IL
NUOVO CIMENTO
ORGANO DELLA SOCIETÀ ITALIANA DI FISICA
SOTTO GLI AUSPICI DEL CONSIGLIO NAZIONALE DELLE RICERCHE

VOL. III, N. 4 *Serie decima* 1° Aprile 1956

Determination of the Ultrasonic Absorption Coefficient in Liquids by the Thermal Method.

E. GROSSETTI
Istituto di Fisica dell'Università - Napoli

(ricevuto il 9 Dicembre 1955)

Summary. (*). — In liquids with a high ultrasonic absorption coefficient as, f.i. benzol, has been observed that an augmentation of the power of the piezoelectric quartz might be a cause of energy dissipation to be ascribed to cavitation and acoustic flow which whould be the origin of the high absorption coefficient. Measures are reported from which it appears that the augmentation of power really produces some uncertainty in the measure of ΔT and therefore of the coefficient α; but, anyway, by a proper proceeding it is possible to obtain for α concordant values with respect to several measurements and one sees therefore that for benzol the thermal method gives a value of the absorption coefficient very greater as the theoretical value.

(*) *Editor's Translation.*

There is presently a lot of criticism on the measurement of the 2nd viscosity coefficient. It is very interesting to notice that in the meeting on the 1st and 2nd viscosity coefficient of fluids, held in April 1953, RICHARDSON pointed out that no abnormal heating was found in liquids whith great values of the acoustic absorption coefficient in the measurements of PARTHASARATHY [1], and therefore the abnormal values found were attributed to variations of specific dielectric capacity, thermal conductivity and so on. Moreover it has been remembered that the liquids with very high absorption coefficient have all a high volatility and may easily give cavitation phenomena.

For the above mentioned reasons RICHARDSON believes that these liquids

[1] S. PARTHASARATHY, S. S. CHARI and P. P. MAHENDROO: S. *Journ. Phys. et Rad.*, **14**, 366 (1953).

have also great speeds of acoustic flow, as it appears from LIEBERMANN's experiences.

It is indeed possible to see clearly the cavitation nuclei take place when the liquids in question are irradiated with ultrasonic waves of sufficient power to produce the acoustic wind. These authors conclude that the excess of ultrasonic energy absorbed by such liquids and changed into heat must be attributed only to the density fluctuations of the medium, fluctuations which in turn facilitate the phenomena of acoustic flow and cavitation.

It is interesting to remark that in our experiments on benzol (2) we found indeed some difficulties for the measurements of the absorption coefficient with the thermal method (3); it will be therefore useful to return again on the subject in order to clarify some aspects of the question.

We used the experimental arrangement already described in our preceding paper (3); the pattern of temperature after the stopping of the ultrasonic waves was very regular for the liquids having low values of the absorption coefficient, so that, after some five minutes, it was possible to measure the final temperature; *on the contrary* for benzol the temperature pattern is less regular and it was necessary to wait a longer time for the determination of the final temperature.

In Fig. 1 we report the pattern of the temperature of Benzol before and after the ceasing of the ultrasonic disturbance. In this way we determine the increase ΔT of temperature at the frequency of 1.8 MHz. This figure presents

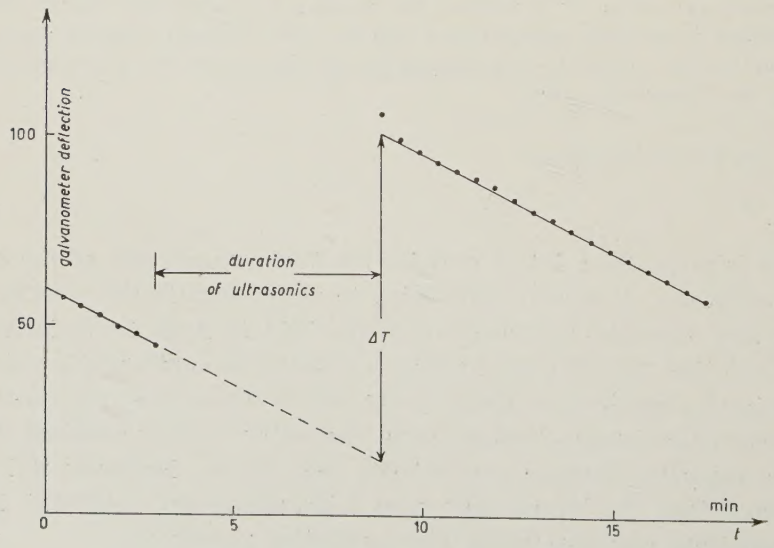

Fig. 1.

(2) E. GROSSETTI: *Nuovo Cimento*, **1**, 525 (1955).
(3) E. GROSSETTI: *Nuovo Cimento*, **11**, 250 (1954).

a case in which the pattern, becomes very regular after some five minutes, so that it is possible to determine the ΔT with precision.

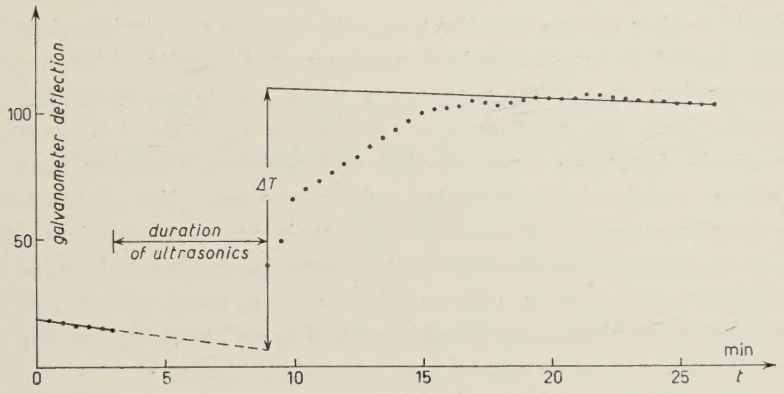

Fig. 2.

This is the general case when the increase of temperature is determinable in a relatively small time and with little ultrasonic power. When instead great power is employed, we have higher ΔT's but the temperature pattern

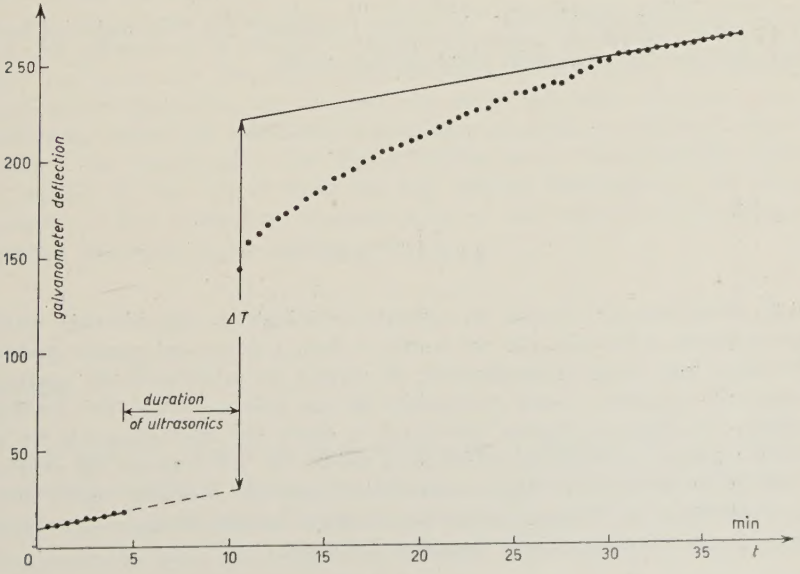

Fig. 3.

after the ceasing of the ultrasonic waves is somewhat irregular, and it is necessary to wait a longer time to obtain the conditions of thermal equilibrium, as can be seen in Figs. 2 and 3.

In such cases the determination of ΔT is rather uncertain and uncertain is therefore also the value of the absorption coefficient of the acoustic waves.

These irregularities must be ascribed evidently to an abnormal heating of the liquid taking place when the power fed to the quartz is not sufficiently low. But it ought to be put clearly in evidence that in spite of these anomalies, in both cases the absorption coefficients which I obtained for benzol did not differ much from one another $\alpha = 2.45 \cdot 10^{-2} \sim 3.01 \cdot 10^{-2} \pm 0.17 \cdot 10^{-2}$ cm^{-1}).

Whe should therefore conclude that the abnormal heating presented by this substance must not be attributed only to the formation of cavitation and acoustic flow because, if such were the case, an increase of the ultrasonic power applied on the quartz would have determined increasing values of the absorption coefficient, *which we did not observe.* One must then think that the great absorption coefficient for these liquids is to be attributed to the 2nd viscosity coefficient.

Anyhow it will be useful to undertake—as we have in mind to do—some systematic measurements of the absorption coefficient of benzol with different powers in order to determine which is the contribution of the cavitation phenomena on this coefficient.

* * *

I am much indebted to Prof. Antonio Carrelli for the material assistance provided and for the valuable suggestions given.

RIASSUNTO

È stato osservato per i liquidi ad elevato coefficiente di assorbimento ultrasonoro, quali, per esempio, il benzolo, che un aumento della potenza del quarzo piezoelettrico potrebbe essere una causa di dissipazione di energia da attribuirsi alla cavitazione ed allo scorrimento acustico, il che porterebbe ad un valore elevato del coefficiente di assorbimento. Si riportano misure dalle quali si rileva che effettivamente un aumento della potenza porta a qualche incertezza nella misura del ΔT e quindi del coefficiente α, ma in ogni modo procedendo opportunamente è possibile ottenere valori concordanti di α relativamente a varie misure e che quindi per il benzolo il metodo termico dà un coefficiente di assorbimento molto maggiore del teorico.

IL NUOVO CIMENTO Vol. III, N. 4 1° Aprile 1956

Explicit Non-Central Potentials and Wave Functions for Given S-Matrices (*).

T. Fulton (+)

Institute for Advanced Study - Princeton, New Jersey

R. G. Newton

Indiana University - Bloomington, Indiana

(ricevuto il 27 Dicembre 1955)

Summary. — Wave functions and potentials are obtained for non-central forces coupling angular momenta l and $l+2$, with the scattering matrix and bound state energies as a starting point. The method, an extension of the techniques developed by Bargmann for central forces, is based on the solution of an integral equation developed and discussed recently by Gel'fand and Levitan, Jost, Kohn and Newton. The ensuing non-central potentials are the first spin-orbit and tensor potential combinations known for which the Schrödinger equation is solvable in closed form. The results allow the approximation of an experimentally given S-matrix by one whose elements are rational functions of the wave number k and subsequent determination of the wave function and potential by purely finite algebraic means.

Introduction.

R. Jost and W. Kohn [1] have developed a method for the construction of all central potentials which give rise to a given phase shift of one angular momentum and given bound states of the same angular momentum. Their work has recently been generalized to include the effects of a tensor force and

(*) Most of this work was done at The Institute for Advanced Study while both authors held Frank B. Jewett Fellowships.

(+) National Science Foundation Postdoctorate Fellow.

(1) R. Jost and W. Kohn: *Kgl. Danske Videnskab. Selskab, Mat.-Fys. Medd.*, **27**, No. 9 (1953).

spin-orbit coupling ([2,3]). The problem of obtaining all combinations of central, tensor and spin-orbit potentials of short range that can be associated with two eigenphaseshifts given as functions of the energy, a mixture parameter (also given as a function of energy), and any number of bound states for the same two angular momenta with given binding energies and mixtures, has been reduced to the solution of Fredholm equations.

It is the purpose of the present work to apply the above-mentioned methods to the explicit construction of non-central potentials which give rise to an S-matrix (referring to two angular momenta and including coupling between them) whose matrix elements are rational functions of $k = E^{\frac{1}{2}}$.

BARGMANN ([4]) has explicitly constructed all *central* potentials leading to an S-matrix element of one angular momentum which is a rational function of k. The present paper is an extension of his work. In principle it is possible to approximate any given $(l, l+2)$ sub-matrix of the S-matrix arbitrarily closely by one whose elements are rational functions of k. The results can be used to exhibit explicitly the potentials which give rise to the latter by purely finite algebraic means.

It may be remarked that the non-central potentials obtained in the present paper are the first ones known for which the set of coupled radial Schrödinger equations for angular momenta l and $l+2$ is solvable in closed form. They are all finite at the origin and decrease at least like r^{-2} at infinity. Certain sub-families of potentials decrease more strongly and some of them are asymptotic to decreasing exponentials.

We shall henceforth use the expression « S-matrix » for the (2×2) sub-matrix of the latter which refers to, and couples, angular momenta l and $l+2$. The potential to be determined is a real, symmetric (2×2) matrix which enters the set of non-relativistic Schrödinger equations for the two components of the radial wave function belonging to angular momenta l and $l+2$ of two spin $\frac{1}{2}$ particles in a triplet state ([5]).

In Sec. 1, we outline the general procedure for constructing potentials and wave functions that is given in Ref. ([3]). In Sec. 2, we discuss a method of specifying an S-matrix whose elements are rational functions of k, and of obtaining from it the parameters needed subsequently. We demonstrate an algebraic method of obtaining the matrix function $F(k)$ (which is required in the construction) from the S-matrix. Sec. 3 contains the explicit deter-

([2]) R. G. NEWTON and R. JOST: *Nuovo Cimento*, **1**, 590 (1955).

([3]) R. G. NEWTON: *Phys. Rev.*, **100**, 412 (1955).

([4]) V. BARGMANN: unpublished. The authors are greatly indebted to Professor BARGMANN for the use of his manuscript before publication.

([5]) For the connection between the elements of the potential matrix and the central, tensor, and spin orbit potentials, see the introduction in Ref. ([3]). The notation of the present paper is generally the same as that of Ref. ([3]).

mination of potentials and wave functions in the general case which is « non-degenerate » and has no bound states. In Sec. 4 a general bound state case is treated. Sec. 5 offers some illustrations. Appendix A treats special cases excluded in Sections 3 and 4 which have some practical interest. Appendix B lists the most important properties of the functions used.

A future publication elsewhere will contain the application of the present construction to the specific case of the neutron-proton interaction.

1. – Outline of the General Construction Procedure (6).

We begin with an S-matrix for angular momenta l and $l+2$ (including a coupling of the two) as a function of $k = E^{\frac{1}{2}}$, given over the entire range $0 \leqslant E < \infty$, and a prescribed number of bound states with given binding energies and given amounts of mixing of the two angular momenta. All of these quantities are entirely independent of each other, except for the requirement that

$$\log \det S(0) = 2\pi m i \,, \tag{1.0}$$

where m is the number of bound states (7) (provided that the logarithm is defined continuously from the value zero at $k = \infty$). The amount of mixing in the σ-th bound state will be specified by means of the mixture angle ε_σ so that the asymptotic ratio of the two components of the bound state wave function is $\operatorname{tg} \varepsilon_\sigma$.

The (2×2)-matrix $S(k)$ has the properties (8)

$$S(k) = \tilde{S}^T(k) \,, \tag{1.1}$$

and

$$S(k)\, S^\dagger(k) = S(k)\, S(-k) = \mathbf{1} \,. \tag{1.2}$$

If it is associated with a short range potential (9) then there exists a matrix funktion $F(k)$ with the following properties: Both $F(k)$ and $F^{-1}(k)$ are analytic for $\operatorname{Im} k < 0$ and continuous for $\operatorname{Im} k \leqslant 0$, except for simple poles of

(6) Proofs for the statements in this section can be found in Ref. (3).

(7) We shall, for the sake of simplicity, neglect the exceptional case of a « resonance » at $k=0$ for $l=0$; see References (2) and (3). We shall also exclude the possibility of degeneracy, the case for which every mixture of angular momenta l and $l+2$ has a bound state of the same binding energy.

(8) We use a « T » for the transposed, a dagger for the hermitean conjugate, and an asterisk for the complex conjugate. The derivative with respect to r will sometimes be indicated by a prime.

(9) In the weak sense of the existence of a second absolute moment of the potential.

$F^{-1}(k)$ at $-i\varkappa_\sigma$ if $-\varkappa_\sigma^2$ is the energy of a bound state, and

$$S(k) = F(k)\,F^{-1}(-k)\,. \tag{1.3}$$

Furthermore, $F(k)$ satisfies, for $\operatorname{Im} k \leqslant 0$,

$$\lim_{|k|\to\infty} F(k) = \mathbf{1}\,, \tag{1.4}$$

and for real k

$$F(-k) = F^*(k)\,, \tag{1.5}$$

$$F^T(-k)F(k) = F^T(k)F(-k)\,. \tag{1.6}$$

The singularity of the matrix $F(-i\varkappa_\sigma)$ is such that

$$P_\sigma F(-i\varkappa_\sigma) = 0\,, \tag{1.7}$$

where P_σ is a real, symmetric projection constructed from the mixture angle ε_σ:

$$P_\sigma = \frac{1}{2}\begin{pmatrix} 1+\cos 2\varepsilon_\sigma & -\sin 2\varepsilon_\sigma \\ -\sin 2\varepsilon_\sigma & 1-\cos 2\varepsilon_\sigma \end{pmatrix}. \tag{1.8}$$

By means of the function $F(k)$ one can construct the « spectral function » $P(E)$ as follows:

$$P(-\infty) = 0\,,$$

$$\frac{\mathrm{d}P(E)}{\mathrm{d}E} = \begin{cases} \pi^{-1}E^{l+\frac{1}{2}}\Upsilon_0(E^{\frac{1}{2}})T(E)\Upsilon_0(E^{\frac{1}{2}})\,, & E > 0\,, \\ \sum\limits_\sigma C_\sigma\,\delta(E-E_\sigma)\,, & E \leqslant 0\,, \end{cases} \tag{1.9}$$

where E_σ are the energies of the bound states [10],

$$\Upsilon_l(k) = k^l(\mathbf{1}-P) + k^{l+2}P\,, \qquad P = \begin{pmatrix} 0 & 0 \\ 0 & 1 \end{pmatrix}, \tag{1.10}$$

the matrix function

$$T(k^2) = [F^T(k)F(-k)]^{-1} \tag{1.11}$$

is real and positive definite, and

$$C_\sigma \equiv c_\sigma(-1)^l\,\Upsilon_l(-i\varkappa_\sigma)\Big[\lim_{k\to -i\varkappa_\sigma}(k^2+\varkappa_\sigma^2)^2F^{-1}(k)F^{T-1}(k)\Big]\,\Upsilon_l(-i\varkappa_\sigma)\,. \tag{1.12}$$

---

[10] $\Upsilon_l(k)$ was called $\mathcal{R}_l(k)$ in Ref. [3].

Here c_σ is an arbitrary positive parameter.

We define the function

$$\mathrm{G}(s, r) = \int_{-\infty}^{\infty} G_0^T(k^2, s)\,\mathrm{d}(P - P_0)/\mathrm{d}E\, G_0(k^2, r)\,\mathrm{d}E\,, \tag{1.13}$$

where

$$\frac{\mathrm{d}P_0}{\mathrm{d}E} = \begin{cases} \pi^{-1}E^{l+\frac{1}{2}}\Upsilon_0^2(E^{\frac{1}{2}})\,, & E > 0\,, \\ 0\,, & E \leqslant 0\,, \end{cases} \tag{1.14}$$

and

$$G_0(k^2, r) = k^{-1}\Upsilon_l^{-1}(k)\,\Phi_0(k, r)\,, \tag{1.15}$$

$$\Phi_0(k, r) = \begin{pmatrix} u_l(kr) & 0 \\ 0 & u_{l+2}(kr) \end{pmatrix}. \tag{1.16}$$

The function $u_l(x)$ satisfies the equation

$$[(\mathrm{d}^2/\mathrm{d}x^2) + 1 - l(l+1)/x^2]u_l(x) = 0\,, \tag{1.17}$$

and is the particular solution

$$u_l(x) = x j_l(x)\,, \tag{1.18}$$

where $j_l(x)$ is the customarly defined spherical Bessel function.

The Gel'fand Levitan integral equation has the form

$$K(s, r) + \mathrm{G}(s, r) + \int_0^r \mathrm{d}t\,\mathrm{G}(s, t)K(t, r) = 0\,, \qquad s \leqslant r\,. \tag{1.19}$$

Equation (1.19) always has a unique solution $K(s, r)$. This function has the property that

$$G(k^2, r) = G_0(k^2, r) + \int_0^r \mathrm{d}t\, G_0(k^2, t)K(t, r) \tag{1.20}$$

is a regular solution of the Schrödinger equation

$$\left(\frac{\mathrm{d}^2}{\mathrm{d}r^2} + k^2\right) G(k^2, r) = G(k^2, r)\left[V(r) + \frac{l(l+1)}{r^2}\,(\mathbf{1} - P) + \frac{(l+2)(l+3)}{r^2}\,P\right]$$

with the potential

$$V(r) = 2(\mathrm{d}/\mathrm{d}r)K(r, r) . \tag{1.21}$$

The spectral function $P(E)$ is the weight function in the integral expressing the completeness of the wave functions $G(k^2, r)$. Due to the interference of the two angular momenta, a boundary condition that would select G uniquely is hard to specify ([11]); G is the generalization of that solution which, in the absence of coupling, satisfies ([12])

$$(2l+1)!! \lim_{r\to 0} \varphi(k, r) r^{-(l+1)} = 1 .$$

If $V(r)$ is of short range ([9]), then the original S-matrix can be obtained from the form of G at large r. The « physical » solution which is asymptotic to

$$\frac{1}{k} U \begin{pmatrix} i^l e^{i\delta_l}(2l+1)\sin[kr+\delta_l - \frac{1}{2}\pi l] & 0 \\ 0 & i^{l+2} e^{i\delta_{l+2}}(2l+5)\sin[kr+\delta_{l+2} - \frac{1}{2}\pi(l+2)] \end{pmatrix} U^{-1},$$

where

$$U(k) = \begin{pmatrix} \cos\varepsilon(k) & \sin\varepsilon(k) \\ -\sin\varepsilon(k) & \cos\varepsilon(k) \end{pmatrix}, \qquad \operatorname{Im}\varepsilon(k) = 0, \tag{1.22}$$

is obtained from G as

$$i^l U(k) \begin{pmatrix} 2l+1 & 0 \\ 0 & -(2l+5) \end{pmatrix} U^{-1}(k) F^{T-1}(-k) Y_l(k) G(k^2, r) .$$

The real functions δ_l and δ_{l+2} are the two eigenphases for angular momenta l and $l+2$. The S-matrix for these angular momenta is given by

$$S(k) = U(k) \begin{pmatrix} \exp[i\delta_l(k)] & 0 \\ 0 & \exp[i\delta_{l+2}(k)] \end{pmatrix} U^{-1}(k) . \tag{1.23}$$

The solution $G(k^2, r)$ can be expressed in terms of solutions $F(k, r)$ and $F(-k, r)$ which satisfy the boundary condition

$$\lim_{r\to\infty} (-i)^l \exp[ikr] \mathcal{E} F(k, r) = \mathbf{1} , \tag{1.24}$$

([11]) See Eq. (2.6) of Ref. ([3]) for the unique definition of G by means of an integral equation.

([12]) For the definition of $(2l+1)!!$, see Appendix B.

where

$$\mathcal{E} = \begin{pmatrix} 1 & 0 \\ 0 & -1 \end{pmatrix}, \tag{1.25}$$

as follows:

$$\Phi(k, r) \equiv k\,\mathcal{Y}_l(k) G(k^2, r) = \tfrac{1}{2} i [F^T(-k) F(k, r) - (-1)^l F^T(k) F(-k, r)]\,. \tag{1.26}$$

The function $F(k)$, on the other hand, can be directly expressed in terms of $F(k, r)$ and $G(k^2, r)$ by means of the Wronskian matrix

$$F(k) = [F(k, r) G'^T(k^2, r) - F'(k, r) G^T(k^2, r)] \mathcal{Y}_l(k)\,. \tag{1.27}$$

Finally, the parameter c_σ is related to the normalization in the sense that the two-component bound state wave function

$$\chi_\sigma(r) \equiv (\chi_{\sigma_1}(r), \chi_{\sigma_2}(r)) \equiv c_\sigma^{-\frac{1}{2}} (\cos \varepsilon_\sigma, -\sin \varepsilon_\sigma) F(-i\varkappa_\sigma, r) \tag{1.28}$$

is normalized to unity:

$$\int_0^\infty \mathrm{d}r [\chi_{\sigma_1}^2(r) + \chi_{\sigma_2}^2(r)] = 1\,.$$

2. – The Rational S-Matrix and its Separation into $F(k)$.

The general method for obtaining $F(k)$ from the S-matrix, when a suitably well-behaved $F(k)$ exists, has been given elsewhere ([13]). In this section we shall develop a purely algebraic procedure applicable when all elements of the submatrix corresponding to angular momenta l and $l+2$ of the S-matrix are rational functions of k.

To begin with, we shall discuss some general properties of rational S-matrices. We shall indicate how these properties may be used to prescribe an S-matrix that approximates an experimentally given one in a form convenient for our purpose.

If bound states exist for the angular momenta we are considering, we first « remove » them from the S-matrix by methods discussed in Refs. ([2]) and ([3]). The matrix S in this section will be assumed to be that which is left after possible bound states have been removed.

([13]) The procedure due to PLEMELJ, see References ([2]) and ([3]).

Let a rational S-matrix be given [14]. Let it have (simple) poles at and only at

$$i\zeta_j, \quad j=1,...,\nu, \qquad i\xi_j, \quad j=1,...,\mu,$$

where $\mathrm{Re}\,\zeta_j<0$, $j=1,...,\nu_1$; $\mathrm{Re}\,\zeta_j>0$, $j=\nu_1+1,...,\nu$; $\mathrm{Re}\,\xi_j<0$, $j=1,...,\mu_1$, $\mathrm{Re}\,\xi_j>0$, $j=\mu_1+1,...,\mu$, and so that

$$S(-i\zeta_j)=0\,, \quad j=1,...,\nu\,; \qquad S(-i\xi_j)\neq 0\,, \quad j=1,...,\mu\,. \tag{2.1}$$

Complex ζ_j and ξ_j must occur in conjugate pairs. We define a matrix whose elements are polynomials:

$$s(k)\equiv\prod_1^{\nu}\frac{k-i\zeta_j}{k+i\zeta_j}\prod_1^{\mu}(k-i\xi_j)S(k)\,. \tag{2.2}$$

It satisfies

$$\lim_{|k|\to\infty}s(k)k^{-\mu}=\mathbf{1}\,. \tag{2.3}$$

Then by (1.2)

$$s^{-1}(k)=(-1)^{\mu}s(-k)/\Delta(k^2)\,, \qquad \Delta(k^2)=\prod^{\mu}(k^2+\xi^2)\,, \tag{2.4}$$

and

$$|\det s(k)|=\Delta(k^2)\,. \tag{2.5}$$

Now, because of (1.2) and (2.1), $\det S(k)$ cannot have double poles at $k=i$, ξ_j, $j=1,...,\mu$. Consequently $\det s(\pm i\xi_j)=0$, $j=1,...,\mu$. Therefore Eqs. (2.3) and (2.5), together with the fact that $\det s(k)$ is a polynomial, imply that

$$\det s(k)=\Delta(k^2)\,. \tag{2.5'}$$

The effective absence of bound states entails that [15]

$$\mu=2(2\nu_1+\mu_1-\nu)\,, \tag{2.6}$$

---

[14] To illustrate the general discussion which follows, it is convenient to keep a special simple but non-trivial rational S-matrix in mind. A convenient example of such an S-matrix is:

$$S(k)=\frac{1}{k^4+\chi^4}\begin{pmatrix}\chi^2 & k^2\\ -k^2 & \chi^2\end{pmatrix}\frac{k-i\psi}{k+i\psi}\begin{pmatrix}\dfrac{k+i\varphi_1}{k-i\varphi_1} & 0\\ 0 & \dfrac{k+i\varphi_2}{k-i\varphi_2}\end{pmatrix}\begin{pmatrix}\chi^2 & -k^2\\ k^2 & \chi^2\end{pmatrix}.$$

[15] Equation (1.0) means that $\det S$ for the case of no bound states has the same number of zeros and poles in the lower half of the k-plane. The same statement holds for the upper half of the k-plane.

and therefore

$$s^{-1}(k) = s(-k)/\Delta(k^2)\,. \tag{2.4'}$$

It follows from the symmetry of S that

$$s_{11}(k) = s_{22}(-k)\,, \qquad s_{12}(-k) = s_{12}^*(k) = -s_{12}(k)\,.$$

We therefore write

$$s(k) = \begin{pmatrix} s_1(k) & iks_2(k^2) \\ iks_2(k^2) & s_1(-k) \end{pmatrix}, \tag{2.7}$$

where

$$s_1(k) = \prod_1^{\mu}(k - i\gamma_n)\,, \qquad s_2(k^2) = \prod_1^{m}(k^2 + \delta_j^2)\,, \qquad 0 \leqslant m \leqslant \tfrac{1}{2}\mu - 1, \tag{2.8}$$

and

$$\prod_1^{\mu}(k^2 + \gamma_u^2) + k^2 \prod_1^{m}(k^2 + \delta_j^2)^2 = \prod_1^{\mu}(k^2 + \xi_j^2)\,, \tag{2.9}$$

while

$$\frac{S_{12}}{S_{11}} = \frac{s_{12}}{s_{11}} = ik\,\frac{\prod_1^{m}(k^2 + \delta_j^2)}{\prod_1^{\mu}(k - i\gamma_n)}\,. \tag{2.10}$$

On the other hand, the symmetry and unitarity of the S-matrix imply the relations

$$\frac{S_{22}}{S_{11}} = -\frac{S_{12}/S_{11}}{(S_{12}/S_{11})^*}\,, \tag{2.11}$$

and

$$|S_{11}|^2 = (1 + |S_{12}/S_{11}|^2)^{-1}\,, \tag{2.12}$$

so that, in addition to S_{12}/S_{11} only the phase of S_{12} need be specified to determine S completely. Furthermore, $\det S = -S_{12}/S_{12}^*$ and hence

$$\prod_1^{\mu}\frac{k - i\xi_j}{k + i\xi_j}\det S = \prod_1^{\nu}\left(\frac{k + i\zeta_j}{k - i\zeta_j}\right)^2. \tag{2.13}$$

One may, then, approximate an experimentally given S-matrix by one with rational elements and obtain the ζ's and ξ's as follows:

The ratio S_{12}/S_{11} determines the γ's and δ^2's by (2.10). Eq. (2.9) then determines the ξ's to within their signs. The latter are determined by the *simple* poles (zeros) of det S, which have to be at $+i\xi_j$ ($-i\xi_j$). Finally, the ζ's are given by (2.13), the determinant of S (the sum of the eigenphases). Eq. (2.6) must, in the effective absence of bound states, be automatically fulfilled.

We now wish to obtain $F(k)$ from the above S-matrix. This is done most simply by means of the matrix $s(k)$. The elements of the latter are polynomials, its determinant vanishes at $k = \pm i\xi_n$, $n = 1, ..., \mu$, and it satisfies (2.3). Let us, for the moment, use the notation

$$\bar{\xi}_n \equiv \xi_n \operatorname{sgn} \operatorname{Re} \xi_n , \qquad n = 1, ..., \mu,$$

so that

$$\operatorname{Re} \bar{\xi}_n > 0 , \qquad n = 1, ..., \mu.$$

We now pick from the ξ's one pair, say ξ_1 and ξ_2, with the only restriction that [16]

$$\text{kernel } s(i\bar{\xi}_1) \not\equiv \text{kernel } s(i\bar{\xi}_2) . \tag{2.14}$$

There exists then a unique projection [17] P_1 such that

$$\begin{cases} \text{range } (\mathbf{1} - P_1) \equiv \text{kernel } P_1 \equiv \text{kernel } s(i\bar{\xi}_1) , \\ \text{range } P_1 \equiv \text{kernel } s(i\bar{\xi}_2) . \end{cases} \tag{2.15}$$

If we define a new matrix

$$\begin{aligned} s_1(k) = [(\mathbf{1} - P_1)(k - i\bar{\xi}_1)^{-1} + P_1(k - i\bar{\xi}_2)^{-1}] \cdot \\ \cdot s(k)[(\mathbf{1} - P_1)(k + i\bar{\xi}_2)^{-1} + P_1(k + i\bar{\xi}_1)^{-1}] , \end{aligned} \tag{2.16}$$

then $s_1(k)$ will still have no poles, due to (2.15) and because it follows from (2.4) that

$$\text{range } s(-i\bar{\xi}_n) \equiv \text{kernel } s(i\bar{\xi}_n) , \qquad n = 1, ..., \mu.$$

---

[16] We use the following terminology: The kernel of a matrix M is the space of all vectors a annihilated by it: $aM = 0$; the range of M is the space onto which M transforms the entire vector space, i.e., the set of all vectors b for which there exist vectors c so that $b = cM$.

[17] By a projection we mean an idempotent matrix $P = P^2$. It is uniquely determined by its range and its kernel, both of which can be independently prescribed.

Furthermore, $\det s_1(k)$ will have zeros only at [18] $k = \pm i\bar{\xi}_n$, $n = 3, \ldots, \mu$ and (2.16) readily shows that

$$\lim_{|k|\to\infty} k^{-(\mu-2)} s_1(k) = \mathbf{1} .$$

This process of removing the zeros of $\det s$ in pairs is repeated until we are left with a matrix $s_f(k)$ which has no poles and whose determinant has no zeros. That matrix also satisfies

$$\lim_{|k|\to\infty} s_f(k) = \mathbf{1} .$$

Consequently, $s_f(k) \equiv \mathbf{1}$, and we have obtained a split

$$S(k) = A(k)B(k) , \tag{2.17}$$

where

$$A(k) = \frac{\prod_{1}^{\nu_1}(k - i\bar{\zeta}_j)}{\prod_{\nu_1+1}^{\nu}(k - i\bar{\zeta}_j)\prod_{\mu_1+1}^{\mu}(k - \bar{\xi}_j)} [(\mathbf{1} - P_1)(k - i\bar{\xi}_1) + P_1(k - i\bar{\xi}_2)] \ldots , \tag{2.18}$$

$$B(k) = \frac{\prod_{\nu_1+1}^{\nu}(k + i\bar{\zeta}_j)}{\prod_{1}^{\nu_1}(k + i\zeta_j)} \frac{1}{\prod_{1}^{\mu_1}(k + i\bar{\xi}_j)} \ldots [(\mathbf{1} - P_1)(k + i\bar{\xi}_2) + P_1(k + i\bar{\xi}_1)] \cdots \tag{2.19}$$

$$= \left[\frac{\prod_{1}^{\nu_1}(-k - i\bar{\zeta}_j)}{\prod_{\nu_1+1}^{\nu}(-k - i\bar{\zeta}_j)}\right]^{-1} \prod_{1}^{\mu_1}(-k - i\bar{\xi}_j)\{[(\mathbf{1} - P_1)(-k - i\bar{\xi}_1) + P_1(-k - i\bar{\xi}_2)] \ldots\}^{-1} ,$$

by the use of (2.6). Since $A(k)$ has no poles in the lower half of the complex k-plane and $\det A(k)$ has no zeros there, and owing to (2.6), $A(\infty) = \mathbf{1}$, we have

$$A(k) = F(k) , \qquad B(k) = F^{-1}(k) . \tag{2.20}$$

In general, however, this procedure may not quite succeed, because we may arrive at a point where we can no longer satisfy (2.14) for the remaining matrix s_r. Then at all the remaining 2ι zeros in the upper half plane s_r has the same kernel. The same holds for all the 2ι zeros in the lower half plane.

[18] The proof of this is entirely analogous to that given in Sec. 3 of Ref. [2].

Moreover,

$$\lim_{|k|\to\infty} k^{-2\iota} s_r(k) = \mathbf{1}\,. \tag{2.21}$$

If the common kernel at the zeros in the lower half of the k plane were also equal to the kernel of the zeros in the upper half plane, then there would exist vectors γ_1 and γ_2, such that

$$\gamma_1 s_r(k) = \prod_1^{2\iota} (k^2 + \xi_n^2)\gamma_2\,,$$

and that would contradict (2.21). The common kernel of s_r at the zeros of $\det s_r$ in the lower half plane must therefore be disjoint from that of those in the upper. Consequently there exists a projection P_r so that

$$s_r(k) = \prod_1^{2\iota} (k - i\bar{\xi}_n) P_r + \prod_1^{2\iota} (k + i\bar{\xi}_n)(\mathbf{1} - P_r) = \tag{2.22}$$

$$= A \begin{pmatrix} \prod_1^{2\iota} (k + i\bar{\xi}_n) & 0 \\ 0 & \prod_1^{2\iota} (k - i\bar{\xi}_n) \end{pmatrix} A^{-1} =$$

$$= \prod_1^{2\iota} (k - i\bar{\xi}_n) A \begin{pmatrix} \dfrac{\prod_1^{\iota} (k - i\varrho_n)}{\prod_1^{2\iota} (k - i\bar{\xi}_n)} & 0 \\ 0 & \dfrac{\prod_1^{\iota} (k - i\varrho_n)}{\prod_1^{2\iota} (k - i\eta_n)} \end{pmatrix} \cdot$$

$$\cdot \begin{pmatrix} \prod_1^{\iota} \dfrac{(k + i\varrho_n)}{(k - i\varrho_n)} & 0 \\ 0 & \prod_1^{\iota} \dfrac{(k + i\varrho_n)}{(k - i\varrho_n)} \prod_1^{2\iota} \dfrac{(k - i\eta_n)}{(k + i\eta_n)} \end{pmatrix} \cdot \begin{pmatrix} \dfrac{\prod_1^{2\iota} (k + i\xi_n)}{\prod_1^{\iota} (k + i\varrho_n)} & 0 \\ 0 & \dfrac{\prod_1^{2\iota} (k + i\eta_n)}{\prod_1^{\iota} (k + i\varrho_n)} \end{pmatrix} A^{-1},$$

where A diagonalizes P_r, and the ϱ's and η's are arbitrary. By setting all $\varrho_n = \eta_n = 1$, we accomplish the separation according to Plemelj's theorem [13]:

$$S(k) = F(k) N(k) F^{-1}(-k)\,,$$

where

$$N = \begin{pmatrix} z^{\mu} & 0 \\ 0 & z^{-\mu} \end{pmatrix}, \qquad z = \frac{k+i}{k-i}\,,$$

and μ are the « Plemelj indices ».

Plemelj's theorem assures us that we could not have reduced μ by removing the zeros in a different order or in different pairs ([19]). Therefore the original S-matrix can not be split into matrices $F(k)$ and $F^{-1}(-k)$ with properties appropriate to short range potentials ([9]).

A criterion that allows us to recognize the index μ of S without first going through the relatively complicated procedure described above, is not known. In view of some readily constructed examples, it may be conjectured that such a criterion is that, in the absence of bound states, the eigenphases must individually vanish at $k = 0$ (Eq. (1.0) asserts this only about their sum.) In the presence of bound states, the same must then be true for the matrix S from which the bound states have been removed by the methods of Refs. ([2]) and ([3]).

3. – Construction of Potentials and Wave Functions in the General Case of No Bound States.

3·1. *Preliminaries.* – We turn to the solution of the Gel'fand Levitan equation in the case when the elements of the matrix $T(k^2)$ of (1.11) are rational functions of k^2:

$$T(k^2) = \mathcal{F}(k^2)/\prod_{i=1}^{\nu_\alpha}(k^2+\alpha_i^2), \quad \mathrm{Re}\,\alpha_i > 0, \quad i = 1, ..., \nu_\alpha, \tag{3.1}$$

where $\mathcal{F}$ is a symmetric matrix all of whose elements are polynomials in k^2. We shall, in this section, assume that the determinant of $\mathcal{F}$ has simple zeros only, at the point $k^2 = -\beta_n^2$, $\mathrm{Re}\,\beta_n > 0$, $n = 1, ..., \nu_\beta$. The reality of T for real k^2 implies that the α's and the β's, if complex, occur in complex conjugate pairs. We shall assume for simplicity that they are all real, but the results are easily modified to complex α's and β's. We shall also assume in this section that no two α's and β's coincide.

It follows from (1.4) and (1.11) that

$$T(\infty) = \mathbf{1}\,; \tag{3.2}$$

([19]) Suppose the S-matrix which we are trying to separate into $F(k)$ and $F^{-1}(-k)$ as obtained by a rational approximation to an experimentally given S-matrix over a certain finite range of energies, and we find that the index does not come out equal to zero. Then one might be tempted to choose the ϱ's and η's (real and) large compared to the k-interval within which the S-matrix was approximated, and then set the matrix in the center of (2.20) equal to $\mathbf{1}$. This would, however, destroy the unitarity of the S-matrix and is therefore not feasible.

consequently

$$\lim_{|k|\to\infty} k^{-2\nu_\alpha}\mathcal{F}(k^2) = \mathbf{1}\,, \tag{3.3}$$

and

$$\nu_\beta = 2\nu_\alpha\,. \tag{3.4}$$

Since $\det \mathcal{F}(k^2)$ was assumed to have only simple zeros, the range of $\mathcal{F}(-\beta_n^2)$ does not vanish for $n = 1, ..., \nu_\beta$. We specify these ranges ([20]) by a set of vectors $\gamma^{(\beta)}$ so that

$$\gamma^{(\beta)} \text{ represents range } \mathcal{F}(-\beta^2)\,, \quad \beta = \beta_n,\ n = 1, ..., \nu_\beta. \tag{3.5}$$

3·2. *Construction of the Potential.* – We now turn to the construction of the potential. Let us write ([21])

$$T(k^2) = \mathbf{1} + \sum_{(\alpha)} (k^2+\alpha^2)^{-1} M_\alpha\,, \tag{3.6}$$

where the (2×2) matrices M_α are symmetric and non-singular (owing to the assumption that all β's differ from all α's). We can then write, in the notation of (1.13) and (1.16)

$$\mathrm{G}(s, r) = \sum_{(\alpha)} \mathrm{G}_\alpha(s, r)\,, \tag{3.7}$$

where

$$\mathrm{G}_\alpha(s, r) = \pi^{-1}\int_{-\infty}^{\infty} \mathrm{d}k\,(k^2+\alpha^2)^{-1}\Phi_0(ks) M_\alpha \Phi_0(kr)\,. \tag{3.8}$$

We define the matrix operator

$$\mathcal{D}_r = \begin{pmatrix} r^{-(l+1)}(\mathrm{d}/\mathrm{d}r) r^{l+1} & 0 \\ 0 & -r^{l+2}(\mathrm{d}/\mathrm{d}r) r^{-(l+2)} \end{pmatrix}, \tag{3.9}$$

([20]) Since we are dealing with (2×2)-matrices, the ranges and kernels of these matrices are one-dimensional subspaces (unless they consist of the whole space or the zero element alone). They can therefore be represented by a single vector in the sense that all other points in the subspace are multiples of that vector. We shall write, then, for example γ rep. range $\mathcal{F}$.

([21]) We shall, in the following, frequently employ this notation. The summation here runs over the set α_i, $i = 1, ..., \nu_\alpha$. If the $\sum$ carries the symbol (β), then it runs over β_n, $n = 1, ..., \nu_\beta$.

and the Green's function [22]

$$(3.10)\qquad g_\alpha^l(s,r)\equiv\pi^{-1}\int_{-\infty}^{\infty}\mathrm{d}k\,(k^2+\alpha^2)^{-1}u_l(ks)\,u_l(kr)=\alpha^{-1}\begin{cases}U_\alpha^l(r)V_\alpha^l(s)\,, & r>s\,,\\ V_\alpha^l(r)U_\alpha^l(s)\,, & r<s\,.\end{cases}$$

The function $g_\alpha^l(s,r)$ satisfies the differential equation

$$(3.11)\qquad (D_s^l-\alpha^2)g_\alpha^l(s,r)=-\delta(s-r)\,,$$

where

$$(3.12)\qquad D_s^l=\mathrm{d}^2/\mathrm{d}s^2-l(l+1)s^{-2}\,.$$

By means of the recursion relations (B.4) and (B.5) (see Appendix B) for u_l, we obtain

$$\begin{aligned}\mathrm{G}_\alpha(s,r)&=\mathcal{D}_s M_\alpha\mathcal{D}_r\pi^{-1}\int_{-\infty}^{\infty}\mathrm{d}k\,k^{-2}(k^2+\alpha^2)^{-1}u_{l+1}(ks)\,u_{l+1}(kr)\,,\\&=\mathcal{D}_s M_\alpha\mathcal{D}_r\alpha^{-2}(g_0^{l+1}(s,r)-g_\alpha^{l+1}(s,r))\,.\end{aligned}$$

If we define

$$(3.13)\qquad \mathrm{V}_\alpha(r)\equiv\begin{pmatrix}V_\alpha^l(r) & 0\\ 0 & -V_\alpha^{l+2}(r)\end{pmatrix},\qquad \mathrm{U}_\alpha(r)=\begin{pmatrix}U_\alpha^l(r) & 0\\ 0 & -U_\alpha^{l+2}(r)\end{pmatrix},$$

we can write (see (1.10) for definition of P)

$$(3.14)\qquad \mathrm{G}_\alpha(s,r)=\alpha^{-1}\{(2l+3)(s/r)^{l+1}(\alpha r)^{-1}(\mathbf{1}-P)M_\alpha P+\mathrm{V}_\alpha(s)M_\alpha\mathrm{U}_\alpha(r)\}\,,\quad r\geqslant s\,,$$

and

$$(3.15)\qquad \mathrm{G}_\alpha(s,r)=\alpha^{-1}\{(2l+3)(r/s)^{l+1}(\alpha s)^{-1}PM_\alpha(\mathbf{1}-P)+\mathrm{U}_\alpha(s)M_\alpha\mathrm{V}_\alpha(r)\},\quad r\leqslant s.$$

We define another matrix operator

$$(3.16)\qquad \Theta_r=\begin{pmatrix}r^{l+1}(\mathrm{d}/\mathrm{d}r)r^{-(l+1)} & 0\\ 0 & -r^{-(l+2)}(\mathrm{d}/\mathrm{d}r)r^{l+2}\end{pmatrix},$$

[22] The functions U and V, also used in BARGMANN's work, are defined as follows: $V_\alpha^l(r)=(-i)^{l+1}u_l(i\alpha r)$, $U_\alpha^l(r)=(-i)^l w_l(-i\alpha r)$, where $w_l(x)=i(-1)^{l+1}h_l^{(1)}(-x)$ and $h_l^{(1)}$ is the spherical Hankel function of the first kind. Some of their most important properties are listed in Appendix B.

and can then write, using the recursion relations of Table II,

$$\Theta_s \mathrm{G}_\alpha(s, r) = - M_\alpha \mathcal{D}_r g_\alpha^{l+1}(s, r) . \tag{3.17}$$

For $r > s$, partial integration yields [23]

$$\Gamma_\alpha(s, r) \equiv \Theta_s \int_0^r \mathrm{d}t\, \mathrm{G}_\alpha(s, t) K(t, r) = \tag{3.18}$$

$$= M_\alpha \left[\int_0^r \mathrm{d}t\, g_\alpha^{l+1}(s, t) \mathcal{K}(t, r) - \alpha^{-1} \mathcal{E} U_\alpha^{l+1}(r) V_\alpha^{l+1}(s) K(r, r) \right] ,$$

where

$$\mathcal{K}(t, r) \equiv \Theta_t K(t, r) . \tag{3.19}$$

If we now apply the operator Θ_s to the left of the Gel'fand Levitan equation, then we obtain for $r > s$

$$\mathcal{K}(s, r) + \sum_{(\alpha)} M_\alpha V_\alpha^{l+1}(s) \mathrm{U}_\alpha(r) + \sum_{(\alpha)} \Gamma_\alpha(s, r) = 0 . \tag{3.20}$$

We operate on this equation with $\prod_{(\alpha)} (\alpha^2 - D_s^{l+1})$ and use (3.11) and (3.18) to obtain

$$[\prod_{(\alpha)} (\alpha^2 - D_s^{l+1}) + \sum_{(\alpha)} \prod_{(\alpha' \neq \alpha)} (\alpha'^2 - D_s^{l+1}) M_\alpha] \mathcal{K}(s, r) = 0 .$$

The bracket is recognized as

$$\prod_{(\alpha)} (\alpha^2 - D_s^{l+1}) T(- D_s^{l+1}) = \mathcal{F}(- D_s^{l+1}) ,$$

so that $\mathcal{K}(s, r)$ satisfies the differential equation

$$\mathcal{F}(- D_s^{l+1}) \mathcal{K}(s, r) = 0 . \tag{3.21}$$

Since the determinant of $\mathcal{F}$ vanishes at $k^2 = - \beta_n^2$, $n = 1, ..., \nu_\beta$, the solutions of (3.21) regular at the origin are linear combinations of $V_{\beta_n}^{l+1}(s)$:

$$\mathcal{K}(s, r) = \sum_{(\beta)} \beta V_\beta^{l+1}(s) \mathcal{K}_\beta(r) , \tag{3.22}$$

[23] See (1.25) for the definition of $\mathcal{E}$.

where the matrices $\mathcal{K}_\beta(r)$ must satisfy, identically in r,

$$\mathcal{F}(-\beta^2)\mathcal{K}_\beta(r) = 0\,, \qquad \beta = \beta_n,\ n = 1, \ldots, \nu_\beta, \tag{3.23}$$

or, in view of (3.5),

$$\gamma^{(\beta)}\mathcal{K}_\beta(r) = 0\,, \qquad \beta = \beta_n,\ n = 1, \ldots, \nu_\beta. \tag{3.24}$$

We now substitute (3.22) in (3.20) and observe that, due to (B.8) (see App. B)

$$\int_0^r \mathrm{d}t\, g^l_\alpha(s, t) V^l_\beta(t) = x^l_{\alpha\beta}(r) V^l_\alpha(s)\alpha^{-1} + (\alpha^2 - \beta^2)^{-1} V^l_\beta(s)\,, \tag{3.25}$$

where

$$x^l_{\alpha\beta}(r) \equiv (\alpha^2 - \beta^2)^{-1} W[V^l_\beta(r);\ U^l_\alpha(r)]\,, \tag{3.26}$$

and W denotes the Wronskian of the functions in the brackets.

We then obtain

$$\sum_{(\beta)} \beta V^{l+1}_\beta(s)\mathcal{K}_\beta(r) + \sum_{(\alpha)} M_\alpha V^{l+1}_\alpha(s)\,\mathrm{U}_\varkappa(r) - \sum_{(\alpha)} \alpha^{-1} M_\alpha \mathcal{E} U^{l+1}_\varkappa(r) V^{l+1}_\alpha(s) K(r, r) + \tag{3.27}$$
$$+ \sum_{(\alpha),(\beta)} M_\alpha \beta [x^{l+1}_{\alpha\beta}(r)\alpha^{-1} V^{l+1}_\alpha(s) + (\alpha^2 - \beta^2)^{-1} V^{l+1}_\beta(s)]\mathcal{K}_\beta(r) = 0\,.$$

Since by hypothesis no α's and β's coincide, it follows from (3.23) that

$$\sum_{(\beta)} [\mathbf{1} + \sum_{(\alpha)} (\alpha^2 - \beta^2)^{-1} M_\alpha] \beta V^{l+1}_\beta(s)\mathcal{K}_\beta(r) = 0\,. \tag{3.28}$$

Furthermore, since the matrices M_α are non-singular and the functions $V^{l+1}_\varkappa(s)$ are linearly independent, the coefficient of every $V^{l+1}_\varkappa(s)$ in (3.27) must vanish and we may divide by M_α to obtain

$$\alpha \mathrm{U}_\alpha(r) + \sum_{(\beta)} \beta x^{l+1}_{\alpha\beta}(r)\mathcal{K}_\beta(r) - U^{l+1}_\alpha(r)\mathcal{E}K(r, r) = 0\,, \qquad \alpha = \alpha_i,\ i = 1, \ldots, \nu_\varkappa. \tag{3.29}$$

In order to recover $K(s, r)$ from $\mathcal{K}(s, r)$ using (3.19), we have to introduce an undetermined function of r. Eq. (3.22) and the recursion relations yield

$$K(s, r) = \sum_{(\beta)} \mathrm{V}_\beta(s)\mathcal{K}_\beta(r) + s^{l+1}(\mathbf{1} - P)A(r)\,. \tag{3.30}$$

We substitute (3.30) in (3.29) and make use of the identity

$$\mathbf{1}\beta x_{\alpha\beta}^{l+1} - U_\alpha^{l+1}\mathcal{E}\mathrm{V}_\beta = \alpha\begin{pmatrix} x_{\alpha\beta}^{l} & 0 \\ 0 & x_{\alpha\beta}^{l+2}\end{pmatrix} \equiv \alpha X_{\alpha\beta}\,. \tag{3.31}$$

The result is

$$\mathrm{U}_\alpha + \sum_{(\beta)} X_{\alpha\beta}\mathcal{K}_\beta - \alpha^{-1}U_\alpha^{l+1}r^{l+1}(\mathbf{1}-P)A = 0\,, \qquad \alpha = \alpha_i,\ i = 1, \ldots, \nu_\alpha. \tag{3.32}$$

Eqs. (3.24) and (3.32) impose $4\nu_\beta$ conditions on the $4\nu_\beta+2$ variables $\mathcal{K}_\beta$ and $(\mathbf{1}-P)A$. The remaining two equations are obtained if we observe that (3.20) does not contain the restrictions on the s^{l+1}-terms which the Gel'fand Levitan equation imposes. We must therefore separately examine the terms of order s^{l+1} in (1.19).

Let the symbol $\{\!|\ |\!\}$ select the factor of s^{l+1} in a function of s. Then [12]

$$\{\!|K(s,r)|\!\} = \sum_{(\beta)}[(2l+1)!!]^{-1}\beta^{l+1}(\mathbf{1}-P)\mathcal{K}_\beta(r) + (\mathbf{1}-P)A(r)\,, \tag{3.33}$$

and for $r \geqslant s$,

$$\{\!|\mathrm{G}_\alpha(s,r)|\!\} = (2l+3)\alpha^{-2}r^{-l-2}(\mathbf{1}-P)M_\alpha P + [(2l+1)!!]^{-1}\alpha^l(\mathbf{1}-P)M_\alpha \mathrm{U}_\alpha(r). \tag{3.34}$$

Use of the recursion relations and of the integral

$$\int_0^r \mathrm{d}t\, U_\alpha^l(t)V_\beta^l(t) = x_{\alpha\beta}^l(r) + \beta(\alpha^2-\beta^2)^{-1}(\beta/\alpha)^l \tag{3.35}$$

leads to

$$\Lambda_{\alpha\beta}(r) \equiv \{\!|\int_0^r \mathrm{d}t \mathrm{G}_\alpha(s,t)\mathrm{V}_\beta(t)|\!\} = \tag{3.36}$$

$$= (\mathbf{1}-P)M_\alpha\left[-\frac{2l+3}{\alpha^2}P\left(\frac{V_\beta^{l+1}(r)}{\beta r^{l+2}} - \frac{\beta^{l+1}}{(2l+3)!!}\right) + \frac{\alpha^l}{(2l+1)!!}\left(X_{\alpha\beta}(r) - X_{\alpha\beta}(0)\right)\right],$$

and

$$\Xi_\alpha(r) \equiv \{\!|\int_0^r \mathrm{d}t \mathrm{G}_\alpha(s,t)t^{l+1}|\!\}(\mathbf{1}-P) = (\mathbf{1}-P)\left[\frac{1}{\alpha^2} - \frac{\alpha^{l-1}r^{l+1}}{(2l+1)!!}U_\alpha^{l+1}(r)\right]. \tag{3.37}$$

Finally, we use (3.32) together with (3.36) and (3.37) to obtain

$$\begin{aligned}\{\!|\Gamma_\alpha(s,r)|\!\} &= \sum_{(\beta)}\Lambda_{\alpha\beta}(r)\mathcal{K}_\beta(r) + \Xi_\alpha(r)A(r) = \\ &= (\mathbf{1}-P)M_\alpha\left\{\sum_{(\beta)}\left[\frac{\beta^{l+1}}{(2l+1)!!}\frac{1}{\alpha^2-\beta^2} - \frac{2l+3}{\alpha^2 r^{l+2}}P\frac{V_\beta^{l+1}(r)}{\beta}\right]\cdot\mathcal{K}_\beta(r) - \right. \\ &\quad \left. - \frac{\alpha^l}{(2l+1)!!}\mathrm{U}_\alpha(r) + \alpha^{-2}(\mathbf{1}-P)A(r)\right\}.\end{aligned} \tag{3.38}$$

Use of (3.28), and the fact that

$$\mathbf{1} + \sum_{(\alpha)} \alpha^{-2} M_\alpha = T(0)\,, \tag{3.39}$$

leads to the equation

$$(\mathbf{1} - P)A(r) = -(2l+3)r^{-(l+2)}N[\mathbf{1} - \sum_{(\beta)} \beta^{-1} V_\beta^{l+1}(r)\mathcal{K}_\beta(r)] = \tag{3.40}$$

$$= -r^{-(l+1)}N\{\mathbf{1}(2l+3)r^{-1} - \sum_{(\beta)} [V_\beta^{l}(r) - V_\beta^{l+2}(r)]\mathcal{K}_\beta(r)\}\,,$$

where

$$N \equiv [T_{12}(0)/T_{11}(0)] \begin{pmatrix} 0 & 1 \\ 0 & 0 \end{pmatrix}. \tag{3.41}$$

We now resubstitute (3.40) in (3.32) and obtain the equations

$$\sum_{(\beta)} \mathcal{Q}_{\alpha\beta}(r)\mathcal{K}_\beta(r) = -\mathcal{U}_\alpha(r)\,, \qquad \alpha = \alpha_i,\ i = 1, \ldots, \nu_\alpha, \tag{3.42}$$

$$K(s, r) = \sum_{(\beta)} \mathcal{V}_\beta(s, r)\mathcal{K}_\beta(r) - (2l+3)r^{-1}(s/r)^{l+1}N\,, \tag{3.43}$$

with

$$\mathcal{Q}_{\alpha\beta}(r) \equiv X_{\alpha\beta}(r) - (2l+3)(\alpha\beta r)^{-1}U_\alpha^{l+1}(r)V_\beta^{l+1}(r)N = \tag{3.44}$$

$$= X_{\alpha\beta}(r) + [x_{\alpha\beta}^{l}(r) - x_{\alpha\beta}^{l+2}(r)]N\,,$$

$$\mathcal{U}_\alpha(r) \equiv \mathrm{U}_\alpha(r) - [U_\alpha^{l}(r) - U_\alpha^{l+2}(r)]N\,, \tag{3.45}$$

$$\mathcal{V}_\beta(s, r) \equiv \mathrm{V}_\beta(s) + (s/r)^{l+1}[V_\beta^{l}(r) - V_\beta^{l+2}(r)]N\,. \tag{3.46}$$

If we consider (3.42) together with (3.24), we can write the equations that determine $\mathcal{K}_\beta$ in matrix notation,

$$\mathfrak{M}\mathfrak{K} = -\mathfrak{U}\,, \tag{3.47}$$

where $\mathfrak{K}$ is a « super » column vector of ν_β components, each of which is a (2×2)-matrix, $\mathcal{K}_\beta(r)$; $\mathfrak{U}$ is the same kind of vector with the first ν_α components equal to $\mathcal{U}_\alpha(r)$, respectively, and null matrices in the last ν_β places; $\mathfrak{M}$ is a « super » square matrix consisting of $(\nu_\beta \times \nu_\beta)$ components, each of which is

a (2×2)-matrix. Schematically, $\mathfrak{M}$ can be written as follows: [24]

$$\mathfrak{M}(r) = \begin{pmatrix} & & & & & \mathcal{Q}_{\alpha\beta}(r) & \\ \cdots & \cdots & \cdots & \cdots & \cdots & \cdots & \cdots \\ \gamma_1^{(1)} & \gamma_2^{(1)} & 0 & 0 & 0 & 0 & \\ 0 & 0 & \gamma_1^{(2)} & \gamma_2^{(2)} & 0 & 0 & \\ 0 & 0 & 0 & 0 & \gamma_1^{(3)} & \gamma_2^{(3)} & \ddots \end{pmatrix} \tag{3.48}$$

With the abbreviation

$$\mathcal{Q}_\beta(r) \equiv \mathcal{Q}_\beta(r, r)\,,$$

the derivative of Y can be written

$$(\mathrm{d}/\mathrm{d}r)\mathcal{Q}_{\alpha\beta}(r) = \mathcal{U}_\alpha(r)\mathcal{V}_\beta(r) = \mathcal{E}\mathcal{V}_\beta(r)\mathcal{U}_\alpha(r)\mathcal{E}\,, \tag{3.49}$$

and $K(r, r)$ becomes

$$K(r, r) = -\,\mathfrak{V}^{\mathfrak{T}}\mathfrak{M}^{-1}\mathfrak{U} - (2l+3)r^{-1}N\,. \tag{3.50}$$

Here $\mathfrak{V}^{\mathfrak{T}}$ is a « super » row vector whose components are $\mathcal{V}_\beta(r)$. Equations (3.49) and (3.50) readily yield

$$\mathrm{tr}\, K(r, r) = -\,\mathrm{Tr}\, \mathfrak{M}'\mathfrak{M}^{-1} = -\,(\mathrm{d}/\mathrm{d}r)\log\det\mathfrak{M}\,,$$

where tr denotes the 2-dimensional trace, and Tr, the $2\nu_\beta$-dimensional trace. Since, furthermore,

$$\mathrm{tr}\,(\mathfrak{V}^{\mathfrak{T}}\mathfrak{M}^{-1}\mathfrak{U})^2 = \mathrm{Tr}\,(\mathfrak{M}'\mathfrak{M}^{-1})^2\,,$$

and for (2×2)-matrices $\mathrm{tr}\, A^2 = (\mathrm{tr}\, A)^2 - 2\det A$, we can obtain the eigenvalues of $\mathfrak{V}^{\mathfrak{T}}\mathfrak{M}^{-1}\mathfrak{U}$ from $\mathrm{Tr}\,\mathfrak{M}'\mathfrak{M}^{-1}$ and $\mathrm{Tr}\,(\mathfrak{M}'\mathfrak{M}^{-1})^2$.

The potential is obtained from (3.50) and (1.21):

$$\tfrac{1}{2}V(r) = -\,\mathfrak{V}^{\mathfrak{T}'}\mathfrak{M}^{-1}\mathfrak{U} - \mathfrak{V}^{\mathfrak{T}}\mathfrak{M}^{-1}\mathfrak{U}' + (\mathfrak{V}^{\mathfrak{T}}\mathfrak{M}^{-1}\mathfrak{U})^2 + (2l+3)r^{-2}N\,, \tag{3.51}$$

by the use of (3.49). The recursion relations for the functions U^l and V^l lead to

$$\mathcal{V}'_\beta(r) = r^{-1}C\mathcal{V}_\beta(r) + \beta V_\beta^{l+1}(r)\mathcal{E}\,, \tag{3.52}$$

$$\mathcal{U}'_\alpha(r) = r^{-1}\mathcal{U}_\alpha(r)C - \alpha U_\alpha^{l+1}(r)\mathcal{E}\,, \tag{3.53}$$

[24] $\gamma^{(\beta_n)} = (\gamma_1^{(n)}, \gamma_2^{(n)})$.

where

$$C = (l+1)(\mathbf{1} - P) - (l+2)P - (2l+3)N \,. \tag{3.54}$$

As a result, we can write [25],

$$\tfrac{1}{2}V(r) = -r^{-1}\{C, \mathfrak{B}^{\mathfrak{T}}\mathfrak{M}^{-1}\mathfrak{U}\} + \\ + \mathfrak{B}^{\mathfrak{T}}\mathfrak{M}^{-1}\mathfrak{U}_1 - \mathfrak{B}_1^{\mathfrak{T}}\mathfrak{M}^{-1}\mathfrak{U} + (\mathfrak{B}^{\mathfrak{T}}\mathfrak{M}^{-1}\mathfrak{U})^2 + (2l+3)r^{-2}N \,, \tag{3.55}$$

where $\mathfrak{U}_1$ is the « super » column vector whose first ν_α elements are the (2×2)-matrices $\alpha U_\alpha^{l-1}\mathcal{E}$, respectively, and whose last ν_α elements are null matrices; and $\mathfrak{B}_1^{\mathfrak{T}}$ is the « super » row vector whose elements are $\beta V_\beta^{l-1}\mathcal{E}$.

3·3. *Construction of the Wave Function.* – The regular solution $G(k^2, r)$ or $\Phi(k, r)$ of (1.25) is obtained from

$$K(s, r) = -\mathfrak{B}^{\mathfrak{T}}(s, r)\mathfrak{M}^{-1}(r)\mathfrak{U}(r) - (2l+3)r^{-1}(s/r)^{l+1}N \tag{3.56}$$

(with an obvious generalization of $\mathfrak{B}(r)$ to a « super » vector with components $\mathcal{U}_\beta(s, r)$ by Eq. (1.20).) Use of the identities

$$\int_0^r \mathrm{d}t\, u_l(kt)V_\beta^l(t) = (k^2+\beta^2)^{-1}W\,[u_l(kr);\, V_\beta^l(r)]$$

and

$$\int_0^r \mathrm{d}t\, t^{l+1}u_l(kt) = k^{-1}r^{l+1}u_{l+1}(kr)$$

leads to the wave function

$$\Phi(k, r) = \Phi_0(k, r) + \mathfrak{W}^{\mathfrak{T}}([u], k, r)\mathfrak{R}(r) - (2l+3)(kr)^{-1}u_{l-1}(kr)N \,, \tag{3.57}$$

where Φ_0 is given by (1.16) and $\mathfrak{W}^{\mathfrak{T}}$ is the « super » row vector whose components are, respectively,

$$\mathcal{W}_\beta([u], k, r) = (k^2+\beta^2)^{-1}W[u_l(kr);\, V_\beta^l(r)](\mathbf{1} - P) - \\ - (k^2+\beta^2)^{-1}W[u_{l-2}(kr);\, V_\beta^{l+2}(r)]P - k^{-1}u_{l-1}(kr)[V_\beta^l(r) - V_\beta^{l+2}(r)]N \,. \tag{3.58}$$

It is apparent from (1.26) that replacement of $u_l(kr)$ by $w_l(kr)$ everywhere

[25] The curly bracket is here used to denote the anti-commutator: $\{A, B\} = AB + BA$.

in (3.57) must give us $F^T(-k)F(k, r)$:

$$F^T(-k)F(k, r) = F_0(k, r) + \mathfrak{W}^{\mathfrak{T}}([w], k, r)\mathfrak{K}(r) - (2l+3)(kr)^{-1}w_{l+1}(kr)N\,, \tag{3.59}$$

with [22]

$$F_0(k, r) = \begin{pmatrix} w_l(kr) & 0 \\ 0 & w_{l+2}(kr) \end{pmatrix}.$$

We can now obtain $F(k)$ from (3.59) by letting r tend to infinity. The asymptotic forms of the relevant constituents are obtained from Table I in Appendix B as

$$x^l_{\alpha\beta}(r) \sim \tfrac{1}{2}(\beta-\alpha)^{-1}\exp[(\beta-\alpha)r]\,,$$

and

$$(k^2+\beta^2)^{-1}W[w_l(kr);\, V^l_\beta(r)] \sim \tfrac{1}{2}i^{l+1}(k+i\beta)^{-1}\exp[(\beta-ik)r]\,.$$

The matrix $\mathcal{Y}_{\alpha\beta}$ of (3.44) therefore becomes asymptotically

$$\mathcal{Y}_{\alpha\beta}(r) \sim \tfrac{1}{2}(\beta-\alpha)^{-1}\exp[(\beta-\alpha)r]\,\mathbf{1}\,,$$

and (3.45) goes over into

$$\mathcal{U}_\alpha(r) \sim \mathcal{E}\exp[-\alpha r]\,.$$

Therefore, if we define

$$a^{(0)T}_\beta \equiv -\tfrac{1}{2}\lim_{r\to\infty} e^{\beta r}\mathcal{K}_\beta(r)\mathcal{E}\,, \tag{3.60}$$

then (3,42) becomes asymptotically

$$\mathbf{1} - \sum_{(\beta)}(\beta-\alpha)^{-1}a^{(0)}_\beta = 0\,, \qquad \alpha=\alpha_i,\ i=1, ..., \nu_\alpha, \tag{3.61}$$

and (3.24) is simply

$$\gamma^{(\beta)}a^{(0)T}_\beta = 0\,, \qquad \beta=\beta_n,\ n=1, ..., \nu_\beta. \tag{3.62}$$

Finally, we multiply (3.59) by $\mathcal{E}(-i)^l\exp[ikr]$ on the right and let r tend to infinity. Reference to (1.24) shows that

$$(-i)^l\exp[ikr]F^T(-k)F(k, r)\mathcal{E} \xrightarrow[r\to\infty]{} F^T(-k)\,.$$

Use of the asymptotic forms, (3.60), and transposition then yield

$$F(k) = \mathbf{1} + i \sum_{(\beta)} (k - i\beta)^{-1} a_\beta^{(0)} . \tag{3.63}$$

In order to show that we have actually closed the circle, i.e., that (3.63) is the $F(k)$ from which we started, we observe that the $F(k)$ corresponding to (3.1) and (1.11) can be written

$$F(k) = \mathbf{1} + i \sum_{(\beta)} (k - i\beta)^{-1} a_\beta \tag{3.64}$$

because of (1.4). Equation (3.1) further implies that

$$F(i\alpha_j) = 0 , \qquad j = 1, ..., \nu_\alpha . \tag{3.65}$$

The matrices a_β must therefore satisfy

$$\mathbf{1} - \sum_{(\beta)} (\beta - \alpha)^{-1} a_\beta = 0 , \qquad \alpha = \alpha_j ,\ j = 1, ..., \nu_\beta . \tag{3.66}$$

Since, moreover, necessarily [26]

$$\text{range } T(-\beta_n^2) \equiv \text{kernel residue } T^{-1}(-\beta_n^2) ,$$

it follows from (1.11) that

$$\text{kernel residue } F^T(i\beta_n) \equiv \text{range } T(-\beta_n^2) ,$$

and hence by (3.5),

$$\gamma^{(\beta)} a_\beta^T = 0 , \qquad \beta = \beta_n ,\ n = 1, ..., \nu_\beta . \tag{3.67}$$

The $4\nu_\beta$ equations (3.66) and (3.67) must determine the $4\nu_\beta$ elements of a_n, $n = 1, ..., \nu_\beta$, uniquely. Otherwise there would be two functions, $F_1(k)$ and $F_2(k)$, with the same zeros, poles, and kernels:

$$F_1(k) = \mathbf{1} + i \sum_{(\beta)} (k - i\beta)^{-1} a_\beta^{(1)} , \qquad F_2(k) = \mathbf{1} + i \sum_{(\beta)} (k - i\beta)^{-1} a_\beta^{(2)} .$$

The difference

$$\Delta F(k) \equiv F_1(k) - F_2(k) = i \sum_{(\beta)} (k - i\beta)^{-1} (a_\beta^{(1)} - a_\beta^{(2)})$$

[26] Because of the simplicity of the zeros of $\det T$; see Ref. [2], Appendix A.

can then have its poles removed by multiplication with ν_α factors of the form

$$P_j(k - i\beta_{1j}) + (\mathbf{1} - P_j)(k - i\beta_{2j}) .$$

The remainder is a matrix all of whose elements are polynomials which vanish at the ν_α points α_i and at infinity are $O(k^{\nu_\alpha - 1})$; hence it must vanish. The difference ΔF is therefore naught and equations (3.66) and (3.67) determine the a's uniquely.

It follows from a comparison of (3.61) and (3.62) with (3.66) and (3.67) that the limit (3.60) exists and

$$a_\beta^{(0)} = a_\beta , \qquad \beta = \beta_n ,\ n = 1, ..., \nu_\beta . \tag{3.68}$$

Thus (3.63) is the same $F(k)$ we started with.

Solutions of the Gel'fand Levitan equation for functions $F(k)$ with various special properties of some interest in computations are given in Appendix A.

4. – Solutions in the General Case with Bound States.

The methods used in Section 3 to obtain solutions to the Gel'fand Levitan equation, with the potential and the wave function as final results, can be followed in this section with small modifications. Only a comparatively brief outline of the present derivation will be given therefore.

If there are m bound states, $F(k)$ will depend on the m binding energies. This dependence can be explicitly exhibited by writing, for the general case [2,3]

$$F(k) = R^{-1}(k) F_N(k) , \tag{4.1}$$

where $F_N(k)$ has poles, and $\det F_N(k)$ has zeros, only in the upper half of the complex k-plane, and $R^{-1}(k)$ is defined by

$$\begin{cases} R^{-1}(k) = R_m^{-1}(k) , \\ R_n^{-1}(k) = R_{n-1}^{-1}(k)\left[(\mathbf{1} - P_n') + P_n' \dfrac{k + i\varkappa_n}{k - i\varkappa_n}\right] , & n = 1, ..., m , \\ R_0^{-1}(k) = \mathbf{1} . \end{cases} \tag{4.2}$$

The projection P_σ' is chosen symmetric and is defined in terms of P_σ of (1.8) by the relation,

$$\text{range } P_\sigma' = \text{kernel}\,(\mathbf{1} - P_\sigma') = \text{kernel}\,[R_{\sigma-1}(-i\varkappa_\sigma)(\mathbf{1} - P_\sigma)R_{\sigma-1}^{-1}(-i\varkappa_\sigma)] . \tag{4.3}$$

F_N can be written in the form (3.64) and we shall assume that it satisfies (3.65), where all α's, β's and $\varkappa$'s are different from each other ([27]). The S-matrix then has double poles at $i\varkappa_\sigma$, and det S has double zeros at $-i\varkappa_\sigma$.

The matrix R^{-1} then introduces m additional poles at $i\varkappa_\sigma$ into $F(k)$, and m additional zeros at $-i\varkappa_\sigma$ into det $F(k)$. However, the spectral function for $E > 0$ will contain no reference to these singularities since from (1.11) one easily obtains the relation

$$T(k^2) = [F_N^T(k)F_N(-k)]^{-1} . \tag{4.4}$$

Eqs. (3.1) and (3.6) therefore follow immediately, and again contain no reference to bound states.

Since the determinants of $F^T(k)$ and $\mathcal{F}(k^2)$ have only simple zeros, ranges and kernels associated with these matrices are non-zero and we can set

$$\begin{cases} \gamma^{(\beta)} \text{ rep. range } \mathcal{F}(-\beta^2) , & \beta = \beta_n,\ n = 1, ..., \nu_\beta, \\ \gamma^{(\varkappa)} \text{ rep. kernel}[\text{res. } F^T(i\varkappa)] , & \varkappa = \varkappa_\sigma,\ \sigma = 1, ..., m, \\ \chi^{(\varkappa)} \text{ rep. kernel } F^T(-i\varkappa) , & \varkappa = \varkappa_\sigma,\ \sigma = 1, ..., m, \end{cases} \tag{4.5}$$

It is convenient to define the auxiliary quantity

$$\mathcal{C}_\varkappa \equiv (-1)^l \varkappa^{-2} Y_l^{-1}(-i\varkappa) C_\varkappa Y_l^{-1}(-i\varkappa) . \tag{4.6}$$

It follows from the definition, Eq. (1.12), of C_σ that

$$\text{kernel } \mathcal{C}_\varkappa \equiv \text{kernel}[\text{res. } F^{-1}(-i\varkappa)] . \tag{4.7}$$

The relation

$$\text{kernel } MA \equiv \text{kernel } A)M^{-1} \tag{4.8}$$

for a non-singular matrix M, leads to

$$(\text{kernel } \mathcal{C}_\varkappa)F_N^{-1}(-i\varkappa) = \text{kernel res. } R(-i\varkappa) = \text{kernel res. } R^{T\,-1}(i\varkappa) . \tag{4.9}$$

It follows that

$$(\text{kernel } \mathcal{C}_\varkappa)T(-\varkappa^2) \quad [\text{kernel res. } R^{T\ -1}(i\varkappa)]F_N^{T\ -1}(i\varkappa) \quad \text{rep. by } \gamma^{(\varkappa)}, \tag{4.9}$$

([27]) A special case of interest where m α's are equal to m $\varkappa$'s is treated in Appendix A.

or

$$\gamma^{(\varkappa)} T^{-1}(-\varkappa^2) \text{ rep. kernel } \mathcal{C}_\varkappa . \tag{4.10}$$

Since $\mathcal{C}_\varkappa$ is symmetric ([28])

$$\text{range } \mathcal{C}_\varkappa \equiv \text{o.c. kernel } \mathcal{C}_\varkappa .$$

However, by (4.7) ([29])

$$\text{o.c. kernel } \mathcal{C}_\varkappa \equiv \text{kernel } F^T(-i\varkappa) . \tag{4.11}$$

Therefore it follows that

$$\chi^{(\varkappa)} \text{ rep. range } \mathcal{C}_\varkappa , \tag{4,12}$$

and we can define a positive number $d_\varkappa$ by

$$\chi^{(\varkappa)} \mathcal{C}_\varkappa = d_\varkappa \chi^{(\varkappa)} . \tag{4.13}$$

By taking partial fractions, we can write

$$F(k) = \mathbf{1} + i \sum_{(\beta)} (k - i\beta)^{-1} a_\beta + i \sum_{(\varkappa)} (k - i\varkappa)^{-1} b_\varkappa , \tag{4.14}$$

and Eq. (3.4) still applies.

It can be shown in a manner analogous to the discussion at the end of Section 3 that the $4\nu_\beta$ components of the a_β's and the $4m$ components of the $b_\varkappa$'s are uniquely determined by the $4\nu_\beta + 4m$ equations

$$\mathbf{1} - \sum_{(\beta)} (\beta - \alpha)^{-1} a_\beta - \sum_{(\varkappa)} (\varkappa - \alpha)^{-1} b_\varkappa = 0 , \quad \alpha = \alpha_j , \ j = 1, \ldots, \nu_{\alpha_j} \tag{4.15}$$

$$\chi^{(\varkappa)} \mathbf{1} [- \sum_{(\beta)} (\beta + \varkappa)^{-1} a_\beta^T - \sum_{(\varkappa')} (\varkappa' + \varkappa)^{-1} b_{\varkappa'}^T] = 0 , \ \varkappa = \varkappa_\sigma , \ \sigma = 1, \ldots, m \tag{4.16}$$

$$\gamma^{(\beta)} a_\beta^T = 0 , \qquad \beta = \beta_n , \ n = 1, \ldots, \nu_{\beta_n} \tag{4.17}$$

and

$$\gamma^{(\varkappa)} b_\varkappa^T = 0 , \qquad \varkappa = \varkappa_\sigma , \ \sigma = 1, \ldots, m . \tag{4.18}$$

These equations are the analogues of (3.66) and (3.67).

([28]) The symbol « o.c. » signifies orthogonal complement, i.e., $A \equiv$ o.c. B if A is the largest subspace such that for all vectors a in A and all vectors b in the subspace B, $a \cdot b = 0$. It is a general theorem that range $M \equiv$ o.c. kernel $M^\dagger$.

([29]) It can be shown (see for example Appendix A of Ref. ([2])) that range $F(-i\varkappa) =$ $=$ kernel res. $F^{-1}(-i\varkappa)$.

The kernel of the Gel'fand Levitan equation for the present case is modified by the bound state spectrum:

$$\mathcal{G}(s, r) = \mathrm{G}(s, r) + Q(s, r) . \tag{4.19}$$

$\mathrm{G}(s, r)$ is the function defined in Eq. (3.7), and

$$Q(s, r) = \sum_{(\varkappa)} Q_\varkappa(s, r) , \tag{4.20}$$

with

$$Q_\varkappa(s, r) = G_0^T(-i\varkappa, s) C_\varkappa G_0(-i\varkappa, r) . \tag{4.21}$$

Alternative forms of $Q_\varkappa$ are given by

$$\left\{ \begin{aligned} Q_\varkappa(s, r) &= \mathrm{V}_\varkappa(s) \mathcal{C}_\varkappa \mathrm{V}_\varkappa(r) \\ &= \varkappa^{-2} \mathcal{D}_s \mathcal{C}_\varkappa \mathcal{D}_r V_\varkappa^{l+1}(s) V_\varkappa^{l+1}(r) . \end{aligned} \right. \tag{4.22}$$

$Q_\varkappa$ is not a singular function like G_α. In fact, it satisfies the homogeneous equation,

$$(D_s^{l+1} - \varkappa^2) \Theta_s Q_\varkappa(s, r) = 0 . \tag{4.23}$$

After an integration by parts, we obtain the equation involving $Q_\varkappa$ which corresponds to (3.18):

$$\begin{aligned} \Omega_\varkappa(s, r) \equiv \Theta_s \int_0^r \mathrm{d}t Q_\varkappa(s, t) K(t, r) = \\ = - \mathcal{C}_\varkappa V_\varkappa^{l+1}(s) \left[\int_0^r V_\varkappa^{l+1}(t) \mathcal{K}(t, r) \, \mathrm{d}t - \mathcal{E} V_\varkappa^{l+1}(r) K(r, r) \right] . \end{aligned} \tag{4.24}$$

If we now apply the operator Θ_s to the left of the Gel'fand Levitan equation, then we obtain for $r > s$

$$\begin{aligned} \mathcal{K}(s, r) + \sum_{(\alpha)} M_\alpha V_\alpha^{l+1}(s) \mathrm{U}_\alpha(r) + \sum_{(\varkappa)} \varkappa \mathcal{C}_\varkappa V_\varkappa^{l+1}(s) \mathrm{V}_\varkappa(r) + \\ + \sum_{(\alpha)} \Gamma_\alpha(s, r) + \sum_{(\varkappa)} \Omega_\varkappa(s, r) = 0 . \end{aligned} \tag{4.25}$$

Operation on the left of Eq. (4.25) with $\prod_{(\varkappa)} (\varkappa^2 - D_s^{l+1}) \prod_{(\alpha)} (\varkappa^2 - D_s^{l+1})$ and

use of (3.11), (3.18), (4.23) and (4.24) leads to

$$\prod_{(\varkappa)}(\varkappa^2 - D_s^{l+1})\mathcal{F}(-D_s^{l+1})\mathcal{K}(s, r) = 0\,. \tag{4.26}$$

$\mathcal{K}(s, r)$ is therefore of the form

$$\mathcal{K}(s, r) = \sum_{(\beta)} \beta V_\beta^{l+1}(s)\mathcal{K}_\beta(r) + \sum_{(\varkappa)} \varkappa V_\varkappa^{l+1}(s)\mathcal{K}_\varkappa(r)\,, \tag{4.27}$$

and the $\mathcal{K}_\beta(r)$ satisfy the equations

$$\gamma^{(\beta)}\mathcal{K}_\beta(r) = 0\,, \qquad \beta = \beta_n,\ n = 1, ..., \nu_\beta. \tag{4.28}$$

We resubstituite (4.27) in (4.25), use the methods of Section 3, and note that all the functions $V_\alpha^{l+1}(s)$ and $V_\varkappa^{l+1}(s)$ are linearly independent. We also require the integral

$$z_{\varkappa\gamma}^l(r) \equiv \int_0^r V_\varkappa^l(t)V_\gamma^l(t) = (\varkappa^2 - \gamma^2)^{-1}W[V_\gamma^l(r);\ V_\varkappa^l(r)]\,. \tag{4.29}$$

The resulting equations are

$$\alpha U_{\alpha i}(r) + \sum_{(\beta)} \beta x_{\alpha\beta}^{l+1}(r)\mathcal{K}_\beta(r) + \sum_{(\varkappa)} \varkappa x_{\alpha\varkappa}^{l+1}(r)\mathcal{K}_\varkappa(r) - \mathcal{E}U_\alpha^{l+1}(r)K(r, r) = 0\,, \tag{4.30}$$

$$\alpha = \alpha_i,\ i = 1, ..., \nu_\alpha$$

and

$$\varkappa T(-\varkappa^2)\mathcal{K}_\varkappa(r) + \mathcal{C}_\varkappa\Big\{\varkappa V_{\varkappa i}(r) - \sum_{(\beta)} \beta z_{\varkappa\beta}^{l+1}(r)\mathcal{K}_\beta(r) - \tag{4.31}$$

$$- \sum_{(\varkappa')} \varkappa' z_{\varkappa\varkappa'}^{l+1}(r)\mathcal{K}_{\varkappa'}(r) + \mathcal{E}V_\varkappa^{l+1}(r)K(r, r)\Big\} = 0\,, \qquad \varkappa = \varkappa_\sigma,\ \sigma = 1, ..., m.$$

When $\varkappa' = \varkappa$, the appropriate limiting process must be carried out to obtain $z_{\varkappa\varkappa}^{l+1}(r)$.

The matrix equations, (4.31), when multiplied by the vectors representing the range and kernel of $\mathcal{C}_\varkappa$, can be rewritten as two sets of vector equations

$$\gamma^{(\varkappa)}\mathcal{K}_\varkappa(r) = 0\,, \qquad \varkappa = \varkappa_\sigma,\ \sigma = 1, ..., m, \tag{4.32}$$

and

$$\chi^{(\varkappa)}[\varkappa V_{\varkappa i}(r) + \varkappa d_\varkappa^{-1}T(-\varkappa^2)\mathcal{K}_\varkappa(r) - \sum_{(\beta)} \beta z_{\varkappa\beta}^{l+1}(r)\mathcal{K}_\beta(r) - \tag{4.33}$$

$$- \sum_{(\varkappa')} \varkappa' z_{\varkappa\varkappa'}^{l+1}(r)\mathcal{K}_{\varkappa'}(r) + \mathcal{E}V_\varkappa^{l+1}(r)K(r, r)] = 0\,, \qquad \varkappa = \varkappa_\sigma,\ \sigma = 1, ..., m.$$

The analysis of Section 3 can now be followed in detail. The terms of order s^{l+1} are obtained as previously. We finally obtain (3.40), (3.42) through (3.46), but the indices of summation now run over all the β's and the $\varkappa$'s. We illustrate with the analogue of (3.42):

$$(3.42a) \qquad \sum_{(\beta)} \mathcal{Q}_{\alpha\beta}(r)\mathcal{K}_\beta(r) + \sum_{(\varkappa)} Y_{\alpha\varkappa}(r)\mathcal{K}_\varkappa(r) = -\mathcal{U}_\alpha(r), \qquad \alpha = \alpha_i,\ i = 1, \ldots, \nu_\alpha.$$

To complete our list of equations of type (3.42) through (3.46) we require the identities

$$(4.34) \qquad \beta z_{\varkappa\beta}^{l+1} - \varepsilon V_\varkappa^{l+1}\mathrm{V}_\beta = -\varkappa \begin{pmatrix} z_{\varkappa\beta}^{l} & 0 \\ 0 & z_{\varkappa\beta}^{l+2} \end{pmatrix} \equiv -\varkappa Z_{\varkappa\beta},$$

and

$$(4.35) \qquad (\varkappa\beta r)^{-1}(2l+3)V_\varkappa^{l+1}V_\beta^{l+1} = z_{\varkappa\beta}^{l} - z_{\varkappa\beta}^{l+2}.$$

The set of equations in addition to those of Section 3 are obtained from (4.33) and are

$$(4.36) \qquad \chi^{(\varkappa)}\Big[\sum_{(\beta)} \mathcal{Z}_{\varkappa\beta}(r)\mathcal{K}_\beta(r) + \sum_{(\varkappa')} (\mathcal{Z}_{\varkappa'\varkappa}(r) + \Delta_{\varkappa'\varkappa})\mathcal{K}_{\varkappa'}(r) + \mathcal{U}_\varkappa^{(1)}(r)\Big] = 0,$$

$$\varkappa = \varkappa_\sigma, \quad \sigma = 1, \ldots, m,$$

where

$$(4.37) \qquad \mathcal{Z}_{\varkappa\gamma}(r) \equiv Z_{\varkappa\gamma}(r) + (z_{\varkappa\gamma}^{l}(r) - z_{\varkappa\gamma}^{l+2})N,$$

$$(4.38) \qquad \Delta_{\varkappa\varkappa'} \equiv \delta_{\varkappa\varkappa'} d_\varkappa^{-1} T(-\varkappa^2),$$

and

$$(4.39) \qquad \mathcal{U}_\varkappa^{(1)}(r) \equiv \mathrm{V}_\varkappa(r) - (V_\varkappa^{l}(r) - V_\varkappa^{l+2}(r))N.$$

Equation (3.47) is also still applicable.

The « super » matrix $\mathfrak{M}$ becomes

$$(4.40) \qquad \mathfrak{M}(r) = \left(\begin{array}{c|c} \mathcal{Q}_{\alpha\beta} & \mathcal{Q}_{\alpha\varkappa'} \\ \hline \chi^{(\varkappa)}\mathcal{Z}_{\varkappa\beta} & \chi^{\varkappa}(\mathcal{Z}_{\varkappa\varkappa'} + \Delta_{\varkappa\varkappa'}) \\ \hline \begin{matrix} \gamma_1^{(\beta 1)}\gamma_2^{(\beta 1)} & 0 & 0 \\ 0 & 0 & \ddots \end{matrix} & 0 \\ \hline 0 & \begin{matrix} \gamma_1^{(\varkappa 1)}\gamma_2^{(\varkappa 1)} & 0 & 0 \\ 0 & 0 & \ddots \end{matrix} \end{array}\right).$$

$\mathfrak{M}$ is a $(\nu_\beta + m)\times(\nu_\beta + m)$ « super » matrix. $\mathfrak{N}$ is a « super » column vector of $\nu_\beta + m$ components and the new $\mathfrak{U}$ has its first ν_α components equal to the

(2×2)-matrices $\mathcal{U}_\alpha$, the next m components to *row vectors* $\chi^{(\varkappa)}\mathcal{U}_\varkappa^{(1)}$, and has null (2×2)-matrices for the remaining components.

If one observes that in the asymptotic limit (4.36) becomes

$$\chi^{(\varkappa)}[\sum_{(\beta)} Z_{\varkappa\beta}^{(\infty)}\mathcal{K}_\beta^{(\infty)} + \sum_{(\varkappa')} Z_{\varkappa\varkappa'}^{(\infty)}\mathcal{K}_{\varkappa'}^{(\infty)}] = 0\,,$$

and if one goes through an analysis similar to that at the end of Section 3, one obtains the starting equations (4.15) through (4.18) and the solution can once again be « taken around in a circle ».

5. – Illustrations.

5·1. *S-Matrices Diagonalizable by Transformations Independent of k.* – In order to illustrate the general approach developed in the preceding pages, we consider, for the case of no bound states, and S-matrix which is a rational function of k, and which is diagonalizable by the real orthogonal transformation T, where

$$T = \begin{pmatrix} u & v \\ -v & u \end{pmatrix}, \qquad u^2 + v^2 = 1, \tag{5.1}$$

and u and v are independent of k. For the type of S-matrix under consideration, F can be simply written as

$$F(k) = Tf(k)T^T\,, \tag{5.2}$$

where

$$f(k) = \prod_{j=1}^{\nu}(k - i\alpha_j)\begin{pmatrix} (k-i\beta_j)^{-1} & 0 \\ 0 & (k-i\lambda_j)^{-1} \end{pmatrix}. \tag{5.3}$$

The present example is of mathematical interest only, since for the physically acceptable solutions $v \sim 0(k^2)$ in the vicinity of the origin ([30]).

If we define the symmetric projection $\mathcal{P}$,

$$\mathcal{P} \equiv TPT^T = \begin{pmatrix} v^2 & uv \\ uv & v^2 \end{pmatrix}, \tag{5.4}$$

where P is defined in Eq. (1.10), and the function

$$D_\eta^{(n)}(x) \equiv \prod_j (x - \eta_j^n)\,, \tag{5.5}$$

([30]) J. M. Blatt and V. F. Weisskopf: *Theoretical Nuclear Physics* (New York, 1952), p. 112.

then Eq. (3.64) can be written in the form

$$F(k) = \mathbf{1} + i \sum_{(\beta)} (k - i\beta)^{-1} a_\beta + i \sum_{(\lambda)} (k - i\lambda)^{-1} a_\lambda \,. \tag{5.6}$$

The a's have the simple form

$$a_\beta = (D_\alpha^{(1)}(\beta)/D_\beta^{(1)'}(\beta))(\mathbf{1} - \mathcal{P}) \,, \tag{5.7}$$

and

$$a_\lambda = (D_\alpha^{(1)}(\lambda)/D_\lambda^{(1)'}(\lambda))\mathcal{P} \,, \tag{5.8}$$

where

$$D_\beta^{(1)'}(\beta_j) \equiv \lim_{\eta \to \beta_j} (\eta - \beta_j)^{-1} D_\beta^{(1)}(\eta) \,. \tag{5.5a}$$

The matrix $\mathcal{F}(k^2)$, defined in Eq. (3.1) has the simple explicit form

$$\mathcal{F}(k^2) = \prod_j [(\mathbf{1} - \mathcal{P})(k^2 + \beta_j^2) + \mathcal{P}(k^2 + \lambda_j^2)] \,, \tag{5.9}$$

and the M_α of Eq. (3.6) are

$$M_\alpha = -[D_\alpha^{(2)'}(\alpha^2)]^{-1} [(\mathbf{1} - \mathcal{P}) D_\beta^{(2)}(\alpha^2) + \mathcal{P} D_\lambda^{(2)}(\alpha^2)] \,. \tag{5.10}$$

Finally, the range of $\mathcal{F}(-\beta_j^2)$ is represented by the same vector $\gamma^{(\beta)}$ for all j, and the range of $\mathcal{F}(-\lambda_j^2)$ by the vector $\gamma^{(\lambda)}$. The two vectors are

$$\gamma^{(\beta)} = (u, -v) \,, \tag{5.11}$$

and

$$\gamma^{(\lambda)} = (v, u) \,. \tag{5.12}$$

5·2. *An Explicit Solution.* – Consider the case of the sub-matrix S which refers to angular momenta zero and two, depends on two arbitrary parameters, and is diagonalizable by a constant matrix. We assume further that there are no bound states, and choose the model

$$F(k) = Tf(k)T^T \,, \qquad S(k) = Ts(k)T^T \,, \tag{5.13}$$

where

$$T = \sqrt{\frac{1}{2}} \begin{pmatrix} 1 & 1 \\ -1 & 1 \end{pmatrix} \,, \tag{5.14}$$

and

$$f(k) = \begin{pmatrix} \dfrac{k - i\alpha}{k - i\beta} & 0 \\ 0 & 1 \end{pmatrix}, \qquad s(k) = \begin{pmatrix} \dfrac{k - i\alpha}{k + i\alpha}\dfrac{k + i\beta}{k - i\beta} & 0 \\ 0 & 1 \end{pmatrix}. \tag{5.15}$$

This is a more special case than that treated in Section 3, and corresponds to some of the α's and β's being equal. Though a case of this type is further discussed in Appendix A, in the present particularly simple example explicit solutions may be obtained directly quite rapidly. We make no claim of physical significance for the present case, but merely cite it to illustrate the general features of a typical solution.

The solution of the Gel'fand Levitan equation is

$$K(s, r) = \mathrm{V}_\beta(s)\mathcal{K}_\beta(r) + s(\mathbf{1} - P)A(r)\,, \tag{5.16}$$

where

$$\mathcal{K}_\beta = \begin{pmatrix} \mathcal{K}_1 & \mathcal{K}_2 \\ -\mathcal{K}_1 & -\mathcal{K}_2 \end{pmatrix}, \tag{5.17}$$

and

$$A = -r^{-1}N[(3/r) - (V^0_\beta(r) - V^2_\beta(r))\mathcal{K}_\beta]\,, \tag{5.18}$$

$$N = \frac{\alpha^2 - \beta^2}{\alpha^2 + \beta^2}\begin{pmatrix} 0 & 1 \\ 0 & 0 \end{pmatrix} \equiv \Gamma\begin{pmatrix} 0 & 1 \\ 0 & 0 \end{pmatrix}. \tag{5.19}$$

If we define

$$Y(r) \equiv 2(\alpha^2 + \beta^2)^{-1}(\beta^2 x^0_{\alpha\beta}(r) + \alpha^2 x^2_{\alpha\beta}(r))\,, \tag{5.20}$$

then we obtain

$$\mathcal{K}_1(r) = -Y(r)^{-1}U^0_\alpha(r)\,, \tag{5.21}$$

and

$$\mathcal{K}_2(r) = -Y(r)^{-1}[U^2_\alpha(r) - \Gamma(U^0_\alpha(r) - U^2_\alpha(r))]\,. \tag{5.22}$$

The result for the potential which gives rise to the S-matrix (5.13) is

$$V(r) = -2\frac{\mathrm{d}}{\mathrm{d}r}\left\{\frac{1}{Y(r)}\left[\frac{2}{\alpha^2 + \beta^2}\begin{pmatrix} \beta^2 V^0_\beta(r)U^0_\alpha(r) & 0 \\ 0 & \alpha^2 V^2_\beta(r)U^2_\alpha(r) \end{pmatrix} + \right.\right. \tag{5.23}$$

$$\left.\left. + V^2_\beta(r)U^0_\alpha(r)\begin{pmatrix} \Gamma & 1 \\ 1 & -\Gamma \end{pmatrix}\right]\right\}.$$

The asymptotic behavior of this potential is

$$V(r) \sim \frac{3}{r^2}\frac{\alpha-\beta}{\alpha^2+\beta^2}\begin{pmatrix}\alpha-\beta & \alpha+\beta\\ \alpha+\beta & \beta-\alpha\end{pmatrix}. \tag{5.24}$$

Finally, we contrast the above results with the two parameter scalar case, where

$$T = \mathbf{1}, \tag{5.25}$$

and

$$F(k) = f(k) = \frac{k-i\alpha}{k-i\beta}\mathbf{1}. \tag{5.26}$$

For this example

$$\mathcal{K} = \begin{pmatrix}\mathcal{K}_1 & 0\\ 0 & \mathcal{K}_2\end{pmatrix}, \tag{5.27}$$

$$\mathcal{K}_1(r) = -(x^0_{\alpha\beta}(r))^{-1}U^0_\alpha(r), \tag{5.28}$$

$$\mathcal{K}_2(r) = -(x^2_{\alpha\beta}(r))^{-1}U^2_\alpha(r), \tag{5.29}$$

and

$$\Gamma = 0.$$

We obtain the potential

$$V(r) = -2\frac{\mathrm{d}}{\mathrm{d}r}\begin{pmatrix}(x^0_{\alpha\beta}(r))^{-1}V^0_\beta(r)U^0_\alpha(r) & 0\\ 0 & (x^2_{\alpha\beta}(r))^{-1}V^2_\beta(r)U^2_\alpha(r)\end{pmatrix}, \tag{5.30}$$

which asymptotically approaches

$$V(r) \sim 8\beta^2\frac{\alpha-\beta}{\alpha+\beta}\begin{pmatrix}\exp[-2\beta r] & 0\\ 0 & (\tfrac{3}{2})(\alpha+\beta)\alpha^{-1}(\beta r)^{-3}\end{pmatrix}. \tag{5.31}$$

If we wish to obtain potentials of shorter range than those obtained in the above two examples, we have to use more parameters than were presently employed. The details of the solutions are somewhat more tedious, but results are of the same general type as listed above.

* * *

We are indebted to Prof. Res Jost for helpful discussions and to Prof. V. Bargmann for the use of his unpublished manuscript on the solution of the Gel'fan Levitan equation for scalar potentials. We should further like to thank the Institute for Advanced Study for its hospitality.

Appendix A

Solution of the Gel'Fand Levitan Equation for Special Cases.

a) *Not All Zeros of* $\det F(k)$ *make* $F(k) = 0$. – This example represents the case of no bound states where for some i and j

$$\beta_i = \alpha_j \,. \tag{A.1}$$

The β_i's will no longer appear. We call α's of type (A.1) λ_j, and assume further that none of the α's, λ's and the remaining β's are equal. The analogue of (3.1) is

$$\mathcal{F}(k^2) = \prod_{(\alpha)} (k^2 + \alpha^2) \prod_{(\lambda)} (k^2 + \lambda^2)\, T(k^2). \tag{A.2}$$

Eq. (A.2) defines a polynomial matrix, the determinant of which has simple zeros at $-\beta_n^2$ and $-\lambda_j^2$.

We define the vectors

$$\gamma^{(\beta)} \text{ rep. range } \mathcal{F}(-\beta^2)\,, \qquad \beta = \beta_n,\ n = 1, \ldots, \nu_\beta, \tag{A.3}$$

$$\chi^{(\lambda)} \text{ rep. range } \mathcal{F}(-\lambda^2)\,, \qquad \lambda = \lambda_j,\ j = 1, \ldots, \nu_\lambda, \tag{A.4}$$

and observe that

$$\text{range } \mathcal{F}(-\lambda^2) \equiv \text{range res. } T(-\lambda^2) \equiv \text{kernel } F^T(i\lambda)\,. \tag{A.5}$$

Equation (3.64) is still correct in the present case, but the a_β's satisfy the set of equations

$$\mathbf{1} - \sum_{(\beta)} (\beta - \alpha)^{-1} a_\beta = 0\,, \qquad \alpha = \alpha_i,\ i = 1, \ldots, \nu_\alpha, \tag{A.6}$$

$$\chi^{(\lambda)}\Big(\mathbf{1} - \sum_{(\beta)} (\beta - \lambda)^{-1} a_\beta^T\Big) = 0\,, \qquad \lambda = \lambda_j,\ j = 1, \ldots, \nu_\lambda, \tag{A.7}$$

and

$$\gamma^{(\beta)} a_\beta^T = 0\,, \qquad \beta = \beta_n,\ n = 1, \ldots, \nu_\beta, \tag{A.8}$$

where

$$\nu_\beta = 2\nu_\alpha + \nu_\lambda\,. \tag{A.9}$$

Eqs. (A.6)–(A.8) define the a_β's uniquely. The derivation of Section 3 is followed in most details. Only a few salient differences need therefore be

pointed out. The partial fractions form of $T(k^2)$ is

$$T(k^2) = \mathbf{1} + \sum_{(\alpha)} (k^2+\alpha^2)^{-1} M_\alpha + \sum_{(\lambda)} (k^2+\lambda^2)^{-1} S_\lambda \,. \tag{A.10}$$

The S_λ are singular matrices. As we proceed with the solution, we obtain Eq. (3.21) (with the new $\mathcal{F}$'s appearing in it), so that

$$\mathcal{K}(s,r) = \sum_{(\beta)} \beta V_\beta^{l+1}(s)\mathcal{K}_\beta(r) + \sum_{(\lambda)} \lambda V_\lambda^{l+1}(s)\mathcal{K}_\lambda(r) \,, \tag{A.11}$$

and

$$\gamma^{(\beta)}\mathcal{K}_\beta(r) = 0 \,, \qquad \beta = \beta_n,\ n = 1, \ldots, \nu_\beta, \tag{A.12}$$

$$\chi^{(\lambda)}\mathcal{K}_\lambda(r) = 0 \,, \qquad \lambda = \lambda_j,\ j = 1, \ldots, \nu_\lambda. \tag{A.13}$$

Next we prove that the $\mathcal{K}_\lambda$'s vanish. Resubstitution of (A.11) in the analogue of (3.20) and the usual arguments of linear independence lead to the analogue of (3.29), and the further equation

$$\lambda S_\lambda \mathrm{U}_\lambda(r) + \Psi_\lambda \mathcal{K}_\lambda(r) + \sum_{(\lambda \neq \lambda')} \lambda' x_{\lambda\lambda'}^{l+1}(r) S_\lambda \mathcal{K}_{\lambda'}(r) + \sum_{(\beta)} \beta x_{\lambda\beta}^{l+1}(r) S_\lambda \mathcal{K}_\beta(r) - \\ - S_\lambda U_\lambda^{l+1}(r) K(r,r) = 0 \,, \qquad \lambda = \lambda_j,\ j = 1, \ldots \nu_\lambda, \tag{A.14}$$

where

$$\Psi_\lambda \equiv \lim_{k^2 \to -\lambda^2} \lambda^2 [T(k^2) - (k^2+\lambda^2)^{-1} S_\lambda] \,. \tag{A.15}$$

We define a vector $\eta^{(\lambda)}$ so that $\eta^{(\lambda)}\chi^{(\lambda)T} = 0$. Then, because of (A.4) and the symmetry of $\mathcal{F}(k^2)$

$$\eta^{(\lambda)} \text{ rep. kernel } \mathcal{F}(-\lambda^2) \equiv \text{kernel res. } T(-\lambda^2) \,.$$

Multiplication of (A.14) by $\eta^{(\lambda)}$ on the left yields,

$$\eta^{(\lambda)}\Psi_\lambda \mathcal{K}_\lambda(r) = 0 \,, \qquad \lambda = \lambda_j,\ j = 1, \ldots, \nu_\lambda. \tag{A.16}$$

Since $\beta_n \neq \lambda_j$, the inverse of $T(k^2)$ exists at $k^2 = -\lambda^2$, and we can write

$$T(k^2) = T_1(k^2) + S_\lambda (k^2+\lambda^2)^{-1} \,, \qquad T_1(-\lambda^2) = \lambda^{-2}\Psi_\lambda \,, \tag{A.15a}$$

$$T^{-1}(k^2) = R_\lambda + L(k^2)(k^2+\lambda^2) \,. \tag{A.17}$$

We must have

$$S_\lambda R_\lambda = 0 \,, \tag{A.18}$$

$$\lambda^{-2}\Psi_\lambda R_\lambda + S_\lambda L(-\lambda^2) = \mathbf{1} \,. \tag{A.18a}$$

If we multiply (A.18a) by $\eta^{(\lambda)}$ on the left and use (A.18), we obtain

$$\eta^{(\lambda)} = \lambda^{-2}\eta^{(\lambda)}\Psi_\lambda R_\lambda \neq 0 \,. \tag{A.19}$$

Equation (A.18) shows that

$$\chi^{(\lambda)}R_\lambda = 0 \,. \tag{A.20}$$

It follows that $\chi^{(\lambda)}$ and $\eta^{(\lambda)}\Psi_\lambda$ are linearly independent. Equations (A.13) and (A.16) together therefore imply

$$\mathcal{K}_\lambda(r) = 0 \,, \qquad \lambda = \lambda_j,\ j = 1, \ldots, \nu_\lambda .$$

Eq. (A.14) can be reduced to a set of vector equations on multiplication by $\chi^{(\lambda)}$:

$$\chi^{(\lambda)}[\lambda U_\lambda(r) + \sum_{(\beta)} \beta x_{\lambda\beta}^{l+1}(r)\mathcal{K}_\beta(r) - U_\lambda^{l+1}(r)\mathcal{E}K(r, r)] = 0 \,.$$

The final results are now obtained quite straightforwardly, and we obtain again (3.40) and (3.42) through (3.46). We have the additional set of equations for the λ's,

$$\chi^{(\lambda)}[\sum_{(\beta)} \mathcal{Q}_{\lambda\beta}(r)\mathcal{K}_\beta(r) + \mathcal{U}_\lambda(r)] = 0 \,, \qquad \lambda = \lambda_j,\ j = 1, \ldots, \nu_\lambda . \tag{A.22}$$

Eq. (3.47) is applicable. The « super » matrix $\mathfrak{M}$ becomes

$$\mathfrak{M}(r) = \begin{pmatrix} & \mathcal{Q}_{\alpha\beta} & & \\ & \chi^{(\lambda)}\mathcal{Q}_{\lambda\beta} & & \\ \gamma_1^{(\beta_1)} & \gamma_2^{(\beta_1)} & 0 & 0 \\ 0 & 0 & & \ddots \end{pmatrix} . \tag{A.23}$$

The « super » vector $\mathfrak{U}$ has components $\mathcal{U}_\alpha$, $\chi^{(\lambda)}\mathcal{U}_\lambda$, and for the remaining components (2×2) null matrices.

b) *$F(k)$ has Multiple Zeros or Poles.* – We again restrict ourselves to the case of no bound states. We will treat only two examples of the large number of special cases which can arise under this category.

Consider first the case when all components of the S-matrix have poles simultaneously at m $i\eta$'s. The remaining poles we still call β, and also split the α's arbitrarily into two groups, α and λ, so that $F(k)$ and $T(k^2)$ can be written as, respectively,

$$F(k) = \prod_1^m \left(\frac{k - i\lambda_j}{k - i\eta_j}\right)\left[\mathbf{1} + i\sum_{(\beta)} \frac{a_\beta}{k - i\beta}\right], \tag{A.24}$$

and

$$T(k^2) = \prod_1^m \frac{k^2+\eta_j^2}{k^2+\lambda_j^2}\left[\mathbf{1} + \sum_{(\alpha)} \frac{M_\alpha}{k^2+\alpha^2}\right]. \tag{A.25}$$

We note that the range of $\mathcal{F}(-\eta^2)$ vanishes, since

$$T(-\eta^2) = \mathcal{F}(-\eta^2) = 0\,, \qquad \eta = \eta_j,\ j = 1, \ldots m. \tag{A.26}$$

For the β's we can still define

$$\gamma^{(\beta)} \text{ rep range } \mathcal{F}(-\beta^2) \qquad \beta = \beta_n,\ n = 1, \ldots, \nu_\beta. \tag{A.27}$$

The a_β's are defined uniquely by the equations (3.4), (3.66) and (3.67) but, of course, in the present case F has the m additional zeros λ_j and poles η_j.

The analysis of Section 3 once again follows. The index α of Equations (3.42) through (3.46) runs over all λ's and α's in the present case and the index β over all η's and β's. However, in the case treated at present, we get only

$$\gamma^{(\beta)}\mathcal{K}_\beta(r) = 0\,, \qquad \beta = \beta_n,\ n = 1, \ldots, \nu_\beta. \tag{A.28}$$

There is no similar restriction on the $\mathcal{K}_\eta(r)$.

Next we treat the case when two of the α's, say α_1 and α_2, coincide. This can be done by letting α_1 approach α_2 directly in the inversion of (3.47):

$$\mathfrak{K} = -\mathfrak{M}^{-1}\mathfrak{U}\,. \tag{A.29}$$

Now, if in a matrix A the first row, a function of x, approaches the second as $x \to x_0$ and at the same time the first component of the vector a approaches the second, then by L'Hospital's rule (we consider all other rows resp. components, independent of x) gives,

$$\lim_{x\to x_0} \sum_j (A^{-1})_{ji} a_j = \lim_{x\to x_0} (\det A)^{-1} \sum_j (\!(A)\!)_{ji} a_j = \\ = \lim_{x\to x_0} [(\det A)']^{-1} \left[\sum_{j\neq 1} (\!(A)\!)'_{ji} a_j + (\!(A)\!)_{1i} a'_1\right],$$

where $(\!(A)\!)_{ij}$ is the cofactor of A_{ij}. The result is equivalent to replacing the first row of A and the first element of a by their derivatives with respect to x.

The situation in (A.29) is precisely the same, with two rows of $\mathfrak{M}$ and two components of $\mathfrak{U}$ approaching two others. Letting α_0 coincide with another α therefore results in the replacement

$$\mathcal{Y}_{\alpha_0\beta} \to \frac{\partial}{\partial\alpha_0}\mathcal{Y}_{\alpha_0\beta}\,,$$

$$\mathcal{U}_{\alpha_0} \to \frac{\partial}{\partial\alpha_0}\mathcal{U}_{\alpha_0}\,.$$

Everything else is left unchanged.

c) *The Case for Which S has Simple Poles, and* det *S Simple Zeros at the Bound States.* – R^{-1} is given for this case by:

$$\text{(A.30)} \qquad \begin{cases} R^{-1} = R_m^{-1}\,, \\ R_n^{-1}(k) = R_{n-1}^{-1}(k)\left[(\mathbf{1} - P_n') + P_n' \dfrac{k + i\varkappa_n}{k - i\varkappa_n}\right], & n = 1, \ldots, m, \\ R_0^{-1}(k) = \mathbf{1}\,. \end{cases}$$

All the parameters $\varkappa$, λ, α and β are assumed to be different. Eqs. (4.1) and (4.3) still hold. $R^{-1}(k)$ introduces additional poles into F at $i\lambda_\sigma$ and additional zeros into det F at $-i\varkappa_\sigma$. The function T is given by

$$\text{(A.31)} \qquad T(k^2) = [F_N^T(k) R^{T\,-1}(k) R^{-1}(-k) F_N(-k)]^{-1}\,,$$

and is a function of the $\varkappa$'s. $\mathcal{F}(k^2)$ is defined in a manner analogous to (A.2) as

$$\mathcal{F}(k^2) = \prod_{(\varkappa)} (k^2 + \varkappa^2) \prod_{(\alpha)} (k^2 + \alpha^2)\, T(k^2)\,.$$

$F(k)$ has the familiar form

$$\text{(A.32)} \qquad F(k) = \mathbf{1} + i \sum_{(\beta)} (k - i\beta)^{-1} a_\beta + i \sum_{(\lambda)} (k - i\lambda)^{-1} a_\lambda\,.$$

If one defines the vectors

$$\text{(A.33)} \qquad \begin{cases} \gamma^{(\beta)} \text{ rep. range } \mathcal{F}(-\beta^2)\,, \\ \gamma^{(\lambda)} \text{ rep. range } \mathcal{F}(-\lambda^2)\,, \\ \chi^{(\varkappa)} \text{ rep. range } \mathcal{F}(-\varkappa^2)\,, \end{cases}$$

and observes the relation

$$\text{(A.34)} \qquad \text{range } \mathcal{F}(-\varkappa^2) \equiv \text{kernel } T^{-1}(-\varkappa^2) \equiv \text{kernel } F^T(-i\varkappa)\,,$$

one can show that the a_β's and a_λ's are uniquely defined by the equations

$$\text{(A.35)} \qquad \mathbf{1} - \sum_{(\beta)} (\beta - \alpha)^{-1} a_\beta \sum_{(\lambda)} (\lambda - \alpha)^{-1} a_\lambda = 0\,, \qquad \alpha = \alpha_i,\ i = 1, \ldots, \nu_\alpha,$$

$$\text{(A.36)} \qquad \chi^{(\varkappa)}\Big[\mathbf{1} - \sum_{(\beta)} (\beta + \varkappa)^{-1} a_\beta^T - \sum_{(\lambda)} (\lambda + \varkappa)^{-1} a_\lambda^T\Big] = 0\,, \qquad \varkappa = \varkappa_\sigma,\ \sigma = 1, \ldots, m,$$

$$\text{(A.37)} \qquad \gamma^{(\beta)} a_\beta^T = 0\,, \qquad \beta = \beta_n,\ n = 1, \ldots, \nu_\beta,$$

$$\text{(A.38)} \qquad \gamma^{(\lambda)} a_\lambda^T = 0\,, \qquad \lambda = \lambda_\sigma,\ \sigma = 1, \ldots, m,$$

and

$$\nu_\beta = 2\nu_\alpha\,.$$

Equations (4.6) through (4.13) are still applicable. If we define

$$\chi^{(\varkappa)} \text{ res. } T(-\varkappa^2) = n_\varkappa \chi^{(\varkappa)}, \tag{A.39}$$

where $n_\varkappa$ is a number, and use the techniques of Section 4 and Appendix (A.a), we obtain as solutions involving α's (3.40) through (3.46) with the indices of summation running over the β's and λ's but not the $\varkappa$'s. Finally, for the solutions involving $\varkappa$'s, we obtain the set of vector equations

$$\chi^{(\varkappa)}\Big\{\sum_{(\beta)}[n_\varkappa \mathcal{Q}_{\varkappa\beta}(r) + d_\varkappa \mathcal{Z}_{\varkappa\beta}(r)]\mathcal{K}_\beta(r) + \sum_{(\lambda)}[n_\varkappa \mathcal{Q}_{\varkappa\lambda}(r) + d_\varkappa \mathcal{Z}_{\varkappa\lambda}(r)]\mathcal{K}(r) +$$

$$+ n_\varkappa \mathcal{U}_\varkappa(r) + d_\varkappa \mathcal{U}_\varkappa^{\sim}(r)\Big\} = 0\,, \qquad \varkappa = \varkappa_\sigma,\ \sigma = 1, \ldots, m.$$

Appendix B

Useful Properties of Relevant Functions.

The two tables below summarize properties of functions useful in the preceding derivations.

The symbol $(2l-1)!!$ is defined as

$$(2l-1)!! = (2l-1)(2l-3)\ldots 1\,; \tag{B.1}$$
$$(2l-1)!! = 1\,, \qquad \text{for } l = 0\,.$$

Useful forms for U and V are

$$V_\alpha^l(r) = \left(\frac{r}{\alpha}\right)^l \left(\frac{\mathrm{d}}{\mathrm{d}r}\frac{1}{r}\right)^l \sinh \alpha r\,, \tag{B.2}$$

and

$$U_\alpha^l(r) = \left(-\frac{r}{\alpha}\right)^l \left(\frac{\mathrm{d}}{\mathrm{d}r}\frac{1}{r}\right)^l e^{-\alpha r}\,. \tag{B.3}$$

Recursion relations for u_l are given by

$$u_{l-1}(kr) = k^{-1}r^{-l}(\mathrm{d}/\mathrm{d}r)r^l u_l(kr)\,, \tag{B.4}$$

and

$$u_l(kr) = -\,k^{-1}r^l(\mathrm{d}/\mathrm{d}r)r^{-l}u_{l-1}(kr)\,. \tag{B.5}$$

An integral property of two functions $A_\alpha^l(r)$ and $B_\alpha^l(r)$ which satisfy the

TABLE I. – *General Properties of the Functions Used.*

Function	Annihilated by operator	Behaviour at		Expressed in terms of	
		0	∞	Spher. Bess. Fns.	Each other
$u_l(kr)$	$D_r^l + k^2$	$\sim \dfrac{(kr)^{l+1}}{(2l+1)!!}$	$\sim \sin(kr - \frac{1}{2}l\pi)$	$krj_l(kr)$	$u_l(kr) = \frac{1}{2}i[w_l(kr) - (-1)^l w_l(-kr)]$
$w_l(kr)$	$D_r^l + k^2$	$\sim \dfrac{(2l-1)!!}{(kr)^l}$	$\sim i^l e^{-ikr}$	$i(-1)^{l+1}krh_l^{(1)}(-kr)$	—
$V_\alpha^l(r)$	$D_r^l - \alpha^2$	$\sim \dfrac{(-\alpha r)^{l+1}}{(2l+1)!!}$	$\sim \frac{1}{2}e^{-\alpha r}$	$(-1)^{l+1}(i\alpha r)j_l(i\alpha r)$	$V_\alpha^l(r) = \frac{1}{2}[U_{-\alpha}^l(r) - (-1)^l U_\alpha^l(r)]$
$U_\alpha^l(r)$	$D_r^l - \alpha^2$	$\sim \dfrac{(2l-1)!!}{(-\alpha r)^l}$	$\sim e^{-\alpha r}$	$(i)^{l+1}(i\alpha r)h_l^{(1)}(i\alpha r)$	—

TABLE II. – *Recursion Relations.*

V_α^l	U_α^l
$V_\alpha^l = \alpha^{-1}r^l(\mathrm{d}/\mathrm{d}r)r^{-l}V_\alpha^{l-1}$	$U_\alpha^l = -\alpha^{-1}r^l(\mathrm{d}/\mathrm{d}r)r^{-l}U_\alpha^{l-1}$
$V_\alpha^{l-0} = \alpha r^l \int_0^r t^{-l}V_\alpha^l(t)\,\mathrm{d}t + [(2l-1)!!]^{-1}(\alpha r)^l$	$U_\alpha^{l-1} = -\alpha r^l \int_\infty^r t^{-l}U_\alpha^l(t)\,\mathrm{d}t$
$V_\alpha^{l-1} = \alpha^{-1}r^{-l}(\mathrm{d}/\mathrm{d}r)r^lV_\alpha^l$	$U_\alpha^{l-1} = -\alpha^{-1}r^{-l}(\mathrm{d}/\mathrm{d}r)r^lU_\alpha^l$
$V_\alpha^l = \alpha r^{-l}\int_0^r t^lV_\alpha^{l-1}(t)\,\mathrm{d}t$	$U_\alpha^l = -\alpha r^{-l}\int_0^r t^lU_\alpha^{l-1}(t)\,\mathrm{d}t + [(2l-1)!!](\alpha r)^{-l}$
$\alpha(V_\alpha^{l-1} - V_\alpha^{l+1}) = r^{-1}(2l+1)V_\alpha^l$	$-\alpha(U_\alpha^{l-1} - U_\alpha^{l+1}) = r^{-1}(2l+1)U_\alpha^l$

equations

$$(D_r^l - \alpha^2) A_\alpha^l(r) = 0 , \tag{B.6}$$

and

$$(D_r^l - \beta^2) B_\beta^l(r) = 0 , \tag{B.7}$$

is

$$\int_a^b A_\alpha^l(r) B_\beta^l(r) \mathrm{d}r = (\alpha^2 - \beta^2)^{-1} W[B_\beta^l(r); A_\alpha^l(r)] \Big|_a^b . \tag{B.8}$$

RIASSUNTO (*)

Partendo dalla matrice di scattering e dalle energie degli stati legati si ottengono le funzioni e i potenziali d'onda per le forze non centrali d'accoppiamento dei momenti angolari l e $l+2$. Il metodo, estensione del procedimento elaborato da Bargmann per forze centrali, è basato sulla soluzione di un'equazione integrale recentemente sviluppata e discussa da Gel'fand e Levitan, Kohn e Newton. I potenziali non centrali che ne derivano sono le prime combinazioni note di potenziali di spin-orbita e tensoriali per i quali l'equazione di Schrödinger in forma chiusa sia risolvibile. I risultati consentono di approssimare una matrice S sperimentale per mezzo di una matrice i cui elementi siano funzioni razionali del numero d'onde k e della susseguente determinazione della funzione e del potenziale d'onda con sole espressioni algebriche finite.

(*) *Traduzione a cura della Redazione.*

Evidence for a Double Covalent Bond from Paramagnetic Resonance, Optical Absorption and X-Ray Data (*).

M. B. Palma-Vittorelli, M. U. Palma, D. Palumbo

Istituto di Fisica dell'Università - Palermo

F. Sgarlata

Istituto di Mineralogia dell'Università - Palermo

(ricevuto il 31 Dicembre 1955)

Summary. — Data on paramagnetic resonance absorption, on the distance between the levels responsible for optical absorption, on polarized light absorption and on the structure deduced with X-rays are given which, consistently in agreement with theoretical considerations, confirm the hypothesis previously advanced of the existence of a double covalent bond in the vanadyl group of a vanadylsulphate.

1. – Introduction.

In the study of the magnetic properties of salts containing paramagnetic ions of the iron group, the experimental investigation and the theoretical interpretation of the results for ions having a single $3d$ electron, has been particularly difficult and fruitful. The two examples of such ions are Ti^{+++} and V^{++++}. For the first, the experimental difficulty arises substantially from the exceptionally short spin-lattice relaxation time: because of it, absorption

(*) This work forms part of a program of research undertaken with the financial support of the Consiglio Nazionale delle Ricerche, through the Comitato per la Fisica, for which the authors wish to express their sincere gratitude.

measurements have not been possible except below 4 °K. Furthermore, there have been difficulties in fitting the experimental and theoretical results ([1-4]).

One of the first difficulty presented by salts of V^{++++} is that it is difficult to obtain them in a definite hydration form, and to obtain single crystals of sufficient size for the measurements ([5]). Furthermore, information on the crystal structure of these salts is generally not available.

For these reasons, we have preferred to study as thorougly as possible the paramagnetic resonance absorption, the crystal structure and the optical properties of only one of the salts of V^{++++}, namely $VOSO_4 \cdot 5H_2O$. Further, on the displacement of the maximum of the paramagnetic resonance absorption line as a function of the number of water molecules of crystallization, a little more than qualitative investigation has been carried out, since a perfect discrimination among the different states of hydration of this salt is not always possible.

In fact, vanadylsulphate crystallizes in many different hydration states, among which certainly exist the ones with 6.5, 5, 3.5, and 2 molecules of water ([5]). They are obtained by evaporation of aqueus solutions in very similar and not always completely and surely known physical conditions. Thus we get an uncertainty in the number of water molecules of crystallization, in the attempt to get the different hydration states.

2. – Experimental Results.

An account has been previously given ([6]) about preliminary measurements on the paramagnetic resonance absorption, about the elementary cell, containing 4 ions of Vanadium, in slightly inequivalent positions, about the expected configuration of the ions surrounding the Vanadium ion, consisting of a deformed octohedron whose vertices are occupied by four water molecules, one O of the SO_4 group, and the O of the VO group. The axis of the VO group lies almost parallel to the twofold y axis.

Further measurements of paramagnetic absorption in X-band and K-band have been carried out at the Massachusetts Institute of Technology. The experimental method consisted essentially in the modulation of the magnetic

([1]) C. J. Gorter: *Paramagnetic Relaxation* (Amsterdam, 1947).

([2]) D. Bijl: *Proc. Phys. Soc.*, A **63**, 405 (1950).

([3]) B. Bleaney, K. W. H. Stevens: *Rep. on Progr. in Phys.*, **16**, 108 (1953).

([4]) B. Bleaney, J. S. Bogle, A. H. Cooke, R. J. Duffus, M. C. M. O'Brian, and K. W. H. Stevens: *Proc. Phys. Soc.*, A **68**, 57 (1955).

([5]) Koppel and Behrendt: *Zeits. Anorg. Chem.*, **35**, 154 (1903).

([6]) M. B. Palma-Vittorelli, M. U. Palma, D. Palumbo and M. Santangelo: *Suppl. Nuovo Cimento*, **12**, 154 (1954).

field (7) and narrow-band amplification. The sample was put in a cavity which was fed by an arm of a magic T. The latter was so arranged as to give in its 4-th arm a signal proportional to the absorbed power. The derivative of the absorption line was recorded. The magnetic field and the frequency were electronically stabilized and measured respectively by means of a proton resonance signal and by comparison with a frequency standard.

At the temperature of liquid helium, in K-band, and with a high-Q silver cylindrical cavity, it has been possible to detect the resonance signal of one single crystal. However, it has not been possible to obtain single crystals of the necessary dimensions to allow accurate measurements. The results obtained for the powder at various temperatures are listed in Table I.

TABLE I. *g-values for* $VOSO_4 \cdot 5H_2O$, *powder, at different temperatures* ($\nu \simeq 9000$ MHz).

Temperature	g, powder	$\Delta g = 2.0023 - g$
300 °K	1.990 ± 0.003	$12 \cdot 10^{-3}$
77 °K	1.999 ± 0.003	$3 \cdot 10^{-3}$
4 °K	1.994 ± 0.004	$8 \cdot 10^{-3}$

With the decrease of the number of water molecules of crystallization a decrease of the g-values of the powder has also been observed.

Using the recorded derivative of the absorption line, the following values have been obtained:

$$\Delta H_{\text{m.sl.}} = 128 \pm 5 \text{ gauss}, \qquad (\Delta H^2)^{\frac{1}{2}}_{\text{av.}} = 60 \pm 15 \text{ gauss},$$

where $\Delta H_{\text{m.sl.}}$ is the distance between the H-values corresponding to the two points of maximum slope in the absorption curve, and:

$$\sqrt{(\Delta H^2)_{\text{av.}}} = \sqrt{\frac{\int_{-\infty}^{+\infty} I(H) H^2 \, dH}{\int_{-\infty}^{+\infty} I(H) \, dH}} = \sqrt{\frac{\int_{-\infty}^{+\infty} (dI/dH) H^3 \, dH}{3 \int_{-\infty}^{+\infty} (dI/dH) \, dH}}.$$

The relation $\Delta H_{\text{m.sl.}} = 2\sqrt{(\Delta H^2)_{\text{av.}}}$ which holds for a gaussian line, gives, for the above value of $\sqrt{(\Delta H^2)_{\text{av.}}}$, $\Delta H_{\text{m.sl.}} = 120$ gauss which, compared with the experimental value, shows (8) that the gaussian assumption is not necessarily a bad one.

(7) R. MALVANO and M. PANETTI: *Nuovo Cimento*, **7**, 28 (1950).
(8) J. H. VAN VLECK: *Phys. Rev.*, **74**, 1168 (1948).

In addition, measurements of optical absorption have been performed for the purpose of determining the distance between the orbital levels, between which a transition is allowed. The measurements were carried out by illuminating the sample with white light, and recording

$$\log \frac{\text{Incident luminous flux}}{\text{Transmitted luminous flux}}$$

as a function of the frequency. The absorption band turned out to be centred at approximately $\lambda = 7\,700$Å. The distance between the orbital levels responsible for the transition is thus about 13000 cm^{-1}.

Investigations on crystal's pleochroism which will be later described, have shown that the optical transition occurs when the radiating magnetic field is orthogonal to the V–O axis. On the contrary, it has not been possible to detect any noticeable absorption within the optical range, with a radiating magnetic field parallel to this axis.

3. – Remarks on the Experimental Data.

It seems worthwhile to note that, although for the reasons given above, it has not been possible to perform measurements on single crystals, the given g-values for the powder, nevertheless do give significant informations.

In fact, let us assume that:

1) The shape of the single crystal's line is gaussian.
2) The system has an axial symmetry.
3) The line-width of the single crystal is isotropic.

Then, as it will be discussed in a forthcoming paper, the following limitations hold:

$$(1) \qquad \begin{cases} \dfrac{3g_\perp + g_\parallel}{4} \geqslant g_{\text{powder}} \geqslant g_\perp & \text{if} \quad g_\parallel > g_\perp \\ \dfrac{3g_\perp + g_\parallel}{4} \leqslant g_{\text{powder}} \leqslant g_\perp & \text{if} \quad g_\parallel < g_\perp . \end{cases}$$

Concerning the above assumptions, assumption 1) is not very restrictive, because, in obtaining eq. (1), the shape of the line of the single crystal is of some importance only in the vicinity of the maximum, and this is the truer, the closer the principal g-values are.

Assumption 2) is satisfied for each V-ion in an axial-symmetric crystalline electric field. Let us now consider that in our case, the elementary cell contains

a number of equal paramagnetic ions, in inequivalent positions. In this case, it is well known that, if an exchange interaction is effective, the elementary cell may behave as one single paramagnetic unit. More precisely, as it will be discussed in details in the section concerning X-ray structure, our elementary cell contains four V-ions. The symmetry axes of the electric field surrounding these ions, are disposed in parallel pairs, each pair lying at an angle $2\varphi = 30°$ with respect to the other.

An effective exchange coupling, gives, for the elementary cell the following principal g-values:

$$(2) \qquad \begin{cases} g_\alpha = g_\parallel + (g_\perp - g_\parallel) \sin^2 \varphi \\ g_\beta = g_\perp - (g_\perp - g_\parallel) \sin^2 \varphi \\ g_\gamma = g_\perp \end{cases}$$

where α, β, γ, respectively, stand for the internal bisector, the external bisector and the perpendicular to the directions of the two pairs of symmetry axes. In this case it is impossible to distinguish the above relations, deduced from [9]

$$g_\vartheta = g_\parallel \cos^2 \vartheta + g_\perp \sin^2 \vartheta \,,$$

from the ones that one could have obtained using the:

$$g_\vartheta^2 = g_\parallel^2 \cos^2 \vartheta + g_\perp^2 \sin^2 \vartheta \,.$$

Even in the less favourable hypothesis concerning the difference $(g_\perp - g_\parallel)$, due to the small value of the angle φ, the characteristic surface of the g-values, may still be considered as a revolution ellipsoid: assumption 2) is then justified, provided that in eq. (1), $g_\perp$ is substituted by $(g_\perp + g_\beta)/2$.

According with the small value of φ, assumption 3) too appears a reasonable one.

The above considerations, in specifying the play of the quantities $g_\parallel$ and $g_\perp$ upon the g-value of the powder, give the possibility of increasing the quantity of information that it is possible to derive from the experimental results on the powder.

4. – Theoretical Interpretation of the Results.

4·1. *Inadequacy of the ionic model.* – An attempt was first made to interpret these data according with the usual scheme of a crystalline electric field [10].

---

[9] M. B. Palma-Vittorelli, M. U. Palma, D. Palumbo and M. Santangelo: *Nuovo Cimento*, **2**, 811 (1955).

[10] J. H. Van Vleck: *El. and Magn. Suscept.* (Oxford, 1932).

Concerning the symmetry of this field, various hypothesis can be formulated. One which agrees with the octohedral coordination of the V^{++++} ion is that the crystal potential should contain a term of cubic symmetry and a term of tetragonal symmetry around the V–O axis.

The ${}^2D_{\frac{1}{2}}$ state is an orbital quintuplet, described by the functions $R(r)Y_2^m$ ($m = 2, 1, 0, -1, -2$). The cubic term splits the quintuplet into a fundamental triplet and a doublet. The tetragonal term further splits the levels as shown in Fig. 1. Then, the perturbation of the spin-orbit interaction on the ground level, which is a spin doublet, yields (besides $R(r)$):

$$(3)\qquad \begin{cases} \dfrac{Y_2^2 - Y_2^{-2}}{i\sqrt{2}}\begin{pmatrix}1\\0\end{pmatrix} - \dfrac{\lambda}{i\sqrt{2}D}\,Y_2^{-1}\begin{pmatrix}0\\1\end{pmatrix} - \dfrac{2\lambda}{D'}\,\dfrac{Y_2^2 + Y_2^{-2}}{i\sqrt{2}}\begin{pmatrix}1\\0\end{pmatrix} \\ \dfrac{Y_2^2 - Y_2^{-2}}{i\sqrt{2}}\begin{pmatrix}0\\1\end{pmatrix} - \dfrac{\lambda}{i\sqrt{2}D}\,Y_2^{1}\begin{pmatrix}1\\0\end{pmatrix} - \dfrac{2\lambda}{D'}\,\dfrac{Y_2^2 + Y_2^{-2}}{i\sqrt{2}}\begin{pmatrix}0\\1\end{pmatrix}, \end{cases}$$

The magnetic field splits this doublet; the separation is $g\beta H$, where g depends on the orientation of H with respect to the symmetry axis of the electric field. The principal g-values are:

$$(4)\qquad \begin{cases} g_{\parallel} = 2.0023\left(1 - \dfrac{4\lambda}{D'}\right), \\ g_{\perp} = 2.0023\left(1 - \dfrac{\lambda}{D}\right), \end{cases}$$

and, calling $\Delta g = 2.0023 - g$:

$$(5)\qquad \Delta g_{\parallel} \cong \frac{8\lambda}{D'} \qquad g_{\perp} \cong \frac{2\lambda}{D},$$

where D and D' are the distances between the orbital levels, as shown in Fig. 1.

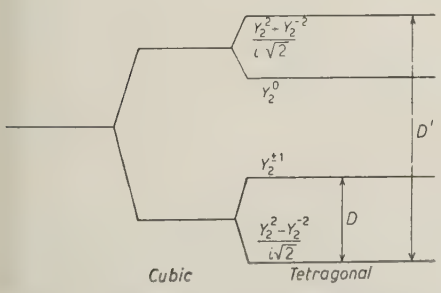

Fig. 1. – Splitting of the ${}^2D_{\frac{1}{2}}$ orbital quintuplet, under the action of an electric field containing a dominant cubic term, and a tegtraonal term (not in scale).

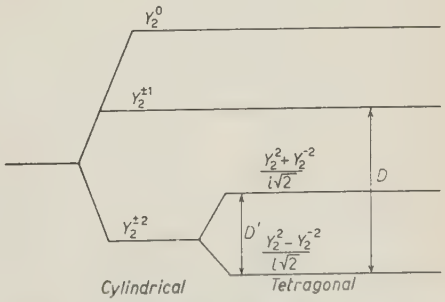

Fig. 2. – Splitting of the ${}^2D_{\frac{1}{2}}$ orbital quintuplet, under the action of an electric field containing a dominant cylindrical term, and a tetragonal term (not in scale).

As it can be deduced from the results obtained with polarized light, the optical transition occurs between the two levels whose distance is labelled by D in Fig. 1 and 2. Further, the experimental results with polarized light show that the transition corresponding to the distance labelled by D' is out of the optical range. In the case of Fig. 1 it is then necessary that $D' \geqslant 25000\ \mathrm{cm}^{-1}$.

Concerning the value of λ, the spin-orbit interaction coefficient, accurate experimental data are not available. Extrapolation of the data of LAPORTE ([11]), indicates that it is not less than $200\ \mathrm{cm}^{-1}$.

Assuming for D' a value even as large as $5 \cdot 10^4\ \mathrm{cm}^{-1}$, eq. (5) yields the values

$$\Delta g_{\parallel} = 3 \cdot 10^{-2}\,, \qquad \Delta g_{\perp} = 3 \cdot 10^{-2}\,, \tag{6}$$

which are not in agreement with the experimental values of Table I. It is to be noted that the arbitrary choice in the D' value is at any rate not important, due to eq. (1).

Next, an attempt was made to take a better account of the presence of the oxygen in the group VO, assuming as the dominant term of the crystal potential a cylindrical term, followed by a tetragonal one. A similar procedure yields the separation of the levels shown in Fig. 2, and again the ground doublet given in eq. (3). But now it is $D' < D$, so that $\Delta g_{\perp}$ is the same given by eq. (6), and $\Delta g_{\parallel}$ is even in a more striking disagreement with the experimental data (*).

4·2. *Evidence for the covalent bond.* – The above assumptions concerning the symmetry of the crystalline electric potential yield, as it has been shown, results which are in disagreement with the experimental data. Now, the crystalline electric potential can be expanded in spherical harmonics and all terms of order higher than the 4-th have zero matrix elements in this case. It follows that the possible assumptions on the symmetry are limited; whatever the hypothesis, the Δg's will be always of the form

$$k \frac{\lambda}{D}\,. \tag{7}$$

([11]) O. LAPORTE: *Zeits. f. Phys.*, **47**, 761 (1928).

(*) It is of interest to remark that Dr. I. M. WARD has investigated at the Clarendon Laboratory, Oxford, the paramagnetic resonance of an undiluted single crystal of $K_2(VO(C_2O_4)_2)$, finding a magnetic behaviour corresponding to an effective spin $S = \frac{1}{2}$. He has not found possible to explain the g-values on an ionic model.

We are pleased to thank here Dr. I. M. WARD for private communication of his unpublished results.

It is easily seen that none of these leads to results which are in better accord with experiment, even choosing rather arbitrary values of D'.

In order to fit the experimental results, it is therefore necessary to seek, by means of a more detailed consideration of the V–O bond, a cause which would justify the choice, in eq. (7), of values of λ or of K considerably lower than those previously assumed. In fact, it is to be observed that the V^{+++} is present in the group VO^{++} and that therefore its magnetic properties should be considered in the light of this fact ([10]). So one comes to the conclusion that the hypothesis of a purely ionic double V=O bond has to be abandoned since, as has been seen, it can not justify the experimental data, with any reasonable choice of parameters. The hypothesis of a double covalent bond has been then advanced ([12]).

In this case, the two bonds (σ and π respectively), may be formed by two $2p$ or $2s2p$ hybrid oxygen's orbitals, and by two $3d$ or $3d4s$ hybrid vanadium's orbitals. The binding electrons have in this case the double effect of further decreasing the effective nuclear charge acting upon the paramagnetic electron, and of modifying the spherical symmetry of the atomic electric field.

Such hypothesis previously advanced by the authors ([12]), has independently been called upon by EISENSTEIN and PRYCE ([13]) for the interpretation of the paramagnetic properties of the transuranic ions in groups of the uranylic type, and more precisely of $(NpO_2)^{++}$. Other cases of not ionic binding, pointed out by a study of the magnetic properties, are those of the cyanides of some elements of the iron group which have been studied by VAN VLECK ([14,15]), HOWARD ([16]) and KOTANI ([17]), and those discussed by STEVENS ([18]) and OWEN ([19]).

The mentioned modification of the spherical symmetry of the atomic electric field should forbid, for a strict treatment, the use of orbitals of the kind hitherto assumed.

Nevertheless, and as a first approximation, the non spherical-symmetric part of the atomic electric field may be considered as included in the crystalline electric field.

In this approximation, it seems reasonable to assume the fundamental state to be again the one given by eq. (3), thanks also to the fact that the

([12]) M. B. PALMA-VITTORELLI, M. U. PALMA, and D. PALUMBO: *Suppl. Nuovo Cimento*, **2**, 938 (1955). (Atti Congresso S.I.F., Parma, 1954).
([13]) J. C. EISENSTEIN and M, H. L. PRYCE: *Proc. Roy. Soc.*, A **229**, 20 (1955).
([14]) J. H. VAN VLECK: *Journ. Chem. Phys.* **3**, 807 (1935).
([15]) J. H. VAN VLECK: *Ann. Inst. H. Poincaré*, **10**, 57 (1948).
([16]) J. B. HOWARD: *Journ. Chem. Phys.*, **3**, 813 (1935).
([17]) M. KOTANI: *Journ. Phys. Soc. Jap.*, **4**, 293 (1935).
([18]) K. W. H. STEVENS: *Proc. Roy. Soc.*, A **219**, 542 (1953).
([19]) J. OWEN: *Proc. Roy. Soc.*, A **227**, 183 (1955).

related charge density is condensed on the plane orthogonal to the V – O axis.

The $\Delta g_{\parallel}$ and $\Delta g_{\perp}$ values will then undergo the following changes:

1) A drastic diminution due to the decreasing of the effective nuclear charge: the value of the spin-orbit coupling constant will no longer be given by extrapolation of the data of LAPORTE [11] concerning Ti^{+++}, but it has rather to be deduced using the value related to the $^4F_{\frac{3}{2}}$ state of the V^{++}, which suggests a value of about 80 cm^{-1}.

2) A decreasing of the matrix element of the spin-orbit coupling between the fundamental state and the states of axial momentum equal to ± 1, due to the fact that these states are partially occupied by the bonding electrons. Such a decreasing involves only the $\Delta g_{\perp}$ value, and it seems likely to be of the order of a factor $1/\sqrt{2}$.

Besides, one more reason of decrease of the $\Delta g_{\parallel}$ and $\Delta g_{\perp}$ values may be due to a certain amount of δ bond, interesting the paramagnetic electron, as discussed by STEVENS [18] and later by OWEN [19]. Such a decrease would anyway not be sufficient by himself to fit the experimental results.

From the above considerations, it follows:

$$g_{\perp} \cong 1.993 , \qquad g_{\parallel} \cong 1.990 . \tag{8}$$

This new theoretical assumption therefore fits the experimental results. Nevertheless, it was believed advisable to find one more proof of the validity of the assumptions, by determining in details the crystal structure of the salt under investigation.

5. – Crystal Structure.

5·1. *Crystallographic determination.* – Small crystals of the substance with well defined prismatic faces were chosen. Four faces parallel to the elongation's direction were found with the goniometer; on the microscope the same extinction angle (about 8°) was measured on two adjacent faces. Taking the elongation's direction as the direction of the z-axis, the form is shown to be the monoclinic prism (110). With the goniometer it is found that $(110):(\bar{1}10) = 112°20'$. The value $a \sin\beta/b = 0.6703$ is calculated.

The angle of the prism being $\alpha = 67° 40'$, the refraction index for sodium light has been measured by deviation method, under the following conditions:

1) With a wave polarized in a direction approximately normal to the wedge of the prism, and with incidence angle $i = 57° 24'$, one finds a devia-

tion of 47°10′; thus the refraction index is $n = 1.513$. We can assume this to be the index in the direction parallel to the « b »-axis, i.e., $n_{\parallel b} = 1.513$.

2) With a wave polarized in a direction approximately parallel to the wedge of the prism, and with incidence angle $i = 59° 27'$, one finds a deviation of 50° 57′, and therefore $n_{\perp b}$, 1.544.

The crystals are strongly pleochroic, and they show a deep blue color when observed with polarized light, whose polarization plane is orthogonal to the wedge of the prism; on the contrary they are practically transparent for a wave polarized in a plane parallel to the wedge of the prism.

5'2. X-*ray determinations*. – The method of the rotating crystal and Weissenberg's method of the equiinclination have been applied, using a camera with the radiant-diameter, and Cu radiations.

A rotation around the « c »-axis has shown the absence of symmetry perpendicular to this axis; the period is $c_0 = 13.02$ Å. The equatorial Weissenberg shows the $2/m(C_{2h})$ symmetry. The period T_1 and T_2 have been measured along the symmetry elements giving $T_1 = 6.57$ Å, and $T_2 = 9.71$ Å. The 1st order equiinclination Weissenberg shows that the binary axis is the direction with maximum period, that is, $b_0 = 971.1$ Å. Measuring the distance between the two reflections (011) and $(0\bar{1}1)$ with the method suggested by BUERGER, one obtains $\beta = 111° 23'$, and it is then possible to calculate $a_0 = 7.06$ Å. The value $a_0 \sin\beta / b_0 = 0.6766$ then results.

With a solution of bromoform and xylol the density has been measured to be 2.00 g/cm³; thus it is found that four $VOSO_4 \cdot 5H_2O$ molecules are present in the monoclinic cell. The observed extinctions ($(0k0)$ only with $k=2n$; and $(h0l)$ only with $l=2n$), imply the spatial group $P2_{1/c}(C_{2h}^5)$.

With the intensities of the reflections $(hk0)$ measured in the equatorial Weissenberg, the Patterson projection on the xy plane has been calculated. From the distribution of the secondary maxima of this projection, one finds that the atoms with the higher atomic numbers (i.e., Vanadium and Sulphur) occupy the general position (e) and have an y coordinate such that in the projection on the xy plane there are two atoms superposed. The most likely interpretation of the Patterson projection gives:

for Vanadium	$x = 0.335$	$y = 0.250$
for Sulphur	$x = 0.000$	$y = 0.000$

From these coordinates it is found that the distance between the superposed atoms of Vanadium is $\frac{1}{2}c = 6.51$ Å; and the distance between the Sulphur atoms depends on the z-values. Since each atom of Sulphur arranges the

group SO_4^{--} independently of the others, the most likely value of the Sulphur-Sulphur distance is found for a z-value about 0.250.

TABLE II. – *Coordinates of atoms.*

	x/a_0	y/b_0	z/c_0
V	0.335	0.302	0.407
O	0.382	0.467	0.390
$H_2O(1)$	0.286	0.075	0.431
$H_2O(2)$	0.402	0.260	0.271
$H_2O(3)$	0.283	0.314	0.572
$H_2O(4)$	0.670	0.240	0.479
S	0.017	0.976	0.192
O(1)	0.058	0.333	0.365
O(2)	0.932	0.085	0.141
O(3)	0.005	0.951	0.300
O(4)	0.257	0.952	0.184
$H_2O(5)$	0.377	0.710	0.210

The z coordinate of Vanadium can be determined by taking into account, for example, that the reflection (042) has zero intensity; with the y-values from the Patterson projection, in order to let the contributions of the Vanadium and Sulphur atoms to be in opposition for the reflection (042), the difference of the z-values has to be about 0.250; hence a coordinate of about 0 must be assigned to Vanadium. On the basis of these coordinates assigned to the atoms of higher atomic number, it has been possible to define approximately an initial distribution of the particles in the monoclinic cell of the spatial group, by geometrical considerations developed in such a manner as to provide

TABLE III. – *Interionic distances.*

V – O	1,67 Å	$H_2O(1) – O(1)$	2.93 Å
$V – H_2O(1)$	2.27 »	$H_2O(1) – H_2O(2)$	3.08 »
$V – H_2O(2)$	2.03 »	$H_2O(1) – H_2O(3)$	2.96 »
$V – H_2O(3)$	2.31 »	$H_2O(1) – H_2O(4)$	3,01 »
$V – H_2O(4)$	2.29 »		
V – O(1)	1.85 »	$O(1) – H_2O(2)$	3.16 »
		$O(1) – H_2O(3)$	2.5.9»
O – O(1)	2.57 »		
$O – H_2O(2)$	2.57 »	$H_2O(4) – H_2O(2)$	2.69 »
$O – H_2O(3)$	3.08 »	$H_2O(4) – H_2O(3)$	3.35 »
$O – H_2O(4)$	2.94 »		

a tetrahedral configuration around the Sulphur, and an octohedral configuration around Vanadium.

The coordinates obtained in this way have been adjusted by the method of steepest descent; the method has been used on the reflections whose intensities are zero or almost zero in the equinclination Weissenberg from 0-order to the 3rd order. It has been possible in this way to avoid the calculation of the absolute values of the structure factors. Using the values of the coordinates given in Table II, the interionic distances given in Table III have been calculated.

5·3. *Discussion of the structure.* – The initial distribution of the particles in the cell of the lattice, shows that among the atoms surrounding the Vanadium atom, one Oxygen is found to be closer to the central atom than the others. The higher approximations confirm and define the particular behaviour of this Oxygen atom, and give a distance of about 1.67 Å. This behaviour can be interpreted by assuming that the V–O group, chemically defined, maintains its identity in the crystal lattice.

An analogous case occurs in the lattice of the Uranyl compounds. Uranium shows a cubic arrangement, but, for instance, in the uranylfluoride UO_2F_2, among the eight atoms surrounding the Uranium, the two Oxygens are closer to the central atom than the fluorines, which fact is consistent with the existence of a covalent bond. Concerning the VO group, one must bear in mind that the sum of the ionic radii is 2.03 Å, while that of the atomic radii is 1.94 Å. Since the observed V–O distance is considerably less than these values, one has to conclude that a double covalent bond is established between the two atoms.

X-ray, paramagnetic and optical absorption, and polarized light measurements are then in consistent agreement to point out the existence of this double covalent bond.

* * *

We wish to express our gratitude to Dr. K. W. H. Stevens for many helpful discussions on the theoretical aspects of the subject; and also to thank Professors A. Bellanca, N. Carrara and M. Kotani for their interest in our work.

We are particularly indebted to Prof. J. H. Van Vleck for his interest in the present work.

Finally, we thank Prof. M. W. P. Strandberg and all his group and particularly Drs. C. F. Davis Jr., J. H. Solt Jr., M. Tinkham, for their kind hospitality, their assistance and the use of their equipment in the Paramag-

netic Laboratory in the Massachusetts Institute of Technology, which was kindly extended to two of us (M.B.P.V. and M.U.P.) during a stay at M.I.T.

This stay has been kindly supported by the Comm. Am. Scambi Cult. and by the Ministero P. I., which support we gratefully acknowledge.

RIASSUNTO

Lo studio dell'assorbimento di risonanza paramagnetica su polvere di $VOSO_4 \cdot 5H_2O$ ha fornito i dati di Tab. I. L'assorbimento ottico in luce naturale e polarizzata, permette di stabilire la distanza tra i due livelli responsabili della transizione, permettendone anche l'individuazione. È data una limitazione (che verrà discussa in un successivo lavoro), che, precisando il ruolo di $g_\perp$ e $g_\parallel$ nel g della polvere, permette una più completa utilizzazione dei dati sperimentali. Non è possibile fornire una interpretazione unitaria di tali dati in termini di un campo elettrico cristallino. L'interpretazione è invece fornita sulla base di un doppio legame covalente (un legame σ ed un legame π) nel gruppo VO, che può essere formato da due orbitali $2p$ dell'Ossigeno e da due $3d$ del Vanadio, eventualmente mescolati con orbitali s. Gli elettroni del legame schermano ulteriormente la carica nucleare, diminuendo notevolmente il coefficiente di accoppiamento spin-orbita, che deve ora essere dedotto dal valore relativo al V^{++}. Inoltre, poichè tali elettroni occupano parzialmente gli stati di momento assiale ± 1, l'elemento di matrice dell'accoppiamento spin-orbita che interviene nel $g_\perp$ viene ancora ridotto. Un eventuale legame δ potrebbe sovrapporsi a tale legame, ma non sarebbe da solo sufficiente a render conto dei dati sperimentali. Si è comunque ritenuto molto utile cercare una ulteriore conferma della validità dell'ipotesi formulata, determinando con raggi X la struttura del cristallo in esame. I principali risultati sono elencati in Tab. II e III. Uno degli atomi di O è risultato particolarmente avvicinato al V (1.67 Å), il che, tenuto conto del fatto che la somma dei raggi ionici è 2.03 Å e quella dei raggi atomici è 1.94 Å conferma inequivocabilmente l'esistenza di un doppio legame covalente.

IL NUOVO CIMENTO Vol. III, N. 4 1° Aprile 1956

K-Mesons in Emulsions Exposed to a 6.2 GeV Proton Beam.

J. Crussard, V. Fouché, J. Hennessy, G. Kayas, L. Leprince-Ringuet, D. Morellet et F. Renard

Laboratoire de Physique de l'École Polytechnique - Paris

(ricevuto il 30 Gennaio 1956)

Summary. — A large emulsion stack has been exposed in the 6.2 GeV proton beam of the Berkeley Bevatron. 414 K^+ decaying at rest have been observed. Their probable time of flight is $\sim 5 \cdot 10^{-10}$ s. 57 flat secondaries at or near minimum ionization have been extensively measured. The proportions of K_μ, χ, K_β, $\varkappa$, τ and τ' are found to be respectively around 54%, 26%, 8%, 4%, 7% and 1%. They are not significantly different from the proportions in stacks exposed to the K^+ focused beam of the bevatron or to cosmic radiation, which indicates similarity in lifetimes and in relative frequencies of production for the different types of K's. The average range of 8 stopping secondaries of K_μ and of 4 stopping secondaries of χ are respectively 202.0 ± 1.9 mm and 118.8 ± 1.7 mm. The masses of K_μ and χ deduced from these ranges are very close to the masses found by direct measurement in the K beam. Two $\varkappa$ events with secondaries of 61.5 and 90.5 MeV have been observed. The whole evidence on $\varkappa$-mesons in large emulsion stacks is examined: it is felt that the results are so far consistent with the $\varkappa \to \pi^0 + \mu + \nu$ scheme. Five K^--events have been found and are described.

1. – Introduction.

Several experiments have recently been performed in order to study K-meson secondaries by means of large nuclear emulsion blocks. In particular, the « G-stack » group [1] have flown emulsions at high altitude. The K-mesons are produced by cosmic ray particles of different and unknown energies, and have ranges of the order of a few centimetres, corresponding to times of flight

[1] G-Stack Collaboration: *Nuovo Cimento*, **2**, 1063 (1955).

of 1 to $5 \cdot 10^{-10}$ s. Other workers have used emulsions exposed to the focused K-beam of the Berkeley Bevatron ([2,3]), in which the K-mesons are produced by protons of known energy (generally 6 GeV) and have times of flight of the order of 10^{-8} s.

In the present experiment, emulsions have been exposed directly in the 6.2 GeV proton beam of the Berkeley Bevatron. There is no marked difference between the production conditions of the K-mesons we observe at rest and those of the « K-beam ». Not only are the producing particles of the same nature and energy, but the energy and direction of emission of the K's are also very similar. However, our times of flight are much shorter, and close to those of the « G-stack ». By comparing our results with those of the two experiments mentioned above, information should be obtained both on the mean lifetimes of the various types of K-mesons and on their relative frequencies of production by different kinds of primaries.

The first results have been given at the Pisa Conference (1955).

2. – Experimental Procedure.

The stack consisted of 120 stripped emulsions of 25 cm × 35 cm × 600 μm. This 6.5 litre block was introduced in a straight section of the Bevatron, with the 25 cm dimension parallel to the beam. It was placed on a carriage, and was shot forward in time to cross the beam just before the end of a pulse (the energy of the proton then being 6.2 GeV). In order to concentrate the protons in a certain part of the stack, the « lip target » design has been used ([1]). One thus obtains a roughly exponential track density which is maximum near the edge of each plate and is reduced to about half its value every 7 mm.

The sides of the stack were marked with X-rays at Berkeley. After processing, these marks were used as guides in cutting the plates, in order to obtain directly the alignment necessary to follow a track from one plate to another.

Scanning consisted in a systematic examination of all stopping tracks, in order to detect K-mesons decaying at rest. Scanned areas were in a band parallel to the beam, extending from 8.5 to 17.5 cm from the edge of the plate where the beam is strongest (see Fig. 1). From the directions of most of the K-mesons found, we gather that they come mainly from the region where the beam is strongest. Most of them, therefore, have a range of 5 to 20 cm corresponding to a time of flight of 3 to $9 \cdot 10^{-10}$ s.

([2]) D. M. Ritson, A. Pevsner, S. C. Fung, M. Widgoff, G. T. Zorn, S. Goldhaber: Private communication (October 1955).

([3]) R. W. Birge, R. P. Haddock, L. T. Kerth, J. R. Peterson, J. Sandweiss, D. H. Stork and M. N. Whitehead: *Proc. Pisa Conference* (June 1955).

([1]) E. McMillan: *Rev. Sci. Instr.*, **22**, 117 (1951).

3. – Preliminary Classification of the Positive K-Particles.

We have made a preliminary classification of K-particles according to their appearance at first sight.

1) K_L-mesons: one secondary with ionization at or near the minimum;

2) τ-mesons;

3) K-mesons with one « grey » secondary that is noticeably more ionizing than minimum. The corresponding ionization limit is badly defined (roughly 1.5 to 2 times minimum). This class consists of τ' and $\varkappa$ (or $K_{\mu 3}$) mesons, which are identified by following the secondary to its stopping point.

The numbers and percentages found are given in the Table I. They are compared with the corresponding numbers from the « G-stack » and from two experiments in the Berkeley K^+ beam.

TABLE I.

Type	Present experiment		« G-Stack » [1]		RITSON *et al.* [2]		BIRGE *et al.* [3]	
	Number	%	Number	%	Number	%	Number	%
K_L	376	91	315	89	693	90.5	460	90
τ	30	7.2	30	8.5	58	7.6	41	8
τ'	4–5 (*)	1–1.2	6	1.7	10	1.3	10	2
$\varkappa$ with slow μ	3–4 (*)	0.7–1	3	0.8	5	0.6	?	—
Total	414		354		766		511	

(*) One very steep secondary goes out of the stack after 19.3 mm. It could not be identified.

These proportions are completely consistent with one another, as regards the τ/K_L and τ'/τ ratios, and the number of $\varkappa$-mesons with slow secondaries. However, this good agreement may not be as significant as it seems at first, because of scanning biases. These are negligible in the fourth column (the K's have been found by following their tracks until they stop), and probably very small in the third. In our experiment, they are probably rather small, since the results obtained by our different scanners are quite similar. This can be explained by two favourable facts: most of the K's come from the area where the 6 GeV protons pass, and their tracks are therefore generally flat, which makes them much easier to detect; also the minimum grain density is high (23 to 24 blobs per 100 μm at plateau).

The energies of the « grey » secondaries are: energies of π's of τ''s: 14.6, 14.8, 25.2, 35.3 MeV; energies of μ's of $\varkappa$'s: 15.7, 24.4, 29.3 MeV. The ratio

of stopped π's to K's is 36674/372, or 98/1; it is of the same order as that found in plates exposed to cosmic rays.

4. – Observations on Secondaries of K_L-Mesons.

Among the 376 K_L's, we have selected 57 by using the following criteria: the direction of the secondary at the start must have a dip smaller than 20% and it must correspond to a length of at least 50 mm in the stack. These secondaries have either been followed to their end, or followed and measured (scattering and grain density) over a sufficient length to allow almost certain identification.

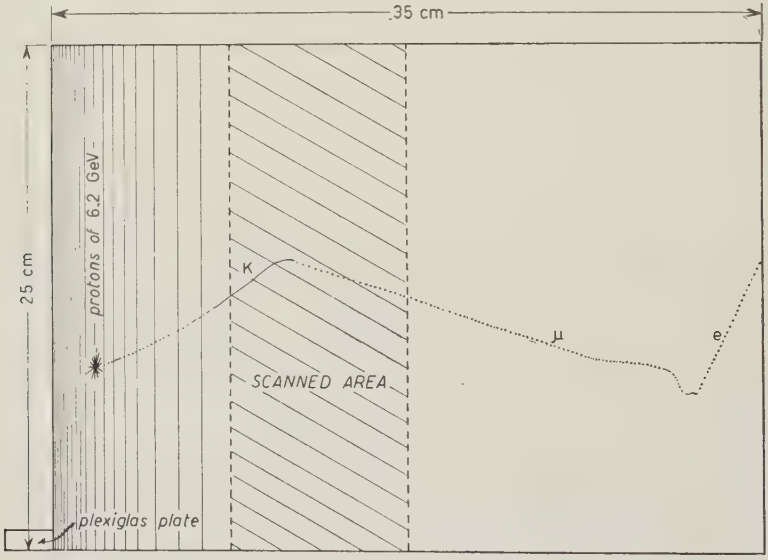

Fig. 1.

Table II gives a list of these measurements. In an appendix we supply some details on the way they have been made.

In the case of secondaries stopping in the emulsion, the range given in the next to last column is the measured range. The error includes that due to straggling. In the case of secondaries that were not followed to the end, the range indicated is generally derived from scattering measurements, using the range-energy curve of BARONI *et al.* [5]. However, the ranges of the secondaries of K_{157}, K_{283} and K_{322} are deduced from grain counting.

---

[5] G. BARONI, M. CASTAGNOLI, G. CORTINI, C. FRANZINETTI and A. MANFREDINI: *CERN*, BS 9 (1954).

The secondaries of K_ρ-mesons have been followed with great care by several observers. In order to be sure that these events are not coincidences between stopping protons and random electrons, the masses of the K_ρ's found have been measured by gap count. The masses found are all of the order of $950 \pm 150\ m_e$. In one case (K_{63}) a mass measurement was also made by grain counting; the result is $(915 \pm 40)\ m_e$.

One of the stopping K's gives an electron pair and another secondary ($g/g_{pr} = 1.2$) producing a star ($3+0\pi$) after 5.7 mm. This is very probably a case of $\chi \to \pi^- + e^- + e^- + \gamma$. It is not shown in Table II, as the secondary has a dip larger than 20%. A similar event has been observed by the Dublin group ([6]).

4·1. *Masses of the particles derived from measurements on the secondaries.*

1) *The* K_μ (or $K_{\mu 2}$).

a) If we take the 8 secondaries stopping in the emulsion, and one that leaves the stack at less than one millimetre from its stopping point (K_{283}), we find for the K_μ secondary a mean range of

$$R_\mu = 202.0 \pm 1.9 \text{ mm}.$$

The mean dispersion of the 9 values is 2.9 mm, whereas the formula used for computing straggling ([7]) predicts 5.7 mm.

This range is very close to those found in the « G-stack » (205.7 ± 2.4 mm) and by RITSON *et al.* ([2]) (204 ± 2.5 mm) in emulsions of almost the same density (3.84 to 3.85).

If we use the range-energy relation of BARONI *et al.* ([5]), this range corresponds to an energy of 151.1 ± 1.1 MeV and to a mass

$$M_{K_\mu} = (958 \pm 3)\ m_e\,.$$

If we use the Barkas relation ([8]), we find $E_\mu = 148.8 \pm 1.1$ MeV and

$$M_{K_\mu} = (952 \pm 3)\ m_e\,.$$

Various measurements made at low and medium ([9,10]) energies indicate that both the BARONI *et al.* and the BARKAS *et al.* curves are satisfactory

([6]) F. ANDERSON, G. LAWLOR and F. NEVIN: *Nuovo Cimento*, **2**, 608 (1955).

([7]) B. ROSSI: *High Energy Particles* (New York, 1952).

([8]) W. H. BARKAS and D. M. YOUNG: *University of California Radiation Laboratory, Report N. UCRL* 2579 Rev.

([9]) O. HEINZ: *UCRL* 2458 (January 12, 1954).

([10]) H. G. DE CARVALHO and J. I. FRIEDMAN: *Rev. Sci. Instr.*, **26**, 261 (1955).

TABLE II. – *Measurements made on 57 flat secondaries of* K_L*'s.*

No.	Type	Observed lenght	Scattering measurement		Grain counts		Total range mm	Remarks
			$p\beta c$ MeV	at (*) mm	g/g_{pr}	at (*) mm		
K_{80}	K_μ	198.7	—	—	—	—	198.7 ± 5.7	stops $\mu \rightarrow$ e decay
K_{97}	K_μ	205.1	—	—	—	—	205.1 ± 5.8	»
K_{105}	K_μ	201.3	—	—	—	—	201.3 ± 5.7	»
K_{108}	K_μ	206.5	—	—	—	—	206.5 ± 5.8	»
K_{246}	K_μ	198.6	—	—	—	—	198.6 ± 5.7	»
K_{250}	K_μ	197.6	—	—	—	—	197.6 ± 5.8	»
K_{267}	K_μ	204.0	—	—	—	—	204.0 ± 5.8	
K_{292}	K_μ	205.8	—	—	—	—	205.8 ± 5.8	»
K_{283}	K_μ	199.2	—	—	4.65 ± 0.90	198.6	200.0 ± 5.9	—
K_{157}	K_μ	187.3	—	—	1.71 ± 0.053	183.7	208.0 ± 9	—
K_{140}	K_μ	168.3	83 ± 10	163.0	—	—	203 ± 10	—
K_{124}	K_μ	100.0	209 ± 14	6.0	—	—	202 ± 19	—
K_{220}	K_μ	109.0	128 ± 14	102.0	1.198 ± 0.022	103.5	190 ± 17	—
K_{255}	K_μ	71.4	170 ± 13	65.4	—	—	208 ± 19	—
K_{289}	K_μ	54.4	190 ± 14	42.0	—	—	212 ± 20	—
K_{139}	K_μ	82.6	192 ± 18	8	1.045 ± 0.045	22.0	182 ± 25	—
		—	—	—	1.125 ± 0.060	66	—	—
K_{231}	K_μ	53.0	162 ± 18	37.0	1.030 ± 0.045	6	168 ± 26	—
		—	—	—	1.102 ± 0.045	26	—	—
		—	—	—	1.067 ± 0.034	34	—	—
K_{130}	K_μ	51.9	185 ± 19	7.0	—	—	—	—
		—	152 ± 17	35.0	1.07 ± 0.035	35	160 ±17	—
K_{132}	K_μ	125.3	202 ± 14	12.0	1.09 ± 0.023	12	—	—
		—	115 ± 18	125.0	1.24 ± 0.064	125	197 ± 13	—
$K_{\ldots}$	$K_\ldots$	138.0	131 ± 13	113.6	1.13 ± 0.034	116.1	103 ± 14	—

K_{298}	K_μ	47.9	202 ± 17	35.0	1.02 ± 0.036	31.1	222 ± 25	—
K_{146}	K_μ	44.1	201 ± 16	8.0	1.025 ± 0.058	42.8	194 ± 24	—
K_{237}	K_μ	51.1	172 ± 13	47.5	—	—	195 ± 19	
K_{68}	K_μ	23.3	206 ± 12	7.0	1.015 ± 0.020	7.0	199 ± 16	—
K_{94}	K_μ	37.4	215 ± 18	4.0	1.055 ± 0.031	10.8	209 ± 25	—
K_{166}	K_μ	27.9	201 ± 15	9.0	1.033 ± 0.025	9.5	195 ± 20	—
K_{151}	K_μ	26.0	196 ± 13	10.8	1.10 ± 0.025	9.5	190 ± 18	—
K_{73}	K_μ	13.8	217 ± 19	6.9	1.02 ± 0.040	3.6	214 ± 25	—
K_{180}	K_μ	34.0	216 ± 19	24.5	1.04 ± 0.032	27.4	229 ± 24	—
K_{85}	χ	112.2	—	—	—	—	112.2 ± 3.3	stops with $\pi \to \mu \to e$
K_{123}	χ	120.8	—	—	—	—	120.8 ± 3.3	»
K_{265}	χ	120.5	—	—	—	—	120.5 ± 3.3	»
K_{93}	χ	117.1	—	—	—	—	117.1 ± 3.3	»
K_{155}	χ	117.0	—	—	—	—	117.0 ± 3.3	»
K_{274}	χ	29.4	—	—	1.14 ± 0.044	3.6	—	gives $1+0\pi$ in flight
K_{230}	χ	28.7	163 ± 28	27.0	1.20 ± 0.041	6.5	134 ± 34	gives $4+0\pi$ in flight
K_{122}	χ	36.5	—	—	1.32 ± 0.16	36.1	—	gives $3+0\pi$ in flight
K_{99}	χ	0.4	—	—	1.32 ± 0.16	0.2	—	gives $4+0\pi$ in flight
K_{174}	χ	30.7	—	—	1.27 ± 0.043	28	—	scatter. of 48° after 30 mm
K_{226}	χ	65.6	134 ± 14	56.5	—	—	129.5 ± 19	—
K_{203}	χ	62.1	114 ± 14	52.1	1.49 ± 0.015	52.1	106 ± 15	—
K_{276}	χ	63.7	—	—	1.28 ± 0.072	17.3	—	—
		—	—	—	1.47 ± 0.044	60.7	—	—
K_{386}	χ	39.7	161 ± 14	12	1.22 ± 0.025	12	124 ± 19	—
K_{216}	χ	52.0	161 ± 20	22.5	—	—	—	—
		—	143 ± 19	43.9	1.31 ± 0.037	43.9	127 ± 15	—
K_{247}	χ	38.9	156 ± 13	12.8	1.17 ± 0.030	8.6	111 ± 16	—
		—	—	—	1.26 ± 0.06	30.5	—	—

(*) This is the distance from the decay point of the K to the middle point of the measured interval.

TABLE II (*continued*).

No.	Type	Observed length	Scattering measurement		Grain counts		Total range mm	Remarks
			$p\beta c$ MeV	at (*) mm	g/g_{pr}	at (*) mm		
K_{2C0}	K_β	42.9	250 ± 60	9.4	—	—	—	—
		—	152 ± 28	34.0	—	—	—	—
		—	41 ± 7	36.4	—	—	—	—
K_{141}	K_β	41.1	111 ± 10	3.9	—	—	—	—
		—	91 ± 11	10.1	—	—	—	—
		—	80 ± 9	15.2	1.04 ± 0.017	25.0	—	—
		—	67 ± 11	37.8	—	—	—	—
		—	38 ± 8	39.9	—	—	—	—
K_{190}	K_β	35.1	180 ± 24	13.2	—	—	—	—
		—	85 ± 10	16.0	1.10 ± 0.050	15	—	—
K_{63}	K_β	6.2	99 ± 14	1.8	1.04 ± 0.049	1.8	—	—
		—	28 ± 5	4.8	—	—	—	—
K_{100}	K_β	13.0	100 ± 11	4.3	—	—	—	—
		—	58 ± 9	10.8	1.05 ± 0.040	10.8	—	—
K_{75}	$\varkappa$	57.2	94 ± 11	6.0	1.35 ± 0.050	6.0	57.5 ± 1.8	—
		—	71 ± 8	33.9	1.43 ± 0.031	14.8	—	—
		—	—	—	1.67 ± 0.041	33.9	—	—
K_{322}	$\varkappa$	93.5	123 ± 6	13.7	1.21 ± 0.019	13.7	—	—
		—	—	—	2.15 ± 0.07	90.0	100.9 ± 1.3	—

(*) This is the distance from the decay point of the K to the middle point of the measured interval.

at these energies (although the former has been computed for a density of 3.96 instead of 3.85, which is the figure for the emulsions in general use). They differ slightly at high velocities ($\beta \sim 0.8 \div 0.9$) such as that of the K_μ secondary at the start. Since there are no experimental data on this part of the curve, it is impossible to choose between those two relations. Besides, the small value of the above given error will be significant only when this part of the range-energy relation will also be known with accuracy from experiment. Presently, we can but add to this error an arbitrary uncertainty. For instance, if we take $\pm 3\%$ in range, we are led to an error of $\pm 15\ m_e$ on the mass of the K_μ.

b) One can also derive the mass of the K_μ from scattering measurements made on the secondaries. The range-energy relation interferes again (since the measurements are made at various distances from the stopping point) but to a much smaller extent.

If we use the curve of BARONI *et al.*, we find for the mean range derived from scattering measurements on 19 K_μ, $R_\mu = 205.3 \pm 6.1$ mm. This corresponds to $E_\mu = 153.1 \pm 3.7$ MeV and to $M_{K_\mu} = (967 \pm 15)\ m_e$. This value is in agreement with that derived from the secondaries stopping in the emulsion.

2) *The* χ (or $K_{\pi 2}$).

a) The mean range of the four stopping secondaries is

$$R_\pi = 118.8 \pm 1.7 \text{ mm} .$$

The BARONI *et al.* range-energy relation then gives $E_\chi = 110.1 \pm 1.1$ MeV and $M_\chi = (971 \pm 4)\ m_e$.

The BARKAS *et al.* relation gives $E_\pi = 109.5 \pm 1.1$ MeV and $M_\chi = (969 \pm 4)\ m_e$.

An additional 3% uncertainty in range corresponds to $\pm 9\ m_e$.

b) The range derived from scattering measurements on five π secondaries is $R_\pi = 118.6 \pm 8.2$ mm, using the BARONI *et al.* relation. We thus get $E_\pi = 110.0 \pm 5.2$ MeV and $M_\chi = (971 \pm 20)\ m_e$.

The masses of the various K-mesons have been measured with accuracy at Berkeley by comparing their ranges with those of τ-mesons of the same momentum, in the K-beam. Thus HECKMAN, SMITH and BARKAS [11] have recently given:

$$M_{K_\mu} = (962.5 \pm 3.2)\ m_e$$

and

$$M_\chi = (972.2 \pm 4.7)\ m_e .$$

[11] *UCRL* 3156 (October 14, 1955).

These values are very close to those derived from secondary range measurements.

4·2. *Proportions of the various types of* K_L. – In Table III are given the numbers and percentages of the various types of K of Table II. As a comparison, we give the corresponding numbers observed in the G-stack (1) and in a stack exposed to the K-beam (RITSON *et al.* (2)).

TABLE III.

Type of K_L	Present experiment		« G-Stack »		RITSON *et al.*	
	Number	%	Number	%	Number	%
K_μ	34	60	37	55	13	60
χ	16	28	22	33	7	32
K_β	5	9	5	7	1	5
$\varkappa$ with fast μ	2	3	2–4	5	—	3 (*)
Total	57	100	66–68	100	21	100

(*) Two out of 60 K_L's have been identified by grain count.

No significant difference shows up in the proportions obtained in the three experiments. It must be remembered, however, that these proportions may be altered by scanning biases. These biases are probably negligible for RITSON *et al.*: they look for K's in a small area where they are easy to observe. On the contrary, the G-stack group have estimated that the percentage of K's missed is quite different for the different types of K; in their opinion, the number of K_μ's should be multiplied by 3.9, that of χ's by 1.8. In the present experiment, it seems that very few K's are missed in the parts of the plate furthest from the beam; however, more would be missed in the area closest to the beam, where there is a great density of tracks of all kinds. Yet we are inclined to think that the various types of K's are missed in much the same way, due to the two circumstances mentioned above (flat K's, high minimum grain density).

Besides, the various types of K's identified are spread out in a completely comparable manner over the area of the plates. The same can be said about the direction of the primaries near the end of the tracks.

5. – Discussion on the Relative Proportions.

Taking into account both the results of the first classification and of the 57 measured secondaries of K_L, the proportions in this stack of the different

types of K's are found to be approximately:

K_μ	χ	K_β	$\varkappa$	τ	τ'	all
54	26	8	4 (*)	7	1	100

These proportions are not significantly different from those found in the K-beam or in the G-stack.

What can we conclude from this?

1) The similarity of our results and those obtained in the Berkeley focused K^+-beam indicates similarity of mean life. The mean life of the K_μ, χ and τ have been measured recently by means of counters ([12,13]), and found to be very nearly the same. *Our results confirm this, and we can extend it to the* K_β *and the* $\varkappa$: *one can say that the mean life of the two latter particles is certainly not much shorter than that of the first three.*

2) Despite the possibility of biases, the similarity between the proportions given in the G-stack and in our results seems to shows that there is no marked difference in the relative frequencies of production of the various types of K by 6.2 GeV protons or by high-altitude cosmic radiation. This result concerns only the K's having a low energy in the stack.

6. – Study of the $\varkappa$ (or $K_{\mu 3}$).

6·1. *Description of two* $\varkappa$ *events with a fast secondary.* – There are two $\varkappa$-mesons mentioned in Table II. The secondary of the second one has, as far as we know, the highest energy so far observed in $\varkappa$'s.

The secondary of the first one (K_{75}) stops between two plates: hence its disintegration has not been observed. From a scattering measurement made on the last plate, its residual range as it leaves it is $0.3^{+0.5}_{0.3}$ mm. Its $\varkappa$ nature is clearly shown by grain counts made on 2/3 of its range. Its energy is 61.5 ± 1.4 MeV.

The secondary of K_{322} is flat at first, then its dip increases up to a value of 0.4. It leaves the stack after 93.5 mm. The scattering has been measured only on the flat part of the track (27 mm from the decay point), using cell-lengths of 50 μm, 100 μm and 150 μm. From this measurement and from the

(*) This number is derived from the study of the $\varkappa$-decay given below.

([12]) V. Fitsch and R. Motley: Private communication (November 1955).

([13]) L. W. Alvarez, F. S. Crawford, M. L. Good and M. L. Stevenson: *UCRL* 3165 (October 1955).

grain count made on the same interval, the mass of the secondary is $(205 \pm 13)\ m_e$. In this computation, we use our calibration curve of grain density vs. range (Fig. 2). The uncertainties both on this curve (± 0.02 on g/g_{pr}) and on the scattering constant ($\pm 2\%$) are included in the error. Besides, if this event were a χ-meson, g/g_{pr} of the secondary at 90 mm from the decay would be 1.72 ± 0.04, instead of 2.15 ± 0.07 observed which agrees with the energy of the particle (supposed to be μ) deduced from the scattering measurement. The energy of this secondary is 90.5 ± 2.1 MeV.

The secondaries of both K_{75} and K_{322} are emitted in the backward hemisphere: it is necessary to see if these events could not be K_μ's decaying in flight. The residual ranges of such K_μ's at the point of decay can be calculated; they are found to be respectively 29 mm and 17.4 mm. This is quite inconsistent with the appearance of both tracks, which is normal for decays at rest.

6·2. *The κ-decay mode.* – It is interesting to study what information is conveyed by present experimental data in large emulsion blocks about the κ-decay mode.

We can reject the $\kappa \to \mu + \nu + \nu$ decay, and also $\kappa \to \mu + \nu + \gamma$; a K giving a slow μ and an electron pair has recently been observed [11]. From its geometry, this case is inconsistent with the two decay modes given above, and suggests the presence of one or more neutral pions.

Supposing the κ to be a boson, two possible decay schemes are:

(1) $$\kappa \to \pi^0 + \mu + \nu,$$

(2) $$\kappa^+ \to \pi^0 + \pi^0 + \mu + \nu\ .$$

1) In mode (2), the maximum energy of the muon is 78 MeV, assuming $M_\chi = 965\ m_e$. Since the mass of the κ giving a slow μ has been found to be very near the mass of the τ [11], our observation of a secondary of 90 MeV is inconsistent with this scheme (unless there are two kinds of κ's with different masses). Besides, there is another serious objection against decay (2): the decay mode $\kappa \to \pi^+ + \pi^- + \mu + \nu$ (2′) should occur at least as often as (2). From the four experiments mentioned earlier, the κ/τ ratio is 20/159 (about 1/8). There should therefore be at least one (2′) in 8 apparent τ-decays. Yet at the Pisa meeting, E. Amaldi cited 54 τ's completely analyzed, whereas only one possible $\kappa \to \pi^+ + \pi^- + \mu + \nu$ decay has been mentioned so far [15]. Moreover, over 250 secondaries of τ have been followed to the end of their range. If

[14] G. Yekutieli, M. F. Kaplon and T. F. Hoang: Private communication (October 1955).

there is one (2′) in eight τ decays, approximately 10 of these should have been μ's. Only one possible μ has been found ([15]).

2) The main difficulty for scheme (1) ($\varkappa \to \pi^0 + \mu + \nu$) seems to be that the number of fast muons found is much too small. The energy spectrum, assumed proportional to phase-space volume (see for instance the curve given by RITSON *et al.* ([2])), ends at 130 MeV and has its maximum around 75 MeV. Such a spectrum seems in complete disagreement with the observed energies, most of which are less than 40 MeV.

It may be however that this disagreement is more apparent than true: many fast secondaries are probably missed because of scanning biases and of the difficulty in telling a $\varkappa$ with fast μ from a χ or a K_μ.

RITSON *et al.* ([2]) have already discussed this question and concluded nevertheless to a too small number of observed fast secondaries. In a similar way, let us assume that for $E_\mu < 25$ MeV ($g/g_{\text{plateau}} > 2$), all the $\varkappa$'s are found at first scanning. If we add the results of the four experiments already mentioned (G-stack ([1]), RITSON *et al.* ([2]), BIRGE *et al.* ([3]), and the present experiment) we get 10 $\varkappa$'s with $E_\mu < 25$ MeV for 1853 K_L's observed. If we suppose that decay scheme (1) is correct and that its energy spectrum is proportional to phase-space volume, this corresponds to one $\varkappa$ (all energies) for every 21 K_L's. Let us now consider the other end of the spectrum: $\varkappa$'s with secondaries between 80 and 130 MeV. From the proportion of one $\varkappa$ in 21 K_L, one would have 33 such events in the four experiments, whereas only one has been observed. But in practice, these are not recognized at first sight, and even if measurements have been made on a few cm of secondary track, there is a strong chance of their being taken for χ or K_μ. To be sure to recognize such a secondary of $\varkappa$, one must either follow it to the end, or follow it for at least half the track length and measure it carefully. In the four experiments mentioned above, only ~ 77 K_L's have been measured in this way. Therefore, one can expect to have observed not 33, but $(77/1853)\cdot 33 \sim 1.4$ such secondaries.

For intermediate energy values, a similar discussion shows that there is also no major disagreement between the number of $\varkappa$'s found and the number that could reasonably be expected. This comparison is summarized in Table IV; the figures given must naturally be taken only as rough approximations.

In spite of its obvious weaknesses, this line of thought seems to show that it is so far possible to attribute all $\varkappa$-decays to the $\varkappa \to \pi^0 + \mu + \nu$ scheme. It also shows that, in order to confirm this, it is important to follow to the

([15]) K. R. DIXIT: *Zeits. f. Naturforsch.*, **9***a*, 355 (1954).

end as many K_L secondaries as possible, especially those appearing to be χ-mesons.

TABLE IV.

Energy	Number of $\varkappa$ found	Corresponding number of K_L's	Expected number of $\varkappa$
$E_\mu < 25$ MeV	10	1853	10
25 MeV $< E_\mu <$ 50 MeV	6	1215 (+)	< 12 (*)
50 MeV $< E_\mu <$ 80 MeV	3	180 (−)	2.7
80 MeV $< E_\mu <$ 130 MeV	1	77	1.4

(+) This class corresponds to $1.4 < g/g_{\text{plateau}} < 2.0$. Some of the $\varkappa$'s are probably not detected on the first scanning.

(−) It seems that RITSON *et al.* have only tried to detect these $\varkappa$'s among 60 secondaries on which a quick grain count had been performed, and not among the 700 − odd K_L's found.

(*) Such $\varkappa$'s are generally not recognized as such at first sight, but are found only after measurements of the secondary.

7. – Negative K-Particles.

In addition to the 414 observed K^+-mesons, 5 negative K-mesons have been found. The K^+/K^- ratio is not different from that observed in the 350 MeV/c beam at Berkeley ([16]).

The characteristics of the capture stars formed by the K^--particles are listed in the Table V.

TABLE V.

K_1^-	Σ^+ of 780 μm. Stops and gives a proton of 1630 μm. ($\Sigma^+ \to p + \pi^0$).
K_2^-	Σ^+ of 110 μm. Stops and gives a proton of 1625 μm. π^- of 35.3 mm ($E_\pi = 50.5$ MeV). Gives a σ-star. 1 evaporation proton. 2 recoil tracks.
K_3^-	Σ^+ of 1755 μm. Stops and gives a proton of 1615 μm. 1 evaporation track.
K_4^-	π^- of 34.3 mm ($E_\pi = 49.5$ MeV). Gives a one prong σ-star.
K_5^-	(*a*) Hyperfragment of 4 μm. (*b*) π^+ of 68.1 mm giving π-μ-e decay ($E_\pi = 76$ MeV). (*c*) Proton-like track of 270 μm. (*d*) 1 recoil track.

([16]) W. W. CHUPP, S. GOLDHABER, G. GOLDHABER, W. R. JOHNSON and S. WEBB: *Proc. Pisa Conference* (June 1955).

The first three events are probably examples of the scheme:

$$K^- + p \rightarrow \Sigma^+ + \pi^- ,$$

the negative pion of N°'s 1 and 3 being absorbed in the nucleus. If the proton were free, the π^- would have 85 MeV energy (range 81 mm) and the Σ^+ 13 MeV (range 730 μm). The difference with the observed ranges is easily explained by the Fermi momentum of the proton in the nucleus, and by secondary interactions of the reaction products.

In the K_5^- star, prong (*a*) is a black track of 4 μm giving rise to a secondary star consisting of a proton of 130 MeV (stopping in the stack), an evaporation track of 62 μm and a recoil track of 18 μm.

The most probable interpretations of this event seem to be

$$K^- + p + p \rightarrow \text{bound } \Lambda^0 + \pi^+ + n ,$$

or

$$K^- + p \rightarrow \text{bound } \Lambda^0 + \pi^0,$$

followed by $\pi^0 + p \rightarrow n + \pi^+$.

The geometry of the secondary star fits rather well with the non-mesonic decay of an hyperfragment of $Z = 5$ or 6.

Other simple interpretations of the K_5^- event would be:

1) $K^- + p \rightarrow \Lambda^0 + \pi^+ + \pi^- + 36$ MeV, the π^- being reabsorbed. This scheme is ruled out by the too high energy of the π^+.

2) $K^- + p \rightarrow \Sigma^- + \pi^+$: (*a*) would represent the capture of the Σ^-. This seems rather improbable from the high energy of the proton of the supposed Σ^- star; a very high Fermi momentum would be necessary in order to get such a fast proton in a reaction of the type Σ^- + nucleus $\rightarrow \Lambda^0$ + nucleus + p. Besides, FRY *et al.* [16] do not mention any fast proton in the Σ^- stars.

The masses of the negative K-mesons have been measured by gap count at the end of the track. They are all of the order of $(1000 \pm 250)\, m_e$.

It may seem surprising to have found such a large proportion of stars containing a Σ (3/5), whereas, according to various authors [17-20] this ratio

---

[17] J. HORNBOSTEL and E. O. SALANT: *Phys. Rev.*, **98**, 218 (1955).

[18] W. F. FRY, J. SCHNEPS, G. A. SNOW and M. S. SWAMI: *Phys. Rev.*, **100**, 350 (1955).

[19] W. W. CHUPP, G. GOLDHABER, S. GOLDHABER and F. H. WEBB: *Proc. Pisa Conference* (1955).

[20] E. P. GEORGE, A. J. HERZ, J. N. NOON and N. SOLNSTEFF: Private communication (October 1955).

should be about 1/4. This may be a mere fluctuation. It may also indicate that some K^-'s have been missed.

* * *

In the course of this work, several hyperfragments have been found. An analysis of these will be given in a later paper. The parent stars of the K-mesons observed in the stack are also under study.

* * *

We are glad to express our great indebtedness to Professor B. LAWRENCE and Professor E. J. LOFGREN for having arranged the exposure of the emulsions, thus allowing us the privilege of taking part in the research program on K-mesons performed with the use of the Bevatron. We also particularly thank Dr. W. W. CHUPP, Dr. G. GOLDHABER and the other members of the Bevatron staff for their kind cooperation and efficiency in preparing and performing the irradiation. It was the first time a large stack was exposed inside the accelerator, and it was therefore necessary to devise and manufacture special apparatus, and perform preliminary tests.

We also thank Mr. WALLER and his colleagues at Ilford, who, despite a particularly heavy manufacturing schedule, successfully and punctually prepared this large stack.

This work was performed with the financial support of the Centre National de la Recherche Scientifique, to which we express our gratitude.

We finally thank the scanning staff of the laboratory, consisting of Mmes J. COURTOIS, C. SEROPIAN, M.elles M. BOURDILLON, M. DUCROS, S. MERRENS, M.M. RANÇON, A. VANHOVE, and recently M.lles Y. CORRE, M. LEPLÉ, R. LHÉRAULT, for the considerable work they have done in finding the K's.

APPENDIX

Details on the methods used for measuring secondaries.

1. *Range measurements.* – We have added to the measured length the emulsion equivalent to the sheets of paper placed between consecutive emulsions; these are roughly equivalent to 5 μm of emulsion, which corresponds to an increase in range of about 0.8%.

The various sources of error (errors on the appraisal of the entry and exit point in each emulsion, distortions, uncertainty on the emulsion equivalent of the passage in paper etc.) are quite small when compared to the uncertainty due to straggling. For instance, in the case of a K_μ secondary (μ of 20 cm range),

they add up to about 0.3 to 1.5%, whereas straggling corresponds to 2.8%. In the few cases where distortions are not negligible, the shortening or lengthening of the track has been estimated by comparison with neighbouring steep tracks, and the necessary corrections were made. To do this, we have assumed that the real direction of a track is that of its « air » end. (This has been cheeked many times with fast tracks, and is practically always true).

2. *Scattering.* – The noise has been eliminated in the usual manner between two different cell-lengths; cells of 75 μm and 150 μm have been used. We have not taken into account track deformations, but we have checked in each case that their influence is negligible. The scattering constants used are those of PICKUP and VOYVODIC ([21]). An uncertainty of 2% on this constant ([1]) is included in the error given on $p\beta c$.

3. *Grain density.* – For each measurement, we have taken as standard in each plate a number of beam protons located at different depths in the vicinity of the measured track. Such protons are easily found all over the stack, and easily recognized from their direction. Their energy is certainly very close to 6 GeV.

In Table II, we have indicated the ratio of measured track grain density (g), to 6 GeV proton track grain density (g_{pr}). By measuring K_β secondaries and other electrons, we have found

$$g_{pr}/g_{plateau} = 0.931 \pm 0.010 .$$

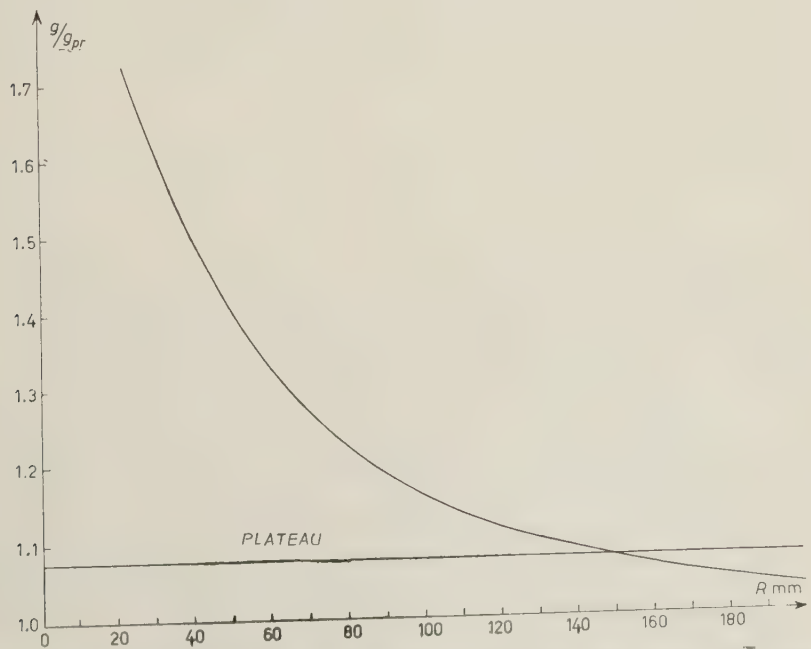

Fig. 2. – Calibration curve giving the grain density vs. range for the μ-mesons.

([21]) L. VOYVODIC and E. PICKUP: *Phys. Rev.*, **85**, 91 (1955).

We have generally used grain density only as a confirmation of the nature of the secondaries, and not to calculate their range. Fig. 2 gives g/g_{pr}^{*} against residual range for the μ-meson. This curve is derived from measurements made on the secondaries (both stopping and not stopping).

RIASSUNTO (*)

Un grosso pacco di emulsioni è stato esposto al fascio protonico di 6.2 GeV del bevatrone di Berkeley. Sono stati osservati 414 K^{+} disintegranti a riposo. Il loro probabile tempo di volo è $\sim 5 \cdot 10^{-10}$ s. Sono stati misurati in dettaglio 57 secondari piani al minimo o prossimi al minimo di ionizzazione. Le proporzioni di K_{β}, χ, K_{μ}, $\varkappa$, τ e τ' risultano rispettivamente del 54%, 26%, 8%, 4%, 7% e 1%. Non differiscono, cioè, in modo significativo dalle proporzioni riscontrate in pacchi esposti al fascio focheggiato di K^{+} del bevatrone o alla radiazione cosmica, il che è indice di similitudine nella vita media e nelle frequenze relative di produzione dei differenti tipi di K. I range medi di 8 secondari di K_{μ} e di 4 secondari di χ giunti a riposo sono rispettivamente 202 ± 1.9 mm e 118.8 ± 1.7 mm. Le masse del K_{μ} e del χ dedotte da questi range sono assai prossime a quelle risultanti dalla misura diretta nel fascio dei K. Sono stati osservati 2 eventi $\varkappa$ con secondari di 61.5 e 90.5 MeV. Si esaminano tutti i dati noti sui $\varkappa$ nei grossi pacchi di emulsioni; si esprime il parere che finora i risultati sono compatibili con lo schema $\varkappa \to \pi^{0}+\mu+\nu$. Si sono trovati e si descrivono 5 eventi K^{-}.

(*) *Traduzione a cura della Redazione.*

IL NUOVO CIMENTO Vol. III, N. 4 1° Aprile 1956

Charge Conjugation, a New Quantum Number G, and Selection Rules Concerning a Nucleon-Antinucleon System.

T. D. Lee

Columbia University - New York, N.Y.

C. N. Yang

Institute for Advanced Study - Princeton, N.J.

(ricevuto il 30 Gennaio 1956)

Summary. (*). — A new quantum number is introduced which leads to selection rules concerning transitions between states with heavy particle number = 0. They are applied to the system nucleon-antinucleon; it is also shown that they can be extended to include the conservation of strangeness.

(*) *Editor's care.*

Whenever several conservation laws operate for the same system it is oftentimes possible to obtain new quantum numbers and new selection rules. For the pion-nucleon-antinucleon system in strong interaction one has besides the usual spin parity conservation laws the additional conservation laws of isotopic spin, charge conjugation and heavy particle number. We shall see that these conservation laws together do lead to a new quantum number for all systems with heavy particle number = 0. Application of this result to a nucleon-antinucleon system gives the selection rules tabulated in Tables I and II.

We shall be concerned with these operators:

$$I_1, I_2, I_3 = \text{isotopic spin operators},$$

$$G = C \exp[i\pi I_2],$$

and $N =$ number of heavy particles.

TABLE I. – *Selection Rules for* $\bar{p} + n \to m\pi$.

State	Spin parity	I	G	$\pi^- + \pi^0$	$2\pi^- + \pi^+$	$\pi^- + 2\pi^0$	$2\pi^- + \pi^+ + \pi^0$	$\pi^- + 3\pi^0$	$3\pi^- + 2\pi^+$	$2\pi^- + \pi^+ + 2\pi^0$	$\pi^- + 4\pi^0$
$^1S_0$	0^-	1	—	×			—	—			
$^3S_1$	1^-	1	+		—	—			—	—	—
$^1P_1$	1^+	1	+	×	—	—			—	—	
$^3P_0$	0^+	1	-	—	×	×	—	—			
$^3P_1$	1^+	1	—	×			—	—			
$^3P_2$	2^+	1	—	—			—	—			

× means strictly forbidden and — means forbidden so far as the isotopic spin is a good quantum number.

Here C is the charge conjugation operator. The advantage of using the operator G instead of C is that G commutes with I_1, I_2, and I_3, while C does not.

To see this one need only write down in the rest system the explicit form for these operators between the four states (1) with the same z component of spatial spin:

$$\begin{pmatrix} p \\ n \\ \bar{n} \\ -\bar{p} \end{pmatrix}.$$

They are

$$I_1 = \begin{pmatrix} 0 & 1 & 0 & 0 \\ 1 & 0 & 0 & 0 \\ 0 & 0 & 0 & 1 \\ 0 & 0 & 1 & 0 \end{pmatrix}, \quad I_2 = \begin{pmatrix} 0 & -i & 0 & 0 \\ i & 0 & 0 & 0 \\ 0 & 0 & 0 & -i \\ 0 & 0 & i & 0 \end{pmatrix}, \quad I_3 = \begin{pmatrix} 1 & 0 & 0 & 0 \\ 0 & -1 & 0 & 0 \\ 0 & 0 & 1 & 0 \\ 0 & 0 & 0 & -1 \end{pmatrix}$$

$$G = \begin{pmatrix} 0 & 0 & 1 & 0 \\ 0 & 0 & 0 & 1 \\ -1 & 0 & 0 & 0 \\ 0 & -1 & 0 & 0 \end{pmatrix}, \quad N = \begin{pmatrix} 1 & 0 & 0 & 0 \\ 0 & 1 & 0 & 0 \\ 0 & 0 & -1 & 0 \\ 0 & 0 & 0 & -1 \end{pmatrix}.$$

(1) Notice the minus sign in front of the $\bar{p}$ state in the convention here. The definition of $\bar{n}$ and $\bar{p}$ as the antineutron and antiproton states is here so chosen that they are identically related to the neutron and proton states. In other words, charge conjugation is here defined in the same way for the neutron and the proton.

TABLE II. – *Selection Rules for* $\bar{p}+p \to m\pi$ *or* $\bar{n}+n \to m\pi$.

State	Spin parity	C	I	G	$2\pi^0$	$\pi^+ + \pi^-$	$3\pi^0$	$\pi^+ + \pi^- + \pi^0$	$4\pi^0$	$\pi^+ + \pi^- + 2\pi^0$	$2\pi^+ + 2\pi^-$	$5\pi^0$	$\pi^+ + \pi^- + 3\pi^0$	$2\pi^+ + 2\pi^- + \pi^0$
$^1S_0$	0^-	$+$	0	$+$	×	×	–	–				–	–	–
			1	–	×	×				–				
$^3S_1$	1^-	–	0	–	×	–	×		×	–		×		
			1	$+$	×		×	–	×			×		–
$^1P_1$	1^+	–	0	–	×	×	×		×	–	–	×		
			1	$+$	×	×	×	–	×			×	–	–
$^3P_0$	0^+	$+$	0	$+$			×	×					–	–
			1	–	–	–	×	×	–	–				
$^3P_1$	1^+	$+$	0	$+$	×	×	–	–				–	–	–
			1	–	×	×			–	–				
$^3P_2$	2^+	$+$	0	$+$				–						–
			1	–	–	–			–	–	–			

× means strictly forbidden and – means forbidden so far as the isotopic spin is a good quantum number.

For a multiple particle system, I and N are additive and G multiplicative. One therefore has *in general*

$$[I_i, G] = [I_i, N] = 0 , \tag{1}$$

$$GN + NG = 0 , \tag{2}$$

$$G^2 = (-1)^N . \tag{3}$$

Besides G is unitary by definition and N has integral eigenvalues. Solving the relations (1) to (3) one obtains the following:

(1) For a state with a definite value $\neq 0$ for N, the quantum numbers are N, I^2 and I_3. The operation of G on the system gives a state with the same I^2, I_3 but changes the sign of N.

(2) For a state with $N = 0$ the quantum numbers are $N = 0$, I^2, I_3 and $G = \pm 1$. Besides, *all components of the same I-multiplet have the same value for G*. The pions obviously belong to this category, with $I^2 = 1(1+1)$ and $I_3 = \pm 1$ or 0. To find their value for G we notice that a π^0 has matrix elements connecting it to the $^1S_0$ state of a proton-antiproton system. Such a system has $C = +1$ ([2]). Now π^0 has a total I-spin equal to 1. Therefore $\exp[i\pi I_2]$ for π^0 is -1. Hence by definition $G = -1$ for π^0. *Therefore $G = -1$ for all pions, charged or neutral.*

The existence of the quantum number G leads to interesting selection rules ([3]) concerning transitions between states with $N = 0$. In particular one sees that *an even number of pions cannot by strong interaction go into an odd number of pions*. When applied to a system consisting of a nucleon and an antinucleon one obtains the selection rules tabulated in Tables I and II.

The above consideration can easily be extended to include the conservation ([4]) of strangeness S. (S is defined to be $2Q - 2I_3 - N$). The commutation relations between S and the other operators are

$$[N, S] = [S, I_i] = 0 ,$$

$$GS + SG = 0 ,$$

([2]) L. Wolfenstein and D. G. Ravenhall: *Phys. Rev.*, **88**, 279 (1952); A. Pais and R. Jost: *Phys. Rev.*, **87**, 871 (1952).

([3]) Most of these results have been stated in the literature in various forms. See A. Pais and R. Jost: *Phys. Rev.*, **87**, 871 (1952); L. Michel: *Nuovo Cimento*, **10**, 319 (1953); D. Amati and B. Vitale: *Nuovo Cimento*, **2**, 719 (1955).

([4]) M. Gell-Mann: *Phys. Rev.* (in press); T. Nakano and K. Nishijima: *Prog. Theor. Phys.*, **10**, 581 (1954).

and

$$G^2 = (-1)^{N+S}.$$

Solving these commutation relations one obtains results similar to (1) and (2) discussed above, except that S is now an additional quantum number. G is a good quantum number $= \pm 1$ in this case only if both N and S are zero.

RIASSUNTO (*)

Si introduce un nuovo numero quantico G che porta a regole di selezione riguardanti le transizioni fra stati con un numero N di particelle pesanti nullo. Tali regole sono poi applicate al sistema nucleone-antinucleone e viene anche mostrato che esse possono essere estese in modo da comprendere la conservazione della « stranezza » S.

(*) *A cura della Redazione.*

^{160}Tb Decay.

G. Bertolini, M. Bettoni and E. Lazzarini

Istituto di Fisica Sperimentale del Politecnico - Milano

(ricevuto il 4 Febbraio 1956)

Summary. — By means of an intermediate β spectrometer and a scintillation spectrometer, the decay of ^{160}Tb has been studied. Coincidences between β^- continuous spectrum and selected γ-rays allows the resolution of the β^- spectra of low energy. β^- spectra of 367 ± 12, 564 ± 6.5, 861 ± 1.8, and 1711 ± 7 keV have been resolved. From their photospectrum relative intensities of γ-rays have been taken. Conversion coefficients of some γ-rays have been obtained. A decay scheme is suggested. The possibility of the rotational character of some of the excited levels, predicted by the Bohr-Mottelson theory, is discussed.

1. – Introduction.

The β^- decay of ^{160}Tb and the γ decay of ^{160}Dy have been studied by several investigators ([1-6]) and their results are summarized in Table I and Table II.

Magnetic spectrographs have been used to resolve β^- decays and γ lines. β^--γ, β^--e^- and e^--e^- coincidence studies have suggested many decay schemes. A careful study of decay scheme has been performed by Burson and coworkers ([5]) by γ-γ coincidences. In this way the predominant γ transitions

---

([1]) J. M. Cork, R. G. Shreffler and C. M. Fowler: *Phys. Rev.*, **74**, 240 (1948).

([2]) S. B. Burson, K. W. Blair and D. Saxon: *Phys. Rev.*, **77**, 403 (1950).

([3]) J. M. Cork, C. E. Branyan, W. C. Rutledge, A. E. Stoddard and J. M. Le Blanc: *Phys. Rev.*, **78**, 304 (1950).

([4]) L. Y. Shavtvalov: *Izv. Akad. Nauk SSSR, Sez. Fiz.*, **17**, 503 (1953).

([5]) S. B. Burson, W. C. Jordan and J. M. Le Blanc: *Phys. Rev.*, **94**, 103 (1954).

([6]) V. Keshishian, H. W. Krusc, R. J. Klotz and C. M. Fowler: *Phys. Rev.*, **96**, 1050 (1954).

of ^{160}Dy was put in evidence. Among the investigators there is no agreement about the β^- decays of ^{160}Tb and this lack of consistency is due to the difficulty of resolving all the possible β^- spectra present in the decay.

TABLE I. – *β-decay observed in early experiments.*

References		(1)	(2)	(4)	(6)
β^--decay energy in keV	β_1	—	—	—	280 (19 %)
	β_2		396 (16 %)		461 (19 %)
	β_3	546	521 (41 %)	540 ÷ 590 (60 %)	557 (32 %)
	β_4	882	860 (43 %)	850 (40 %)	851 (30 %)

TABLE II. – *γ-ray energies observed in early experiments.*

γ_1	86.3 (1-3,5,6)	γ_7	282 (3,6)	γ_{13}	873 (3,5,6)
γ_2	93.4 (3,5,6)	γ_8	297.6 (1-3,5,6)	γ_{14}	960 (3,5,6)
γ_3	112.1 (1)	γ_9	375.2 (3)	γ_{15}	1174 (1,5,6)
γ_4	176.2 (3)	γ_{10}	391.3 (3,5,6)	γ_{16}	1265 (5,6)
γ_5	196.1 (1-3,5,6)	γ_{11}	410.3 (3,6)		
γ_6	24.18 (3,5,6)	γ_{12}	759 (5,6)		

V. KESHISHIAN and coworkers (8) observed a great number of γ-rays of low intensity, but only a few energies have been incorporated into the table.

Hence, further investigations on the β^- continuous spectrum in coincidence with different γ-rays for the purpose of obtaining additional information concerning the decay scheme in question, seemed worthwhile.

2. – Sources.

The sources were obtained with the method of SCHAFER and HARKEV (7) and the uniformity of the active layer was controlled with the autoradiographic method.

Different sources were used in the course of the experiment:

a) Investigation of β^- spectrum: mean thickness of the source $\sim 7 \cdot 10^{-4}$ mg/cm^2; backing ~ 0.7 mg/cm^2 of aluminium or ~ 0.16 mg/cm^2 of nylon.

(7) V. J. SCHAFER and D. HARKEV: *Journ. Appl. Phys.*, **13**, 427 (1942).

b) β^--γ coincidences: mean thickness ~ 0.1 mg/cm^2; backing ~ 0.7 mg/cm^2 of alluminium.

c) Investigation of higher energy β^- spectrum and photospectrum: mean thickness ~ 1 mg/cm^2; backing ~ 0.7 mg/cm^2 of alluminium.

3. – Experimental Apparatus.

A high trasmission intermediate image magnetic spectrometer ([8]) was used to investigate the β^- spectra. In the β-γ coincidence arrangement a NaI(Tl) cylindrical crystal, 1″ diameter $\times$ 1″ thickness was mounted behind the source to detect the γ-rays, and an anthracene cylindrical crystal, $\frac{1}{2}$″ diameter $\times$ $\frac{1}{2}$″ thickness, detected the focalized electrons. The apparatus was the same used in a previous work ([9]). A fast single channel allowed the sending of only γ-rays of a determined energy interval in the coincidence stage.

In order to investigate γ lines energies and their relative intensities, converters of lead, gold and bismuth were prepared by vacuum evaporation on copper 0.7 mm thick. The distance source-converter was 2 mm.

4. – β^--Spectrum.

The Fermi plot of β^- spectrum shows 4 components of maximum energy: 367, 564, 861 and 1711 keV (Fig. 1). The existence of a β^- component of maximum energy higher than 860 keV had been suggested by SHAVTVALOV ([4]) but not clearly observed.

In Table III are shown the energies, relative intensities and log *ft* values of the β^- spectra. As appears from Fig. 1, the evaluation of the maximum energy of the β_1 spectrum is affected by big error. Similar analysis of the

TABLE III. – *β-decay energy, intensities and* log *ft*.

E_{max} keV	From total spectrum		From coincidence β^--$\gamma > 800$ keV	
	intensity	log *ft*	intensity	log *ft*
1711 ± 7	0.3 %	12	—	—
861 ± 1.8	34.8 %	8.8	20.6 %	9.03
564 ± 6.5	51.5 %	8.2	55.5 %	7.9
367 ± 12	13.9 %	7.9	23.9 %	7.65

([8]) G. BOLLA, S. TERRANI and L. ZAPPA: *Nuovo Cimento*, **12**, 875 (1954).
([9]) G. BERTOLINI, M. BETTONI and E. LAZZARINI: *Nuovo Cimento*, **2**, 273 (1955).

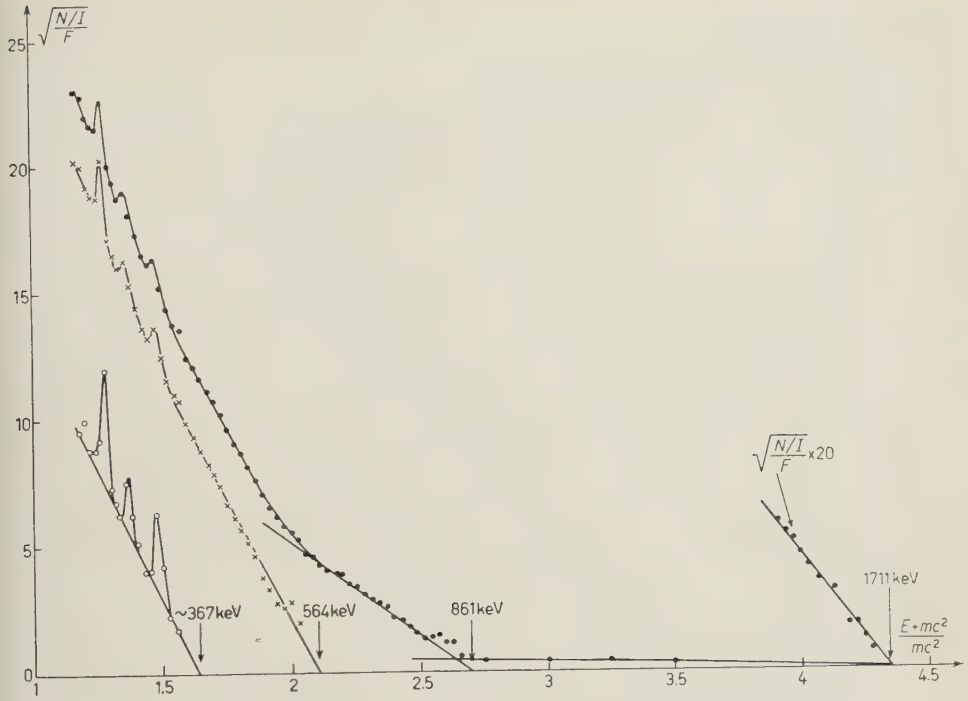

Fig. 1. – ^{160}Tb Fermi plot.

β^- spectrum made by V. KESHSHIHIAN and coworkers (6) had given in the low energy region two components of maximum energy of 461 and 280 keV.

5. – β^--γ Coincidences.

Fig. 2 shows the γ-ray spectrum detected by the NaI(Tl) crystal. The vertical lines indicate the interval of the spectrum, which was successively

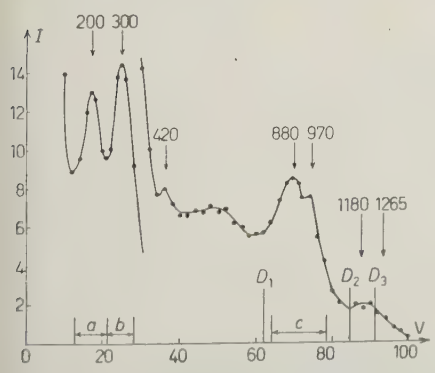

Fig. 2. – γ-ray scintillation spectrum of ^{160}Tb. The energies are in keV.

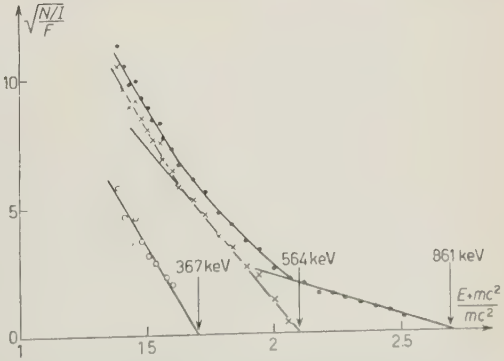

Fig. 3. – Fermi plot of the β-spectrum in coincidence with γ-rays of 200 keV.

limited by the single channel and the bias of the discriminator in the two sets of measurements. Fig. 2, 3, 4, 5, 6 give the experimental results, Tables IV, and III summarize them.

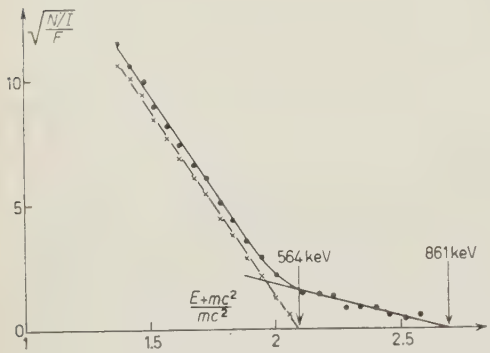

Fig. 4. – Fermi plot of the β-spectrum in coincidence with γ-rays of 300 keV.

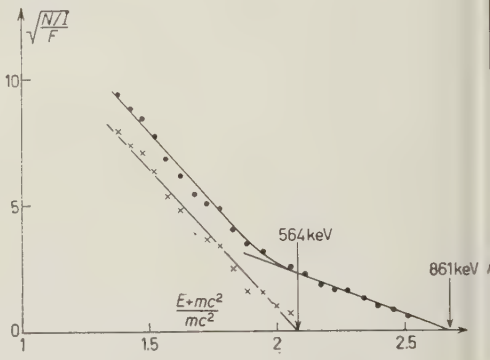

Fig. 5. – Fermi plot of the β-spectrum in coincidence with γ-rays of 970 and 880 keV.

TABLE IV. – β-γ *coincidence results.*

The numbers are proportional to the area of the β^- spectra in coincidence. Columns *a*), *b*) and *c*) represent the results of the coincidences with γ-rays of 200, 300 and 800 ÷ 970 keV respectively. Columns D_1, D_2 and D_3 represent the results of the coincidences with γ-rays of energies higher than 800, 1100 and 1180 keV respectively.

	E_{max} keV	*a*	*b*	*c*	D_1	D_2	D_3
		200	300	970 ÷ 880	> 800	> 1100	> 1180
β_3	861	12.2 *	5.8 *	8.6	10.8	1.3	1.1
β_2	564	23.3 *	41.1 *	28.9	29.5	7.3	6.9
β_1	367	13	·	—	12.5	13.2	8.4

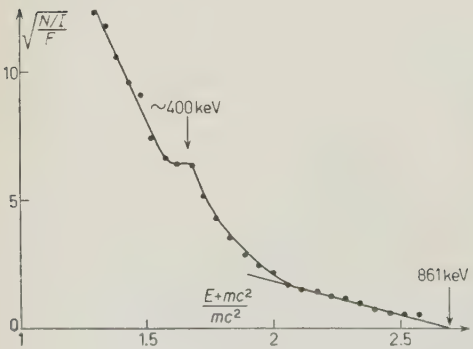

Fig. 6. – Fermi plot of the β-spectrum in coincidence with γ-rays of energy higher than 1100 keV.

The numbers of the Table IV signed with an asterisk should be corrected for coincidences due to the presence of pulses in the energy interval of 200 or 300 keV belonging to Compton distribution of the 800 and 970 keV γ-rays. For the correction it is necessary to know the response of the crystal to γ-rays of ~ 900 keV and the effect of the light pipe; the latter consists of a widening of the spectrum and the former is derived from a previous study (⁹). Taking into account

the width of the γ channel in the β^--γ coincidences *a*), *b*) and *c*) (see Table IV), the areas of β^- spectra β_2^- and β_3^- in coincidence with γ-rays of 200 and 300 keV, which are equal to 12.2, 5.8, 23.3 and 41.1 become of the order of ~ 9, 4, 13 and 37 respectively. However this correction is not significant as for what concerns the determination of the relative intensity of the β^- spectra.

6. – Internal Conversion Coefficients.

The complexity of the β^- decay of ^{160}Tb and the big number of γ-rays found (KESHISHIAN and coworkers ([6]) found 29 of them) makes it impossible to assign the conversion coefficients of the most intense γ-rays through a given decay scheme. For this reason we tried to obtain the K-conversion coefficients of some of the 8 γ-rays clearly seen in our spectrometer by means of a well known technique described in Siegbahn's book ([10]).

This method consists of measuring the γ-ray intensity from the photoelectron spectrum obtained in the spectrometer with different converters and to compare it with the internal conversion lines. This measurement can be affected by some error due to the angular distribution of the photoelectrons ([11]).

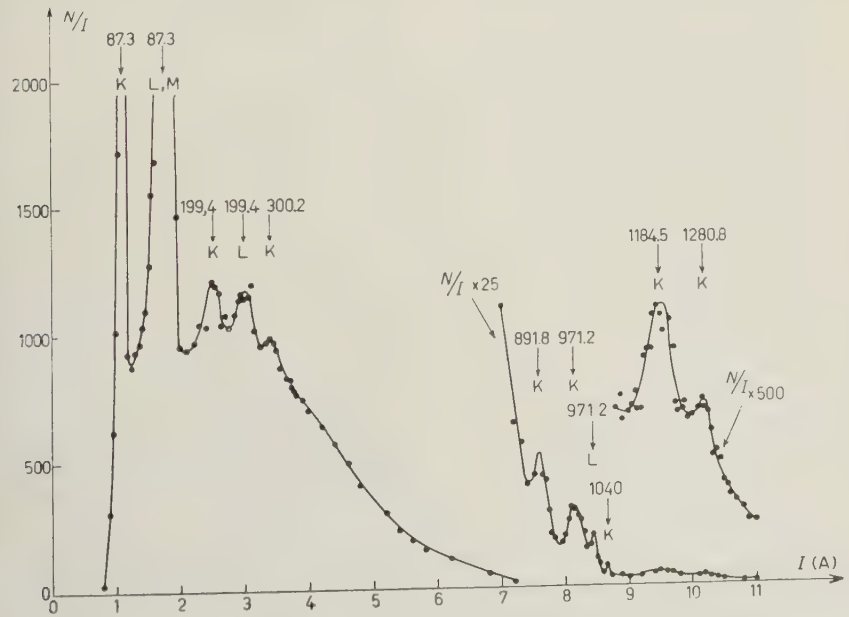

Fig. 7. – Internal conversione lines and β-spectrum of ^{160}Tb.

([10]) K. SIEGBAHN: *β and γ-Ray Spectroscopy* (Amsterdam, 1955), p. 234.
([11]) C. M. DAVIDSON and R. D. EVANS: *Rev. Mod. Phys.*, **24**, 79 (1952).
([12]) H. O. W. RICHARDSON: *Proc. Phys. Soc.*, A **63**, 234 (1950).

The area under a given photoelectric line A in the case of a thin converter is given by

$$A_\gamma = KI_\gamma \tau_K(E_\gamma) \,. \tag{1}$$

Where I_γ is the intensity of the γ-radiation, $\tau_K(E_\gamma)$ is the photoelectric efficiency of the converters in (mg/cm²) and K is a constant dependent on the geometry of the experiment and on the spectrometer transmission.

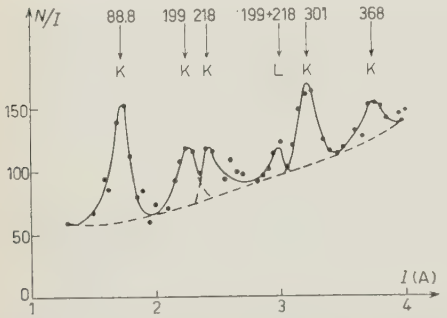

Fig. 8. – Partial photospectrum of ^{160}Dy γ-rays. Au converter 1.8 mg/cm². The energies are in keV.

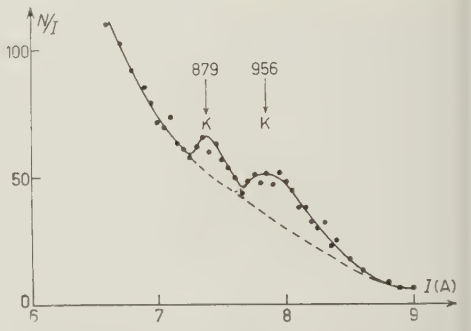

Fig. 9. – Partial photospectrum of ^{160}Dy γ-rays. Au converter 5.2 mg/cm². The energies are in keV.

According to Davidson and Evans' paper the expression (1) would be further multiplied by a corrective term, which is a function of the γ-ray energy, the acceptance solid angle of the spectrometer being known. An evaluation of this effect has been made with three γ-rays of known conversion coefficients; the energies were: 661 keV (^{137}Cs), 800 keV (^{134}Cs) and 1.33 MeV (^{60}Co). Within experimental errors the constant K was found to be independent from the γ-ray energies. This result is perhaps due to the small distance source-converter (2 mm) and to the high transmission of the β-spectrometer.

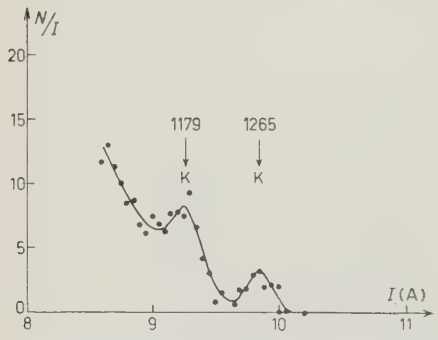

Fig. 10. – Partial photospectrum of ^{160}Dy γ-rays. Au converter 24.4 mg/cm². The energies are in keV.

Considering the thickness of the source, copper and converters, no corrections have been necessary for the area of the photoelectric lines ([12]).

Examples of photoelectron and conversion electron spectra are shown in Fig. 7, 8, 9, 10. Table V gives the results. Conversion coefficients have been evaluated only for γ-rays in the

energy range in which the effect of the anisotropy of photoelectron emission has been measured.

TABLE V. – *Summary of the results obtained from internal conversion spectra and photospectra.*

No. of γ-rays	Energy from Internal Conversion (keV)	Energy from Photoelectric Conversion	γ-rays Relative Intensity %	K-Conversion Coefficients
1	87.3 ± 0.1	88.8 ± 0.6	—	—
2	199.4 ± 1.0	199.4 ± 1.0	2.2	—
3	—	218.7 ± 1.1	2.1	—
4	300.2 ± 0.8	301.6 ± 1.2	11.6	—
5	393	368.0 ± 2.7	—	—
6	891.8 ± 2.2	879.0 ± 3.6	27.5	$2.3 \cdot 10^{-3}$ ($E2$)
7	971.2 ± 0.2	956.3 ± 3	100	$4.07 \cdot 10^{-3}$ ($E2$)
8	1040	—	—	—
9	1184.5 ± 2.6	1179.4 ± 2.9	1.4	$0.9 \cdot 10^{-3}$ ($E1$)
10	1280.8 ± 2	1265.1 ± 5.1	0.8	$0.7 \cdot 10^{-3}$ ($E1$)

7. – Discussion.

From the results obtained by us and from the γ-γ coincidence results of BURSON and coworkers we suggest the decay scheme of Fig. 11.

In attempting to construct a decay scheme it is interesting to take into account the probable existence in ^{160}Dy of excited levels belonging to the rotational bands predicted for this nucleus by the Bohr-Mottelson theory ([13,14]).

To a first approximation the energies should be given by the simple formula $E = (\hbar^2/2J)I(I+1)$, where J is the moment of inertia and I is the total angular momentum of the level.

In the theory of Bohr-Mottelson, a new quantum number K is introduced,

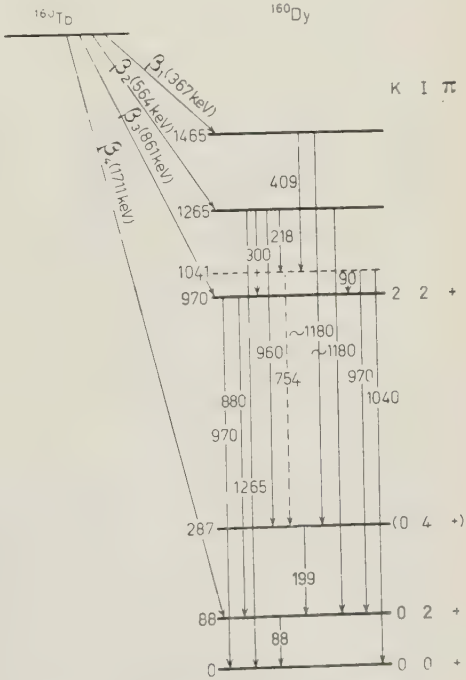

Fig. 11. – Decay scheme of ^{160}Tb.

([13]) G. ALAGA, K. ALDER, A. BOHR and B. R. MOTTELSON: *Kgl. Danske Videnskab. Selskab., Dan. Mat. Fys. Medd.*, **29**, no. 9 (1955).

([14]) K. SIEGBAHN: *β and γ-Ray Spectroscopy* (Amsterdam, 1955), p. 468.

which is the projection of the total angular momentum along the nuclear symmetry axis. K is the same for all the the levels of a rotational band and is equal to the spin of the base level of the rotational band. The relative transition probability for emission of a given multipole L radiation from a level i to different levels f is given by eq. (12) of ALAGA *et al.* ([13]):

$$\frac{B(L,\, I_i \to I_f)}{B(L,\, I_i \to I_{f'})} = \frac{\langle I_i L K_i K_f - K_i | I_i L I_f K_f \rangle^2}{\langle I_i L K_i K_f - K_i | I_i L I_{f'} K_f \rangle^2}.$$

where $\langle I_i L K_i K_f - K_i | I_i L I_f K_f \rangle$ are the Clebsch-Gordon coefficients in the notation of CONDON and SHORTLEY ([15]).

From previous coincidence measurements, the 88 keV γ-ray is assumed to decay from the first excited level to ground state. MCGOWAN ([16]) found a K conversion coefficient of the 88 keV γ-ray consistent with E 2 polarity. Spin 2 and parity + of the first excited level seem therefore correct. The 88 keV level represents probably the first rotational excitation of the ground state $(0, 2+)$.

The next rotational excitation $(0, 4+)$ is expected at an energy of 293 keV. An energy of $199 + 88 = 287$ keV fits quite well. γ-γ coincidences between 88 keV and 199 keV γ-rays make it possible to put this γ transition between the second and the first excited levels. But the lack of experimental information on the polarity of 199 keV γ-rays (it was not possible to resolve the electron conversion lines of the 218 and 199 keV γ-rays), makes it uncertain that the 287 keV level belongs to the first rotational band of ^{160}Dy.

From γ-γ coincidence experiments of BURSON and coworkers and from our β-γ coincidence results, we assume that the 970 keV excited level decays mostly with the two γ-rays of 880 and 970 keV.

The internal conversion coefficients of the 880 and 970 keV γ-rays are consistent with E 2 polarity. Thus if the 88 keV level belongs to the first rotational band with $K = 0$ the assegnment $(2, 2+)$ to the 970 keV level seems rather plausible.

Furthermore it seems that the existence of a level of about 1040 keV is probable, owing to the observation of a weak γ line of ~ 1040 keV in the β-spectrometer, a γ-ray of ~ 410 keV with a crystal detector and an electron line in the β-spectrometer corresponding to a gamma of ~ 400 keV in coincidence with γ-rays of energy higher than 1000 keV. In this way the 218 keV transition would then have to be interpreted as taking place between the 1265 and 1041 keV levels. To interpret this level as belonging to the same

([16]) E. U. CONDON and G. H. SHORTLEY: *The Theory of Atomic Spectra* (Cambridge, 1953), p. 76.

([17]) F. K. MCGOWAN: *Phys. Rev.*, **85**, 151 (1952).

rotational band of 970 keV level is rather difficult because in that case a branching to the 1041 keV level from the ^{160}Tb ground state would be expected, which, however, was not verified experimentally.

In the β^--γ coincidences between 300 keV gamma and β^- continuous spectrum the 564 keV E_{max} β^- spectrum appears predominantly. This suggests that the 300 keV transition takes place between 1265 and 970 keV states. Moreover, the absence of the decay of 367 keV E_{max} in coincidence with 300 keV γ-rays suggests a very weak transition between the 1465 and 1265 keV levels.

* * *

The authors wish to thank Dr. AAGE BOHR for helpful criticism in the interpretation of the experimental results, and Prof. G. BOLLA for his kind interest in the present work.

RIASSUNTO

Il decadimento del ^{160}Tb e del ^{160}Dy è stato studiato mediante uno spettrografo β ad immagine intermedia e mediante uno spettrometro a scintillazione. La componente β^- di bassa energia è stata accuratamente risolta mediante studi di coincidenze. I coefficienti di conversione interna di alcune transizioni sono stati ottenuti dagli spettri di conversione interna ed esterna. Si propone uno schema di decadimento consistente con i risultati sperimentali.

General Properties of the Fixed Source Meson Theory.

M. Cini

Istituto di Fisica dell'Università - Catania
Istituto Nazionale di Fisica Nucleare - Sezione di Torino

S. Fubini

Istituto di Fisica dell'Università - Torino
Istituto Nazionale di Fisica Nucleare - Sezione di Torino

(ricevuto il 7 Febbraio 1956)

Summary. — Three relationships connecting the renormalized and unrenormalized coupling constants to the scattering amplitudes are deduced as a rigorous consequences of the fixed source meson theory. The expressions for the scattering amplitudes deduced in the framework of the one-meson approximation and fitted to experiment in the low energy region do not satisfy these sum rules. It is shown that agreement between theory and experiment at low energy requires the high energy (above the cut-off) contributions to the sum rules to be dominant.

1. – Introduction.

Some recent important advances have been made in the study of the fixed-source meson theory, by investigating the general properties of Heisenberg operators (1). The starting point of these investigations is the connection between the matrix elements of the source operators in Heisenberg representation and the scattering matrix elements.

(1) H. Lehmann, K. Symanzik and W. Zimmermann: *Nuovo Cimento*, **1**, 205 (1955); M. L. Goldberger: *Phys. Rev.*, **97**, 508 (1955); F. Low: *Phys. Rev.*, **97**, 1992 (1955); Y. Nambu: *Phys. Rev.*, **98**, 803 (1955); M. Cini and S. Fubini: *Nuovo Cimento*, **2**, 860 (1955).

In this paper these techniques will be used to deduce some relationships connecting the renormalized and the unrenormalized coupling constants to the scattering amplitudes. These results are a direct consequence of the algebraic properties of the σ and τ operators ([2]).

The expressions for the scattering amplitudes deduced recently in the framework of the one-meson approximation ([3]) (with the values of the parameters which fit the experiments in the low energy region), can be introduced in these sum rules. If the form factor is such that, as usually assumed, the contributions from the energy range above the nucleon mass become negligible (e.g. square cut-off), a definite inconsistency is obtained. Only if the high energy range contributions are dominant, the conditions can be satisfied.

In the limiting case in which the form factor tends to zero as $1/k$ for high momenta ([4]), the sum rules diverge and the inconsistency does not seem to hold any more.

2. – Theory.

The relationships we are going to derive in this section are essentially based on the algebra of the σ and τ operators. Throughout this derivation an extensive use of the results of CHEW and LOW ([2]) will be made. However we find convenient to use a slightly modified notation keeping a different label for momentum and isotopic spin of the meson, and introducing explicitly an index for the nucleon state.

In our notation the interaction Hamiltonian is:

$$H_I = \sum_{k,\alpha} (V^{(0)}_{k\alpha} a_{k\alpha} + V^{(0)+}_{k\alpha} a^{+}_{k\alpha}), \tag{1}$$

with

$$V^{(0)}_{k\alpha} = i(4\pi)^{\frac{1}{2}} \frac{f^{(0)}}{\mu} \frac{\boldsymbol{\sigma}\cdot\boldsymbol{k}}{\sqrt{2\omega_k}} v(k)\tau_\alpha \,. \tag{2}$$

We denote with Ψ_r the four dressed nucleon states, and with $\Psi^{(-)}_n$ the complete set of the « incoming » eigenstates of the total Hamiltonian. The

([2]) G. CHEW and F. LOW (to be published) have previously derived one of these relations. We are indebted to Drs. CHEW and LOW for having made the results of their work available to us prior to publication. Their work will be quoted in the following with CL.

([3]) L. SARTORI and V. WATAGHIN: *Nuovo Cimento*, **12**, 145 (1954). The results obtained by these authors have been derived in CL in the framework of Low's equation.

([4]) This type of cut-off gives the same asymptotic behaviour at high momenta as the relativistic γ_5 theory in all Feynman integrals. Simple considerations on the Low equation (to be published elsewhere) show that cut-off going to zero more slowly than $1/k$ make the theory inconsistent.

main result of *CL* used here is the relationship between the matrix elements

$$(\Psi_n^{(-)}, V_{p\alpha}^{(0)}\Psi_r)$$

and the elements of the scattering matrix S. If the transition matrix T is defined by

$$\langle n|(S-1)|p\alpha; r\rangle = -2\pi i\langle n|T|p\alpha; r\rangle\delta(E_n-\omega_p)\,, \tag{3}$$

this result can be written as [5]

$$\langle n|T|p\alpha; r\rangle = (\Psi_n^{(-)}, V_{p\alpha}^{(0)}\Psi_r) \qquad (E_n=\omega_p) \tag{4}$$

where $|n\rangle$, $|p\alpha; r\rangle$ are eigenstates of the free Hamiltonian, the latter referring to a state with one pion of momentum and isotopic spin p, α and a nucleon r.

The unitarity of the S matrix can be stated in the form:

$$\langle p\alpha; r|T^+-T|p'\alpha'; r'\rangle = 2\pi i\sum_n\langle p\alpha; r|T^+|n\rangle\langle n|T|p'\alpha'; r'\rangle\delta(E_n-\omega_p), \tag{5}$$

with $\omega_p=\omega_{p'}$.

By introducing eqs. (2) (4) in the right hand side of eq. (5) we get:

$$\langle p_\alpha; r|T^+-T|p'\alpha'; r'\rangle = 2\pi i\sum_n\sum_{ll'}\delta(E_n-\omega_p)\frac{4\pi(f^{(\omega)})^2}{\mu^2}\cdot \tag{6}$$

$$\cdot\frac{v^2(p)}{2\omega_p}p'_{l'}p_l(\Psi_r, \tau_\alpha\sigma_l\Psi_n^{(-)})(\Psi_n^{(-)}\tau_{\alpha'}\sigma_{l'}\Psi_{r'})\,.$$

It is useful to go in a representation for T in which eigenstates of the angular momentum of the pion appear. Eq. (6) shows, as is well known, that only p-states contribute. Then we can write:

$$\langle p'\alpha'; r'|T|p\alpha; r\rangle = \sum_{ll'}\langle p'|l'\rangle\langle l'\alpha'; r'|T(\omega_p)|l\alpha; r\rangle\langle l|p\rangle\,, \tag{7}$$

where [6]:

$$\langle l|p\rangle = \left(\frac{6\pi^2}{\omega_p p^2}\right)^{\frac{1}{2}}p_l\,. \tag{8}$$

[5] See formula CL (19).

[6] The numerical coefficient is fixed by normalization requirements: see W. LIPPMANN and J. SCHWINGER: *Phys. Rev.*, **74**, 569 (1950) eqs. from (1.90) to (1.103).

Then eq. (6) becomes:

$$(9)\quad -\frac{3i}{2}\frac{1}{p^3v^2(p)}\langle l\alpha;\, r\,|\,T^+(\omega_p)-T(\omega_p)\,|\,l'\alpha' r'\rangle = \\ = \frac{(f^0)^2}{\mu^2}\sum_n \delta(E_n-\omega_p)(\Psi_r,\, \tau_\alpha\sigma_l\Psi_n^{(-)})(\Psi_n^{(-)},\, \tau_{\alpha'}\sigma_{l'}\Psi_{r'})\,.$$

By integrating on ω_p from μ to infinity and by using the completeness of the set $\Psi_n^{(-)}$ one obtains (7):

$$(10)\quad -\frac{3}{2}i\int_\mu^\infty \frac{\mathrm{d}\omega_p}{p^3v^2(p)}\langle l\alpha;\, r\,|\,T^+(\omega_p)-T(\omega_p)\,|\,l'\alpha';\, r'\rangle = \\ = \frac{(f^{(0)})^2}{\mu^2}\left\{(\Psi_r,\tau_\alpha\sigma_l\tau_{\alpha'}\sigma_{l'}\Psi_{r'})-\sum_{r''}(\Psi_r,\tau_\alpha\sigma_l\Psi_{r''})(\Psi_{r''},\tau_{\alpha'}\sigma_{l'}\Psi_{r'})\right\}.$$

We notice that in the right hand side appear only expectation values of σ and τ operators in the dressed nucleon states. Then, because of invariance requirements, we can write:

$$(11)\quad \begin{cases} (\Psi_r,\, \tau_\alpha\Psi_{r'}) = \dfrac{1}{\varrho_1}\langle r\,|\,\tau_\alpha\,|\,r'\rangle \\ (\Psi_r,\, \sigma_l\Psi_{r'}) = \dfrac{1}{\varrho_1}\langle r\,|\,\sigma_l\,|\,r'\rangle \\ (\Psi_r,\, \tau_\alpha\sigma_l\Psi_{r'}) = \dfrac{1}{\varrho_2}\langle r\,|\,\tau_\alpha\sigma_l\,|\,r'\rangle \end{cases}$$

where ϱ_1, ϱ_2 are unknown constants. As is well known

$$(12)\quad f = \frac{1}{\varrho_2}f^{(0)}$$

is the renormalized coupling constant.

It is useful to introduce the isotopic spin $\boldsymbol{t}$ and the angular momentum $\boldsymbol{l}$ of the meson defined by (8):

$$(13)\quad \begin{cases} \delta_{ll'}\cdot\langle r\,|\,\tau_\alpha\tau_{\alpha'}\,|\,r'\rangle = \langle l\alpha;\, r\,|\,(1-\boldsymbol{t}\cdot\boldsymbol{\tau})\,|\,l'\alpha';\, r'\rangle\,, \\ \delta_{\alpha\alpha'}\cdot\langle r\,|\,\sigma_l\sigma_{l'}\,|\,r'\rangle = \langle l\alpha;\, r\,|\,(1-\boldsymbol{l}\cdot\boldsymbol{\sigma})\,|\,l'\alpha';\, r'\rangle\,. \end{cases}$$

(7) The complete set $\Psi_n^{(-)}$ must contain, of course, also the four single nucleon states Ψ_r. The presence of the δ-function in eq. (6) excludes these states from the sum over n. This is the reason for subtracting the last term on the r.h.s. of eq. (10).

(8) Y. Nambu and Y. Yamaguchi: *Prog. Theor. Phys.*, **6**, 1000 (1951). See also S. Fubini: *Nuovo Cimento*, **10**, 564 (1953), Appendix I.

With this notation eq. (10) can be written in matrix form as follows:

$$(14)\quad -\frac{3}{2}\,i\int_{\mu}^{\infty}\frac{\mathrm{d}\omega_p}{p^3v^2(p)}[T^+(\omega_p)-T(\omega_p)]=$$

$$=\frac{f^2}{\mu^2}\left\{(\varrho_2^2-1)+\left(1-\frac{\varrho_2^2}{\varrho_1}\right)(\boldsymbol{\sigma}\cdot\boldsymbol{l}+\boldsymbol{\tau}\cdot\boldsymbol{t})+(\varrho_2-1)\boldsymbol{\sigma}\cdot\boldsymbol{l}\,\boldsymbol{\tau}\cdot\boldsymbol{t}\right\}.$$

To obtain relationships between the scattering amplitudes we expand the transition matrix T by taking as a basis the projection operators on the states with given total angular momentum J and total isotopic spin I. Let us write:

$$(15)\qquad T(\omega)=-\frac{1}{\pi}\{g_1(\omega)P_{11}+g_2\omega)(P_{13}+P_{31})+g_3(\omega)P_{33}\},$$

where

$$(16)\qquad\begin{cases}P_{11}=\frac{1}{9}(1-\boldsymbol{\tau}\cdot\boldsymbol{t})(1-\boldsymbol{l}\cdot\boldsymbol{\sigma})\\ P_{13}=\frac{1}{9}(1-\boldsymbol{\tau}\cdot\boldsymbol{t})(2+\boldsymbol{l}\cdot\boldsymbol{\sigma})\\ P_{31}=\frac{1}{9}(2+\boldsymbol{\tau}\cdot\boldsymbol{t})(2+\boldsymbol{l}\cdot\boldsymbol{\sigma})\\ P_{33}=\frac{1}{9}(2+\boldsymbol{\tau}\cdot\boldsymbol{t})(2+\boldsymbol{l}\cdot\boldsymbol{\sigma})\,.\end{cases}$$

It is well known that if the scattering is purely elastic

$$(17)\qquad g_i=\exp[i\delta_i]\sin\delta_i,\qquad (i=1,2,3)$$

where δ_i are the (real) phaseshifts (9).

With the use of eqs. (15) (16) one obtains from eq. (14):

$$(18a)\qquad \frac{1}{3\pi}\int_{\mu}^{\infty}\frac{\mathrm{d}\omega_p}{p^3v^2(p)}\,\mathrm{Im}\{g_1(\omega_p)+4g_2(\omega_p)+4g_3(\omega_p)\}=\frac{f^2}{\mu^2}(\varrho_2^2-1)\,,$$

$$(18b)\qquad \frac{1}{3\pi}\int_{\mu}^{\infty}\frac{\mathrm{d}\omega_p}{p^3v^2(p)}\,\mathrm{Im}\{-g_1(\omega_p)-g_2(\omega_p)+2g_3(\omega_p)\}=\frac{f^2}{\mu^2}\left(1-\frac{\varrho_2^2}{\varrho_1}\right),$$

$$(18c)\qquad \frac{1}{3\pi}\int_{\mu}^{\infty}\frac{\mathrm{d}\omega_p}{p^3v^2(p)}\,\mathrm{Im}\{g_1(\omega_p)-2g_2(\omega_p)+g_3(\omega_p)\}=\frac{f^2}{\mu^2}(\varrho_2-1)\,.$$

(9) We use the notation of F. Low; $\delta_1=\delta_{11}$; $\delta_2=\delta_{13}=\delta_{31}$; $\delta_3=\delta_{33}$.

If one recalls that

$$\mathrm{Im}\{g_1 + 4g_2 + 4g_3\} = \frac{3p^2}{8\pi}\{\sigma^+ + \sigma^-\},$$

where σ^+ and σ^- are the total cross-sections for positive and negative pions on protons, formula (18a) reduces to a sum rule already obtained by CHEW and LOW (CL65).

3. – Numerical application and discussion.

Eqs. (18) are the essential result of the present paper. They are sufficient to determine ϱ_1, ϱ_2 and f^2 in terms of the scattering amplitudes. Of course the exact solutions of the fixed-source Hamiltonian must satisfy these relations. These conditions can therefore be used for two essentially different purposes. The first one is to test the approximate solutions known until now, by taking into account the fact that f^2 can be determined independently from experiment ([10]). The second is to investigate to what extent the exact solution of the theory might agree with experiment. Of course one must only ask the theory to reproduce the experimental data for energies such that the nucleon recoil can reasonably be neglected, i.e. well below the cut-off (usually taken at the nucleon mass M). Therefore the sum rules (18) can give an indication about the magnitude of the high energy contributions required from the agreement between theory and experiment in the low energy range. In this paper we will mainly devote our attention to the first point. For sake of definiteness we will concentrate the discussion on the one-meson approximation worked out by CHEW and LOW, which seems the most reliable at this time. All previous approximations had in common with this one the following main features: a) the phaseshift δ_3 is strongly dominant over all others; b) the quantities $\sin^2\delta_i$ are proportional to $v^1(p)$. Let us consider for the moment the square cut-off at M used in most calculations. In this case, because of property b), the range of integration is reduced to the interval from μ to M, where $v^2(p)$ can be taken equal to one. Since in this range the integrands are of the form $\mathrm{Im}\, g_i/p^3$ and $\mathrm{Im}\, g_i \leqslant 1$, the low momenta contributions ($\omega_\nu \lesssim 2.5\,\mu$) will dominate. This means that, because of property a), g_1

([10]) The experimental results can be very well represented by an effective range formula as pointed out in CL. These authors have deduced from this expression a value $f^2 = 0.08$. The general question of the deduction of the coupling constant from experiment will be discussed in detail in a forthcoming publication (M. CINI, S. FUBINI and A. STANGHELLINI: *Nuovo Cimento*, in the press). This investigation gives $f^2 = 0.107 \sim 0.010$, which is not very far from the Low value.

abd g_2 can be neglected in comparison with g_0: By using eq. (17) we obtain:

$$\frac{4}{3\pi}\int_{\mu}^{M}\frac{\sin^2\delta_3(\omega_p)}{p^3}\,\mathrm{d}\omega_p = \frac{f^2}{\mu^2}(\varrho_2^2-1)\,, \tag{19a}$$

$$\frac{1}{3\pi}\int_{\mu}^{M}\frac{\sin^2\delta_3(\omega_p)}{p^3}\,\mathrm{d}\omega_p = \frac{f^2}{\mu^2}(\varrho_2-1)\,. \tag{19b}$$

Eqs. (19) give immediately

$$\varrho_2 = 3$$

and

$$\frac{\mu^2}{6\pi}\int_{\mu}^{M}\frac{\sin^2\delta_3(\omega_p)}{p^3}\,\mathrm{d}\omega_p = f^2\,. \tag{20}$$

The integral in eq. (20) has been evaluated numerically by introducing for $\delta_3(\omega_p)$ the expressions given by CHEW and LOW (CL47) (CL48). The result is:

$$f^2 = 0.013$$

in striking contrast with the value $f^2 = 0.10$ given by experiment ([10]) (*).

The situation is quite different if we consider a form factor such that the high energy range may contribute significantly to the integrals in eqs. (18). In the limiting case when $v(p) \to \mathrm{const}/p$ as $p \to \infty$ the integrals diverge logarithmically (as it happens in any renormalizable local theory) and ϱ_2 becomes infinite for any finite value of f^2. Therefore in this case these equations become meaningless and no inconsistency seems to arise.

The foregoing results allow us to make some remarks about the exact solution of the fixed source theory. If the form factor decreases rapidly enough

---

(*) *Note added in proof.* — Dr. WALTHER THIRRING has communicated to us a result which makes the discrepancy even more striking. By considering the structure of the physical nucleon he has been able to show that:

$$1 + \frac{2}{\varrho_1} - \frac{3}{\varrho_2} > 0\,. \tag{N1}$$

By multiplying eqs. (18*a,b,c*) by 1; -2; -3 respectively and summing one obtains:

$$\frac{1}{\pi}\int\frac{\mathrm{d}\omega_p}{p^3 v^2(p)}\,\mathrm{Im}\left[4g_2(\omega_p) - g_3(\omega_p)\right] = \frac{f^2}{\mu^2}\,\varrho_2^2\left(1 + \frac{2}{\varrho_1} - \frac{3}{\varrho_2}\right) > 0\,. \tag{N2}$$

Since in the low energy range the contribution of g_2 is experimentally only a few percent of g_3; eq. (N2) shows that a strong contribution is required from the high energy region for the consistency of our sum rules.

above the nucleon mass it is reasonable to assume that the high energy contributions in the integrals (18) are negligible also when the exact (unknown) expressions for g_i are used ([11]). This means that in this case, while on the one hand eqs. (18) must be satisfied exactly by the expressions for the scattering amplitudes, on the other hand their behaviour at low energies determines completely the value of the integrals appearing in these equations, which turn out to be too small if agreement with experiment is required.

We conclude that if the common viewpoint is adopted according to which the cut-off factor of the fixed source theory should make all the high energy contributions negligible, the exact solutions of this theory cannot agree with experiment even for low energies. The result of this investigation contrasts with the usual philosophy of the fixed source theory which requires that all high energy contributions are small, even to those quantities which in the relativistic renormalizable local theories are infinite.

([11]) We notice that, in eqs. (18), the factor $v^2(p)$ in the denominator is always cancelled by an identical factor appearing in the expressions of $\mathrm{Im}\, g_i$. In addition one extra factor $v^2(k)$ appears in the numerator for each emitted particle of momentum k. The presence of these factors should limit the high energy contributions.

RIASSUNTO

Si ricavano tre relazioni che connettono le costanti di accoppiamento rinormalizzata e non rinormalizzata con gli elementi della matrice S di scattering. Queste relazioni sono una conseguenza rigorosa della teoria mesonica di sorgente fissa. Queste regole di somma non sono soddisfatte dalle espressioni per la matrice S dedotte nell'approssimazione di un mesone, che sono in accordo con l'esperienza a basse energie. Si dimostra che per avere accordo a bassa energia fra teoria ed esperienza è necessario che nelle regole di somma i contributi al disopra del taglio siano predominanti.

IL NUOVO CIMENTO Vol. III, N. 4 1° Aprile 1956

High Energy Behaviour of Renormalizable Fields.

H. Umezawa, Y. Tomozawa and M. Konuma
Department of Physics, University of Tokyo

S. Kamefuchi
Institute of Theoretical Physics, Nagoya University

(ricevuto il 9 Febbraio 1956)

Summary. — It has been suggested that the renormalized value of the coupling constant is sometimes restricted within a zone, i.e., the normal zone. Gell-Mann and Low showed an intimate relation between the renormalization factor and the asymptotic form of the renormalized propagator. By using this relation to calculate the renormalized propagators and the effective couplings, we shall discuss peculiar features, which appear in results of the renormalization theory in high-energy phenomena when the observed values of the coupling constants are out of the normal zones. The normal zone of the electric charge and the effective charge in the quantum electrodynamics will be discussed in a succeeding paper.

1. – Introduction.

The present quantum field theory has been based on many physical requirements, e.g., Lorentz invariance, causality, unitarity of the S-matrix, etc. However, we have never known the reason why the masses of particles and the coupling constants are of values realized in nature. To answer this question it seems necessary to clarify the internal structure of the elementary particles. The latter problem was studied by many authors in connection with the ultraviolet catastrophe. But this problem has long been a very academic one and it was often expected that more fruitful results might be obtained by searching for the realistic effects of the « proper field » that is immediately connected with the ultraviolet catastrophe.

Such effects were found in phenomena of the Lamb-shift and the anomalous magnetic moment of the electron. The renormalization theory obtained great successes in explaining these phenomena. Now we know that the re-

normalization theory being based on the perturbation expansion is applied only to interactions of the first kind, but not to those of the second kind (1). The electromagnetic interactions of charged particles (with spin $\frac{1}{2}$ or 0) belong to the former.

At first sight, the realistic footing for investigations of the structure of elementary particles disappeared and there is no limit to the applicability of the quantum field theory in case of interactions of the first kind. For, in this case, all of ultraviolet catastrophes can be eliminated by adjusting the renormalized coupling constants (g_r) and masses (m) to their observable values (g_{ob}, m_{ob}). Thus there appeared two distinct standpoints among theoretical physicists; the one is optimistic and says that what we must do is to reformulate the theory in such a way that the unrenormalized constants (g, $\varkappa$) never appear in any place of the theory, and the second is pessimistic and says that the ultraviolet catastrophe remaining in the ratio g_r/g, $m/\varkappa$ ($\varkappa$ = unrenormalized mass) still suggests the existence of the limit of applicability of the quantum field theory. To decide which standpoint we should take, we must know whether or not the renormalized theory is internally consistent and how it can explain experimental results.

In the renormalization theory, all physical results are obtained as functions of g_r and m; S_{F1}, D_{F1}, $\Gamma_{\mu 1}$ in the quantum electrodynamics are functions of the renormalized charge (e_r) and mass m. Furthermore, the renormalized constants g_r and m are functions of the unrenormalized ones g and $\varkappa$:

$$g_r = g_r(g, m)\,, \qquad m = m(g, \varkappa)\,. \tag{1}$$

For example, in the quantum electrodynamics we should have:

$$e_r = e_r(e, m)\,, \tag{2}$$

where e is the unrenormalized charge. In the renormalization theory, however, it is usual to replace g_r (or e_r) and m with the observed values g_{ob} (or e_{ob}) and m_{ob}, without taking into account the relation (1) or (2). Suppose that, when g^2 runs from 0 to ∞, g_r runs over a zone. In this paper such a zone will be called the *normal zone* of g_r and denoted by $N(g_r)$. In a similar way we can define the normal zone $N(m)$ of m. Now, there immediately arises a question as to whether the observable values g_{ob} and m_{ob} are within the normal zones $N(g_r)$ and $N(m)$ respectively. For example, it is an important problem to ask whether or not $e_{ob} = 1/\sqrt{137}$ lies in the $N(e_r)$. In this connection it seems possible to arrive at conditions which restrict the observable values (g_{ob}, m_{ob})

(1) S. Sakata, H. Umezawa and S. Kamefuchi: *Prog. Theor. Phys.*, **7**, 377 (1952). H. Umezawa: *Prog. Theor. Phys.*, **7**, 551 (1952).

of coupling constants and masses within the framework of the present theory; they should be in the normal zones.

It is well known that the renormalization factor $Z(g_r)$ of the one-body propagator $G(x, x')$ being a function of g_r, should be in the domain:

$$0 \leqslant Z(g_r) \leqslant 1 \,. \tag{3}$$

This can be satisfied when the interaction Hamiltonians are hermitic, and therefore g_r is in the normal zone $N(g_r)$. Thus, when $Z(g_{ob})$ does not satisfy (3), g_{ob} is out of the normal zone $N(g_r)$. Such a circumstance has happened in a simple example given by LEE [2]. In this example, when g_{ob} is out of $N(g_r)$, there appears a state of negative probability and therefore the S-matrix is no longer unitary. We shall give, in Sect. **5**, a general discussion, which shows that the appearance of states of negative probability is a general feature in cases where (3) is not satisfied. The Z-factors of propagators for charged particles show some peculiarities, which will also be discussed in Sect. **5**.

However, it is not a nice tactics to examine only Z-factors, since they do not appear explicitly in the renormalized theory. Now, we know that all S-matrix elements are built with the renormalized constants (g_r, m) and renormalized propagators $G_c(g_r)$ and vertices $\Gamma_c(g_r)$. In the renormalization theory, we replace g_r by g_{ob}. Therefore, it is interesting to find essential differences between $G_c(g_{ob})$ with g_{ob} in $N(g_r)$ and with g_{ob} out of $N(g_r)$. This will be discussed in Sect. **4**. There, we shall give a way useful to calculate $G_c(g_r)$. We shall also see that, if g_r is out of the normal zone $N(g_r)$ in such a way that $Z(g_r) < 0$, the renormalized theory can no longer explain the high energy phenomena.

The detailed discussions concerning the normal zones in the quantum electrodynamics and the meson theory will be given in papers to follow.

In order to calculate the renormalized quantities G_c, Γ_c etc., we first cut-off the effects of high internal momenta ($k > \Lambda$). Then, we make the limiting process $\Lambda \to \infty$ and the substitutions $g_r \to g_{ob}$ and $m \to m_{ob}$, after the renormalization, to give $G_c(g_{ob})$ and $\Gamma_c(g_{ob})$. There is a way of cut-off, which leads to $G_c(g_\Lambda)$ and $\Gamma_c(g_\Lambda)$ ($g_\Lambda =$ the renormalized coupling constant in the case of finite Λ) with the following properties: the quantities $G_c(g_\Lambda)$ and $\Gamma_c(g_\Lambda)$ do not depend on Λ except through g_Λ and therefore, the replacement $g_\Lambda \to g_{ob}$ (without the limiting process $\Lambda \to \infty$) immediately leads to the renormalized quantities $G_c(g_{ob})$ and $\Gamma_c(g_{ob})$. We shall call such a cut-off procedure the *renormalization cut-off*. In this way of cut-off, the renormalized theory is independent of the value of Λ, and therefore, we can obtain the ordinary

[2] T. D. LEE: *Phys. Rev.*, **95**, 1329 (1954).

renormalized theory without taking the limit $\Lambda \to \infty$. The renormalization cut-off is very useful for the investigation of high energy behaviours of $G_c(g_{ob})$ and $\Gamma_c(g_{ob})$. Details of the renormalization cut-off will be discussed in Sect. 2.

2. – The renormalization Cut-Off (*).

The one-body propagator G satisfies the equation of the form:

$$h(-k^2)G(k^2) = 1\,, \tag{4a}$$

with

$$h(-k^2) \equiv k^2 + \varkappa^2 + \Sigma(-k^2) \tag{5a}$$

for a field of spin zero and the electromagnetic field (cf. Sect. 5), or that of the form

$$h(-i\gamma p)G(p) = 1\,, \tag{4b}$$

with

$$h(-i\gamma p) \equiv i\gamma p + \varkappa + \Sigma(-i\gamma p) \tag{5b}$$

for a field of spin $\frac{1}{2}$. Here $\varkappa$ denotes the unrenormalized mass. We shall write the mass operators as follows:

$$\Sigma(-k^2) = \Sigma(m^2) + (k^2+m^2)\left(\frac{\partial\Sigma(-k^2)}{\partial k^2}\bigg|_{k^2=-m^2}\right) + \frac{1}{Z(g_r)}(k^2+m^2)A(-k^2, g_r)\,, \tag{6a}$$

or

$$\Sigma(-i\gamma p) = \Sigma(m) + (i\gamma p + m)\left(\frac{\partial\Sigma(-i\gamma p)}{\partial(i\gamma p)}\bigg|_{i\gamma p=-m}\right) + \frac{1}{Z(g_r)}(i\gamma p + m)A(-i\gamma p, g_r)\,. \tag{6b}$$

We assume in the following that the divergences of $\Sigma(-k^2)$ and $\Sigma(-i\gamma p)$ are, at the highest, of the second and first order respectively. This was

(*) It can be shown that this cut-off is similar to the Ward cut-off [3]. We formulate this in a form useful for calculating the renormalized propagator $G_c(k^2)$.

[3] M. GELL-MANN and F. E. LOW: *Phys. Rev.*, **95**, 1300 (1954).

proved for any term of the perturbation expansion of Σ in cases of interactions of the first kind. In (6a, b), m denotes the renormalized mass, and therefore it satisfies the relation:

(7a) $$h(m^2) = 0 \ ,$$

or

(7b) $$h(m) \ = 0 \ ,$$

corresponding to (5a) or (5b) respectively. The symbol g_r means the renormalized coupling constant. The A in (6a, b) are the well-defined functions satisfying the relations

(8a) $$A(m^2, g_r) = 0 \ ,$$

or

(8b) $$A(m, g_r) \ = 0 \ .$$

The $Z(g_r)$ is the renormalization constant defined by

(9a) $$\frac{1}{Z(g_r)} = \frac{\partial}{\partial k^2} h(-k^2) \Big|_{k^2=-m^2} = 1 + \frac{\partial}{\partial k^2} \Sigma(-k^2) \Big|_{k^2=-m^2} ,$$

or

(9b) $$\frac{1}{Z(g_r)} = \frac{\partial}{\partial (i\gamma p)} h(-i\gamma p) \Big|_{i\gamma p=-m} = 1 + \frac{\partial}{\partial (i\gamma p)} \Sigma(-i\gamma p) \Big|_{i\gamma p=-m} ,$$

corresponding to (5a) or (5b) respectively. From (6a,b) and (7a,b), we obtain:

(10a) $$G(k^2) = \frac{1}{h(-k^2)} = \frac{Z(g_r)}{(k^2 + m^2 - i\varepsilon)[1 + A(-k^2, g_r)]} ,$$

or

(10b) $$G(p) = \frac{Z(g_r)}{(i\gamma p + m - i\varepsilon)[1 + A(-i\gamma p, g_r)]} .$$

Thus, the renormalized propagators G_c finally lead to the following forms

(11a) $$G_c(k^2, g_r) = \Delta_F(k^2) \frac{1}{1 + A(-k^2, g_r)} ,$$

or

(11b) $$G_c(p, g_r) = S_F(p) \frac{1}{1 + A(-i\gamma p, g_r)} .$$

Here Δ_F and S_F are the free field propagators:

$$\Delta_F(k^2) = \frac{1}{k^2 + m^2 - i\varepsilon},$$

$$S_F(p) = \frac{1}{i\gamma p + m - i\varepsilon}.$$

We now cut off the contributions of high momenta to $h(-k^2)$ or $h(-i\gamma p)$ in the following way:

$$(12a) \qquad h_\Lambda(-k^2) = k^2 + \varkappa^2 + \Sigma(-k^2) + (k^2 + m^2)\frac{\mathrm{Re}\,[\Sigma(\Lambda^2)] - \Sigma(m^2)}{\Lambda^2 - m^2},$$

or

$$(12b) \qquad h_\Lambda(-i\gamma p) = i\gamma p + \varkappa + \Sigma(-i\gamma p) + (i\gamma p + m)\frac{\mathrm{Re}\,[\Sigma(\Lambda)] - \Sigma(m)}{\Lambda - m}.$$

It is of great importance to note that $\Sigma(\Lambda^2)$ or $\Sigma(\Lambda)$ are, in general, complex quantities. Indeed, the interference thresholds [1] cause the branching points to give imaginary terms in Σ. We introduced the real part of Σ instead of Σ itself in (12*a*,*b*) in order to obtain a real renormalization factor by defining it in a way analogous to (9*a*,*b*). Now we shall apply this cut-off procedure to any of the self-energy and vertex diagrams in the Feynman graphs. Then, the renormalization factor $Z(g_r)$ changes into the function $Z^R(\Lambda, g_\Lambda)$ of Λ. The $Z^R(\Lambda, g_\Lambda)$ is derived in this case from h_Λ by

$$(13a) \qquad \frac{1}{Z^R(\Lambda^2, g_\Lambda)} = \frac{\partial}{\partial k^2} h_\Lambda(-k^2)\Big|_{k^2 = -m^2},$$

or

$$(13b) \qquad \frac{1}{Z^R(\Lambda, g_\Lambda)} = \frac{\partial}{\partial(i\gamma p)} h_\Lambda(-i\gamma p)\Big|_{i\gamma p = -m}.$$

Then, the renormalized charge is now g_Λ defined by

$$g_\Lambda^2 = g^2 Z^R(\Lambda, g_\Lambda).$$

The observable mass m is independent of Λ, because we still have the relations

$$h_\Lambda(m^2) = 0,$$

(1) R. J. Eden: *Proc. Roy. Soc.*, A **210**, 388 (1952).

or

$$h_\Lambda(m) = 0\,,$$

corresponding to (7a) or (7b) respectively.

There is no infinity in (12a,b), when Λ is of finite value. -This can be seen from the following relations:

$$(14a)\qquad h_\Lambda(-k^2) = k^2 + m^2 - \Sigma(m^2) + \Sigma(-k^2) - \\ - (k^2+m^2)\left\{\frac{\partial}{\partial k^2}\Sigma(-k^2)\Big|_{k^2=-m^2} + \frac{1}{Z^R(\Lambda^2, g_\Lambda)}\,\mathrm{Re}\,[A(\Lambda^2, g_\Lambda)]\right\} = \\ = k^2 + m^2 + \frac{1}{Z^R(\Lambda^2, g_\Lambda)}\{A(-k^2, g_\Lambda) - \mathrm{Re}\,[A(\Lambda^2, g_\Lambda)]\}(k^2+m^2),$$

or

$$(14b)\quad h_\Lambda(-i\gamma p) = i\gamma p + m + \frac{1}{Z^R(\Lambda, g_\Lambda)}\{A(-i\gamma p, g_\Lambda) - \mathrm{Re}\,[A(\Lambda, g_\Lambda)]\}(i\gamma p + m)\,.$$

On the other hand, from (12a) and (13a), we obtain

$$(15a)\qquad \frac{1}{Z^R(\Lambda^2, g_\Lambda)} = 1 + \frac{\partial}{\partial k^2}\Sigma(-k^2)\Big|_{k^2=-m^2} + \frac{\mathrm{Re}\,[\Sigma(\Lambda^2)] - \Sigma(m^2)}{\Lambda^2 - m^2}$$

$$(16a)\qquad = 1 - \frac{1}{Z^R(\Lambda^2, g_\Lambda)}\,\mathrm{Re}\,[A(\Lambda^2, g_\Lambda)].$$

In a similar way, (12b) and (13b) lead to

$$(15b)\qquad \frac{1}{Z^R(\Lambda, g_\Lambda)} = 1 + \frac{\partial}{\partial(i\gamma p)}\Sigma(-i\gamma p)\Big|_{i\gamma p=-m} + \frac{\mathrm{Re}\,[\Sigma(\Lambda)] - \Sigma(m)}{\Lambda - m}$$

$$(16b)\qquad = 1 - \frac{1}{Z^R(\Lambda, g_\Lambda)}\,\mathrm{Re}\,[A(\Lambda, g_\Lambda)]\,.$$

Thus, (14a,b) lead to

$$(17a)\qquad h_\Lambda(-k^2) = \frac{(k^2+m^2)}{Z^R(\Lambda^2, g_\Lambda)}\{1 + A(-k^2, g_\Lambda)\},$$

or

$$(17b)\qquad h_\Lambda(-i\gamma p) = \frac{(i\gamma p + m)}{Z^R(\Lambda, g_\Lambda)}\{1 + A(-i\gamma p, g_\Lambda)\},$$

respectively.

Comparing (17*a*,*b*) with (11*a*,*b*), we obtain

$$G_\Lambda(k^2) \equiv \frac{1}{h_\Lambda(-k^2)} = Z^R(\Lambda^2, g_\Lambda) G_c(k^2, g_\Lambda), \tag{18a}$$

or

$$G_\Lambda(p) \equiv \frac{1}{h_\Lambda(-i\gamma p)} = Z^R(\Lambda, g_\Lambda) G_c(p, g_\Lambda)\,. \tag{18b}$$

It should be noted here that G_Λ is just equal to what is obtained from G by substitutions $Z \to Z^R(\Lambda)$ and $g_r \to g_\Lambda$. This remarkable result comes from the following reason; as shown by (6*a*) and (11*a*), the renormalized propagator G_c depends only on the higher derivatives

$$\frac{\partial^n}{\partial(k^2)^n} h(-k^2)\,, \qquad (n \geqslant 2)$$

wich remain unchanged throughout the cut-off procedure (12*a*). By substituting g_{ob} for g_Λ in $G_c(-k^2, g_\Lambda)$, we obtain the renormalized propagator which is independent of Λ.

It is of great importance that (15*a*,*b*) leads to the relation (*)

$$\lim_{\Lambda\to\infty} Z^R(\Lambda^2, g_\Lambda) = Z(g_r)\,, \tag{19a}$$

or

$$\lim_{\Lambda\to\infty} Z^R(\Lambda, g_\Lambda) = Z(g_r) \tag{19b}$$

and therefore to

$$\lim_{\Lambda\to\infty} G_\Lambda = G\,. \tag{20}$$

On the other hand, we can derive from (16*a*,*b*) the relations

$$Z^R(\Lambda^2, g_\Lambda) = 1 + \mathrm{Re}[A(\Lambda^2, g_\Lambda)]\,, \tag{21a}_R$$

or

$$Z^R(\Lambda, g_\Lambda) = 1 + \mathrm{Re}[A(\Lambda, g_\Lambda)]\,. \tag{21b}_R$$

We now introduce

$$Z(\Lambda^2, g_\Lambda) \equiv 1 + A(\Lambda^2, g_\Lambda)\,, \tag{21a}$$

(*) This will be easily understood if we expand Σ in perturbation series.

or

$$Z(\Lambda, g_\Lambda) \equiv 1 + A(\Lambda, g_\Lambda) \tag{21b}$$

and

$$Z^I(\Lambda^2, g_\Lambda) \equiv \mathrm{Im}\,[A(\Lambda^2, g_\Lambda)]\,, \tag{21a}_I$$

or

$$Z^I(\Lambda, g_\Lambda) \equiv \mathrm{Im}\,[A(\Lambda, g_\Lambda)]\,. \tag{21b}_I$$

The imaginary part of A is the contribution from the displaced poles ([4]). Thus, as was shown by DYSON ([5]), it should be finite for any value of Λ (cf. Sect. 6). The $Z(\Lambda^2, g_\Lambda)$ can be obtained in a way similar to the derivation of $Z^R(\Lambda^2, g_\Lambda)$. Let us modify the renormalization cut-off such that $\mathrm{Re}\,[\Sigma(\Lambda^2)]$ in (12a) is replaced by $\Sigma(\Lambda^2)$ itself. Then, $Z(g_r)$ in (6a) should be replaced by $Z(\Lambda^2, g_\Lambda)$ defined by

$$\frac{1}{Z(\Lambda^2, g_\Lambda)} = 1 + \left.\frac{\partial\Sigma(-k^2)}{\partial k^2}\right|_{k^2=-m^2} + \frac{\Sigma(\Lambda^2) - \Sigma(m^2)}{\Lambda^2 - m^2}$$

(cf. (12a)). Here g_Λ is connected with g by the relation

$$g_\Lambda^2 = g^2 Z(\Lambda^2, g_\Lambda)\,.$$

Then, (16a) is changed to be

$$\frac{1}{Z(\Lambda^2, g_\Lambda)} = 1 - \frac{1}{Z(\Lambda^2, g_\Lambda)}\, A(\Lambda^2, g_\Lambda)\,.$$

This leads to

$$Z(\Lambda^2, g_\Lambda) = 1 + A(\Lambda^2, g_\Lambda)\,.$$

This is just (21a), if we replace the argument $g_\Lambda = gZ^{\frac{1}{2}}$ by $g_\Lambda = g(Z^R)^{\frac{1}{2}}$. Substituting g_r and $-k^2$ for g_Λ and Λ^2 respectively, we have

$$Z(-k^2, g_r) = 1 + A(-k^2, g_r)\,, \tag{22a}$$

or

$$Z(-i\gamma p, g_r) = 1 + A(-i\gamma p, g_r)\,. \tag{22b}$$

The relations (11a,b) now become

$$G_c(k^2, g_r) = \Delta_F(k^2)\,\frac{1}{Z(-k^2, g_r)}\,, \tag{23a}$$

([5]) F. J. DYSON: *Phys. Rev.*, **75**, 1736 (1949).

or

$$G_c(p, g_r) = S_F(p) \frac{1}{Z(-i\gamma p, g_r)} . \tag{23b}$$

Furthermore, from (19a,b) and (22a,b) we see the following properties:

$$\begin{cases} \lim\limits_{-k^2\to\infty} Z^R(-k^2, g_r) = Z(g_r) \\ Z(m^2, g_r) = 1 \end{cases} \tag{24a}$$

or

$$\begin{cases} \lim\limits_{-i\gamma p\to\infty} Z^R(-i\gamma p, g_r) = Z(g_r) \\ Z\ (m, g_r) = 1 \end{cases} \tag{24b}$$

To calculate $Z(\Lambda^2, g_\Lambda)$, $Z(\Lambda, g_\Lambda)$ and g_Λ by means of the perturbation expansion, we should formulate the cut-off method for the vertex Γ, because self-energy diagrams contain vertices. This is done as follows. We first consider the electromagnetic interaction of spinor particles. The vertex Γ_μ can be written in the form:

$$\Gamma_\mu(p_1, p_2) = \gamma_\mu + Z_1^{-1} \Lambda_\mu(p_1, p_2) , \tag{25}$$

with

$$\Lambda_\mu(p_1, p_2) = L(e_r)\gamma_\mu + \Lambda_{\mu c}(p_1, p_2) . \tag{26}$$

Here e_r is the renormalized charge, and $\Lambda_{\mu c}$ is a convergent function. The constant Z_1 is defined by

$$Z_1 = 1 - L(e_r) . \tag{27}$$

The renormalized vertex $\Gamma_{\mu c}$ is given by

$$\Gamma_{\mu c}(p_1, p_2) = Z_1 \Gamma_\mu(p_1, p_2) \tag{28}$$

$$= \gamma_\mu + \Lambda_{\mu c}(p_1, p_2) . \tag{29}$$

We shall now introduce

$$\Gamma_{\mu\Lambda}(p_1, p_2) = \gamma_\mu + \frac{1}{Z_1^R(\Lambda, e_\Lambda)} \Lambda_{\mu\Lambda}(p_1, p_2) , \tag{30}$$

with ([3])

$$(31)\qquad \Lambda_{\mu\Lambda}(p_1, p_2) = \Lambda_\mu(p_1, p_2) - \int_0^1 \mathrm{d}x\, \mathrm{Re}^*[\Lambda_\mu(tx + l(1-x), tx + l(1-x))]\,.$$

Here t and l are the energy-momenta satisfying

$$(32)\qquad -i\gamma t = \Lambda\,, \qquad -i\gamma l = m\,.$$

Furthermore, the notation $\mathrm{Re}^*[\Lambda_\mu]$ should be understood $\gamma_\mu \mathrm{Re}[\Lambda]$ with Λ defined by $\Lambda_\mu \equiv \gamma_\mu \Lambda$. Here use is made of the fact that $\Lambda_\mu(p, p)$ is proportional to γ_μ for $i\gamma p = a$ c-number. It is evident that, when Λ is finite, (31) does not contain any divergent integral in itself. By using the well-known relation,

$$(33)\qquad \Gamma_\mu(p, p) = \frac{1}{i}\frac{\partial}{\partial p_\mu}[G(p)]^{-1} = \gamma_\mu + \frac{1}{i}\frac{\partial}{\partial p_\mu}\Sigma(-i\gamma p)\,,$$

we can derive, from (25), the relation

$$(34)\qquad \Lambda_\mu(p, p) = Z_1^R(\Lambda, e_\Lambda)\gamma_\mu \frac{\partial}{\partial(i\gamma p)}\Sigma(-i\gamma p) \qquad \text{for } i\gamma p = -M\,,$$

where $i\gamma p$ is replaced by a c-number M after the derivation in (33). We can understand the reason why there appears $Z^R(\Lambda, e_\Lambda)$ instead of $Z_1(e_r)$ in the following way. The divergent diagrams in general contain self-energy or vertex graphs, and the infinities due to latter graphs lead to the renormalization factors in the final integrations ([6]). The renormalization cut-off should be applied not only to the final integration but to any stage of the calculation.

Equation (34) leads to

$$(35)\qquad \int_0^1 \mathrm{d}x\, \Lambda_\mu(tx + l(1-x), tx + l(1-x)) =$$

$$= -Z_1^R(\Lambda, e_\Lambda)\gamma_\mu \frac{1}{\Lambda - m}\int_0^1 \mathrm{d}x \frac{\partial}{\partial x}\Sigma(\Lambda x + m(1-x))$$

$$(36)\qquad = -Z_1^R(\Lambda, e_\Lambda)\gamma_\mu \frac{\Sigma(\Lambda) - \Sigma(m)}{\Lambda - m}\,.$$

([6]) A. SALAM: *Phys. Rev.*, **82**, 216 (1951).

Thus, (30) and (26) give

$$\Gamma_{\mu\Lambda}(p_1, p_2) = \gamma_\mu + \tag{37}$$
$$+ \frac{1}{Z_1^R(\Lambda, e_\Lambda)} \left[\left\{ L(e_\Lambda) + Z_1^R(\Lambda, e_\Lambda) \frac{\mathrm{Re}\,[\Sigma(\Lambda)] - \Sigma(m)}{\Lambda - m} \right\} \gamma_\mu + \Lambda_{\mu\sigma}(p_1, p_2) \right].$$

By taking $Z_1^R(\Lambda, e_\Lambda)$ as

$$Z_1^R(\Lambda, e_\Lambda) = 1 - L(e_\Lambda) - Z_1^R(\Lambda, e_\Lambda) \frac{\mathrm{Re}\,[\Sigma(\Lambda)] - \Sigma(m)}{\Lambda - m}, \tag{38}$$

we see that the renormalized vertex is independent of Λ:

$$\Gamma_{\mu c}(p_1, p_2) = Z_1^R(\Lambda, e_\Lambda) \Gamma_{\mu\Lambda}(p_1, p_2) \tag{39}$$
$$= \gamma_\mu + \Lambda_{\mu\sigma}(p_1, p_2) \tag{40}$$

(with $e_r \to e_\Lambda$). In other words, the subtraction (31) is the renormalization cut-off for the vertex.

Comparing (37) with (12*b*) and taking account of Ward's identity and (33)

$$\frac{1}{1 - L(e_r)} = 1 + \frac{\partial \Sigma(-i\gamma p)}{\partial(i\gamma p)}\bigg|_{i\gamma p = -m}, \tag{41}$$

we obtain

$$\Gamma_{\mu\Lambda}(p, p) = \frac{1}{i} \frac{\partial}{\partial p_\mu} h_\Lambda(-i\gamma p). \tag{42}$$

Thus, we see that the renormalization cut-off is the gauge-invariant procedure.

From (38) and (41) we obtain

$$\frac{1}{Z_1^R(\Lambda, e_\Lambda)} = 1 + \frac{L(e_\Lambda)}{Z_1^R(\Lambda, e_\Lambda)} + \frac{\mathrm{Re}\,[\Sigma(\Lambda)] - \Sigma(m)}{\Lambda - m} \tag{43}$$
$$= 1 + \frac{\partial \Sigma(-i\gamma p)}{\partial(i\gamma p)}\bigg|_{i\gamma p = -m} + \frac{\mathrm{Re}\,[\Sigma(\Lambda)] - \Sigma(m)}{\Lambda - m}, \tag{44}$$

which leads to

$$Z_1^R(\Lambda, e_\Lambda) = Z^R(\Lambda, e_\Lambda) \tag{45}$$

on account of (15*b*) (with $g_\Lambda \to e_\Lambda$). The relation (45) is the extention of the Ward identity into the case of finite Λ.

It is clear from (19*b*) that

$$\lim_{\Lambda \to \infty} Z_1^R(\Lambda, e_\Lambda) = Z(e_r) = Z_1(e_r). \tag{46}$$

The relation

$$\Gamma_{\mu\Lambda}(p, p) = \frac{1}{i}\frac{\partial}{\partial p_\mu}[G_\Lambda(p)]^{-1} \tag{47}$$

leads to

$$\Gamma_{\mu\Lambda}(p, p) = \frac{1}{i}\frac{\partial}{\partial p_\mu}\left\{(i\gamma p + m)\frac{Z(-i\gamma p, e_\Lambda)}{Z^R(\Lambda, e_\Lambda)}\right\} \approx \tag{48}$$

$$\approx \gamma_\mu\left\{1 + i\frac{Z^I(\Lambda, e_\Lambda)}{Z^R(\Lambda, e_\Lambda)}\right\} \quad \text{for} \quad -i\gamma p = \Lambda \gg m$$

on account of (17*b*) and (18*b*). This leads to

$$\Gamma_{\mu c}(p, p) \approx \gamma_\mu Z(-i\gamma p, e_r) \qquad \text{for} \qquad -i\gamma p \approx \Lambda \gg m. \tag{49}$$

For the scalar (pseudoscalar) meson theory the renormalization cut-off of the vertices can be similarly carried out by (30), (31) and (32) with the replacement $\Gamma_\mu \to \Gamma$ (Γ_5), $\Lambda_\mu \to \Lambda$ (Λ_5) and $\gamma_\mu \to 1$ (γ_5).

The main results obtained in this section shall be summarized in the theorems in the next section.

3. – Miscellaneous Theorems.

Theorem 1. *The propagators $G_\Lambda(k^2)$ and $G_\Lambda(p)$ obtained by the renormalization cut-off are equal to*

$$G_\Lambda(k^2) = \frac{1}{k^2 + m^2 - i\varepsilon}\left(1 - i\frac{Z^I(\Lambda^2, g_\Lambda)}{Z\ (\Lambda^2, g_\Lambda)}\right) \tag{50a}$$

$$G_\Lambda(p) = \frac{1}{i\gamma p + m - i\varepsilon}\left(1 - i\frac{Z^I(\Lambda, g_\Lambda)}{Z\ (\Lambda, g_\Lambda)}\right) \tag{50b}$$

when $k^2 = -\Lambda^2$ or $i\gamma p = -\Lambda$ (cf. (18*a*,*b*) and (23*a*,*b*)).

Theorem 2. *Asymptotic forms of the propagators and vertices are given by:*

$$G(k^2) = \frac{1}{k^2 + m^2 - i\varepsilon}\left\{1 + O\left(\frac{1}{\log\,(k^2/m^2)}\right)\right\}, \tag{51a}$$

$$G(p) = \frac{1}{i\gamma p + m \quad i\varepsilon}\left\{1 + O\left(\frac{1}{\log\,(i\gamma p/m)}\right)\right\}, \tag{51b}$$

$$\Gamma_\mu(p, p) = \gamma_\mu\left\{1 + O\left(\frac{1}{\log\,(i\gamma p/m)}\right)\right\}, \tag{51c}$$

for $-k^2 \gg m^2$ and $-i\gamma p \gg m$.

This follows from theorem 1 and the relations (20), and (48). This is quite a reasonable result, because this theorem means that if we enter the inside of the proper field, we should observe its source particle.

It must be noted that Theorems 1, 2 and following cannot be extended to the case of the interactions of the second kind. Indeed, in the latter case the h_Λ's in (14*a*,*b*) may still contain divergent integrals. To make h_Λ finite, more terms should be subtracted from (14*a*,*b*). Then, almost all results in Sect. 2 do not hold any more. For example, G_c explicitly depends on Λ. This can be understood as follows; the cloud of proper fields due to interactions of the second kind seems to concentrate compactly near the source, and therefore, we cannot separate the cloud from its source. This is one of the essential differences between interactions of the first and of the second kind.

Theorem 3. *The renormalized propagators* $G_c(k^2, g_{ob})$ *and* $G_c(p, g_{ob})$ *with observable charge* g_{ob} (*i.e.* $g_r \to g_{ob}$) *can be obtained by calculating* $Z(\Lambda^2, g_\Lambda)$ *and* $Z(\Lambda, g_\Lambda)$ *with various values of the cut-off* Λ.

In fact, when we have the functions, $Z(\Lambda^2, g_\Lambda)$ and $Z(\Lambda, g_\Lambda)$, of Λ, we can derive G_c by replacing Λ^2, Λ and g_Λ by $-k^2$, $-i\gamma p$ and g_{ob} respectively:

$$G_c(k^2, g_{ob}) = \Lambda_F(k^2)\,\frac{1}{Z(-k^2, g_{ob})}\,, \tag{52a}$$

$$G_c(p, g_{ob}) = S_F(p)\,\frac{1}{Z(-i\gamma p, g_{ob})}\,. \tag{52b}$$

It is the peculiar feature of Theorem 3 that the renormalized quantities defined in the theory without cut-off (or $\Lambda \to \infty$) can be derived from quantities obtained with the cut-off procedure (with various Λ).

In general, it is not so easy to calculate $Z(\Lambda^2, g_\Lambda)$ or $Z(\Lambda, g_\Lambda)$ for all possible values of Λ. However, we occasionally encounter a case where $Z^R(\Lambda, g_\Lambda)$ for $\Lambda \gg m$ can be calculated approximately (error: $O(m/\Lambda)\log(\Lambda/m)$). An example of such a case is given by the Z_3-factor in the quantum electrodynamics as will be discussed in the succeeding paper. About the imaginary part Z^I, we have pointed out in Sect. 2 that it is finite for any value of Λ.

4. – The Renormalized Propagator and the Effective Coupling.

It is well known that, in most cases, the renormalization factor $Z(g_r)$ of propagators satisfies the condition (3). Suppose that

$$Z(g_{ob}) < 0$$

and therefore, g_{ob} is out of the normal zone $N(g_r)$. Then (24*a*) and (24*b*) say

that by taking suitable λ, we obtain

$$Z^R(-k^2, g_{ob}) < 0 \qquad \text{for } -k^2 > \lambda^2, \tag{53a}$$

or

$$Z^R(-ikp, g_{ob}) < 0 \qquad \text{for } -ikp > \lambda. \tag{53b}$$

In other words, $Z^R(-k^2, g_{ob})$, $(Z^R(-i\gamma p, g_{ob}))$ changes its sign at $-k^2 = \lambda^2$ $(-i\gamma p = \lambda)$ (cf. Fig. 1). Then, we see from Theorem 3 that the real part of $G_c(k^2, g_{ob})$ or of $G_c(p, g_{ob})$ also changes its sign at $-k^2 = \lambda^2$ or $-i\gamma p = \lambda$ respectively (*), as is shown in Fig. 2. When $R_c(-k^2, g_{ob})$ defined by the ratio

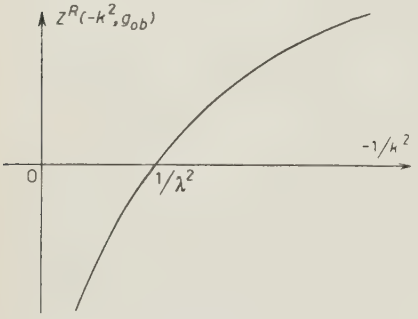

Fig. 1.

$$R_c(-k^2, g_{ob}) = \frac{G_c(k^2, g_{ob})}{\Delta_F(k^2)} = \frac{1}{Z(-k^2, g_{ob})}, \tag{54}$$

we see that the negative sign of the real part of R_c for large $|k^2|$ (or for large $|i\gamma p|$) is an essential feature that occurs when g_{ob} is out of the normal zone $N(g_r)$. If this is the case, the system in the region $|k^2| > \lambda^2$ will behave quite differently from that in the low energy region. For all the S-matrix elements are made up of the renormalized propagator G_c. There may, therefore, be some experiments which will allow the observation of the effects of G_c with $|k^2| > \lambda^2$.

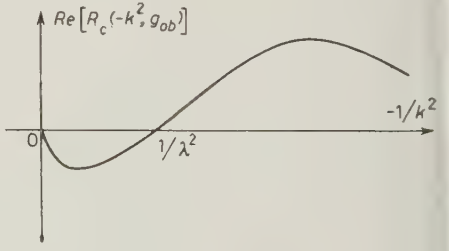

Fig. 2.

If we cut-off the integrations over internal momenta at Λ, then the renormalization factor is given by $Z^R(\Lambda^2, g_\Lambda)$. To obtain the normal zone containing g_{ob}, Λ should be smaller than λ. In other words, the normal zone $N(g_1)$ can contain g_{ob} in itself, only when we disregard the contribution from $G_c(k^2, g_{ob})$ with $-k^2 > \lambda^2$. Thus, we may say that the ordinary renormalization theory is out of the limit of applicability if $-k^2 > \lambda^2$.

To understand the situation clearly, it would be helpful to consider a simple case. Suppose that the $Z(g_r)$ gives the ratio g_r^2/g^2:

$$g_r^2 = Z(g_r)g^2 .$$

(*) Here, the case where Z^R changes its sign discontinuously at $-k^2 = \lambda^2$ is not excluded. Anyhow, the essential fact is that the sign of Z^R is negative for $-k^2 > \lambda^2$.

In such a case the radiative corrections modify the scattering potential due to the propagator Δ_F of the scalar field in two ways: the coupling constant g is replaced by g_r, and the propagator is modified to give $G_c(k^2)$. These two effects can be amalgamated into one effect, i.e. the change of the coupling

$$g^2 \to g_r^2 R_c(-k^2, g_r) ,$$

and the propagator remains unchanged.

In this connection it is convenient to introduce the concept « effective charge » g_{eff} defined by

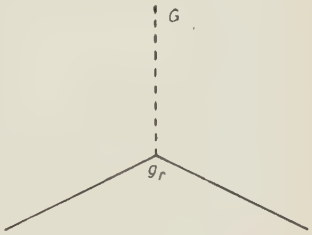

Fig. 3.

$$g_{eff}^2(-k^2, g_r) = g_r^2 R_c(-k^2, g_r) . \tag{55}$$

The relations (23a), (24a) and (54) say that

$$\lim_{-k^2 \to \infty} g_{eff}^2(-k^2, g_r) = g^2 , \tag{56}$$

$$g_{eff}^2(m^2, g_r) = g_r^2 . \tag{57}$$

The relation (56) shows that the charge immediately near the source is nothing but the unrenormalized charge.

The real part of the effective charge Re (g_{eff}^2) depends on the k^2 in the same way as Re (R_c) does. Thus, as shown by Fig. 2, Re (g_{eff}^2) changes its sign at $-k^2 = \lambda^2$. Thus it may well be that the renormalization theory gives wrong answers in the high energy scattering process $(|k^2| > \lambda^2)$.

Since g_Λ is the function of the unrenormalized charge g and Λ:

$$g_\Lambda = f(\Lambda, g) ,$$

to regard g_Λ as g_{ob} is equivalent to assume a value for g. Such a value of g can be easily found from Fig. 4, For we have the relation

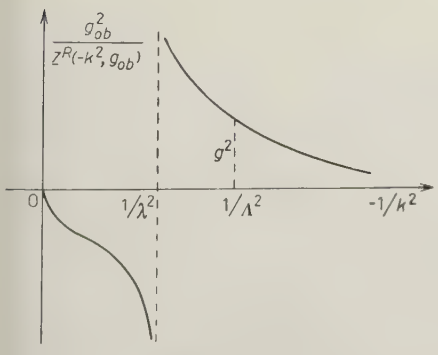

Fig. 4.

$$\frac{g_{ob}^2}{Z^R(-k^2, g_{ob})} = g^2 \quad \text{for} -k^2 = \Lambda^2. \tag{58}$$

Thus, we see that, the unrenormalized charge is imaginary, when Λ is larger than λ. This is just what we have seen; the normal zone $N(g_\Lambda)$ (not $N(g_r)$) can contain g_{ob} only when $\Lambda < \lambda$. At any rate, the renormalization theory cannot

describe the experimental results for the scattering process with high momentum transfer ($-k^2 > \lambda^2$), when $N(g_r)$ (not $N(g_\Lambda)$) does not contain g_{ob}. We shall discuss the effective electric charge in a succeeding paper.

If g_{ob} is out of $N(g_r)$, it may be reasonable to expect that some physical effects have been out of consideration and that to take account of such effects may change the sign of Re $(G_c(k^2))$ with $-k^2 > \lambda^2$ (cf. (54) and Fig. 5).

Since interactions due to particles with masses larger than λ may affect essentially the function $G_c(k^2)$ with $-k^2 > \lambda^2$, it may be of importance to examine how the effects of these heavy particles have influences on the $N(g_r)$. For example, it may be likely that the renormalized propagators of the π-meson and the nucleon for high energy-momenta depend on effects due to heavy mesons and hyperons, and therefore that we should carefully take into account these latter effects in order to obtain the normal zone for the meson-nucleon coupling. This will be discussed in a separate paper. Contrary to the case of meson-nucleon scattering, λ seems to be quite large for the photon propagator $D_c(k^2)$; as will be shown in a succeeding paper, λ is larger than any of the masses of particles which we know at present. Thus, in order to improve the quantum electrodynamics, we should search for effects different from those due to heavy particles.

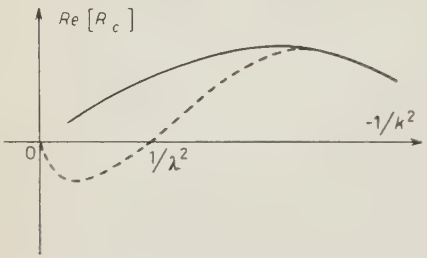

Fig. 5.

We shall end this section by giving a note on $Z^R(\Lambda, g_{ob})$. Since the order of divergence of $Z(g_r)$ is logarithmic, we may approximately calculate $Z^R(\Lambda, g_{ob})$ with $\Lambda \gg m$ by using the simple straight cut-off instead of using the renormalization cut-off; the error introduced in this case amounts to $O(m/\Lambda)\log(\Lambda/m)$. Thus, in order to obtain an approximate form of $G_c(k^2)$ for $-k^2 \gg m^2$, we have only to calculate $Z(g_{ob})$ by use of straight cut-off.

5. – Renormalization Constants.

We shall now briefly review the discussions on the condition (3). We first consider the propagator $G_c(k^2)$ of a scalar field $\varphi(x)$ which is renormalized. As shown by LEHMANN (7), $G_c(k^2)$ can be written in the form

$$G_c(k^2) = \int \frac{\varrho(\varkappa^2)\,\mathrm{d}\varkappa^2}{k^2 + \varkappa^2 - i\varepsilon}\,. \tag{59}$$

(7) H. LEHMANN: *Nuovo Cimento*, **11**, 324 (1954).

By introducing eigenstates $\Phi(k)$ of total energy-monemtum, we can expand the state

$$\varphi(x)\Phi_0 \tag{60}$$

in a following form

$$\varphi(x)\Phi_0 = \sum \Phi(k) \exp[ikx] . \tag{61}$$

Here Φ_0 is the physical vacuum whose energy and momentum are zero. Then, the function $\varrho(\varkappa^2)$ is the probability of the state $\Phi(k)$ with $k^2 = -\varkappa^2$:

$$\varrho(\varkappa^2) = \sum \Phi^*(k)\Phi(k) , \tag{62}$$

where the summation is taken over all states $\Phi(k)$ with $k^2 = -\varkappa^2$. In the state (60), there appear some one-particle states with the masses m_1, m_2, ... and many-particle states with $-k^2 > m_1^2, m_2^2, \ldots$: Thus $\varrho(\varkappa^2)$ has the form

$$\varrho(\varkappa^2) = \sum_i \frac{Z_i}{Z(g_r)} \delta(\varkappa^2 - m_i^2) + \sigma(\varkappa^2) , \tag{63}$$

with

$$\sigma(\varkappa^2) = 0 \qquad \text{for } \varkappa^2 < M^2.$$

Here M^2 is the minimum value of $-k^2$ for many-particle states.

By using (4a) and (59) we can derive

$$\sum_i \frac{Z_i}{Z(g_r)} \frac{h(-k^2)}{k^2 + m_i^2 - i\varepsilon} + \int_{M^2}^{\infty} \frac{h(-k^2)\sigma(\varkappa^2)\,\mathrm{d}\varkappa^2}{k^2 + \varkappa^2 - i\varepsilon} = \frac{1}{Z(g_r)} . \tag{64}$$

This shows that

$$h(m_i^2) = 0 \tag{65}$$

$$\frac{1}{Z_i} = \frac{\partial}{\partial k^2} h(-k^2)\Big|_{-k^2 = m_i^2} . \tag{66}$$

The use of the canonical commutation relation

$$Z(g_r)[\varphi(\boldsymbol{x}, t), \varphi^*(\boldsymbol{x}', t)] = -i\delta(\boldsymbol{x} - \boldsymbol{x}')$$

and of the relation (59) leads to the result:

$$\int \varrho(\varkappa^2)\,\mathrm{d}\varkappa^2 = \sum_i \frac{Z_i}{Z(g_r)} + \int_{M^2}^{\infty} \sigma(\varkappa^2)\,\mathrm{d}\varkappa^2 = \frac{1}{Z(g_r)} . \tag{67}$$

If the interaction is hermitic, $\varrho(\varkappa^2)$ can not be negative on account of (62) and we should have

$$0 \leqslant Z_i \leqslant 1 , \tag{68}$$

on account of (63) and (67). However, if the g_{ob} is out of the normal zone $N(g_r)$, Z_i does not necessarily satisfy (68). If any of the Z_i does not satisfy (68), (63) and (67) say that $\varrho(\varkappa^2)$ is not positive-definite, and therefore there appear some states of negative probability. This means that the interaction with the unrenormalized constant g, which leads to g_{ob} out of $N(g_r)$, is not hermitic.

It is possible to express $\varrho(\varkappa^2)$ in terms of $Z(-k^2, g_r)$ in the following way. Eq. (59) can be rewritten into

$$G_c(k^2) = P\int \frac{\varrho(\varkappa^2)\,\mathrm{d}\varkappa^2}{k^2+\varkappa^2} + i\pi\varrho(-k^2) .$$

On the other hand, the imaginary part of $G(k^2)$ is derived from (23a) to be

$$\mathrm{Im}\,[G(k^2)] = \frac{-Z^I(-k^2, g_r)}{(k^2+m^2)\,|\,Z(-k^2, g_r)\,|^2}$$

for $-k^2 > m^2$. These equations lead to

$$\varrho(\varkappa^2) = \frac{Z^I(\varkappa^2, g_r)}{\pi(\varkappa^2-m^2)\,|\,Z(\varkappa^2, g_r)\,|^2}$$

for $\varkappa^2 > m^2$. This says that, for a region of k_μ where $Z^I(-k^2, g_r)$ is positive, the state $\Phi(k)$ has positive probability. For, in such a case, $\varrho(-k^2)$ must be positive.

It has been noticed by some authors [3] that, in quantum electrodynamics, condition (3) is to be required for Z_3, but not for Z_2. We shall now discuss this point in detail. Since the scalar photon appears with negative probability, we cannot deduce, from (62), the positive definiteness of $\varrho(\varkappa^2)$. Indeed, the renormalization factor Z_2 of the electron depends on the gauge and does not necessarily satisfy (3). However, we show that the renormalization factor $Z_3(e_r)$ of the photon should satisfy (3). Let us denote the propagator of a photon by $D_{\mu\nu}(k)$:

$$D_{\mu\nu}(k) \equiv \langle A_\mu(k),\, A_\nu(k)\rangle_0 . \tag{69}$$

Here $\langle\,\rangle_0$ means that the expectation value is taken for the vacuum state. The $D_{\mu\nu}$ should satisfy the equation

$$\left\{k^2\delta_{\mu\varrho} + \Pi_{\mu\varrho}(k)\right\} D_{\varrho\nu}(k) = \delta_{\mu\nu} . \tag{70}$$

On account of the gauge-invariance of the theory, $\Pi_{\mu\nu}(k)$ should satisfy the relation

$$k_\mu \Pi_{\mu\nu}(k) = 0 . \tag{71}$$

We see from (71) that $\Pi_{\mu\nu}(k)$ should take the form of

$$\Pi_{\mu\nu}(k) = \left(\delta_{\mu\nu} - \frac{k_\mu k_\nu}{k^2}\right) \Pi(k^2) \tag{72}$$

from the requirement of relativistic covariance of the theory. It is convenient to introduce an unit vector $\boldsymbol{e}$, which is orthogonal to $\boldsymbol{k}$:

$$\boldsymbol{ke} = 0 . \tag{73}$$

Then, (72) leads to

$$\sum_{j=1,2,3} e_j \Pi_{j\mu}(k) = \begin{cases} \Pi(k^2) e_\mu & \text{for } \mu = 1, 2, 3. \\ 0 & \text{for } \mu = 4. \end{cases}$$

From this we can derive the equation

$$\{k^2 + \Pi(k^2)\} D(k^2) = 1 , \tag{74}$$

with

$$D(k^2) \equiv \sum_{j,l=1,2,3} (e_j e_l D_{jl}(k)) . \tag{75}$$

$$= \sum_{j,l} \langle e_j A_j(k) A_l(k) e_l \rangle_0 .$$

We see from (74) that $D(k^2)$ depends only on k^2.

In the Gupta-Bleuler formalism [8] of quantum electrodynamics, the expectation value of any operator F is given by

$$\langle F \rangle \equiv \Psi^* \eta F \Psi . \tag{76}$$

Here, η is the operator satisfying the relations:

$$\eta A_4 = -A_4 \eta , \quad \eta A_j = A_j \eta \quad (\text{for } j = 1, 2, 3), \quad \eta^* = \eta^{-1}. \tag{77}$$

[8] S. N. Gupta: *Proc. Phys. Soc.*, **63**, 681 (1950); K. Bleuler: *Helv. Phys. Acta*, **23**, 567 (1950).

The hermitic property of A_j shows that A_j is self-adjoint:

$$A_j^\dagger \equiv \eta^* A_j \eta = A_j \,. \tag{78}$$

Thus, we see that

$$\langle e_j A_j(k),\, e_l A_l(k)\rangle_0 \geqslant 0 \,. \tag{79}$$

Taking into account the relativistic covariance of the theory, $D_{\mu\nu}(k)$ should have the form:

$$D_{\mu\nu}(k) = \left\{\delta_{\mu\nu} - \frac{k_\mu k_\nu}{k^2}\right\} D(k^2) + k_\mu k_\nu D_l(k^2) \,. \tag{80}$$

The D_l depends on the gauge, and therefore can be assumed to be zero. We now calculate the commutation relation:

$$\left\langle \left[\frac{\mathrm{d}}{\mathrm{d}t} A_\mu(\boldsymbol{x}, t),\, A_\nu(\boldsymbol{x}', t)\right] \right\rangle_0 = \lim_{t' \to t} \left\{ \left[\frac{\mathrm{d}}{\mathrm{d}t} D_{\mu\nu}(x - x')\right]_{t>t'} - \left[\frac{\mathrm{d}}{\mathrm{d}t} D_{\mu\nu}(x - x')\right]_{t<t'} \right\} . \tag{81}$$

By writing $D(k^2)$ in the form of (59) and by comparing (81) with the canonical commutation relation

$$Z_3 \left[\frac{\mathrm{d}}{\mathrm{d}t} A_\mu(\boldsymbol{x}, t),\, A_\nu(\boldsymbol{x}', t)\right] = -\, i\, \delta(\boldsymbol{x} - \boldsymbol{x}') \,,$$

we can deduce

$$\int \varrho(\varkappa^2)\, \mathrm{d}\varkappa^2 = 1 + \int_{M^2}^{\infty} \sigma(\varkappa^2)\, \mathrm{d}\varkappa^2 = \frac{1}{Z_3(e_r)} \,. \tag{82}$$

In a way similar to the case of (66), we can define the renormalization factor $Z_3(e_r)$ by

$$\frac{1}{Z_3(e_r)} = \frac{\partial}{\partial k^2} h(-k^2) \Big|_{k^2=0} , \tag{83}$$

with

$$h(-k^2) \equiv k^2 + \Pi(k^2) \,. \tag{84}$$

The relation (79) says that $\varrho(\varkappa^2)$ is positive definite and that

$$0 \leqslant Z_3(e_r) \leqslant 1 \,. \tag{85}$$

Hence, if $Z_3(e_r)$ does not satisfy (85), the observed value e_{ob} of the charge is out of the normal zone $N(e_r)$.

6. – Simple Examples.

To have a clear idea of the general discussions in Sects. 2, 3 and 4, it may helpful to consider some simple examples; they will be discussed here.

6·1. *Vacuum polarization in quantum electrodynamics.* – In the lowest order approximation of the perturbation theory, we obtain [9]

$$k^2 + \Pi(k^2) = \frac{1}{Z_3}\left\{k^2 + k^2 A(k^2)\right\}, \tag{86}$$

with

$$Z_3 = 1 - \frac{e_r^2}{\pi}\int_0^1 \frac{v^2}{1-v^2}\left(1 - \frac{v^2}{3}\right)\mathrm{d}v, \tag{87}$$

and

$$A(k^2) = -\frac{e_r^2 k^2}{4\pi m^2}\int_0^1 v^2\left(1 - \frac{v^2}{3}\right)\frac{\mathrm{d}v}{\left\{1 + (k^2 - i\varepsilon)(1-v^2)/4m^2\right\}}. \tag{88}$$

The variable v is connected with the total energy-momentum P_μ of virtual states in the following way:

$$(P_\mu, P_\mu) = -\frac{4m^2}{1-v^2}.$$

Cut-off of the integration (87) at $(P_\mu P_\mu) = -\Lambda^2$ leads to

$$Z_3 = 1 - \frac{e_r^2}{3\pi}\left[\log\frac{\Lambda^2}{m^2} - \frac{5}{3}\right] + O\left(\frac{m^2}{\Lambda^2}\right)\log\frac{\Lambda^2}{m^2} \qquad \text{for } \Lambda \gg m. \tag{89}$$

By replacing Λ^2 by $-k^2$, we have

$$Z_3^R(-k^2, e_r) = 1 - \frac{e_r^2}{3\pi}\left[\log\frac{-k^2}{m^2} - \frac{5}{3}\right] + O\left(\frac{m^2}{k^2}\right)\log\frac{-k^2}{m^2}. \tag{90}$$

According to Theorem 3, we can derive

$$D_C(k^2) = D_F(k^2)\frac{1}{1 + A(k^2)} = D_F(k^2)\frac{1}{Z_3(-k^2, e_r)}. \tag{91}$$

[9] H. Umezawa and R. Kawabe: *Prog. Theor. Phys.*, **4**, 443 (1949).

This can be proved by a practical calculation. Indeed, when $-k^2 \gg m^2$, the evaluation of (88) leads to

$$A(k^2) = -\frac{e_r^2}{3\pi}\left[\log\frac{-k^2}{m^2} - \frac{5}{3} - i\pi\right] + O\left(\frac{m^2}{k^2}\right). \tag{92}$$

We shall discuss Z_3 without using perturbation approximation in the succeeding paper.

6·2. *Lee's model* (2) (*). – The propagator $S'_V(p_0)$ satisfies the equation:

$$h(p_0)S'_V(p_0) = 1\,,$$

with

$$h(p_0) = p_0 - m - \delta m - \Sigma(p_0) = (p_0 - m)\left\{1 + g^2 \sum \frac{1}{2\omega\Omega(\omega - \delta_m)(\omega - \delta_p)}\right\}. \tag{93}$$

The constant m is the renormalized mass of the V-particle, and the notations δ_m, δ_p mean

$$\begin{cases} \delta_m \equiv m - m_N \\ \delta_p \equiv p_0 - m_N\,. \end{cases} \tag{94}$$

The renormalization cut-off can be used to give $Z(\Lambda, g_\Lambda)$ in the following way:

$$\begin{cases} \dfrac{1}{Z(\Lambda, g_\Lambda)} = \dfrac{\partial}{\partial p_0} h(p_0)\Big|_{p_0=m} + \dfrac{\Sigma(\Lambda) - \Sigma(m)}{\Lambda - m}\,, \\ Z(\Lambda, g_\Lambda) = 1 + g_\Lambda^2 \sum \dfrac{\Lambda - m}{2\omega\Omega(\omega - \delta_m)^2(\omega - \delta_\Lambda)}\,, \end{cases} \tag{95}$$

with

$$\begin{cases} g_\Lambda^2 \equiv g^2 Z^R(\Lambda, g_\Lambda) \\ \delta_\Lambda \equiv \Lambda - m_N\,. \end{cases} \tag{96}$$

According to Theorem 3, the renormalized propagator is

$$S_{Vc}(p_0) = \frac{1}{(p_0 - m + i\varepsilon)Z(p_0, g_{ob})}\,. \tag{97}$$

(*) We shall use, unless otherwise stated, the same notations as those in Lee's paper.

Here $Z(p_0, g_{ob})$ is obtained from $Z(\Lambda, g_\Lambda)$ by replacing Λ and g_Λ by p_0 and g_{ob} respectively. We see that (97) and (95) lead to S_{vc} given by LEE.

By evaluating the integral in (95), we obtain ([10])

$$(98)_R \quad Z^R(p_0, g_{ob}) = 1 - \frac{g_{ob}^2}{4\pi^2}\left[\frac{2(\delta_m\delta_p - \mu^2)}{(\delta_p - \delta_m)\sqrt{\mu^2 - \delta_m^2}}\,\mathrm{tg}^{-1}\sqrt{\frac{\mu + \delta_m}{\mu - \delta_m}} - 1 + \right.$$

$$+ \begin{cases} \dfrac{\sqrt{\delta_p^2 - \mu^2}}{\delta_p - \delta_m}\log\dfrac{\delta_p + \sqrt{\delta_p^2 - \mu^2}}{\mu}\Big] & \text{for } \delta_p > \mu \\ \dfrac{2\sqrt{\mu^2 - \delta_p^2}}{\delta_p - \delta_m}\,\mathrm{tg}^{-1}\sqrt{\dfrac{\mu + \delta_p}{\mu - \delta_p}}\Big] & \text{for } \mu > \delta_p > -\mu \\ \dfrac{\sqrt{\delta_p^2 - \mu^2}}{\delta_p - \delta_m}\log\dfrac{-\delta_p - \sqrt{\delta_p^2 - \mu^2}}{\mu} & \text{for } -\mu > \delta_p \end{cases}$$

$$(98)_I \quad Z^I(p_0, g_{ob}) = \begin{cases} \dfrac{g_{ob}^2}{4\pi^2}\cdot\pi\,\dfrac{\sqrt{\delta_p^2 - \mu^2}}{\delta_p - \delta_m} & \text{for } \delta_p > \mu \\ 0 & \text{for } \mu > \delta_p\,. \end{cases}$$

The $Z^I(p_0, g_{ob})$ is positive definite for the region $p_0 > m_N + \mu_0$: This means that there appear no states of negative probability in the above region. Indeed, the relation

$$S_C(p_0) = \int_{-\infty}^{\infty}\frac{\varrho(\varkappa)\,\mathrm{d}\varkappa}{p_0 - \varkappa + i\varepsilon}\,,$$

with (97) leads to

$$\varrho(\varkappa) = \delta(\varkappa - m) + Z_{m'}\,\delta(\varkappa - m') + \sigma(\varkappa)\,.$$

Here

$$Z_{m'} < 0\,, \qquad m' < m\,,$$

and

$$\sigma(\varkappa) = \begin{cases} \dfrac{Z^I(\varkappa, g_r)}{\pi(\varkappa - m)\,|\,Z(\varkappa, g_r)\,|^2} & \text{for } \varkappa > m_N + \mu \\ 0 & \text{for } m_N + \mu > \varkappa. \end{cases}$$

The fact that $Z_{m'} < 0$ means that the m'-state is of negative probability

([10]) G. KÄLLÉN and W. PAULI: *Dan. Mat. Fys. Medd.*, **30**, no. 7 (1955).

When $\Lambda \gg m,\ \mu,\ m_N$, $(98)_R$ leads to

$$(99) \qquad Z^R(\Lambda, g_{ob}) = 1 - \frac{g_{ob}^2}{4\pi^2}\left[\log\frac{2\Lambda}{\mu} + \frac{2\delta_m}{\sqrt{\mu^2 - \delta_m^2}}\,\mathrm{tg}^{-1}\sqrt{\frac{\mu+\delta_m}{\mu-\delta_m}} - 1\right].$$

Here, we disregarded terms $O(\delta_m/\Lambda)\log(2\Lambda/\mu)$, or $O(m_N/\Lambda)$ and $O(\mu/\Lambda)$. On the other hand, the straight cut-off gives the following renormalization factor,

$$(100) \qquad Z_s(\Lambda) = \left[\frac{\partial}{\partial p_0} h(p_0)\Big|_{p_0 = m}\right]^{-1} = 1 - \frac{g_{ob}^2}{4\pi^2}\int_{\mu}^{\Lambda} \frac{\sqrt{\omega^2 - \mu^2}}{(\omega - \delta_m)^2}\,\mathrm{d}\omega\,.$$

It can be easily shown that (100) leads to (99) except for the omission of a term $O(\delta_m/\Lambda)$. In this way, $S_{VC}(p_0)$ $(p_0 \gg m,\ \mu,\ m_N)$ can be derived from $Z_s(\Lambda)$.

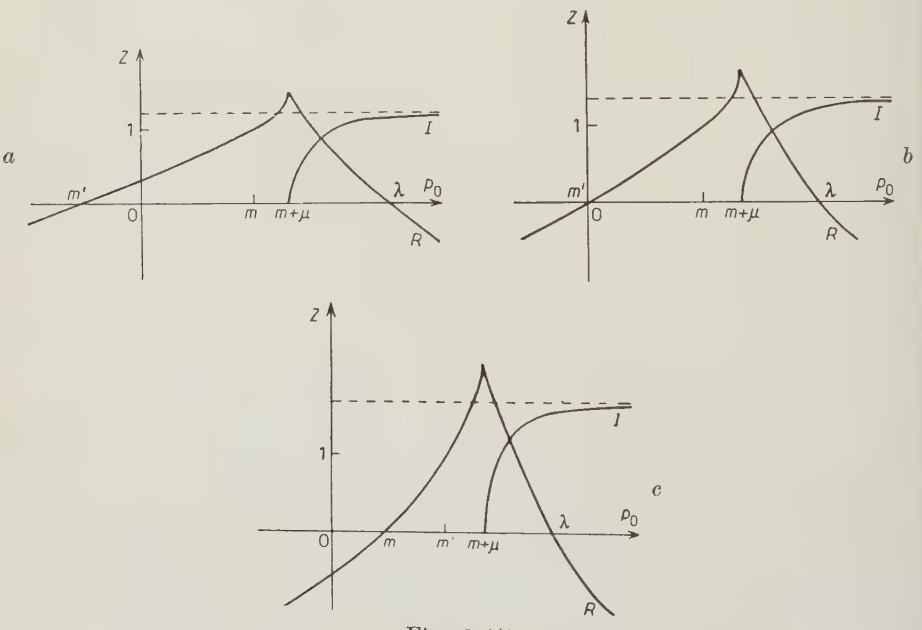

Fig. 6 (*).

The $Z(p_0, g_{ob})$, i.e. (98), is graphically shown in Fig. 6 in case of $m = m_N$. The value m' is the mass of a V-particle state with a negative probability ([10]).

(*) In Fig. 6 and 7,

$$g_0^2 \equiv 4\pi^2\left[\frac{\mu\pi}{2m} - 1 + \frac{\sqrt{m^2-\mu^2}}{m}\log\frac{m+\sqrt{m^2-\mu^2}}{\mu}\right]^{-1}$$

and the symbol R (I) means the real (imaginary) part of Z and g_{eff}^2 respectively.

Following the general discussions in Sect. 4, we introduce the effective charge g_{eff} defined by

$$g^2_{eff}(p_0) = g^2_{ob}/Z(p_0, g_{ob}) \,. \tag{101}$$

It can be seen in Fig. 7 that Re (g^2_{eff}) is negative for $p_0 > \lambda$. The sign of Re (g^2_{eff}) or of Z^R is important to the sign of the scattering phase shift. Indeed, the transition matrix and the phase shift (+) for the (N, θ)-scattering process are given by [11]

$$(N', \theta' \,|\, S \,|\, N, \theta) = \frac{g^2}{2\omega\Omega} S'_F(M+\omega) = \frac{g^2_{eff}(M+\omega)}{2\omega\Omega} S(M+\omega) \,, \tag{102}$$

with

$$S(p_0) = \frac{1}{p_0 - M} \,,$$

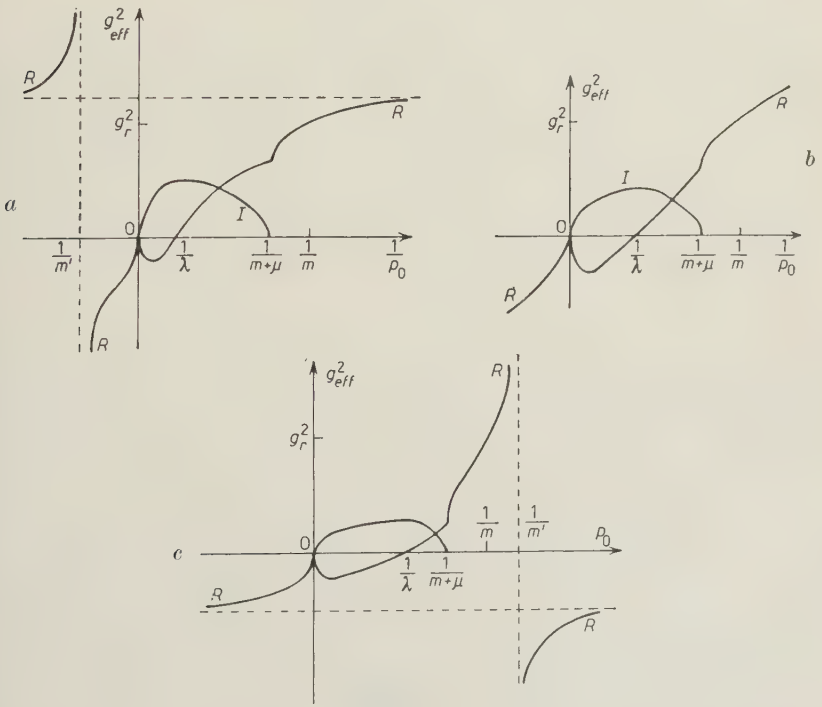

Fig. 7.

(+) Here we give the form different either from Eq. (16) in Ref. [2] or from Eq. (24) in Ref. [11]. It is not a difficult matter to prove the equivalence of the latter expressions to Eq. (103). Here we remark that Eq. (24) in Ref. [11] should be read

$$\mathrm{tg}\,\delta = \frac{-\pi\,|\boldsymbol{k}|}{(\omega + M - m_1)(\omega + M - m_2)} \left[P \int_{\bullet}^{\infty} \mathrm{d}k' \frac{k'^2}{\omega'(\omega' \quad \omega)(\omega' + M \quad m_1)(\omega' + M \quad m_2)} \right]^{-1} .$$

[11] H. Umezawa and A. Visconti: *Nuclear Physics*, **1**, 20 (1956).

and

$$\text{tg}\,\delta = \frac{1}{i}\,\frac{(N', \theta'|S|N, \theta) - (N', \theta'|S|N, \theta)^*}{(N', \theta'|S|N, \theta) + (N', \theta'|S|N, \theta)^*} = \frac{-Z^I(p_0, g_{0b})}{Z^R(p_0, g_{0b})}\,. \tag{103}$$

The phase shift really changes its sign at $p_0 = \lambda$ as shown by Fig. 9. The change of the sign has its origin in the fact that g_{0b} is out of the normal zone $N(g_r)$. Thus, in the present model the conclusion of the renormalization theory for the high energy scattering process can not be justified.

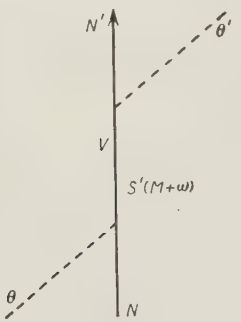

Fig. 8.

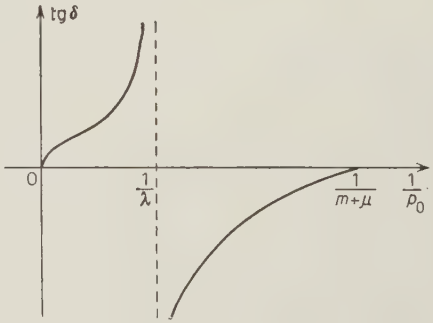

Fig. 9.

If we restrict the momentum space within the region $\omega < \Lambda$, the renormalization factor Z is given by (100). Thus, g_{0b} can lie in the normal zone $N(g_\Lambda)$ only when $\Lambda < \lambda$. When $\Lambda > \lambda$, we have seen ([10]) that there appears, in the region $p_0 < m$, a stable state with a negative probability.

The sign of phase shift is obtained from the sign of Z^R immediately, for Fig. 8 is the only irreducible diagram for N-θ scattering in the present model. It is possible that the relation between the phase shift and the function Z may be more complex. In fact, the scattering matrix elements are given by the many-body propagators. It may be quite important to investigate the relation between the many-body propagators and the one-body propagator which is in close relation to Z^R.

Note added in proof.

The Ward's cut-off ([3]) can be obtained by replacing $\text{Re}\,[\Sigma(\Lambda^2)]$ with $\Sigma(\Lambda^2)$ in (12a), and therefore, leads to a complex renormalization factor, i.e. $Z(\Lambda^2, g_\Lambda)$. This shows the reason why we used $\text{Re}\,[\Sigma(\Lambda^2)]$ in (12a). A short comment on this point will be presently published in *Progress of Theoretical Physics*.

* * *

The authors would like to thank Prof. YUKAWA, Prof. SAKATA, Prof. KOBA and Prof. KATAYAMA for their inspiring discussions. Thanks are also due to stimulating discussions in the symposium held at the Institute for Fundamental Physics in Kyoto University in November, 1955.

RIASSUNTO (*)

È stata avanzata l'ipotesi che il valore rinormalizzato della costante d'accoppiamento sia talvolta contenuto entro una zona, detta zona normale. GELL-MANN e LOW hanno dimostrato l'esistenza di una stretta relazione tra il fattore di rinormalizzazione e la forma asintotica del propagatore rinormalizzato. Servendosi di questa relazione per calcolare i propagatori rinormalizzati e gli accoppiamenti effettivi, si discutono i caratteri particolari assunti dai risultati della teoria della rinormalizzazione nei fenomeni di alta energia, quando i valori osservati delle costanti di accoppiamento cadono fuori dalle zone normali. La zona normale della carica elettrica e la carica effettiva nell'elettrodinamica quantistica saranno discussi in un successivo lavoro.

(*) *Traduzione a cura della Redazione.*

Gamma-Gamma Angular Correlation in ^{46}Ti.

G. Bertolini, M. Bettoni and E. Lazzarini

Istituto di Fisica Sperimentale del Politecnico - Milano

(ricevuto l'11 Febbraio 1956)

Summary. — The directional angular correlation of the γ-γ cascade of the ^{46}Ti, obtained from ^{46}Sc is studied. The correlation function is represented by the formula: $W(\theta) = 1+0.1006P_2(\cos\theta)+0.0178P_4(\cos\theta)$.

1. – Introduction.

In a recent paper Keister and Schmidt [1] propose for the ^{46}Sc the decay scheme shown in Fig. 1. The spin and parity assignment to the ground state of ^{46}Sc is supported by the shape and relative intensity of the β spectra [1] and from the assignment $0+$, $2+$, $4+$ to the excited levels of the ^{46}Ti, as pointed out in the pioneer work on directional correlation and polarization correlation of Brady and Deutsch [2], Novey [3] and Metzger and Deutsch [4]. Indeed their measurements are in agreement with γ-γ cascade in which both γ-rays are electric quadrupole radiations.

It seemed worthwhile to re-measure the directional correlation in order to define the correlation function by using the most recent methods developed in the angular correlation studies [5,6]. More uncertain however, appears to

[1] G. L. Keister and F. H. Schmidt: *Phys. Rev.*, **93**, 140 (1954).
[2] E. L. Brady and M. Deutsch: *Phys. Rev.*, **78**, 558 (1950).
[3] B. Novey: *Phys. Rev.*, **78**, 66 (1950).
[4] F. Metzger and M. Deutsch: *Phys. Rev.*, **78**, 551 (1950).
[5] S. Frankel: *Phys. Rev.*, **83**, 673 (1951).
[6] J. L. Lawson and H. Frauenfelder: *Phys. Rev.*, **91**, 649 (1953).

be the assignment of the spin and parities by measurements of conversion coefficients ([7-9]).

The half life of the excited state of ^{46}Ti has been measured by various workers ([10-12]) with the delayed coincidence method; the recent value $\tau < 5 \cdot 10^{-11}$ s does not conflict with electric quadrupole radiations.

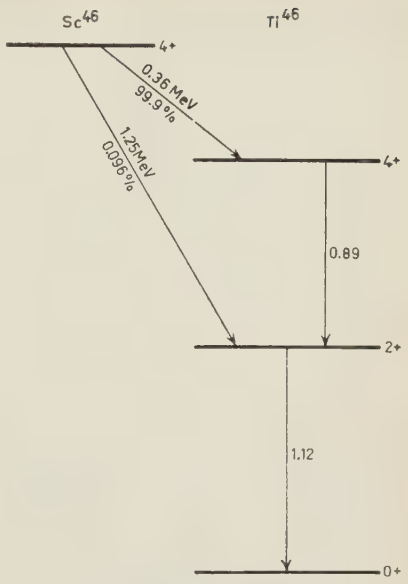

Fig. 1. – Decay scheme of ^{46}Sc.

2. – Apparatus and source.

For the detection of the radiations, scintillation detectors were used consisting of thallium-activated sodium iodide cylindrical crystals, 1″ diameter ×1″ thickness, mounted on RCA type 5819 photomultiplier tubes. The influence of the magnetic field was eliminated by mounting a mu-metal screen around the phototubes. The counters were laterally and frontally shielded against scattered radiation by lead of 1.5 cm minimum thickness. Frontally the screen had a cone-shaped hole, which accepted only γ-rays from a point source in the center of the apparatus; the circular base of the crystal corresponded with the normal section of the cone. The distance crystal-source was 5 cm. The discrimination against counter to counter scattering at angles near 180° was achieved by accepting only pulses corresponding to γ-rays of at least 350 keV.

Fig. 2 shows the γ spectrum obtained with a 1″ × 1″ cylindrical crystal of NaI(Tl). The resolving power of the coincidence circuit was $4.3 \cdot 10^{-8}$ s. It was measured with the method of two independent sources before the experiment and with the method of the delay cable during the experiment. The delay cable inserted in one of the channels corresponded to a delay of $2.5 \cdot 10^{-7}$ s. In the course of the measurements, the resolving power was constant within the 1.5 %.

The source of ^{46}Sc was prepared from Sc_2O_3 irradiated in Harwell with

---

([7]) M. L. Moon, M. A. Waggoner and A. Roberts: *Phys. Rev.*, **79**, 905 (1950).
([8]) F. T. Porter and C. S. Cook: *Phys. Rev.*, **81**, 298 (1951).
([9]) J. A. Whalen, F. T. Porter and C. S. Cook: *Phys. Rev.*, **89**, 902 (1953).
([10]) H. S. Mendoch and A. J. Webb: *Proc. Phys. Soc.*, A **67**, 286 (1954).
([11]) C. E. Whittle and F. T. Porter: *Phys. Rev.*, **90**, 498 (1953).
([12]) R. E. Azuma: *Phil. Mag.*, **46**, 1031 (1955).

200 mC/g specific activity. The Sc_2O_3 was dissolved in HCl and NH_4CNS was added; the resulting $Sc(CNS)_3$ has been reconverted in scandium chloride and

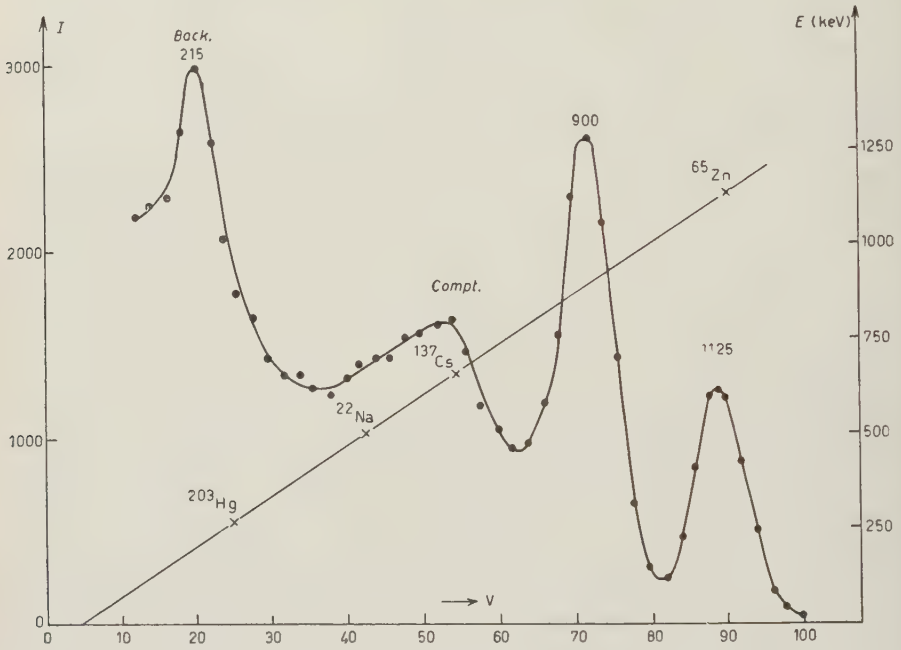

Fig. 2. – γ-spectrum of ^{46}Sc.

with this the source has been prepared. It consisted of about 0.01 ml of solution placed in a plexiglas cylindrical container of 1 mm thickness and 2 mm inner diameter. The activity of the source used during the experiment was of about 150 μC; consequently the ratio true-accidental coincidences was about two.

3. – Experimental measurements and results.

Coincidences were taken for angles between the counter axis of 90°, 112.5°, 135°, 157.5°, 180°, 202.5° 225°, 247.5°, 270°. The results of the measurements relative to simmetric angles with respect to 180° were united in order to correct, in first approximation, a possible non coincidence between the rotational axis of the revelators and the axis of the source. The experimental results show that such effect is less than the standard deviation of the measurements. The single counts N_1 and N_2 were taken by means of two independent scalers, simultaneously with the coincidences in order to evaluate the random

coincidences. The resolving power of the coincidence circuit was measured for 30 minutes at 2 hours intervals. The coincidences at each angle were measured for 30 minutes.

From the measured data, the coincidence ratio $W_s(\theta) = C(\theta)/N_1N_2$ between genuine coincidences and single counts is then formed. This ratio eliminates, in first approximation, the effects of slow drift of the electronic apparatus with consequent variation of the detectors' efficiencies.

The number of the coincidences detected at each angle θ in the same period is a function of θ, that is conveniently expressed in terms of a Legendre polynomial expansion, of which the highest even term is determined by the selection rules:

$$n = \text{Min}\,(2I_b, 2L_1, 2L_2),$$

where I_b is the spin of the intermediate level, L_1 and L_2 the multipolarity of the two radiations. If we suppose a cascade of the type 4 (2) 2 (2) 0, the correlation function is:

$$W_s(\theta) = \alpha_0 + \alpha_2 P_2(\cos\theta) + \alpha_4 P_4(\cos\theta)\,. \tag{1}$$

The calculation of the α_n coefficients by means of experimental values W_s and their comparison with theoretical values calculated by BIEDENHARN and ROSE ([13]) gives information about the nuclear parameters involved in the cascade.

By means of the least square fit of the assumed form of the function, we have obtained with convenient normalization:

$$W_\Omega(\theta) = (1 \pm 0.0035) + (0.0932 \pm 0.0059)P_2(\cos\theta) + (0.0138 \pm 0.0100)P_4(\cos\theta)\,. \tag{2}$$

In order to compare the experimental results with the theoretical values of ROSE calculated for point sources and detectors, it is necessary to correct the coefficients α_n for the finite solid angle of the counters. Using a method suggested by FRANKEL ([5]) and neglecting the correction for the extension of the source, one can write the formula (1) as:

$$W_\Omega(\theta) = \alpha_0 + \frac{Q_2}{Q_0}\alpha_2 P_2(\cos\theta) + \frac{Q_4}{Q_0}\alpha_4 P_4(\cos\theta)\,, \tag{3}$$

where

$$Q_n = J_n^{\mathrm{I}} J_n^{\mathrm{II}}\,, \qquad J_n^i = \int \varepsilon^i(\alpha, \gamma)\, P_n(\cos\theta)\,|\sin\alpha|\,d\alpha\,. \tag{4}$$

([13]) L. C. BIEDENHARN and M. E. ROSE: *Rev. Mod. Phys.*, **25**, 746 (1953).

The super-scripts I and II refer to the two counters respectively and $\varepsilon^i(\alpha, \gamma)$ is the efficiency of a counter i for a γ-ray emitted at an angle α with respect to the counter axis. The formula (4) is corrected for γ-rays of nearly the same energy, in which case it is possible to assume $\varepsilon^i(\alpha, \gamma_1) \cong \varepsilon^i(\alpha, \gamma_2)$.

The angular efficiency of the two detectors has been determined experimentally by using a well collimated γ-ray beam from a 40 mC ^{46}Sc source (width of the beam less than 0.6°). The collimation was obtained by means of a lead block 20 cm long provided with a channel of 1 cm diameter, followed by a second lead block 10 cm long with a channel of 0.2 cm diameter.

The following values were obtained:

$$\frac{Q_2}{Q_0} = 0.926 , \qquad \frac{Q_4}{Q_0} = 0.776 ,$$

therefore the corrected experimental correlation function is represented by

$$W(\theta) = 1 + 0.1006\, P_2(\cos\theta) + 0.0178\, P_4(\cos\theta) .$$

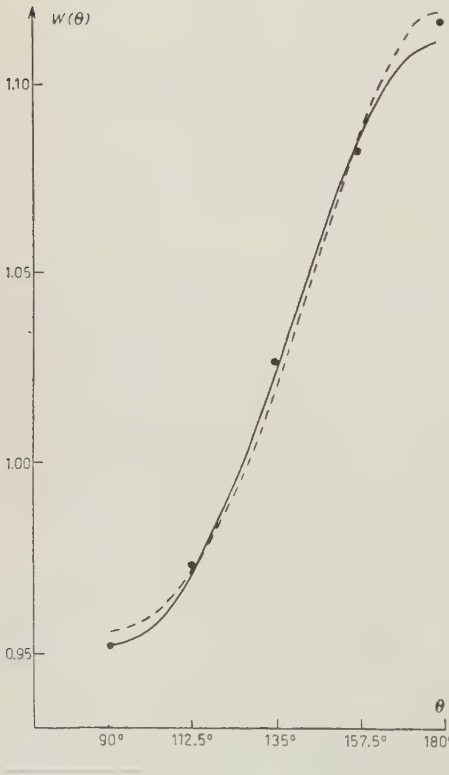

From (5) we obtained

$$A = \frac{W(\pi)}{W(\pi/2)} = 1.169 \pm 0.012 .$$

The theoretical function for a transition of the type 4 (2) 2 (2) 0 is

$$W(\theta)_{\text{theor}} = 1 + 0.1020\, P_2(\cos\theta) + 0.0091\, P_4(\cos\theta).$$

The ratio $\varepsilon_n^2 = (\alpha_n^0 - \alpha_n)^2/\sigma^2(\alpha_n)$, where α_n^0 is the theoretical value and α_n that obtained from formula (2), has been performed according to the formulas suggested by Rose [14]. Our ε^2 va-

Fig. 3. – Correlation function of ^{46}Sc. The solid line represents the theoretical function corresponding to a 4 (2) 2 (2) 0-transition and the dotted line the function expressed by formula (5). The points represent the experimental results.

[14] M. E. Rose: *Phys. Rev.*, **91**, 611 (1953).

lues, less than unity, show that the function used in the least square fit is correct.

Fig. 3 shows the behaviour of the theoretical function (solid line) and of the experimental function expressed by formula (5) (dotted line). The points represent the experimental results.

* * *

We wish to thank the Prof. G. Bolla, for his interest and encouragement in the present work.

RIASSUNTO

È stata studiata la correlazione angolare della cascata γ-γ del ^{46}Ti, ottenuto da ^{46}Sc. La funzione di correlazione è rappresentata dalla formula:

$$W(\theta) = 1 + 0.1006\, P_2(\cos\theta) + 0.0178\, P_4(\cos\theta)\ .$$

The « N » Component of Cosmic Rays in Relation to Oscillations of the Atmosphere.

P. Bassi and F. Ferrari

Istituto di Fisica dell'Università - Padova
Istituto Nazionale di Fisica Nucleare - Sezione di Padova

(ricevuto il 13 Febbraio 1956)

Summary. — Acting on the suggestion implicit in some recent experimental results, we have used Heisenberg's theory to calculate the correlation between oscillations of the Earth's atmosphere and the intensity of the N component of cosmic rays. The theoretical predictions are in qualitative but not in quantitative agreement with the experimental results. However we may note that these latter are, at present, statistically poor.

Various authors [1-4] have measured the variations in intensity of the «N» component of cosmic rays due to « meteorological » variations of the atmospheric pressure. The barometric coefficient which gives the correlation between intensity (N) and pressure (x) is $\beta = 13.6(100/N)(\mathrm{d}N/\mathrm{d}x) \cong 10\%$ per $\mathrm{cm}_{\mathrm{Hg}}$, and does not depend on the energy in an appreciable way, at least up to several tens of GeV.

It is possible to explain the value and the sign of the coefficient β by supposing that an increase in the atmospheric pressure corresponds to an increase in the mass of air over the point of observation: to this corresponds a diminution of the intensity N due to absorption. The absorption length in air for the N component is $\Lambda = 125\ \mathrm{g/cm^2}$, and is almost independent of the energy.

---

(1) L. Jánossy and G. D. Rochester: *Proc. Roy. Soc.*, A **183**, 186 (1944).

(2) C. B. A. McCusker, J. G. Dardis and B. G. Wilson: *Proc. Phys. Soc.*, A **68**, 585 (1955).

(3) C. Baccalin, P. Bassi and C. Manduchi: *Nuovo Cimento*, **1**, 657 (1955).

(4) K. W. Ogilvy: *Toronto Meeting Amer. Phys. Soc.* (1955).

Variations of pressure which we have called « meteorological » concern the lower part of the atmosphere (up to 10 km) and since this is far below the level of the primary collisions the nucleonic cascade may be considered as being in equilibrium at this height, and consequently one may calculate the coefficient β from the absorption length. It is $\mathrm{d}N/N \cong \mathrm{d}x/\Lambda$ (i.e. for $\mathrm{d}x = 1\ \mathrm{cm_{Hg}}$, $\beta \cong -10\%$).

In addition to these irregular variations of pressure, which in reality prove to be those which have the biggest amplitude, there are cyclic variations (tidal variations) ([5]), with periods of 12 and 24 hours, due mainly to oscillations of the atmosphere resulting from thermal phenomena produced by solar heating, and to a lesser degree due to gravitation tidal effects produced by the Sun and the Moon. All these effects are increased by the fact that the atmosphere has a period of oscillation of about 12 hours.

As distinct from the « meteorological » variations these latter concern the whole of the atmosphere and naturally this also includes the levels of the primary collisions of the nucleonic cascade. It is to be expected that the intensity of the N component will depend in different ways on the two types of pressure variations.

In this work, after a brief review of the existing experimental data, we calculate the influence of the atmospheric oscillations on the N component. While a comparison with experiment is at present not very significant, due to the poor statistics, it is to be hoped that more accurate experiments, when compared with our calculations, will furnish information on very high energy nuclear collisions in air and on the variations of the thermodynamical variables in the upper atmosphere.

1. – Experimental data.

C. B. A. McCusker, J. G. Dardis e B. G. Wilson ([2]) have recently analyzed the intensity variations of locally produced penetrating showers at sea level (Dublin, Eire), which were produced by the N component, whose mean energy was taken to be about 20 GeV. For the meteorological variations of pressure the usual barometric coefficient $\beta = -10\%$ per $\mathrm{cm_{Hg}}$ was found: on averaging these results over long periods an intensity variation of a few per cent was found which had a semidiurnal period with respect to solar time. This intensity variation appears to be correlated and in phase opposition to the pressure variation due to the tidal oscillations.

Admitting the existence of such a correlation, which is not however fully confirmed by present statistics, the authors have calculated the new baro-

([5]) M. V. Wilkes: *Oscillation of the Earth's Atmosphere* (Cambridge, 1949).

metric coefficient $\bar{\beta} = -430 \pm 90\%$ per cm_{Hg} due exclusively to the periodic pressure variation (in reality the experimental results will also be compatible with smaller values of $\bar{\beta}$ but anyway they seem to indicate $|\bar{\beta}| > |\beta|$).

C. Baccalin, P. Bassi, C. Manduchi [3] have described a series of measurements on cosmic ray protons of 0.5 GeV at 2000 m (Laboratorio della Marmolada), and have found a meteorological barometric coefficient $\beta \cong -10\%$ per cm_{Hg}. We have re-analyzed the same results, obtained in about two months, and, on averaging intensity and pressure over the whole period, the curves relative to solar time which are shown in Fig. 1 were obtained. Following the example of the above authors and once again admitting a correlation, we have used the « χ^2 » test to find the best correlation coefficient $\bar{\beta}$: in fact we find that to $\bar{\beta} = 0\%$, -10%, -25%, -50%, correspond the values $P = 0.02$, 0.05, 0.65, 0.85.

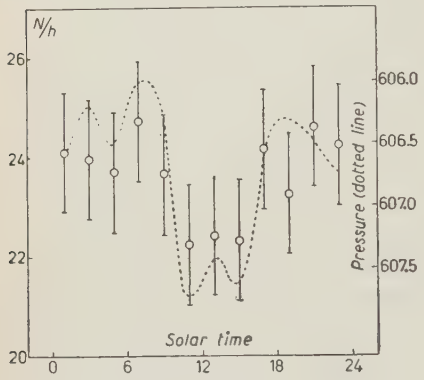

Fig. 1.

At these energies $\bar{\beta}$ should thus be smaller than at higher energies.

Supposing there is a correlation between the periodic variations of pressure and the intensity of the N component, we will see if it is possible to predict for $\bar{\beta}$ both the negative sign and the increase with energy which is found by experiment.

The periodic variations of pressure are an indication which is available at low levels of a very complex phenomenon involving the whole atmosphere. The fact that at a height of about 25 km there is the first temperature inversion, produces in that region a node in the pressure oscillations, and from a detailed calculation ([6,7]) (which only takes account of gravitational oscillations) it results that dx/x is practically constant from sea level to above 20 km. Taking into account both gravitational and thermal oscillations, dx/x is of the order of 10^{-4}.

The nuclear cascade develops below 20 km, and should therefore be influenced by pressure variations, not only in the lower atmosphere where the cascade is in equilibrium, but also in the upper atmosphere, where the major reproduction processes take place.

The oscillations of the atmosphere give rise to changes in the « scale height » $Z_0 = x/\varrho$: the fact that $dZ_0/Z_0 \neq 0$ can have an influence on the competition between decay and nuclear interaction of the π- and K-mesons which, at high

---

([6]) S. K. Mitra: *The Upper Atmosphere* (Calcutta, 1952).

([7]) C. L. Pekeris: *Proc. Roy. Soc.*, A **158**, 650 (1937).

energies and in the first stages, represent an important link in the development of the cascade (this, in a certain sense, is the counterpart of the positive temperature effect on π-μ decay proposed by DUPERIER).

The effect will obviously increase with energy; neither the value nor the sign of $\mathrm{d}Z_0/Z_0$ have been directly measured in the zone of the first collisions (15-20 km). Considering the largely thermal nature of the oscillations we may assume for $\mathrm{d}Z_0/Z_0$ the same sign as for $\mathrm{d}x/x$ and a value of the order of $\mathrm{d}T/T$ (where T is the absolute temperature) at least in correspondence to the diurnal maximum ($\mathrm{d}T/T \sim 10^{-2}$). Thus $\mathrm{d}Z_0/Z_0 \cong 100(\mathrm{d}x/x)$.

The calculations will show that the pressure variations influence the intensity N independently of the energy; variations of scale height produce an effect which grows with the energy and which is greater than that produced by the pressure variations.

2. – Calculation of the « N » Component.

We describe the development of the cascade of the « N » component by means of the following system of integral-differential equations:

$$\frac{\partial \boldsymbol{N}(E, l)}{\partial l} = -\left[\mathbf{1} + \frac{c(z_0)}{El}\,\boldsymbol{\tau}\right]\boldsymbol{N}(E, l) + \int_E^\infty (E_0, E)\,\boldsymbol{N}(E_0, l)\,\mathrm{d}E_0 \tag{1}$$

in which:

$$\boldsymbol{N}(E, l) = \begin{vmatrix} N(E, l) \\ \pi(E, l) \end{vmatrix} \qquad \boldsymbol{\tau} = \begin{vmatrix} 0 & 0 \\ 0 & 1 \end{vmatrix} \qquad \boldsymbol{F} = \begin{vmatrix} F_{NN}(E_0, E) & F_{N\pi}(E_0, E) \\ F_{\pi N}(E_0, E) & F_{\pi\pi})E_0, E) \end{vmatrix}$$

and where $N(E, l)$ and $\pi(E, l)$ are the differential intensities of nucleons and pions; $c(Z_0)$ is a function of the « scale height ». The lateral spread of the cascade can be ignored since, for the energies which interest us, the greater part of the secondary particles lie at small angles with respect to the primary.

The differential production spectra have been written for convenience in the following way:

$$F_{ik} = -\gamma_{ik}\left[(\alpha_{ik} - 1)!\,\frac{E}{E_0}\,\log^{1-\alpha_{ik}}\frac{E}{E_0}\right]^{-1}\frac{1}{E_0}\,, \tag{2}$$

in which γ_{ik} and α_{ik} are experimentally determined constants. System (1) can be resolved by an expansion in series of the « l » of $\boldsymbol{N}(E, l)$

$$\boldsymbol{N}(E, l) = \exp\left[-l\right]\sum_n \boldsymbol{N}_n(E) l^n\,,$$

where $N_n(E)$ and $\pi_n(E)$ represent the energy spectra of the n-th generations of nucleons and of pions respectively. Thus one obtains the following recurrence formula, by means of which the problem may be solved:

$$\left[\boldsymbol{n}+\mathbf{1}+\frac{c(z_0)}{E}\boldsymbol{\tau}\right]\boldsymbol{N}_{n+1}=\int_E^\infty \boldsymbol{F}(E,E_0)\boldsymbol{N}_n(E_0)\,\mathrm{d}E_0\,. \tag{3}$$

However, to study the effects due to oscillations of the atmosphere it is convenient to use another and simpler method, even though it may be less rigorous. Before proceeding we will first consider the following points ([10]): let $g(E)$ be a primary spectrum, and writing $m_{g,1}(s)$ as the relative transformation of Mellin, one can then easily demonstrate that the transformation of Mellin of the spectrum after « n » collisions is:

$$m_{g,n}(s)=m_{g,1}(s)\cdot m_{ik}^n(s) \tag{4}$$

in which $m_{ik}^n(s)$ is the n-th power of:

$$m_{ik}(s)=\int_0^1 \mathrm{d}\eta\,\eta^s F_{ik}(\eta)=\gamma_{ik}s^{-\alpha_{ik}} \qquad \left(\eta=\frac{E}{E_0}\right). \tag{5}$$

Multiplying (4) by $W_n(l)=\exp[-l](l^n/n!)$ (the probability that in the tract considered, there are exactly n collisions) and summing over n, one obtains in a general way the transformation of Mellin of the differential spectrum at a depth l, generated by a primary spectrum:

$$m(s,l)=m_{g,1}(s)\exp\langle -l[1-m_{ik}(s)]\rangle\,. \tag{6}$$

Finally, through an inverse transformation of (6) one obtains the differential spectrum at a depth l:

$$g(E,l)\,\mathrm{d}E=\frac{\mathrm{d}E}{2\pi i}\int_{\sigma-i\infty}^{\sigma+i\infty} m(s,l)E^{-(s+1)}\,\mathrm{d}s\,. \tag{7}$$

Expression (7) may generally be calculated by means of the « saddle point method » and can be put into the form:

$$g(E,l)\,\mathrm{d}E=\left[2\pi\frac{\mathrm{d}^2}{\mathrm{d}s^2}\log m(s,l)\right]^{-\frac{1}{2}} m(s,l)\,E^{-(s+1)}\,\mathrm{d}E\,. \tag{8}$$

For s one must take the value at the peak of the saddle, which turns out

to be connected to E by the equation:

$$\frac{\mathrm{d}}{\mathrm{d}s}\log m(s, l) = \log E\,.$$

Putting:

$$\pi(E, l) = A, l\lambda \frac{E}{E + z_0 m_\pi c/\tau_\pi)} \exp\left[-l\right] E^{-s_\pi},$$

as the differential intensity of pions at a depth l, the differential spectrum of nucleons generated per unit depth (mean free path) will then be:

$$N_\pi(E, l)\,\mathrm{d}E = \mathrm{d}E\int_E^\infty F_{N\pi}(E, E_0)\pi(E_0, l)\,\mathrm{d}E_0\,. \tag{9}$$

In our case (6) becomes:

$$m(s, l) = m_N(s, 0)m(s, l) + \int_0^l m_{N\pi}(s, l')m(s, l-l')\,\mathrm{d}l', \tag{10}$$

where:

$$\begin{cases} m_N(s, 0) = \displaystyle\int_0^\infty \mathrm{d}E\,E^s N(E, 0) \\ m_{N\pi}(s, l) = \displaystyle\int_0^\infty \mathrm{d}E\,E^s N_\pi(E, l) \\ m(s, p) = \exp\left\{-p\left[1 - m_{NN}(s)\right]\right\}. \end{cases} \tag{11}$$

Substituting (10) in (7) one arrives at the differential energy spectrum of nucleons at depth l. This solution may be written as the sum of two terms:

$$N(E, l) = N_N(E, l) + N_\pi(E, l) \tag{12}$$

in which the first refers to a purely nucleonic cascade and the second to a compound cascade in which pions are also present. This solution has been compared to that given in (3), for the zone of the first collision (5-6 collisions), which for us is the most critical region. The results given by the two methods are practically identical.

3. – The intensity of the N component and the oscillations of the atmosphere.

We must now introduce the numerical values of α_{ik}, γ_{ik} and λ in expression ([12]) for $N(E, l)$. We will use the α_{ik} and γ_{ik} determined experimentally by DEUTSCHMANN *et al.* and those given by BUDINI, MOLIÈRE and POIANI ([8-11])

$$\alpha_{N\pi} = 1.5 \; ; \quad \alpha_{NN} = 1.3 \; ; \quad \gamma_{N\pi} = 0.3 \; ; \quad \gamma_{NN} = 0.8 \; .$$

At present these values are by no means definite, however, the numerical calculation which is given in this paper can only serve as a guide since the experimental values of $\mathrm{d}N/N$ and particularly those of ref. ([3]) are highly uncertain: for this reason we have confined our calculations to a sea level determination, despite the fact that one of the experiments to which we have referred ([3]) was carried out at 2000 m.

We will assume that, of the mesons, only pions are present; one may show that the K-mesons will give rise to insignificant effects since their mass is greater than that of the pions, while their mean life-times, and probably also their nuclear cross-section are slightly less ([12]).

Finally we will use a mean free path for nuclear interaction of $\lambda = 60$ g/cm^2 which has been derived from the geometric collision cross-section; the other constants are:

$S_N = 1.6$; $S_\pi = 1.75$; $A_1 = 0.23$ (Energy measured in GeV); $x = 1033$ g/cm^2

Normalizing the experimental spectra one obtains $A_0 = 1.34$.

Let us return to (12):

$$N(E, l) = N_N(E, l) + N_\pi(E, l);$$

it may be interesting to note the values of the ratio N_N/N_π at various energies. It is found that to energies of $E = 1$, 10, 20, 40 GeV correspond the values $N_N/N_\pi = 8.64$, 5.58, 4.62, 2.84. For $E > 120$ GeV the ratio N_N/N_π begins to

([8]) M. DEUTSCHMANN: *Zeits. f. Naturfors.*, **9***a*, 477 (1954).

([9]) M. CRESTI, M. DEUTSCHMANN, W. D. B. GREENING, L. GUERRIERO, A. LORIA and G. ZAGO in course of publication.

([10]) P. BUDINI and G. MOLIÈRE, in W. HEISENBERG: *Kosmische Strahlung* (Berlin, 1953).

([11]) P. BUDINI and G. POIANI: *Nuovo Cimento*, **10**, 1288 (1953).

([12]) G. GOLDHABER, S. GOLDHABER, E. L. JLHOFF, J. E. LANNUTTI, A. PEWSNER and D. RITSON: *Proc. Pisa Conference*, 1955.

([13]) G. PUPPI: *Progress in Cosmic Rays*, Chapter VII, in print.

increase owing to a change in the slope of the spectra, which is due to the dependence of the energy on the decay probability of the pions.

N is a function of x ($x = l\lambda$) not only directly, but also through Z_0. The relation between x and Z_0 is that which has already been given in Sect. **1**, i.e. $\mathrm{d}Z_0/Z_0 = 100(\mathrm{d}x/x)$ which is valid in the upper atmosphere (anyway it may be shown that the integrand function used for the calculation of N and which contains Z_0 contributes to the integral between 0 and l only for the first collisions).

Since one can write $N_\pi = (1/Z_0)N_\pi$ (for $E < 50$ GeV) the barometric coefficient will be:

$$\bar{\beta} = 13.6\,\frac{100}{N}\,\frac{\mathrm{d}N}{\mathrm{d}x} = 13.6\,\frac{100}{N}\left[\left(\frac{\partial N_N}{\partial x}\right) + \left(\frac{\partial N_\pi}{\partial x}\right)_{z_0=\mathrm{const}}\right] + \left[-\frac{N_\pi}{z_0}\,\frac{\partial z_0}{\partial x}\right] \%\ \text{per cm}_{\text{Hg}}:$$

where $\bar{\beta}$ is the sum of two terms $(\bar{\beta})_{z_0=\mathrm{const}}$ and $(\bar{\beta})_{x=\mathrm{const}}$ which respectively represent the influence of the variations of x and of Z_0 on the variations of N. In Table I we have calculated the values of $(\bar{\beta})_{z_0=\mathrm{const}}$; $(\bar{\beta})_{x=\mathrm{const}}$ and $\bar{\beta}$ for various values of the energy E of the nucleons at sea level.

TABLE I.

E (GeV)	1	10	20	40
$(\bar{\beta})_{z_0}$ = constant	— 8.70	— 8.75	— 8.80	— 8.95
$(\bar{\beta})_x$ = constant	— 13.60	— 20.95	— 23.40	— 33.75
$\bar{\beta}$	— 22.30	— 29.70	— 32.20	— 42.70

Thus $\bar{\beta}$ is negative and increases with energy, but not as rapidly as experimental results would lead one to believe. The contribution of the variations x of pressure is practically independent of the energy; that of the variations of scale height is larger and increasing with energy.

Finally it is interesting to note that since $N_\pi < N$ is always the case, this puts an upper limit to the absolute value of $\bar{\beta}$, which for example cannot exceed $|140\%|$ per cm_{Hg} at 40 GeV.

4. – Conclusion.

In the preceding paragraphs we have demonstrated the possibility of interpreting the correlation between the variations of intensity of the N component at sea level with the oscillations of the atmosphere. We would, however, like to point out that, while the existence of the effect and its variations with the

energy are connected with the fact that unstable particles participate in the cascade, the numerical values given in Table I are intimately connected with the hypothesis about the collision cross-section, and on the way in which the energy is distributed between mesons and nucleons in nuclear collisions.

The particular interest of a study of this type lies in the possibility of obtaining from the experimental data certain quantities of importance in nuclear physics (collision cross-sections and inelasticity of nuclear collisions; the production at high energies of mesons other than pions). These would be in addition to information on the thermodynamical parameters of the upper atmosphere of interest in geophysics.

Research along these lines presents considerable advantages over previous and more or less analogous work (positive and negative temperature effects on the chain π-μ-e) due to its simplicity of conception (dx/x constant over the whole atmosphere and dZ_0/Z_0 effective only for the first few collisions).

The only disadvantage of this type of measurement lies in the time required to accumulate a significant amount of data. To avoid this, at least in part, it would be advantageous to carry out similar measurements near the equator where oscillations of the atmosphere are more marked.

RIASSUNTO

Sulla traccia di alcuni recenti risultati sperimentali abbiamo calcolato con la teoria di Heisenberg la correlazione fra le oscillazioni dell'atmosfera terrestre e l'intensità della componente N dei raggi cosmici. Le previsioni teoriche sono in accordo soltanto qualitativo con i risultati dell'esperienza: è da notare però che questi ultimi sono ancora statisticamente poveri.

Comptage d'α à basse temperature; une méthode pour éviter la diffusion du Radon.

E. Picciotto

Laboratoire de Physique Nucléaire, Université Libre de Bruxelles

F. Salvetti

Istituto di Chimica Generale e Inorganica dell'Università - Roma

(ricevuto il 3 Febbraio 1956)

Résumé. — On montre que des erreurs importantes peuvent être faites dans les mesures d'activité α naturelle par suite de la diffusion du Radon. Ces erreurs peuvent être évitées en mesurant l'activité de l'échantillon refroidi à — 180 °C, à l'aide d'un compteur à scintillation.

La radioactivité naturelle des roches est souvent mesurée par l'activité α émise en couche épaisse (couche dont l'épaisseur est supérieur au parcours des α). Bien qu'elle ne donne pas d'information sur le rapport Thorium-Uranium et sur l'état d'équilibre radioactif, cette méthode offre des avantages incontestables de commodité.

Une cause d'erreur qui semble avoir été sous-estimée est la diffusion des gaz radioactifs dans l'échantillon. Cette cause d'erreur est souvent mentionnée, mais considérée comme négligeable, sans autre justification. Les données expérimentales sur le pouvoir émanateur des roches ordinaires sont très rares; on trouvera des renseignements sur le pouvoir émanateur des minéraux radioactifs dans un article récent de Giletti et Kulp [1].

En considérant les périodes, on peut s'attendre à ce que la diffusion du Radon entraîne une erreur par défaut dans la mesure de l'activité α, tandis que celle du Thoron, et à un degré moindre, celle de l'Actinon, une erreur par excès. On peut empêcher la perte des gaz radioactifs en recouvrant l'échantillon d'un film mince; ce procédé est efficace dans le cas de sources minces,

[1] B. J. Giletti et J. L. Kulp: *Am. Miner.*, **40**, 481 (1955).

mais il n'y a aucune garantie que ces films empêchent les déplacements du Radon dans l'échantillon lui-même, dans le cas de source épaisse. Ces déplacements changent la géométrie de l'émission α et entraînent des erreurs sur l'estimation des concentrations en radioéléments.

Une méthode qui empêcherait toute diffusion des gaz radioactifs nous a paru possible en comptant l'échantillon refroidi à très basse température. Le Radon possède un point d'ébullition bien défini à — 62 °C, mais il est probablement déjà immobilisé par adsorption à des températures moins basses.

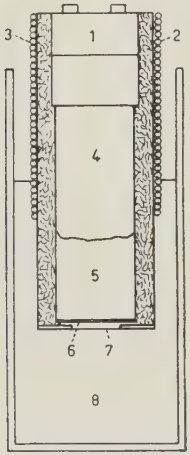

Fig. 1. – 1, socquet et connecteurs amphénol; 2, protection d'amiante; 3, silicagel; 4, photomultiplicateur RCA 5819; 5, conduit de lumière en lucite; 6, couche de sulphure de zinc (environ 5 mg/cm²); 7, cuvette contenant l'échantillon en poudre; 8, oxygène liquide.

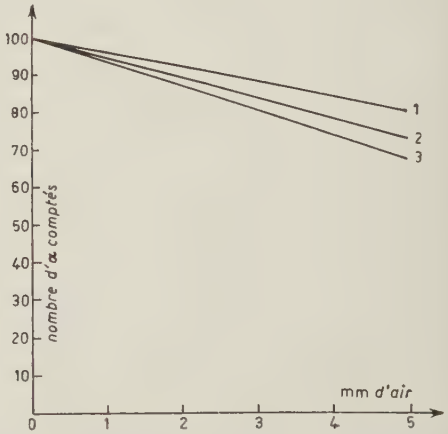

Fig. 2. – Variation théorique du taux de comptage α d'une source épaisse en fonction de l'épaisseur de la couche d'air entre la source et le détecteur, pour un abaissement de température de 160 °C. Nature de la source: 1 = Uranium ($U_I + U_{II}$); 2 = Uranium en équilibre avec ses descendants; 3 = Thorium en équilibre avec ses descendants.

Cette technique est difficilement réalisable avec une chambre d'ionisation ou un compteur proportionnel, mais elle est possible avec l'émulsion photographique [2] et s'adapte très bien au compteur à scintillation où l'effet de la basse température est favorable à la réduction du bruit thermique du photomultiplicateur.

Si la radioactivité de l'échantillon est due seulement à la famille du Thorium, l'équilibre radioactif avec le Thoron ($T = 54$ s) est établi en quelques minutes. Pour des mesures de précision, il faudrait attendre 40 à 50 heures pour être sûr que l'équilibre est rétabli jusqu'au ThB et ThC ($T = 10.6$ h et 60.5 m).

Si la famille de l'Uranium est aussi présente, l'équilibre avec le Radon ($T = 3.8$ j) et ses descendants n'est établi qu'après 30 jours environ. La néces-

---

[2] M. DEBEAUVAIS-WACK: *Nuovo Cimento*, **10**, 1590 (1953).

sité de conserver pendant 30 jours l'échantillon à basse température avant de le mesurer est un inconvénient de la méthode, mais n'introduit pas de difficulté expérimentale sérieuse.

Pour étudier les possibilités du comptage à basse température, nous avons comparé les comptages de diverses sources à température ordinaire et à la température de l'oxygène liquide (— 180°). Le dispositif de comptage à scintillation utilisé est représenté à la fig. 1.

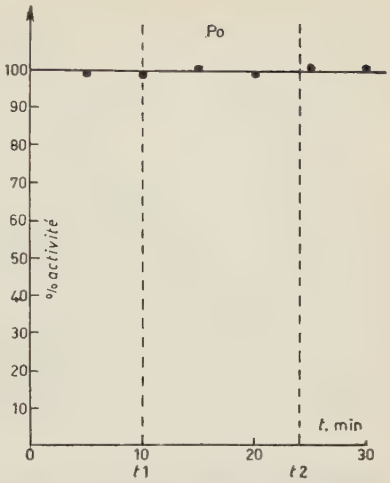

Fig. 3. – Comptage d'une source mince de Polonium. t_1: immersion dans l'oxygène liquide; t_2: retour à la température normale. Déviation standard sur les points expérimentaux: 2 %.

Si on veut comparer les résultats de comptages à des températures différentes, il faut tenir compte de la variation de densité entraînant une variation du pouvoir d'arrêt pour les α de la couche d'air comprise entre la surface de l'échantillon et l'écran de sulfure de zinc.

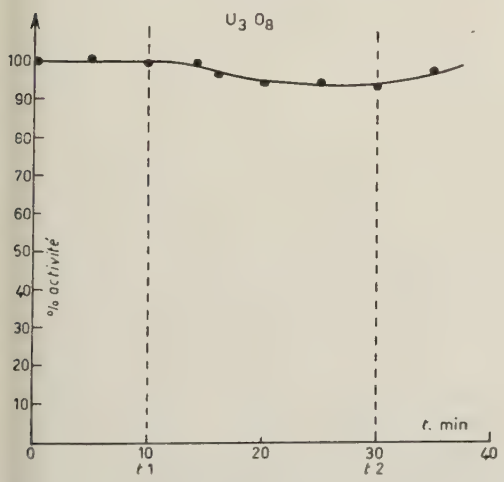

Fig. 4. – Comptage d'une source épaisse d'Uranium ($\sigma = 2$ %).

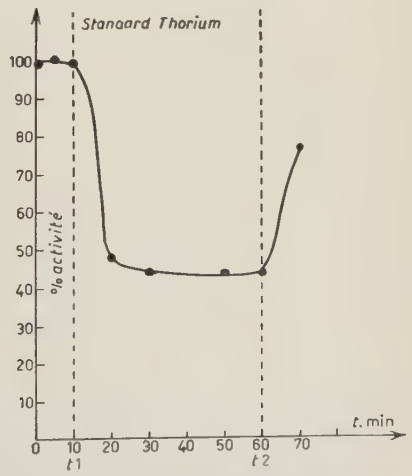

Fig. 5. – Comptage d'un mélange de thorite et de quartz ($\sigma = 2$ %).

Pour une couche d'air de quelques millimètres d'épaisseur, cet effet est négligeable pour une source en couche mince, mais atteint 10 à 20 % pour une source en couche épaisse. Les courbes de la fig. 2 montrent la variation théorique du nombre d'α comptés en fonction de l'épaisseur de la couche d'air

comprise entre la surface de l'échantillon et celle du détecteur, lorsque la température change de +20° à — 140 °C. Ces courbes ont été calculées [3] pour 3 cas, l'activité α étant due:

1) à l'Uranium seul ($U_I + U_{II}$);

2) à la famille de l'Uranium en équilibre;

3) à la famille du Thorium en équilibre.

Les courbes expérimentales 3 à 6 montrent l'évolution du comptage lorsqu'on passe de la température ordinaire à celle de l'oxygène liquide.

Pour démontrer que l'abaissement de température n'introduit pas de variation dans le rendement du compteur, nous avons utilisé deux sources n'émanant certainement pas de gaz radioactifs: une source de Polonium en couche mince (fig. 3) et une source d'oxyde d'urane (U_3O_8) en couche épaisse (fig. 4). Le taux de comptage de la source de Po demeure parfaitement constant. La légère diminution de la source de U_3O_8 correspond à l'augmentation de la densité de la couche d'air entre la source et l'écran de sulfure de zinc.

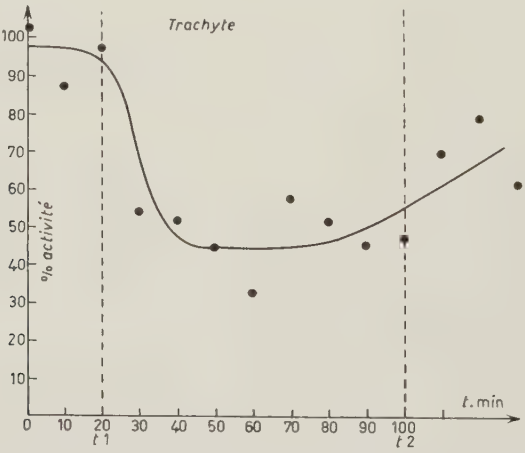

Fig. 6. – Comptage d'une lave en poudre ($\sigma = 10$ %).

La fig. 5 montre la variation du comptage d'un mélange de thorite et de quartz en poudre. De tels mélanges sont souvent utilisés comme étalons de Thorium. La chute de l'activité à basse température ne peut être due qu'à l'immobilisation du Thoron. On voit que le résultat du comptage à température normale est affecté d'une erreur par excès de plus d'un facteur 2 par suite de la diffusion du Thoron.

La fig. 6 montre un effet du même genre obtenu avec une lave trachytique en poudre.

---

[3] R. D. Evans: *Phys. Rev.*, **45**, 24 (1934).

Avec des échantillons contenant seulement la famille de l'Uranium, nous n'avons pas trouvé de différence appréciable de comptage comme on peut s'y attendre pour des périodes de réfrigération de quelques heures seulement, le Radon perdu n'ayant pas eu le temps de se reformer. Pour démontrer la perte de Radon, il aurait fallu conserver quelques jours l'échantillon à basse température.

Nous estimons cependant avoir montré que la diffusion des gaz radioactifs peut introduire des erreurs considérables dans les comptages d'activité α naturelle et que la mesure à basse température offre une solution efficace et simple à ce problème, surtout lorsqu'il s'agit de mesurer des matériaux dont on sait a priori qu'ils ont un grand pouvoir émanateur, tels que: argiles, laves, tuffs, roches altérées.

RIASSUNTO (*)

Si dimostra che nelle misure dell'attività α naturale si possono commettere errori notevoli a causa della diffusione del Radon. Tali errori si possono evitare misurando l'attività del campione raffreddato a — 180 °C per mezzo d'un contatore a scintillazione.

(*) *Traduzione a cura della Redazione.*

Measurements on High Energy Electron Showers.

E. LOHRMANN

Physikalisches Institut der Universität Bern
und Hochspannungslaboratorium Hechingen

(ricevuto il 14 Febbraio 1956)

In a letter in the same issue a high-energy nuclear event is described. Near the core of the jet three electron-positron pairs of high energy were found. They are assumed to be produced by photons from π^0-mesons emitted from the jet. A lower limit of 50 GeV for their energy was determined from relative scattering measurements (the true energy is obtained only if both electrons of the pair have the same energy). In this case however the cascades develop approximately in the same way around both electrons of the pairs (about the same number of tridents on each electron of a pair), so the scattering measurements should not underestimate the true photon energy too much. An upper limit for this energy is given by the energy of the shower particles in the core of the jet, which should agree with the energy of the π^0-mesons producing the photons. This energy was determined by relative scattering measurements to 80 GeV. Thus an upper limit for the mean electron energy in the cascade is 40 GeV. The mean energy of the 3 showers calculated from the opening angle of the first pairs is 12 GeV, thus underestimating the true energy by a factor $4 \div 6$, which is to be expected for great photon energies ([1-3]). The details of the three showers are given in Table I. The correction for spurious tridents was carried out according to KAPLON *et al.* ([4]) assuming a mean electron energy of 50 GeV. The mean free path for trident production is thus slightly overestimated, as the mean electron energy of the showers is 12 GeV, if one takes into account all electrons with energies > 1 GeV. Averaging over all three showers, the mean free path for trident production is $1.7^{+1.7}_{-0.8}\ t$, which is considerably lower than the theoretical mean free path ([5]) of $9\,t$ for an electron energy of 12 GeV and $6\,t$ for an energy of 40 GeV. Even for an assumed mean free path of $6\,t$ the probability of finding the observed number of tridents by a

([1]) G. BARONI, A. BORSELLINO, L. SCARSI and G. VANDERHAEGHE: *Nuovo Cimento*, **10**, 1653 (1953).

([2]) K. HINTERMANN: *Helv. Phys. Acta*, **27**, 125 (1954).

([3]) E. LOHRMANN: *Nuovo Cimento*, **2**, 1029 (1955).

([4]) M. KOSHIBA and M. F. KAPLON: *Phys. Rev.*, **97**, 193 (1955).

([5]) H. Y. BHABHA: *Proc. Roy. Soc.*, A **152**, 559 (1935); M. M. BLOCK, D. T. KING and W. W. WADA: *Phys. Rev.*, **96**, 1627 (1954).

TABLE I.

	L	E_0(BeV)	n_t	BSP	n'_t
I	$0{,}6\,t$	50^{+17}_{-10}	2	1	1,3
II	$0{,}75\,t$	55^{+30}_{-15}	0	3	—
III	$0{,}6\,t$	45^{+35}_{-15}	4	2	2,7

L total investigated length of the shower,

t cascade length (29 mm in the nuclear emulsion),

E_0 primary photon energy as deduced from relative scattering measurements,

n total number of apparent tridents,

BSP total number of bremsstrahlung pairs,

n'_t total number of real tridents corrected according to KAPLON *et al* [4].

fluctuation is 1%. The mean free path found is in agreement with the experimental findings of other authors [4,6,7]. It is also to be noted, that the three showers show an indication of having too many additional electrons created, as compared with Monte Carlo calculations of KAPLON [6].

In addition to these investigations a precise measurement of the blob-density of an electron track was made (the electron did not belong to the above mentioned 3 showers). The shower created by this electron can be followed over 9 cascade lengths; from its development there results a lower limit of 1000 GeV for the energy of the electron [8]. (The probability that it is a particle heavier than an electron is $< 10^{-3}$). The plateau blob density g_{P1} was measured on pair electrons with energies $50\ \text{MeV} < E < 1000\ \text{MeV}$. The blob density of the high-energy electron is accordingly $1.002 \pm 0.011\, g_{P1}$. Thus the existence of the plateau value of blob-density should be established at least up to energies of the order of $2 \cdot 10^6\, mc^2$.

* * *

The author wishes to express his gratitude to Prof. F. G. HOUTERMANS for the hospitality he enjoyed in his Institute, to Prof. E. SCHOPPER for granting a leave of absence, and to Prof. C. PEYROU and Dr. M. TEUCHER for stimulating discussions. He is further indebted to Profs. G. P. S. OCCHIALINI and C. HAENNY for making available to him their parts of the stack. The financial support from the Schweizer Nationalfonds and the Deutsche Forschungsgemeinschaft is gratefully acknowledged.

[6] M. KOSHIBA and M. F. KAPLON: *Phys. Rev.*, **100**, 327 (1955).

[7] A. DEBENEDETTI, C. M. GARELLI, L. TALLONE, M. VIGONE and G. WATAGHIN: *Nuovo Cimento*, **3**, 226 (1956)

[8] G. WATAGHIN: private communication.

IL NUOVO CIMENTO Vol. III, N. 4 1° Aprile 1956

Meson Production at Very High Energies.

E. Lohrmann

Physikalisches Institut der Universität Bern und Hochspannungslaboratorium Hechingen

(ricevuto il 14 Febbraio 1956)

In a stack of stripped emulsions exposed at an altitude of 29 km over Texas a high-energy star (I) of type 5+30p was found. The primary particle is singly charged and forms an angle of 83.5° with the vertical. Relative scattering measurements on four of the shower particles forming angles $\lesssim 10^{-3}$ rad with the primary direction gave a mean energy of 80^{+25}_{-15} GeV. One of these particles makes a secondary interaction of type 2+4p. In addition 3 high-energy electron-positron pairs were found within the first 22 mm from star I. Their angles with the primary direction are $< 7 \cdot 10^{-3}$ rad, their axis points exactly at the center of star I. Their mean energy (from relative scattering measurements) is 50 GeV. If we assume them to be produced by photons from π^0-mesons, emitted from star I, this energy agrees well with the energy of the shower particles given above.

At a distance of 25 mm from star I there is a second one (II) of type 3+55n. The axis of its meson-shower is parallel to the core of jet I, its angular distance from the core is $1.5 \cdot 10^{-3}$ rad; it must therefore have been produced by a neutral particle emitted from jet I (π^0-meson is excluded). The energy of star II can be shown to be 150 GeV. Including all other particles of star I and the energy of the electromagnetic cascades, the total « visible » energy of star I can be shown to be 1100 GeV, which gives a lower limit for the primary energy. An upper limit of 12000 GeV could be derived from scattering measurements on the other shower particles. The inelasticity is thus $> 10\%$, the mean energy E_M of the mesons in the center of mass (CM)-system is 1.7 GeV $> E_M >$ 0.5 GeV. The angular distribution of the particles in the forward cone in the CM-system is strongly anisotropic, 60% of all particles forming angles $< 20°$ with the primary direction even for an assumed primary energy of 12000 GeV. (The angular distribution of the backward cone in the CM-system has no significant meaning, as part of these particles were produced by secondary interactions in the same nucleus). All these data are in agreement with the Heisenberg theory of multiple meson production (1). The

(1) W. Heisenberg: *Zeits. f. Phys.*, **133**, 65 (1952) and **126**, 569 (1949); *Zeits. f. Naturwiss.*,

Fermi theory ([2]) would give a lower limit of 3.6 GeV for the mean energy of the mesons in the CM-system, which can hardly be reconciled with the measurements.

The angular distribution of the particles of star II was transformed into a CM-system, using the exact transformation formulas. For this purpose all particles were assumed to be π-mesons; their energy was measured by their multiple scattering if the transformation dependend on it. Best symmetry in the CM-system resulted for a primary energy of 150 GeV (Fig. 1). From the 22 particles the energy of which had been measured, 14 were selected which were considered to be an unbiased sample. Fig. 2 shows the distribution of their total energy in the CM-system. Their mean energy is greater than the energy calculated from the total energy available in the CM-system and the multiplicity. Agreement can only be reached by assuming that about 6 of the shower particles were produced by secondary interactions (a greater number is improbable because of the small number of evaporation particles observed) and that this is also the case for the 3 mesons with the highest energy in the CM-system. The inelasticity must be 1; no energy in the CM-system is left for the production of particles heavier than π-mesons in appreciable numbers. The mean total energy of the mesons in the CM-system is then 270 MeV assuming a direct production of 60 mesons (including π^0-mesons). The angular distribution of the 14 mesons of Fig. 2 is shown in Fig. 1 (dashed curve). The mesons were divided

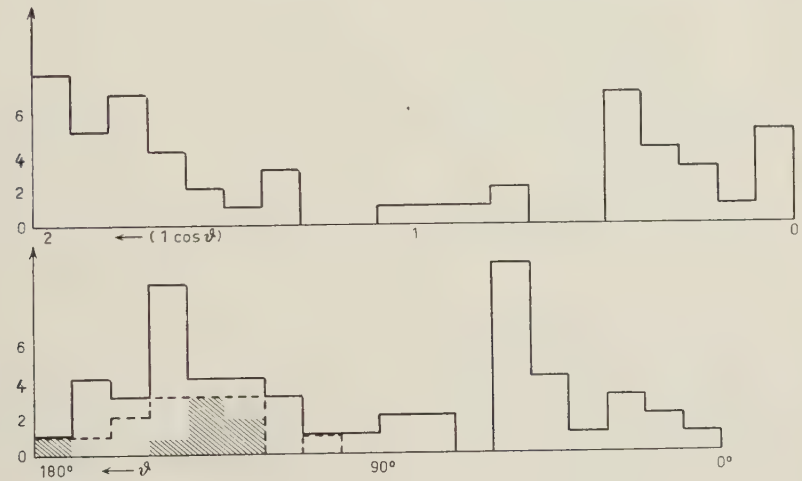

Fig. 1.

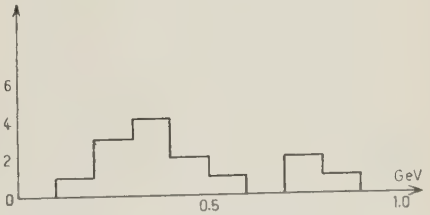

Fig. 2.

39, 69 (1952); *Kosmische Strahlung* (Berlin, 1953), p. 148.

([3]) E. Fermi: *Progr. Theor. Phys.*, **5**, 570 (1950); *Phys. Rev.*, **81**, 570 (1951).

into two groups according to their energy. The area corresponding to mesons with an energy < 0.36 GeV in the CM-system is hatched. One sees that the anisotropy observed is produced by the particles of high energy. All this is again in agreement with the Heisenberg theory ([1]). The Fermi theory ([2]) gives an anisotropic angular distribution only for small multiplicities. Furthermore the expectation value of mesons produced at a primary energy of 150 GeV is only 5 according to Fermi, which is obviously too low (*).

Prior to these measurements extensive calibration work was done on spurious scattering and noise elimination according to PETERS *et al.* ([3]). A more detailed account of this work and of the event described above is going to be published.

* * *

The author wants to express his thanks to Prof. E. SCHOPPER for granting a leave of absence and for encouragement; to Prof. F. G. HOUTERMANS for the hospitality in his Institute and to Prof. C. PEYROU for stimulating discussions. I am also very much indebted to Dr. M. TEUCHER for many valuable discussions. The work was supported by grants from the Schweizer Nationalfonds and the Deutsche Forschungsgemeinschaft.

(*) It is also hardly possible to reach agreement between the FERMI theory and observation by assuming a nuclear cascade according to ROESLER and Mc CUSKER ([4]) and COCCONI ([5]), as these theories do not apply at so low a primary energy and the observed multiplicity would be still too high.

([3]) S. BISWAS, B. PETERS and RAMA: *Proc. Ind. Acad.*, A **41**, 154 (1955).

([4]) F. C. ROESLER and C. B. A. Mc CUSKER: *Nuovo Cimento*, **10**, 127 (1953).

([5]) G. COCCONI: *Phys. Rev.*, **93**, 1107 (1954).

IL NUOVO CIMENTO Vol. III, N. 4 1° Aprile 1956

On the Properties of τ^+-Mesons.

N. N. Biswas, L. Ceccarelli-Fabbrichesi, M. Ceccarelli (*), K. Gottstein
N. C. Varshneya and P. Waloschek
Max-Planck-Institut für Physik - Göttingen

(ricevuto il 20 Febbraio 1956)

It has been shown by Dalitz [1] that it is possible to obtain information on the spin and parity of the τ-meson from the energy and angular distributions of the π-mesons resulting from the τ-decay. The experimental material available at the time of the Pisa Conference [2] indicated that the assumption of a pseudoscalar τ-particle (zero spin, odd parity) was the most plausible one. This was later confirmed by the results of the Berkeley [3] and Bristol [4] groups. Feld and coworkers [5], however, find a certain asymmetry in the energy spectrum of the negative pions which would favour the spin-parity combination [1+]. It might be of interest to add to these results those obtained by our group in a statistically rather unbiassed manner.

In analyzing the data from the previous cosmic ray experiments it has to be kept in mind that often the method of scanning may have produced a bias in favour of events of a certain type, as discussed by the Padua group [6]. Moreover, due to the rather small dimensions of the plates or stacks of emulsions then in use, the probability that a pion could be followed to the end of its range was usually not independent of its energy.

Our sample of τ-mesons has been found in two stacks (« K_1 » and « K_2 ») exposed to the K^+ beam of the Berkeley Bevatron. All tracks were examined which, at a distance of 17 mm from the edge where the beam entered the stack, satisfied the following criteria:

1) Grain-density visibly higher than that of the pions of the beam (the protons stopped before reaching this region of the emulsions).

(*) On leave from Padua University.

(1) R. H. Dalitz: *Phil. Mag.*, **44**, 1068 (1953); *Phys. Rev.*, **94**, 1046 (1954).

(2) E. Amaldi: *Report of the Pisa Conference on Elementary Particles*, 1955; *Suppl. Nuovo Cimento*, in press.

(3) R. Haddock: *Phys. Rev.*, **100**, 1803 (1955).

(4) B. Bhowmik, D. Evans, I. J. Van Heerden and D. J. Prowse: *Nuovo Cimento*, **3**, 574 (1956). We are indebted to the authors for sending us their manuscript prior to publication.

(5) B. T. Feld, A. C. Odian, D. M. Ritson and A. Wattenberg: *Phys. Rev.*, **100**, 1539 (1955).

(6) M. Baldo, G. Belliboni, M. Ceccarelli, M. Grilli, B. Sechi, B. Vitale and G. T. Zorn: *Nuovo Cimento*, **1**, 1180 (1955).

2) Minimum length of track per emulsion:

5 mm (for « K_1 ») and 4 mm (for « K_2 »).

3) Maximum deviation of azimuth angle from the general beam direction: 5°.

These tracks were followed until they either stopped or left the stack (in the 5 first and 5 last plates of each stack only those tracks were followed which were directed towards the inner part of the stack). The end points of all tracks followed were examined very carefully under immersion. A bias of the first type mentioned above can therefore be excluded. In addition, the rather large dimensions of the stacks (« K_1 »: 120 emulsions, 25.5 cm × 40 cm, each 600 μm thick; « K_2 »: 300 emulsions, 25 cm × × 20 cm, each 600 μm thick) and the location of the scanned zone allowed us to determine in each case the charge and energy of all the three pions.

In this way 87 coplanar τ-decays have been observed of which the energies of the three pions and the angles between their tracks have been measured. The Q-values of all the τ's lie within rather narrow limits, the average is

$$Q = 73.5 \pm 0.3 \text{ MeV} .$$

This is in rather good agreement with the value of 75 MeV generally obtained by using the range-energy relation for dry emulsions without correction for the humidity present (7), and shows that no appreciable systematic error has been made.

A survey of the data is presented in Fig. 1 which shows a triangular diagram of the kind suggested by Dalitz (1). The height of the triangle is given by the Q-value (taken as 75 MeV). Each point corresponds to one τ-event, its distance from the base is proportional to the energy of the negative pion. The semicircle encloses the region to which the points are restricted by momentum conservation in non-relativistic approximation. The points are distributed rather

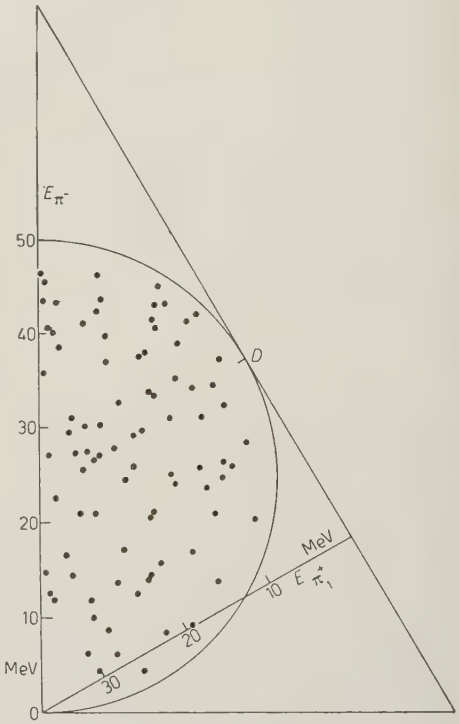

Fig. 1. – Triangular representation of τ-decays.

isotropically; some of them lie near O and D thereby confirming the occasional occurrence of very low energies both for negative and positive pions. This is borne out by Fig. 2 in which the energy distributions for positive (A) and negative (B) pions are plotted separately. The latter is markedly asymmetrical. The lack of low energy negative pions cannot be explained as due to misinterpretation or loss of τ-mesons with short σ_0 tracks since the ratio of σ_0 pions to negative pions causing larger σ-stars is found to be essentially independent of energy.

The experimental material has been

(7) Compare Table I in K. Gottstein: *Nuovo Cimento*, **1**, 284 (1955).

compared with the various theoretical predictions. FABRI ([8]) and, after him, COSTA and TAFFARA ([9]) have calculated, for the spin-parity combinations [0 −], [1+], [1 −], [2+], [2 −], [3 −], [4 −], the probability that the energy E_{π^-} of

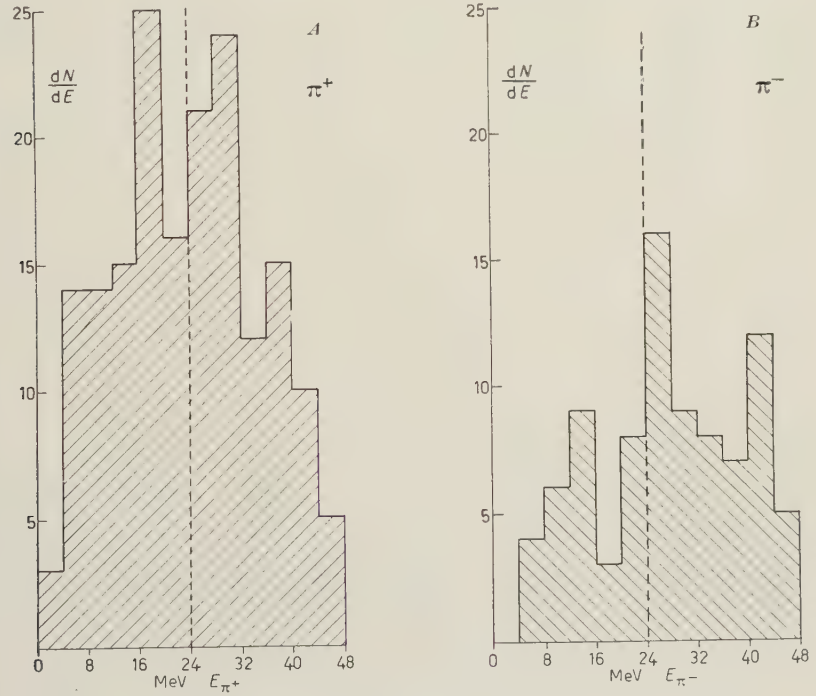

Fig. 2. – Energy distribution of positive (A) and negative (B) pions.

the negative pion obeys one of the three following inequalities:

$$(a) \qquad E_{\pi^-} > E_{\pi 1^+}, \quad E_{\pi 2^+}$$

$$(b) \qquad E_{\pi 1^+} > E_{\pi^-} > E_{\pi 2^+}$$

$$(c) \qquad E_{\pi 1^+}, \quad E_{\pi 2^+} > E_{\pi^-}.$$

Fig. 3A shows these probabilities together with our experimental points. Fig. 3B and 3C give the distributions of angles between the two like pions, and between all the pions, respectively, as calculated by COSTA and TAFFARA ([9]) different spin-parity combinations, and for the corresponding experimental values of ours.

In Fig. 4 the distribution curves of $\cos\theta$ (θ: angle between the directions of the two positive pions in their c.o.m. system and the direction of the negative pion), and in Fig. 5A the energy distribution of the negative pion, for different assumptions on spin and parity, are reproduced from the paper by FELD *et al.* ([5]) and compared with our results. Fig. 5B shows the energy distributions for negative pions as obtained by different groups of workers.

The information from Figs. 3-5, as pertaining to spin and parity, is compiled in Table I. « C » stands for « consistent », « LC » for « less consistent ». The last row contains the judgement at which one arrives by considering the outcome of all the tests.

([8]) E. FABRI: *Nuovo Cimento*, **11**, 479 (1954).
([9]) G. COSTA and L. TAFFARA: *Nuovo Cimento*, **3**, 169 (1956).

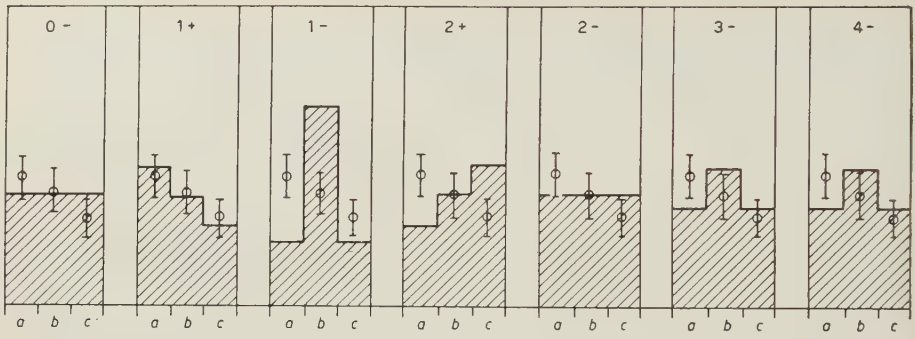

A) Fabri: Energy distributions: *a*) $E_{\pi^-} > E_{\pi_1^+}, E_{\pi_2^+}$; *b*) $E_{\pi_1^+} > E_{\pi^-} > E_{\pi_2^+}$; *c*) $E_{\pi_1^+}, E_{\pi_2^+} > E_{\pi^-}$.

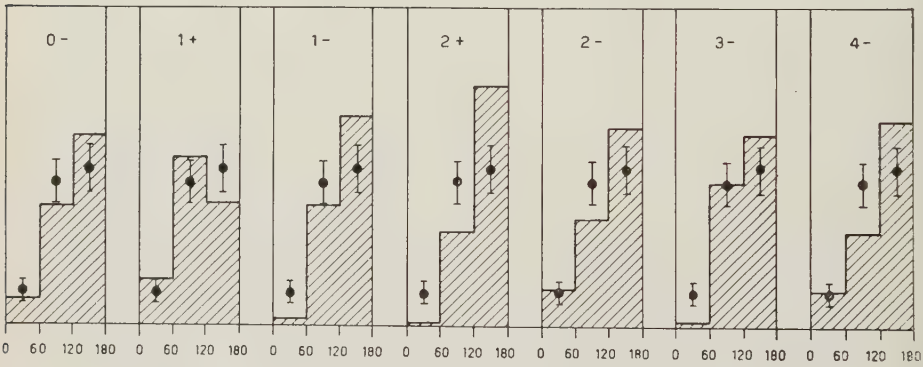

B) Costa and Taffara: Angular distributions. Angles between $\pi^+\pi^+$.

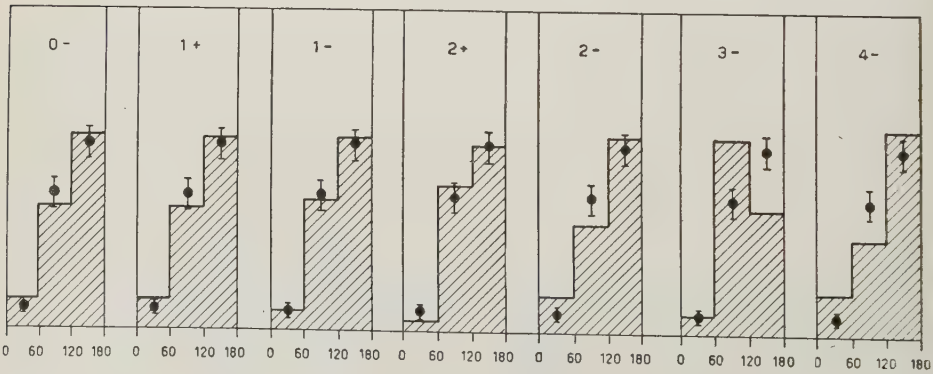

C) Costa and Taffara: Angular distributions. All angles.

Fig. 3. – The three energy distribution cases of Fabri (*A*) and the distributions calculated by Costa and Taffara of the angles between the tracks of the two like pions (*B*) and between those of all pions (*C*), for different spin-parity combinations.

TABLE I.

Theory	Spin and Parity						
	0 —	1+	1 —	2+	2 —	3 —	4 —
FABRI Fig. 3*A*	*C*	*C*	*LC*	*LC*	*C*	*C*	*C*
COSTA and TAFFARA Fig. 3*B*	*C*	*C*	*C*	*LC*	*C*	*C*	*C*
COSTA and TAFFARA Fig. 3*C*	*C*	*C*	*C*	*C*	*C*	*LC*	*C*
DALITZ $\cos\theta$ distribution Fig. 4	*C*	*C*	*LC*	*C*	*C*	*C*	*C*
DALITZ-FELD E_{π^-} distribution Fig. 5*A*	*C*	*C*	*LC*	*LC*	*LC*	*LC*	—
Summary	*C*	*C*	*LC*	*LC*	*LC*	*LC*	*C*

It follows that of the various spin-parity combinations the assumptions [0 —], [1+] and [4 —] are those which are more consistent with the experimental data. As pointed out also by previous Authors it should be noted that the various possibilities of even spin and odd parity cannot be well discriminated by this type of analysis. However at least the case [4 —] is hardly consistent with the absence of any detectable polarization effect.

The ambiguity between the cases [0 —] and [1+] could well be due to a statistical fluctuation. But it is perhaps not without interest to consider the possibility that it is genuine.

One explanation for this could be the existence of two different types of τ-mesons, one pseudoscalar and one vector;

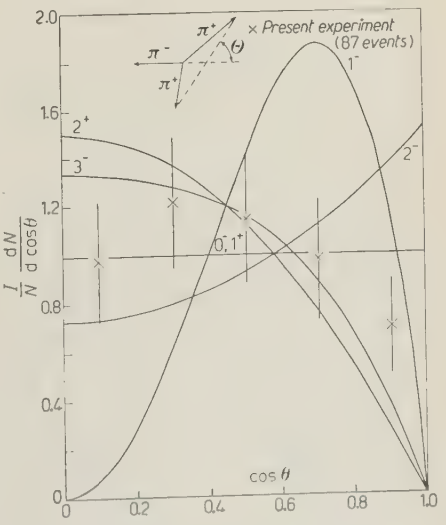

Fig. 4. – Distribution of $\cos\theta$ according to DALITZ.

the former one could be predominant in the cosmic ray events reviewed by AMALDI; it could, e.g., have a shorter mean life than the latter so that it would occur more rarely in emulsions exposed to the focussed K-beam. However, the are of a single [0 —] or [1+] type, and that the theories which predict respectively the two energy distributions are oversimplified. In this connection one might mention the remark by FELD *et al.* [5] that the assumption of certain

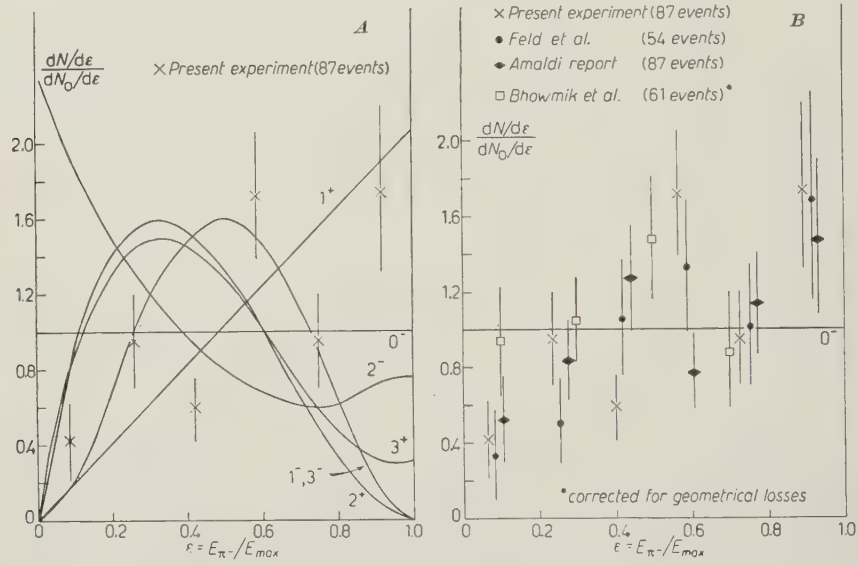

Fig. 5. – Energy distribution of negative pions according to FELD *et al.* *A*: Our results compared with the distributions for different spins and parities. *B*: The result of different groups compared with the assumption [0 —].

Bristol and Berkeley groups were also studying τ-events in emulsions exposed to the Bevatron, and apparently did not find such an ambiguity.

On the other hand, a certain admixture of vector τ-mesons to the total τ-population would result in a more or less strongly pronounced deformation of the negative pion energy distribution towards higher energies whereas this distribution would be symmetrical for a pure [0 —] case. There is indeed a possible indication for such a deformation also in the spectrum given by AMALDI, especially if one considers the possible bias in favour of the detection of pions of low energy.

Another explanation to be perhaps preferred would be that the τ-mesons interactions between the pions would lead to deviations from a symmetrical π^- energy distribution, of the type expected for the [1+] case.

In order to check once more the possibility of a spin different from zero we have made the polarization test proposed by TEUCHER *et al.* [10]. Fig. 6 *A* shows the result. The distribution of the angles between the beam direction and the normals to the planes of decay is isotropic within the limits of experimental errors and therefore does not suggest any polarization effect.

In addition, considering possible re-

[10] M. TEUCHER, W. THIRRING and H. WINZELER: *Nuovo Cimento*, **1**, 733 (1955); H. WINZELER: *Supplement to Amaldi's report* [3].

lations between τ-mesons and K-particles in general, we have also been looking for polarization effects in K_L-events. For this purpose we have measured the angles between beam direction and the projection of the track of the lightly ionizing secondary particle into the plane of the emulsion for 701 K_L secondaries having dip angles $< 45°$. A relative lack of angles around 90° should be expected if the K-particles were polarized with their spins normal to both the beam direction and to the plane of production. Fig. 6 *B* does not show any clear effect of this kind.

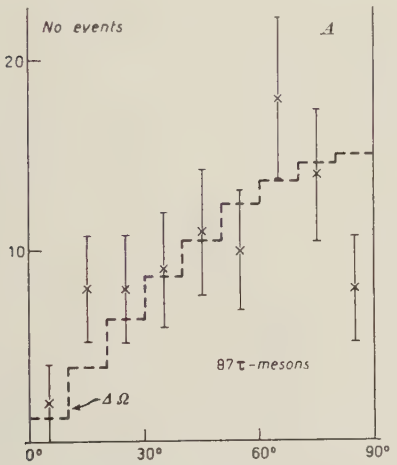

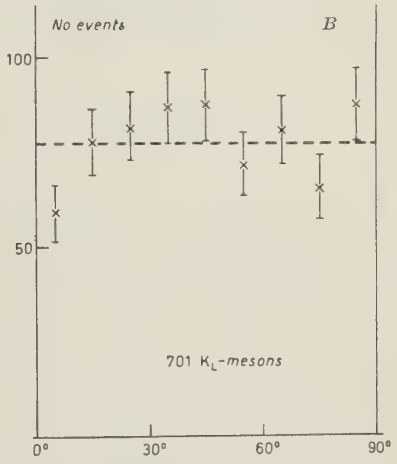

Fig. 6 *A*. – Distribution of angles between beam direction and normal to decay plane. The dotted curve corresponds to isotropy. – Fig. 6 *B*. – Distribution of angles between beam direction and projection of secondary track into plane of emulsion. The dotted curve corresponds to isotropy.

Looking back on all the evidence we feel that our results do not contradict conclusively the view that the τ-meson has zero spin and odd parity. However, there seems to be some indication for second-order effects which have not been considered in the present theories. Only by increasing further in a strictly unbiassed manner the statistical weight of the material available it will be possible to shed more light on this problem.

* * *

We are greatly indebted to Drs. G. and S. Goldhaber and the staff at the Berkeley Bevatron for the exposure of the stacks, to the Bristol group for developing them, and to Prof. G. P. S. Occhialini for allowing us to follow some tracks into the parts of the stacks allotted to the Milan group. Our particular thanks are due to our Göttingen scanning team. Prof N. Dallaporta and Dr. G. Lüders have kindly read the manuscript.

Several of us are grateful to various personalities and institutions for scholarships or maintenance grants: M. C. to Prof. W. Heisenberg, N. N. B. to the Government of India, and P. W. to the Deutscher Akademischer Austauschdienst, Bonn. The latter also wishes to thank the Argentine Comisión Nacional de la Energía Atomica for leave of absence.

The Deutsche Forschungsgemeinschaft has supported our work by the purchase of microscopes.

Campi fermionici e metodo di quantizzazione di Feynman.

P. Bocchieri e A. Loinger

Istituto di Fisica dell'Università - Pavia
Istituto Nazionale di Fisica Nucleare - Sezione di Milano

G. M. Prosperi

Istituto di Scienze Fisiche dell'Università - Milano
Istituto Nazionale di Fisica Nucleare - Sezione di Milano

(ricevuto il 21 Febbraio 1956)

In questa lettera ci proponiamo di rispondere alla seguente questione: è applicabile il metodo di quantizzazione di Feynman [1,2] ai campi fermionici?

A questo scopo, cominciamo col riesaminare brevemente le connessioni esistenti tra l'ordinaria formulazione della meccanica quantistica di una particella e la corrispondente formulazione di Feynman. Indicato con $|\xi', t\rangle$ il vettore di stato relativo a una certa osservazione massima fatta al tempo t e con $q(t)$ l'operatore posizione della particella al tempo t (ci limitiamo, per semplicità di scrittura, al caso di un solo grado di libertà) la legge di composizione delle matrici fornisce:

$$(1) \qquad \langle \xi'', t'' | q(t^{(p)}) q(t^{(p-1)}) \dots q(t^{(1)}) | \xi', t' \rangle =$$

$$= \int \mathrm{d}q_0' \mathrm{d}q_1' \dots \mathrm{d}q_{k_p}' \mathrm{d}q_{k_p}'' \dots \mathrm{d}q_n' \langle \xi'', t'' | q_n', t'' \rangle \cdot$$

$$\cdot \langle q_n', t'' | q_{n-1}', t_{n-1} \rangle \dots \langle q_{k_p+1}', t_{k_p+1} | q_{k_p}', t_{k_p} \rangle \cdot$$

$$\cdot q_{k_p}' \delta(q_{k_p}' - q_{k_p}'') \langle q_{k_p}'', t_{k_p} | q_{k_p-1}', t_{k_p-1} \rangle \dots \langle q_0', t' | \xi', t' \rangle ,$$

ove: $t_r - t_{r-1} = \varepsilon_r > 0$; $t_{k_i} \equiv t^{(i)}$ e supponiamo inoltre $t'' > t^{(p)} > \dots > t^{(1)} > t'$. Ma si

---

(1) P. A. M. Dirac: *The Principles of Quantum Mechanics*, Third Edition (Oxford, 1947), p. 125; R. P. Feynman: *Rev. Mod. Phys.*, **20**, 367 (1948); *Phys. Rev.*, **80**, 440 (1950); C. Morette: *Phys. Rev.*, **81**, 848 (1951); W. Pauli: *Ausgewählte Kapitel aus der Feldquantisierung* (Zürich, 1951), p. 139; Ph. Choquard: *Helv. Phys. Acta*, **28**, 89 (1955); vedi anche le osservazioni concludenti il § 2 del lavoro di J. Schwinger: in *Phys. Rev.*, **82**, 914 (1951).

(2) B. Davison: *Proc. Roy. Soc.*, **225** A, 252 (1954); W. K. Burton e A. H. De Borde: *Nuovo Cimento*, **2**, 197 (1955).

può mostrare che, a meno di termini di ordine superiore a ε_r, è:

$$\langle q'_r, t_r | q'_{r-1}, t_{r-1} \rangle = \frac{1}{N_r} \exp\left[\frac{i}{\hbar} S(q'_r, t_r; q'_{r-1}, t_{r-1})\right], \tag{2}$$

con

$$S(q'_r, t'_r; q_{r-1}, t_{r-1}) = \int_{t_{r-1}}^{t_r} L(q', \dot{q}')\, \mathrm{d}t\,, \tag{2'}$$

ove l'integrazione va eseguita lungo la traiettoria *classica*. Si perviene in tal modo alla formula:

$$\langle \xi'' t'' | q(t^{(p)}) \dots q(t^{(1)}) | \xi', t' \rangle = \lim_{\varepsilon \to 0} \int \mathrm{d}q'_0 \frac{\mathrm{d}q'_1}{N_1} \dots \frac{\mathrm{d}q'_n}{N_n} \cdot \tag{3}$$

$$\cdot \langle \xi'', t'' | q'_n, t'' \rangle q'_{k_p} q'_{k_p - 1} \dots q'_{k_1} \exp\left[\frac{i}{\hbar} \sum_1^n S(q', t_r; q'_{r-1}, t_{r-1})\right] \langle q'_0, t' | \xi', t' \rangle\,,$$

che costituisce la relazione fondamentale del metodo di Feynman. Risulta evidente che *la validità della* (3) *presuppone l'esistenza di una rappresentazione diagonale per le* $q(t)$.

Consideriamo allora gli oscillatori di Bose-Einstein e di Fermi-Dirac. Per l'oscillatore di Bose-Einstein la (3) è ovviamente applicabile, quando esso sia caratterizzato dalla variabile di posizione q e dal momento p. Se però facciamo le sostituzioni

$$q = \sqrt{\frac{\hbar}{2\omega}}\,(a + \bar{a})\,; \qquad p = \frac{1}{i}\sqrt{\frac{\hbar\omega}{2}}\,(a - \bar{a})\,, \tag{4}$$

avremo

$$[a, \bar{a}] = 1\,, \tag{5}$$

da cui consegue che a non è diagonalizzabile e quindi non possiamo scrivere una relazione del tipo (3), in cui la a giochi il ruolo della q.

Una conclusione analoga vale anche per l'oscillatore di Fermi-Dirac se lo si introduce, come si fa di solito, mediante le relazioni

$$\{a, \bar{a}\} = 1\,; \qquad a^2 = \bar{a}^2 = 0\,; \qquad H = \hbar\omega \bar{a} a\,. \tag{6}$$

Ma in questo caso, a differenza di quanto avviene per l'oscillatore di Bose-Einstein, neppure passando a variabili hermitiane q, p tramite le sostituzioni (4), sarà possibile applicare la (3): infatti, così facendo, si ottiene una $q(t)$ diagonalizzabile e si può scrivere una relazione analoga alla (1) avente delle somme su due valori in luogo degli integrali, la (2') però cade necessariamente in quanto essa è fondata su un principio di corrispondenza, mentre la q dell'oscillatore di Fermi-Dirac non possiede un analogo classico.

Per chiarire maggiormente questo punto osserviamo che le (2), (2') coincidono sostanzialmente con la (2.138) del lavoro di SCHWINGER citato in [1], quando l'inter-

vallo di tempo è infinitesimo. Per giungere alla (2.138) è però essenziale poter dedurre dalla (2.136) la (2.137) loc. cit., ma ciò non può farsi nel nostro caso in quanto le variazioni δq e δp delle variabili q e p non sono numeri $-c$ e di conseguenza non possono essere portate fuori dall'elemento di matrice al secondo membro di (2.136).

Un discorso analogo si può evidentemente fare per un qualsiasi sistema a variabili fermioniche, per esempio per il campo di Dirac; sembra pertanto ragionevole concludere che *il metodo di quantizzazione di Feynman è essenzialmente ristretto a variabili bosoniche*, come la maggior parte degli autori ha finora ritenuto; (lo stesso FEYNMAN ha del resto descritto, nel suo lavoro sulla teoria del positone, i fermioni con un opportuno formalismo *configurazionale*). In contrasto con questa conclusione, MATTHEWS e SALAM [3] hanno recentemente ritenuto di poter estendere il metodo di Feynman ai campi fermionici; essi eseguono la « somma sulle storie » corrispondente alla (3) mediante una prescrizione *ad hoc*, la quale costituisce una generalizzazione formale del « metodo parametrico » di Davison [2] valido per la meccanica delle particelle e, forse, pei campi bosonici. Ma noi riteniamo che il successo del procedimento dei suddetti Autori (procedimento che permette loro di ricavare i corretti propagatori dei campi liberi) sia dovuto ad alcune incongruenze di carattere matematico che ci sembra siano contenute nel loro lavoro e pertanto crediamo di non dover modificare l'opinione che abbiamo precedentemente esposto.

[3] P. T. MATTHEWS e A. SALAM: *Nuovo Cimento*, **2**, 120 (1955); vedi anche J. C. POLKINGHORNE: *Proc. Roy. Soc.*, **230** A, 272 (1955).

IL NUOVO CIMENTO Vol. III, N. 4 1° Aprile 1956

On Cut-Off and non Local Theories.

P. Budini

Istituto di Fisica dell'Università - Trieste
Istituto Nazionale di Fisica Nucleare - Sezione di Padova

(ricevuto il 25 Febbraio 1956)

One of the most general non local theories of the pion-nucleon fields in interaction is the form factor theory by Kristensen and Möller [1]. It is based on the Lagrangean:

$$(1) \qquad L = L^0_{\text{Nucleons}} + L^0_{\text{Pions}} - G \int \mathrm{d}^4x_1\, \mathrm{d}^4x_2\, \mathrm{d}^4x_3\, F(x_1x_2x_3)\bar{\psi}'(x_1)\Gamma\psi'(x_2)\varphi'(x_3)\,,$$

where ψ', φ' are the field variables, Γ is a Dirac (eventually differential) operator and $F(x_1x_2x_3)$ the covariant form factor.

The calculations on the low energy pion-nucleon phenomenology are usually based on the knowledge of the canonical field variables for the quantized fields. The problem of their existence has, to our knowledge, not yet been solved in the general case of non local field theories; though, if the form factor is of the normal class, that is such that the initial value problem has the same answer as from the free fields, then canonical field quantities always exist for classical fields and can be constructed, at least in first approximation of perturbation theory, for quantized fields. In this case, if we indicate with ψ, φ the canonical field variables, the Hamiltonian of the system is given by:

$$(2) \qquad H = H^0_{\text{Nucleons}} + H^0_{\text{Pions}} + G \int \mathrm{d}^4x_1\, \mathrm{d}^4x_2\, \mathrm{d}^4x_3\, \delta(t - t_3)\, F(x_1x_2x_3)\,\bar{\psi}(x_1)\,\Gamma\psi(x_2)\varphi(x_3)\,.$$

It is plausible to think [2] that in the case of form factors of the normal class this result is valid not only in the approximation linear in G but also exactly; we shall make this assumption. Then if we put in (2):

$$(3) \qquad F(x_1x_2x_3) = f(\boldsymbol{x}_1 - \boldsymbol{x}_3)\,\delta^4(x_1 - x_2)\,\delta(t_1 - t_3)$$

[1] P. Kristensen and C. Møller: *Dat. King. Dans. Vid.*, **27**, n. 7 (1952).
[2] W. Pauli: *Nuovo Cimento*, **10**, 647 (1953).

and

$$\Gamma = \gamma_5\gamma_\mu \frac{\partial}{\partial x_\mu} \sim \boldsymbol{\sigma}\cdot\boldsymbol{\nabla}$$

we obtain the well known interaction hamiltonian of the extended source theory.

As next non local generalization of the extended source theory we will take into account retardations inside the extended source; that is, we shall eliminate $\delta(t_1 - t_3)$ from (3) and the form factor will be:

$$F(x_1x_2x_3) = f(x_1 - x_3)\,\delta^4(x_1 - x_2)\,,$$

with $f(x_1 - x_3)$ covariant function of $x_1 - x_3$. In momentum space the interaction hamiltonian for the pseudovector symmetrical case (units $c=1$; $\hbar=1$) becomes:

$$H_{\text{int}} = \frac{-iG\boldsymbol{\tau}_i}{(2\pi)^{\frac{3}{2}}} \int \frac{\mathrm{d}^4k'\,\mathrm{d}^3k''}{\sqrt{2\omega'}}\, v(\boldsymbol{k}'', \varepsilon)\,\overline{\psi}(\boldsymbol{k}' - \boldsymbol{k}'')\gamma_5\gamma_\mu k''_\mu \psi(\boldsymbol{k}')\varphi_i(\boldsymbol{k}'')\,, \tag{4}$$

where $v(\boldsymbol{k}, \varepsilon)$ is a covariant function of the fourvector $\boldsymbol{k}$, ε, and is the Fourier transform of the covariant form factor $f(x_1 - x_3)$. ε depends on the energy spectrum of the interacting particles.

Starting from (4) we have deduced the integral equation for the one pion-one nucleon wavefunction $\chi(\boldsymbol{k})$ in first Tamm-Dancoff approximation. In the center of mass system, dropping the fourth term of $\gamma_5\gamma_\mu(\partial/\partial x_\mu)$ (the galilean term) we obtain:

$$\begin{aligned}(E - E_k - \omega)\,\chi_i(\boldsymbol{k}) = \frac{G^2}{(2\pi)^3}\int \frac{\mathrm{d}^3k'}{2\sqrt{\omega\omega'}} \Bigg\{ & \frac{v(\boldsymbol{k}, E - E_k)\,(-\boldsymbol{k}',\, E_{k'} - E)}{E - M}\,(\boldsymbol{\sigma}\cdot\boldsymbol{k})(\boldsymbol{\sigma}\cdot\boldsymbol{k}')\boldsymbol{\tau}_i\boldsymbol{\tau}_j + \\ & + \frac{v(\boldsymbol{k}, E - E_{k+k'} - \omega')\,v(-\boldsymbol{k}',\, E_{k+k'} + \omega - E)}{E - E_{k+k'} - \omega - \omega'}\,(\boldsymbol{\sigma}\cdot\boldsymbol{k}')(\boldsymbol{\sigma}\cdot\boldsymbol{k})\boldsymbol{\tau}_j\boldsymbol{\tau}_i \Bigg\}\,\chi_j(\boldsymbol{k}') + \\ & + \frac{3G^2}{(2\pi)^3}\int \frac{k'^2\,\mathrm{d}^3k'}{2\omega'}\,\frac{v(\boldsymbol{k}', E - E_{k+k'} - \omega)\,v(-\boldsymbol{k}',\, E_{k+k'} - \omega - E)}{E - E_{k+k'} - \omega - \omega'}\,\chi_i(\boldsymbol{k})\,.\end{aligned}$$

In the extended source theory, under the same hypotesis one obtains the same equation but for the dependence of the form factor on the energy of the interacting particles. Thus it is to expect that at low energy with a proper choice of the form factor the covariant non local theory will give results similar to those of the cut-off theory. The presence of the term.

$$E_{k+k'} = (M^2 + k^2 + k'^2 + 2kk'\cos\widehat{\boldsymbol{k}\boldsymbol{k}'})^{\frac{1}{2}}$$

in the form factor will, through the $\cos\widehat{\boldsymbol{k}\boldsymbol{k}'}$, cause a further contribution to S waves (to be added to that of recoil and of the galilean term) in the problem of the pion-nucleon elastic scattering.

A Note on the Analysis of τ-Meson Events.

Y. Eisenberg, S. Rosendorff and Y. Yeivin

Department of Physics, The Weizmann Institute of Science - Rehovoth, Israel

(ricevuto il 27 Febbraio 1956)

It has been suggested by Dalitz [1,2] and Fabri [3] that the spin and parity of the taon (τ-meson) may, in principle, be determined through studying the angular distribution and energy spectra of its secondary pions. Analyses of taons, assuming that π-π interactions are negligible and that all taons decaying at rest are positive, have been recently carried out by Amaldi [4], who collected data available from different laboratories at the Pisa conference (June 1955), and by the M.I.T. group [5], using events observed in an emulsion block exposed to the Berkeley Bevatron. In both works the distribution of Dalitz's angle θ is found to be isotropic. This θ is the angle of decay of the di-pion (the system of the two like pions), in its centre-of-mass system, with respect to the direction of decay of the unlike pion. The isotropic distribution of the experimental data indicates that the spin and parity of the taon are either $(0-)$ or $(1+)$. On the other hand, considering the energy spectrum of the unlike pion in order to distinguish between these possibilities, Amaldi concludes that $(0-)$ is the most probable possibility, whereas the M.I.T. data favour $(1+)$.

The purpose of this note is to point out that the samples considered in the above analyses were somewhat biased and to suggest how one may treat experimental data in order to avoid possible bias. The possibility of systematic bias in the data has already been emphasized by Dalitz [2]. Fig. 1 supports the idea of some bias present in the data we consider. In the two cases, $(0-)$ and $(1+)$, to which we have now confined ourselves, the spectrum of all pions is determined by phase-space considerations only [1], and is therefore

$$\frac{\mathrm{d}N_p}{\mathrm{d}\varepsilon} = \frac{8N}{\pi}\sqrt{\varepsilon(1-\varepsilon)}\,, \tag{1}$$

where $\varepsilon = E_\pi/E_{\max}$, i.e., the pion energy measured in units of the maximum energy which a single pion may have (~ 50 MeV). After normalization by (1) the experimental points should then fall on a flat curve. Inspection of Fig. 1 shows that this is not the case.

In order to understand how this bias arises we notice that the τ-events in emulsions may be classified according to whether all, two, or just one pion stop

---

[1] R. H. Dalitz: *Phil. Mag.*, **44**, 1068 (1953).

[2] R. H. Dalitz: *Phys. Rev.*, **94**, 1046 (1954).

[3] E. Fabri: *Nuovo Cimento*, **11**, 479 (1954).

[4] E. Amaldi: *Provisional report of the International Conference on Elementary Particles*, Pisa, 1955.

[5] B. T. Feld, A. C. Odian, D. M. Ritson and A. Wattenberg: *Phys. Rev.*, **100**, 1539 (1935).

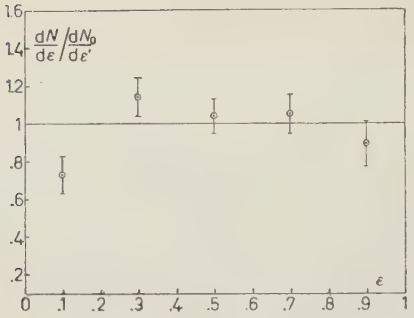

Fig. 1. – The (normalized) experimental spectrum of all pions. The flat curve corresponds to the (0 —) and (1 +) cases.

in the emulsion. The classification of the data is illustrated in Table I.

TABLE I.

Classification of the Taon Sample.

Class	Number of τ-Events		
	AMALDI ([4])	M.I.T. ([5])	Total
1. (+ + —)	49	17	66
2. (+ +)	10	18	28
3. (+ —)	27	13	40
4. (+)	12	—	12
5. (—)	4	7	11
6. (0)	2	—	2
All Classes	104	55	159

The signs of the stopping pions are indicated in the parentheses.

Now, a complete scanning should yield an unbiased sample (consisting of all events of all classes), while each class, taken by itself, is biased. Class 1, for instance, is composed of relatively more events in which all three pions are of intermediate energies ($\varepsilon \sim \frac{1}{2}$), while events with low ($\varepsilon \sim 0$) or high ($\varepsilon \sim 1$) energy pions have a greater chance to fall in other classes, where some pions leave the emulsion. It should now be clear that if some class, or classes, are excluded from the analysis, the resulting sample should be biased. In the M.I.T. analysis, classes 4 and 6 were excluded altogether, while it is not improbable that in the data presented by AMALDI events of classes other than 4 and 6 were more readily reported.

A possible procedure to obtain an unbiased sample is to consider only those events where the potential lengths of the tracks of all three pions are at least 4 cm (corresponding to $\varepsilon = 1$). This procedure, however, has the disadvantage of reducing the statistics very much and is therefore still unpractical. As an alternative, one has to collect data as complete as possible, not discarding events of any of the above classes. Events of class 6 should be considered in testing the data for possible bias, though, of course, they cannot be further used in the analysis proper. Nevertheless, with stripped emulsions it is to be expected that their percentage is small, and that their exclusion introduces a small bias only.

The spectrum of the negative pion may be used to determine whether the spin and parity of the taon are (0 —) or (1+). In the case of class 4 the π^- can alternately be assumed to be the slow or the fast of the two non-stopping pions. One then obtains two spectra between which the true one must lie. It should be noted that these two experimental spectra are quite similar (see Fig. 2), so that this procedure is quite reasonable. It should be mentioned that in this type of analysis one may consider also the $\tau'(\to \pi^+ + 2\pi^0)$ data in order to improve the statistics.

A different approach to the problem is based upon the spectrum of the lower energy positive pion. For the (0 —) case it by is given

$$(2) \qquad \frac{\mathrm{d}N_0}{\mathrm{d}\varepsilon} = \begin{cases} \dfrac{16N}{\pi}\sqrt{\varepsilon(1-\varepsilon)} & 0 \leqslant \varepsilon \leqslant \frac{1}{4} \\ \dfrac{N}{\pi}\left[4\sqrt{3} - 8\sqrt{3}\varepsilon + 8\sqrt{\varepsilon(1-\varepsilon)}\right] & \frac{1}{4} \leqslant \varepsilon \leqslant \frac{3}{4} \end{cases}$$

Obviously, ε cannot exceed $\frac{3}{4}$ in this case. The ratio of the spectrum for the $(1+)$ case to that just given for $(0-)$ case is

$$(3) \qquad \frac{\mathrm{d}N_1}{\mathrm{d}\varepsilon} \Big/ \frac{\mathrm{d}N_0}{\mathrm{d}\varepsilon} =$$

$$= \begin{cases} \frac{3}{2} - \varepsilon & 0 \leqslant \varepsilon \leqslant \frac{1}{4} \\ \frac{9}{4} - \frac{5}{2}\varepsilon - \frac{1}{2}\sqrt{3\varepsilon(1-\varepsilon)} & \frac{1}{4} \leqslant \varepsilon \leqslant \frac{3}{4} \end{cases}$$

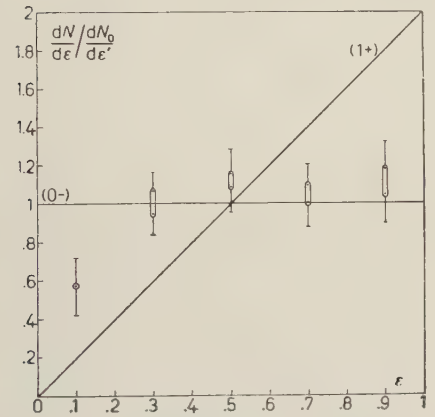

Fig. 2. – The (normalized) experimental π^- spectrum. The double points correspond to the assumption that the π^- is either the slow or the fast of the two non-stopping pions in class 4 events.

The advantage of the π^+_{low} spectrum analysis rests in the fact that in most of the ambiguous class 4 events it can be determined that the stopping pion is the low-energy positive one. In the AMALDI data this could be shown to be the case in 11 out of a total of 12 events in this class. The doubtful events can still be treated by assuming either of the escaping pions to be negative.

Figs. 2 and 3 give the experimental π^- and π^+_{low} spectra respectively, as gathered from the AMALDI and M.I.T. data. Available τ' data ([6,7]) are also included in Fig. 2.

Comparing the experimental results with the theoretical predictions, one

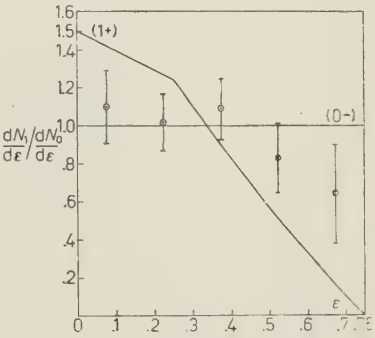

Fig. 3. – The (normalized) experimental π^+_{low} spectrum.

should be able, in principle, to deduce the spin and parity of the taon. Taken at face value, the data seem to indicate that the $(0-)$ is more probable than the $(1+)$ possibility. We think, however, that the experimental data reported till now may be biased against slow and fast pions relative to the complete data.

Omission of class 4 events reduces the numbers of low π^+ and of moderately fast π^+ and π^-. This sort of bias tends to transform the $(1+)$ spectra into the $(0-)$ ones. Thus the slight favouring of the data for $(0-)$ spectra may be fictitious. It is therefore strongly recommended that the *complete* data (classes 1-6) be collected from all laboratories, and it is hoped that with such data available one may come out with a more definite answer.

Added in proof:

Relativistic corrections to this analysis are now being calculated here; there are indications that the classical results may be significantly modified.

(6) G-STACK COLLABORATION: *Nuovo Cimento*, **2**, 1063 (1955).

(7) D. M. RITSON, A. PEVSNER, S. C. FUNG, M. WIDGOFF, G. T. ZORN, S. GOLDHABER and G. GOLDHABER: *Phys. Rev.* (in press).

IL NUOVO CIMENTO Vol. III, N. 4 1° Aprile 1956

A New Effect in the Magnetoresistance of Aluminium.

B. Lüthi and J. L. Olsen

Institut für Kalorische Apparate und Kältetechnik - E. T. H., Zürich

(ricevuto il 28 Febbraio 1956)

Much of the existing experimental data [1] on the magnetoresistance effect in metals can be fitted with remarkable accuracy to a well known formula derivable by very simple theoretical considerations [2]. If ϱ is the resistivity in the absence of a field, and $\Delta\varrho$ the increase in resistivity due to a transverse magnetic field H, then

$$\frac{\Delta\varrho}{\varrho} = \frac{A(H/\varrho)^2}{1 + B(H/\varrho)^2} \tag{1}$$

where A and B are constants of the metal. It is easy to see that this formula yields a quadratic dependence on the magnetic field at low fields, and an asymptotic approach to a constant saturation value at high fields. The high field region is given by the condition $H/\varrho > 2nec$, where n is the number of free electrons per unit volume. Precisely here, however, it is to be expected that the simple theory will break down due to the inapplicability of the Boltzmann equation in the simple form used, when H/ϱ becomes comparable to nec.

In order to examine this interesting region our previously reported magnetoresistance measurements in high magnetic fields at liquid helium temperature [3] were extended to aluminium using the technique previously described. Aluminium was chosen as a substance where the results of other workers [4,5] indicated that the maximum degree of saturation would be achieved with the very high fields available to us [6]. In the figure we show $\Delta\varrho/\varrho$ for two spectroscopically pure polycrystalline aluminium specimens of residual resistance $\sim 2.5 \cdot 10^{-3}$ in transverse fields up to 200 000 gauss at 4.2 °K. The measurements were made by an alternating current method at frequencies of 5 kHz, 10 kHz and 17 kHz. For comparison we show the results of Justi and Scheffers [4] at lower fields and a theoretical curve according to equation (1) with A and B chosen to fit the experimental data in the lower field region.

As is to be expected the fit between

---

(1) E. Justi: *Zeits. f. techn. Phys.*, **21**, 315 (1940).

(2) D. K. C. MacDonald and K. Sarginson: *Rep. Progr. Phys.*, **15**, 249 (1952).

(3) J. L. Olsen and L. Rinderer: *Nature*, **173**, 682 (1954).

(4) E. Justi and H. Scheffers: *Phys. Zeits.*, **39**, 105 (1938).

(5) G. B. Yntema: *Phys. Rev.*, **91**, 1388 (1953).

(6) J. L. Olsen: *Helv. Phys. Acta*, **26**, 798 (1953).

this theoretical curve, and experiment is excellent at the lower fields. In the whole region of JUSTI's measurements the two curves are in fact completely coincident. Then for values of $H/\varrho > 2nec/10$ our observations show a sudden striking departure upwards from the theoretical curve. Instead of approaching saturation $\Delta\varrho/\varrho$ begins to increase approximately as $H^{1.7}$, and we thus have a complete breakdown of the applicability of equation (1). This appears to be the first observed case of a clear cut departure from the magnetoresistive behaviour predicted by the simple model, and raises new theoretical problems. An explanation must probably be sought in considerations of the type given by TITEICA (7), in whose work such an increase at very high fields seems to be implied.

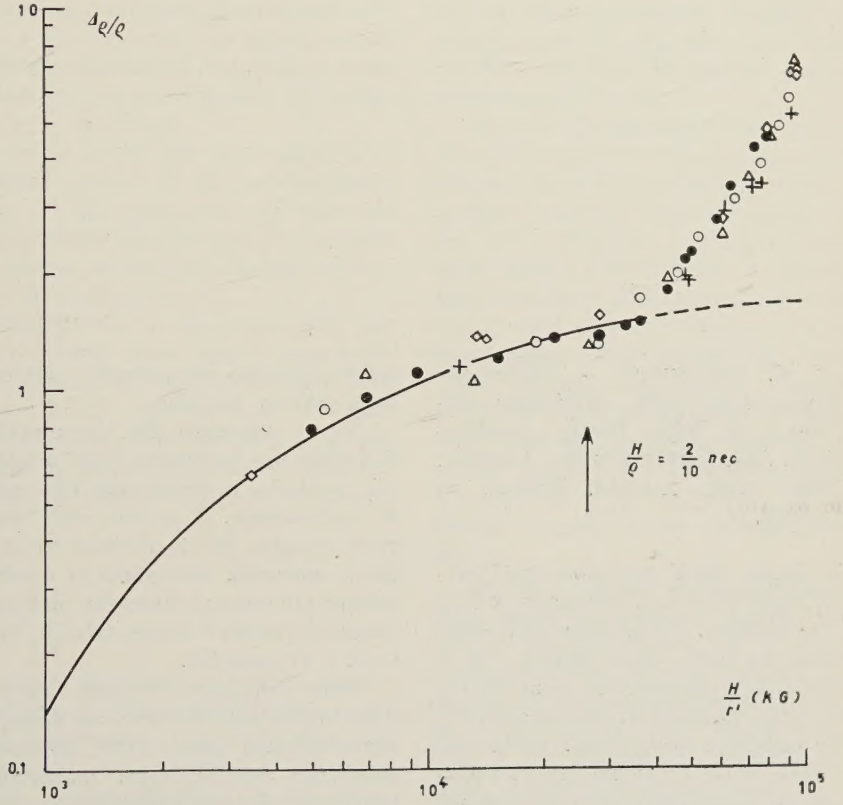

Fig. 1. – Transverse Magnetoresistance $\Delta\varrho/\varrho$ in Aluminium at 4.2 °K plotted against H/r', where $r' = \varrho/\varrho_\theta$; θ is 395 °K, $r = \varrho_{4.2}/\varrho_{293}$: ● Al 3 ($r = 2.6 \cdot 10^{-3}$); ○, △, +, ◇ Al 7 ($r = 2.7 \cdot 10^{-3}$); + 5.7 kHz; ○ 10.0 kHz; △ 17.3 kHz; ◇ 17.4 kHz; —— Justi's result; – – – Theoretical curve.

* * *

We wish to express our thanks to Professor Dr. P. GRASSMANN for his constant interest and support and for placing at our disposal the facilities of his institute, and we are grateful for financial support from the « Arbeitsbeschaffungskredit des Bundes ».

(7) S. TITEICA: *Ann. der Phys.*, **22**, 129 (1935).

LIBRI RICEVUTI E RECENSIONI

ALAN E. CRAWFORD – *Ultrasonic Engineering with Particular Reference to High Power Applications*. Ed. Butterworths, London, 1955; pag. x+344. Prezzo 45 scellini.

In questi ultimi anni sono stati pubblicati molti libri sugli ultrasuoni e sulle loro applicazioni, a cominciare dalla sesta edizione del testo, ormai classico, di L. BERGMANN [1] che contiene senza dubbio la più vasta rassegna di tali argomenti e la più completa bibliografia. Molte cose sono state dette e devono quindi necessariamente essere ripetute in ogni volume dedicato allo studio degli ultrasuoni, ma, dato il continuo progresso scientifico ed applicativo e la grande varietà delle fonti di informazione, ci si può sempre attendere che ogni pubblicazione contenga anche qualche cosa di nuovo e presenti un orientamento particolare.

Questo libro di ALAN CRAWFORD pone l'accento sugli aspetti applicativi e sulla tecnica degli ultrasuoni di grande intensità. L'indiscussa esperienza dell'Autore, che ha lavorato nei laboratori di una delle più importanti ditte che applicano gli ultrasuoni nell'industria, basterebbe a dare una garanzia della serietà del lavoro, peraltro ampiamente confermata dalla lettura del testo.

Si può veramente dire al giorno d'oggi che esiste una ingegneria degli ultrasuoni che ne studia la produzione ed i metodi di applicazione. È questo che l'Autore vuole esporre, da un punto di vista pratico e concreto, servendosi di documentazione abbastanza completa, almeno per quanto riguarda il lavoro fatto in Inghilterra e in America.

Dopo due capitoli dedicati alla teoria, il contenuto del libro si divide sostanzialmente in due parti, l'una dedicata ai generatori (piezoelettrici, magnetostrittivi, a getto ed elettromagnetici) e l'altra alle applicazioni, che sono dettagliatamente esposte in sette capitoli. Risulta particolarmente sviluppato quanto riguarda i trasduttori magnetostrittivi e le loro applicazioni, particolarmente chimiche e metallurgiche. I capitoli dedicati alle applicazioni biologiche e mediche ed agli apparecchi di misura e di controllo basati sugli ultrasuoni, non sembrano invece esaurienti.

Il libro è scritto per gli ingegneri e il suo interesse nel campo della ingegneria è evidente; ma anche chi si interessi di ultrasuoni dal punto di vista della ricerca scientifica può trovare in questa pubblicazione non poche utili notizie. Il contatto con il progresso dell'industria è infatti assolutamente necessario per chi non intenda svolgere il lavoro di labo-

[1] L. BERGMANN: *Der Ultraschall und seine Anwendung in Wissenschaft und Technik* (Zürich, 1954).

ratorio in forma troppo strettamente artigiana, e, d'altra parte, la conoscenza delle soluzioni adottate può fornire idee preziose anche per i dispositivi di ricerca. A questo si deve aggiungere che nel libro non mancano interessanti riferimenti alla teoria e dati ricavati da pubblicazioni non sempre facilmente reperibili; si veda, ad esempio, ciò che riguarda la cavitazione e la corrosione.

Il testo, scritto con la chiarezza e la precisione propri di chi personalmente lavora con gli apparecchi che descrive, fornisce numerosi dati pratici e costruttivi, schemi elettronici, disegni e fotografie di apparecchi.

Concludendo, si può dire che, per quanto questo libro tratti esaurientemente solo alcuni argomenti particolari, tuttavia il suo interesse non si limita esclusivamente al campo tecnico, sicchè esso può degnamente figurare nella biblioteca del fisico che si occupa di ultrasuoni.

F. A. Levi

Giuseppe Pompilj e Diego Napolitani – *Piano degli esperimenti ed elaborazione probabilistica dei risultati con particolare riguardo alla sperimentazione in biologia.* Pag. 206; L. 2000. - Edito come Supplemento a « La Ricerca Scientifica », 1954.

Il volume trae origine da un corso di lezioni tenute dal Pompilj ad un gruppo di ricercatori presso l'Istituto Nazionale della Nutrizione del C.N.R., lezioni raccolte e poi ordinate sistematicamente in volume da Diego Napolitani. Suo scopo è di consentire l'uso sicuro, senza eccessivo sforzo, dei metodi statistici anche a quei ricercatori (e particolarmente ai biologi) che non siano particolarmente versati nelle discipline statistiche e matematiche.

Nel primo breve capitolo vengono poste chiaramente le definizioni ed illustrati i concetti fondamentali (fattori sperimentali e subsperimentali, probabilità a priori, probativa, a posteriori, devianza, varianza, covarianza, codevianza, correlazione, ecc.) e vengono sottolineati i principi e gli atteggiamenti gnoseologici che sono alla base dei metodi statistici correttamente intesi.

Nel secondo capitolo, attraverso una ben scelta successione di casi concreti, si illustra, in varie situazioni, il modo di condurre l'analisi delle frequenze (indice χ^2 di Pearson), il confronto delle medie (indice t di Student), il confronto della varianza e della covarianza ($F(z)$ di Fisher). Alla chiara formulazione del problema segue l'elaborazione dei dati secondo il metodo che meglio si adatta al problema stesso, in modo che il lettore viene condotto, quasi senza sforzo, dai casi più semplici ai più complessi, mentre le peculiarità di ogni problema e di ogni metodo vengono poste chiaramente in luce.

Nel terzo capitolo si tratta infine del piano degli esperimenti, sempre sulla base di esempi concreti, di cui due si riferiscono alla disposizione completa causale, 4 alla disposizione completa a blocchi, 2 alla disposizione a blocchi incompleti, 6 alla disposizione a scacchiera e, infine, 2 alle disposizioni incomplete.

Completano il volume le tavole della distribuzione normale, del χ^2, della t, della F, nonchè le tavole dei quadrati, radici quadrate e inversi (n da 1 a 1000).

Nonostante il Pompilj dichiari nella prefazione di aver rinunziato a qualunque forma di esposizione sistematica, ciò deve intendersi in senso strettamente matematico, in quanto il volume non manca di organicità; il metodo di trattazione usato, a base di esempi concreti con ogni formula seguita dall'effettiva applicazione numerica, e l'esposizione precisa ma non pedantesca fanno ritenere che lo scopo prefissosi dagli Autori sia stato pienamente raggiunto.

Il lettore non specialista non deve

però attendersi che le difficoltà caratteristiche dell'argomento siano state eliminate; dovrà, se mai, guardarsi dalla tentazione opposta; quella cioè, una volta appresa una regola, di sopravalutarne la portata; potrà però evitare anche questo (che allo stato attuale di diffusione dei metodi statistici è pur sempre un male minore), se terrà ben presente la breve ma sostanziosa discussione dei principi, fatta nel primo capitolo. A questo fine, forse, sarebbe stato desiderabile anche in testo nella discussione dei casi particolari un più frequente ed esplicito richiamo ad esse.

Il libro, come si è detto, è rivolto principalmente ai biologi, ma può riuscire utile anche ad altre categorie di ricercatori, non iniziati all'argomento, per esempio ai giovani fisici; naturalmente per questi l'efficacia didattica degli esempi, estranei alla materia più familiare, risulta diminuita.

In conclusione può dirsi che il volume colma veramente una lacuna nella nostra letteratura, mentre regge benissimo il confronto con analoghe pubblicazioni straniere (rivolte sempre ai biologi), dalle quali se mai si differenzia per la maggiore ricchezza di esempi e completezza di argomenti.

Ci sia quindi permesso concludere auspicando, a nome dei fisici, che sorga l'occasione, analoga a quella che originò questo opuscolo del Pompili, per far dedicare anche ad essi un libretto ben fatto del genere di questo e che includa possibilmente anche una moderna trattazione della teoria degli errori, per la quale oggi occorre far ricorso alla sapienza dei padri.

Manlio Mandò

Direttore responsabile: G. POLVANI Tipografia Compositori - Bologna

Questo fascicolo è stato licenziato dai torchi il 29-III-1956